Grid Interaction Performance Evaluation of BIPV and Analysis with Energy Storage on Distributed Network Power Management

Aimie Nazmin Azmi

Grid Interaction Performance Evaluation of BIPV and Analysis with Energy Storage on Distributed Network Power Management

Doctoral Dissertation n for the degree Philosophiae Doctor (PhD) at the
Faculty of Engineering and Science, specialization in Renewable Energy

University of Agder
Faculty of Engineering & Science
2017

Doctoral Dissertations at the University of Agder 154

ISSN: 1504-9272
ISBN: 978-82-7117-848-2

© Aimie Nazmin Azmi, 2017

Printed by the Wittusen & Jensen
Oslo

Nostalgia is like a grammar lesson. You find the present tense and the past perfect….'

In the name of Allah, most Gracious and most Merciful,

For Arwah Abah, and Mama

Your love, support and belief in me, gave me strength.

And always being there for me,

And being the best parents ever.

For family members,

For being the best brothers, sister, and in-laws

For your well wishes and prayers

For my other half (God knows who)

For not being here. Just yet.

And for everyone who has touched my life

I dedicate this to all of you.

Abstract

This research focuses on analysis of photovoltaic (PV) based active generator in microgrid and its utilization in not only for operational planning of the power system but also for instantaneous power flow management in the smart grid environment. The application of this system is part of a solution on handling a large scale deployment of grid connected distributed generators, especially PV system. By implementing the PV based active generator, it will be very flexible able to manage the power delivery from the active generator sources (e.g. PV system, energy storage technologies, active power conditioning devices). In Southern Norway, a smart village Skarpnes is developed for ZEBs. These ZEBs have Building Integrated Photovoltaic (BIPV) system. The energy efficient housing development should consider that a building should produce the same amount of electrical energy as its annual requirements (i.e. ZEB). In future, ZEBs are going to play a significant role in the upcoming smart grid development due to their contribution on the on-site electrical generation, energy storage, demand side management etc. In this work the main objective is to evaluate the usefulness of ZEBs for load matching with BIPV generation profiles and grid interaction analysis. Impact of BIPV system has been investigated on the distributed network power flow as well as on protection and protective relays analysis. Furthermore, techno-economic analysis of BIPV system is presented which will be useful to the utility for developing new business models as well as demand side management (DSM) strategies and for decentralized energy storage. The real operational results of a year are analyzed for annual energy balance with on-site BIPV generation and local load. This work provides quantitative analysis of various grid interaction parameters suitable to describe energy performance of the BIPV. The load matching and grid interaction parameters are calculated for a house to find relationship of BIPV generation and building load. The loss of load probability is analyzed for fulfilling the local load at desired reliability level. Results of this work are going to be useful for developing DSM strategies and energy storage as well as import/export energy to the grid. This work will be beneficial for future planning of the distributed network when the BIPV penetrations are going to increase.

Acknowledgements

Immeasurable appreciation and deepest gratitude for the help and support are extended to the following person in one way or another has contributed in making this study possible;

To Prof. Dr. Mohan Lal Kolhe, whose expertise, understanding and generous guidance and support made it possible for me to go through this rough and tough journey.
To Prof. Dr. Anne Gerd Imenes, for her constructive comments which help me a lot in improving my report writing, and doing technical analysis and for being my co-supervisor.
Universiti Teknikal Malaysia Melaka (UTeM) in providing scholarships throughout my studies in Norway.
To Charly, Gunstein, Stefan, Abozar, Muhammad Tayyib, Giorgi, Abhijit, Sissel, Andet, Ingrid and little Solveig in Grimstad for being a good 'family' throughout my journey in Norway and for making my PhD journey bearable and FUN.
To Emma Elisabeth Horneman for always answered uncountable questions and endured request for thousands of information from all of us in Tekreal. Thank you for being a savior, guardian angel and wonder woman.
I am very much thankful to Konara Mudiyanselage Sandun for having detailed technical discussion on power management of PV system with energy storage and integrating some tasks through his MSc studies. Also I am very grateful to Ivan Nordnes Dahlberg and Su Haocheng for conversation on distributed network analysis with PV system throughout their Master studies.
I am gratefully acknowledges the support of the Research Council of Norway and project partners (i.e. Teknova AS, Agder Energi AS, and Eltek AS) of the project ‘Electricity Usage in Smart Village Skarpnes’ (project no NFR-226139), for providing data and technical information on completing this study.

Thank you all from the bottom of my heart.

Contents

Chapter 1

1 Introduction

This dissertation will cover the photovoltaic (PV) based active generator. The system comprises of a PV system, battery storage, and power electronics power converter devices. The purpose of this project is to analyze PV based active generator in micro-grid and its utilization in operational planning of the power system in a smart grid environment. In order to integrate micro-grid level power management system (EMS) with the centralized EMS, several functions may need proper consideration such as photovoltaic (PV) energy availability, local load consumption and local energy storage availability.

A future smart grid power system network will serve as a dynamic network for bi-directional power flows, linking widely distributed small capacity renewable energy systems (e.g. PV) at consumer level, distribution networks and centralized higher-capacity power generators. It will facilitate active participation of customer choice for energy production and demand management, and will provide real-time information on the performance and optimal operation of the power system network. Many challenges lay ahead in achieving the smart grid network vision. The integration of intermittent renewable energy and other efficient distributed energy resources into existing and future electricity networks represents significant technical and economic challenges. The widespread development of such systems requires a thorough analysis of all technical and commercial aspects of renewable energy sources and other decentralized generation units in the distribution network [1]. A Smart Grid research and technology development effort has to harmonize with expansion of the power system infrastructure, the information and communications infrastructure with modern actuators, and integration of new

monitoring and control applications. These developments are forcing to redesign the power system operation and control [2, 3]. To facilitate higher penetration integration of intermittent renewable energy sources, the EMS of renewable energy sources need to be based on active generator approach.

At present, most of the world-wide grid connected PV systems are operating at maximum power points and not contributing effectively towards the energy management in the power system network [4]. Many studies have been made on techno-economic optimum sizing of standalone (off-grid) PV system [1, 5, 6]. Unless properly managed and controlled, large scale deployment of grid connected PV generators may create problems such as voltage fluctuations, frequency deviations, power quality in the power system network, change in fault currents and protections settings etc. These problems are becoming critical for maintaining the power system stability and control. A solution to some of these problems is the unique concept of PV based active generator. Active generators will be very flexible and able to manage the power delivery as used to be in conventional generator system. This active generator includes the PV array with combination of energy storage technologies and proper power conditioning devices. Figure 1 in the next chapter shows the block diagram of PV based active generator. It is essential to develop unique configurations of the PV based active generator, for delivering the required power in the micro-grid network.

The PV array output is nature dependent and therefore the PV power output predictability is important for operational planning of the micro-grid as well as for centralized generators. PV array output forecasting as well as load forecasting is critical for EMS. The PV power predictions can be adapted more and more accurately by means of predictive models [7]. Markov chain method, artificial neural network, autoregressive and a few more mathematical models are forecasting models used nowadays. The forecasting methodology is required to be incorporated in the EMS in order to make sure that the loop of energy supply will be ongoing and the system stability should be maintained within the prescribed power system network limits.

In power system network, power quality is very important. Due to PV power output fluctuations, there are some chances for power quality disturbances e.g. voltage transients due to intermittency, harmonics, active and reactive power management, power delivery angles etc. In the conventional grid connected PV generators, hybrid filters are used to improve the power quality

[8]. But for multiple PV based active generators (e.g. group of buildings with BIPV), the power quality issues require more analysis.

Higher penetrations of distributed generators may create different possibilities of faults, not only in the micro-grid network but at the higher voltage power system network as well. Fault detection and the isolation mechanism are very important for the power system operation. It is needed to analyze the fault protection system for example fault current levels, relay settings and fault clearing time in the micro-grid environment by considering the PV based active generators [8-10]. The grid may be disconnected during fault or any unwanted events and abnormal conditions at the micro-grid network, thus islanding effect may occur in micro-grid. It will create many problems for grid operation and safety issues. In such type of situations, micro-grid EMS has to be intelligent for effectively managing the power flows within the micro-grid by considering not only voltage and frequency fluctuations but also taking into accounts the safety by using different protection standards [11, 12]. These standards are used to make sure that the PV based active generator grid connections are safe and not going to harm either equipment or personnel. By using these protection standards, the utilities company can envisage the impact of the control strategies of the connection, which includes the performance of voltage deviations, power quality and harmonics.

This research is focusing on the implementations of EMS for a PV based active generator that is connected at micro-grid level in a smart grid environment. In order to integrate micro grid level EMS with the centralized EMS, several functions such as of PV output, local load profile and local energy storage availability may need proper consideration for upgrading the centralized EMS as well as developing new business models for the utility. In this project, the concept of the PV based active generator, the building integrated PV (BIPV) system performance, the grid interaction indicators, operational planning of PV based active generator, and fault analysis in distributed generators are being studied.

1.1 Objectives and Scope

This research focuses on analysis of PV based active generator in microgrid and its utilization in operational planning of the power system in smart grid environment. Impact of PV based active generator is investigated on the distributed network protection and protective relays. Development of energy efficient housing is progressing around the world and most of these houses will

be integrated with PV system. In this work, the real operational results of a BIPV house are analyzed for annual energy balance and to provide quantitative analysis of various grid interaction parameters. Furthermore, techno-economic analysis of BIPV system is presented which will be useful to the utility for developing new business models as well as demand side management (DSM) strategies and for decentralized energy storage. Based on these, the research is divided in following topics:

1) **PV based active generator fundamental**

   This active generator has the capacity to support frequency control and instantaneous power balance. The grid operator adjusts the power dispatch of generators according to power demand fluctuations. PV based active generators can be used as load following generators in the same manner as other power dispatch generators. This new type of distribution system, based on active generator(s), needs new innovative management and operation strategies for increasing the penetration of intermittent renewable energy systems. The considered PV based active generator has three units, i.e., PV array, battery storage and super capacitor. For this research work, the management and operation approaches of PV based active generators are discussed.

2) **Local power management system for PV based active generation for micro-grid management**

   The proposed architecture of the PV based active generator which can meet the load demand while compensating the intermittent nature of the PV power generation is executed by using a random aggregated load from 30 houses. This is to control the active and reactive power demand of a set of AC loads connected with the grid connected PV based active generator with respect to the voltage and frequency stability.

3) **Application of PV based active generator**

   An example of PV based active generator application will be presented. Skarpnes smart house is an example on how the PV based active generator act in a common environment. However, the application on battery storage is still in a trial mode, where there is still lack of information. This project is a pilot project of a ZEB. The energy required in this project will be partially supplied from the PV arrays on the rooftops. It is connected to conventional grid and has a capability of exporting surplus energy

especially in summer. The mismatch loads and generation is calculated to determine the condition of the project.

4) Fault analysis in micro-grid network with PV based active generator

There will be few major issues regarding the protection in the micro-grid network with higher penetration of distributed generators. Fault currents in a micro-grid are not similar to faults in a conventional grid system. In micro-grid network, there are limitations on protection system due to the islanding operation mode. Also the fault clearing time is important for micro-grid stability and operation. In this work, the fault analysis of the PV based active generators in the micro-grid network will be analyzed with the power flow analysis and protective device behavior.

1.2 Thesis Outline

Chapter 1
This chapter consists of a brief introduction of the thesis and the objectives are presented.

Chapter 2
The introduction and definition of PV based active generator as the main idea of this thesis is presented. Literature review and state of the art on how PV based active generator might change the distributed generators in conventional grid is reported.

Chapter 3
In this chapter, the architecture of a PV based active generator which can provide active and reactive power while maintaining the frequency and the voltage stability with grid constraints is presented. With the proposed architecture, the load demand to the grid is reduced and the power flow is managed using a hierarchical approach with stateflow analysis and droop characteristics.

Chapter 4
The application of PV based active generator is presented here. The main concept of the active generator has been executed in the Skarpnes smart house ZEB. The definition of ZEB for this particular project and the data from one of the house has been selected to be examined and discussed.

Chapter 5
With a penetration of PV in DG, what are the effects of the power flow, voltage and how the protective device will act in a case of fault? This will be answered in chapter 5. A simulation using PowerFactory Digsilent ® is used to see the effect.

Chapter 6
Chapter 6 summarizes the inputs from this work and recommends further investigation that can be done based on this work.

1.3 List of Publications

Journal article under review: A.N Azmi, M.L Kolhe, Grid Interaction Performance Evaluation of Zero Energy Building (ZEB) in the Southern Norway, '*Energy and Buildings' (Elsevier),* ISSN: 0378-7788, 2016.

Book Chapter: "PV System Design for Off-Grid Applications," in Solar Photovoltaic System Applications, A guidebook for off-grid electrification, Springer International Publishing, pp: 49-84, 2015 DOI: 10.1007/978-3-319-14663-8_3, Online ISBN: 978-3-319-14663-8

Paper 1: A.N Azmi, M.L Kolhe, *Primary Frequency Control through Grid Connected Photovoltaic Active Generator*, 3rd International Workshop on Integration of Solar Power into Power Systems London, United Kingdom.pp: 32-38, 2013. ISBN: 978-3-9813870-8-7
(Appendix B, Page: 125)

Paper 2: A.N Azmi, M.L Kolhe, A.G Imenes, *Techno-Economic Analysis of On-Grid Smart House in Southern Norway*, 2013 IEEE Conference on Clean Energy and Technology (CEAT 2013), Langkawi, Malaysia. pp: 93 - 97, 2013. DOI: 10.1109/CEAT.2013.6775606
(Appendix B, Page: 130)

Paper 3: A.N Azmi, M.L Kolhe, A.G Imenes, *Technical and Economic Analysis for a Residential Grid Connected PV System with Possibilities of Different Battery Energy Storage Capacities(Case Study: Southern Norway),* 4th International Workshop on Integration of Solar Power into Power Systems Berlin, Germany. Pp: 486 - 491, 2014. ISBN: 978-3-9816549-0-5
(Appendix B, Page: 135)

Paper 4: A.N Azmi, M.L Kolhe, *Photovoltaic Based Active Generator Energy Controlling System by Using Stateflow Analysis*, 11th IEEE International Conference on Power Electronics and Drive Systems (PEDS2015) Sydney, Australia. pp: 18 – 22, 2015.
DOI: 10.1109/PEDS.2015.7203433
(Appendix B, Page: 141)

Paper 5: A.N Azmi, M.L Kolhe, A.G Imenes, *Review on Photovoltaic Based Active Generator*, IEEE International Symposium on Advanced Topics in Electrical Engineering (ATEE 2015), Bucharest, Romania. pp: 812 – 815, 2015.
DOI: 10.1109/ATEE.2015.7133914
(Appendix B, Page: 146)

Paper 6: A.N Azmi, I.N Dahlberg M.L Kolhe, A.G Imenes, *Impact of Increasing Penetration of Photovoltaic (PV) Systems on Distribution Feeders.* IEEE International Conference on Smart Grid and Clean Energy Technologies (2015 ICSGCE), Offenburg, Germany. pp: 70 – 74, 2015. DOI: 10.1109/ICSGCE.2015.745427.
(Appendix B, Page: 150)

Chapter 2

2 Photovoltaic Based Active Generator[1]

At present, most of the world-wide grid connected PV systems are operating at maximum power points and not contributing effectively towards the energy management in the power system network [4]. There are many studies on techno-economic optimum sizing of standalone (off-grid) PV system [5, 13-16]. Unless properly managed and controlled, large scale deployment of grid connected PV generators may create problems; voltage fluctuations, frequency deviations, power quality problems in the power system network, changes in fault currents and protections settings, and congestion in distributed network. These problems are becoming critical for maintaining the power system stability and control. A solution to these problems is the concept of active generator. The active generators will be very flexible and able to manage the power delivery as used to be in conventional generator system. This active generator includes the PV array with combination of energy storage technologies and proper power conditioning devices.

2.1 Introduction

PV array output is nature dependent and therefore the PV power output predictability is important for operational planning of the micro-grid as well as centralized generators. The PV array output forecasting as well as load forecasting is critical for energy management system (EMS). PV power predictions can be adapted more and more accurately by means of predictive models [7]. Markov chain method, artificial neural network, autoregressive and a few more mathematical models are forecasting models used nowadays. The

[1] *Modified from the paper published and presented in a peer reviewed conference. IEEE International Symposium on Advanced Topics in Electrical Engineering (ATEE 2015), Bucharest, Romania. DOI: 10.1109/ATEE.2015.7133914, Pp 812-815, 2015*

forecasting methodology is required to incorporate in EMS in order to make sure that the loop of energy supply would be on-going and the system stability should be maintained within the prescribed power system network limits.

In power system network, the power quality is significant. Due to PV power output fluctuations; there are some chances for power quality disturbances e.g. voltage transients due to intermittency, harmonics, active and reactive power management, power delivery angles etc. In conventional grid connected PV generators, hybrid filters are used to improve the power quality [8]. But for multiple PV based active generators (e.g. group of buildings with BIPV), the power quality issues require more analysis. It seems like analyses on fault protection system is needed due to there will be some unknown situations that might occur and interrupting the power flow on the grid and reducing the efficiency of the grid performance.

The higher penetrations of distributed generators are going to create different possibilities of the faults not only in the micro-grid network but at higher voltage power system network. Fault detection and isolation mechanism is compulsory for power system operation. It is needed to analyses the fault protection system for instance: fault current levels, relay settings and fault clearing time in the micro-grid environment by considering the existence of PV based active generators [9]. During fault or any unwanted events and abnormal conditions at the micro-grid network, the grid may be disconnected, and islanding effect may occur in micro-grid. It will create many problems towards the grid operation and safety issues. In such situations, micro-grid EMS has to be intelligent for effectively managing the power flows within the micro-grid by considering not only voltage and frequency fluctuations but also taking into accounts the safety by using different protection standards [11, 17]. These standards are used to make sure that the PV based active generator and grid connections are safe and not going to harm either equipment or personnel. By using these protection standards, the utilities company can envisage the impact of the control strategies of the connection; which includes the performance of voltage deviations, power quality and harmonics.

2.2 Overview of PV based Active Generator

PV based active generator is a systems that comprise of PV array with a battery storage system with a capacity of storing energy for a long and short term for local usage [18]. From this definition, it can be conclude that this system will be able to generate, store and release energy as long as the electricity

is needed. This can be done with a proper hierarchical monitoring and energy management system. Figure 2.1 shows exactly the system [3].

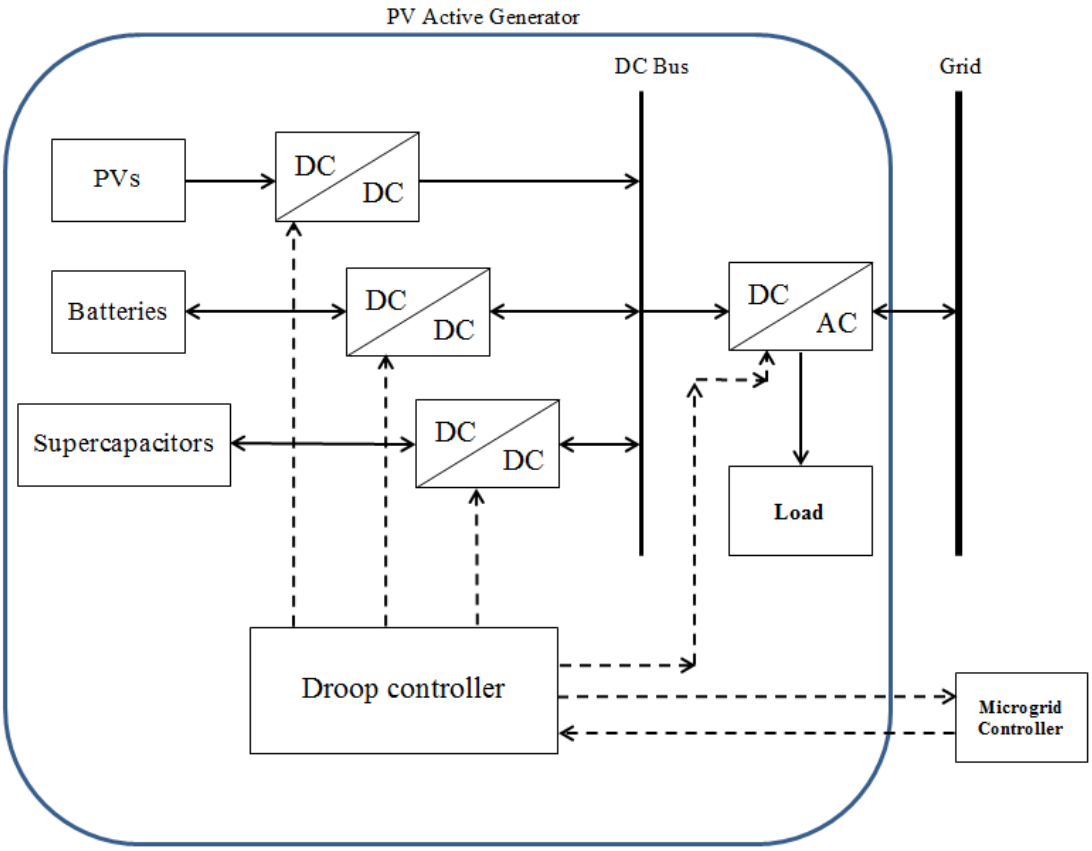

Figure 2.1 Scheme of PV based active generator

Power management is crucial to control the whole energy flow in the PV based active generator. As discussed in [19], the author put an emphasize on the power management algorithm on the active PV station with a battery storage. Four hierarchical positions have been introduced and each level has its own task, as shown in Figure 2.2. These PV based active generator is expected to offers a new flexibilities to the consumer and operator and will be a new dimension of generating electricity through clean energy. This system will be operated in a microgrid environment and will have a lot more parameters that need to be considered.

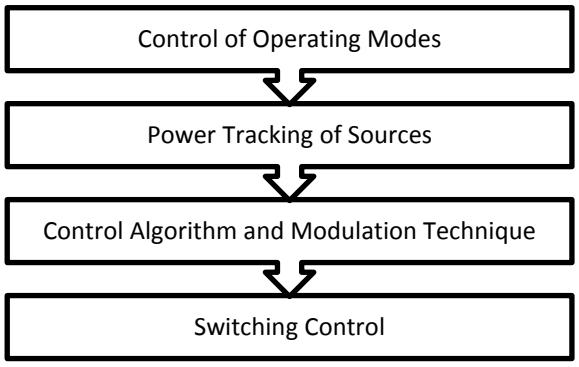

Figure 2.2 PV generator control level

The author stated that the main disadvantage for this system is the stochastic output for solar radiation and the output energy is really dependent on the weather. In order to solve this problem the PV based active generator is introduced by the author. This basic concept of PV based active generator is then discussed in the next paper which is discussed further on the application of PV based active generator and the dimension in the environmental and economical point of view [18, 20].

The system is connected to the battery storage and or supercapacitors and which is then is coupled with choppers and connected to the existing grid (microgrid). With the combination of battery and supercapacitors, it will increase the system efficiency as the battery will be able to store and release energy gradually, while supercapacitor effectively acts as storage device with very high power density. For a complete PV active based generator, a set of battery bank connected in a combination series-parallel in order to provide desired power to the system. The additional supercapacitor will provide a fast response energy storage device that can reduce the effect of short term fluctuations of PV output and will enhance the whole system [21].

The combination of battery storage and supercapacitor will be able to smooth the output from the PV array since it will be fluctuate. For a renewable energy application, the battery storage system will be operated under the partial state of charge duty (PSOC) [22]. In this condition, the battery or supercapacitors will be partially discharge at all time, in order to make sure the system will be able to absorb or discharging power to the grid as it is needed [23]. To charge the supercapacitor, a few methods as discussed in [24] can be used. In this reference, the writers are discussing on the supercapacitor charging efficiency of PV system. Based on simulation that has been done, constant power charging mode is better for charging supercapacitor in PV environment.

However, it is not proven that it will be suit to the microgrid environment yet. For a dynamic equation of supercapacitor, can be seen as;

$$\frac{C_e}{\omega}\frac{\partial V_e}{\partial t} = \frac{1}{R_e}\left[\left(\frac{1-d}{d}\right)V_{dc} - V_e\right] \quad (2.1)$$

Where:

C_e = capacitance value
R_e = series resistance of supercapacitor
V_e = supercapacitor voltage
d = duty cycle.

The duty cycle implemented in the system is proportional and integration controller (PI).

2.3 PV Based Active Generator in Microgrid Environment

Microgrid is a system that operates at low voltage and has a few distributed energy resources (PV, wind, geothermal etc.) With proper energy management and systematic supervision microgrid can be a new dimension of generating and transmitting energy to the load. PV based active generator can be integrated into microgrid and it has been done in Kytnos Island and Mannheim-Wallstadt [18]. It needs a good supervision from the utility operator to make sure it will well operate. Energy supervision for the whole system is compulsory and in [25], the author has divided the system into two different parts: (i) central energy management of the microgrid and (ii) supervision for the active generator. On the microgrid side, the operator needs to manage the energy between source and load. This will includes the active and reactive power, frequency regulation, voltage fluctuations and etc.

From [25] and [20] the author has initiate a strategic framework of executing PV based active generator in a smart grid environment with more consideration and rules. Both have been considered on the long term energy management and short term power balancing this duration of time in monitoring the EMS in smart grid environment is presented in Figure 2.3. In [20] the same approach has been used and the optimization on the environmental and economic criteria has been develop. It is based on 24 hours of PV prediction. The author in [18] describes on the long term operational planning for energy management of a microgrid. In this paper, the author presented a microgrid

system with a source from a three gas turbines and PV based active generator. The microgrid central energy management system (MCEMS) is executed. This system has a different task and parameters such as dealing with the environmental effect, forecasting energy, power prediction, and deal with the power market. Based on all these crucial parameters the microgrid system can be organized properly and the output of the system will be much more efficient and clean.

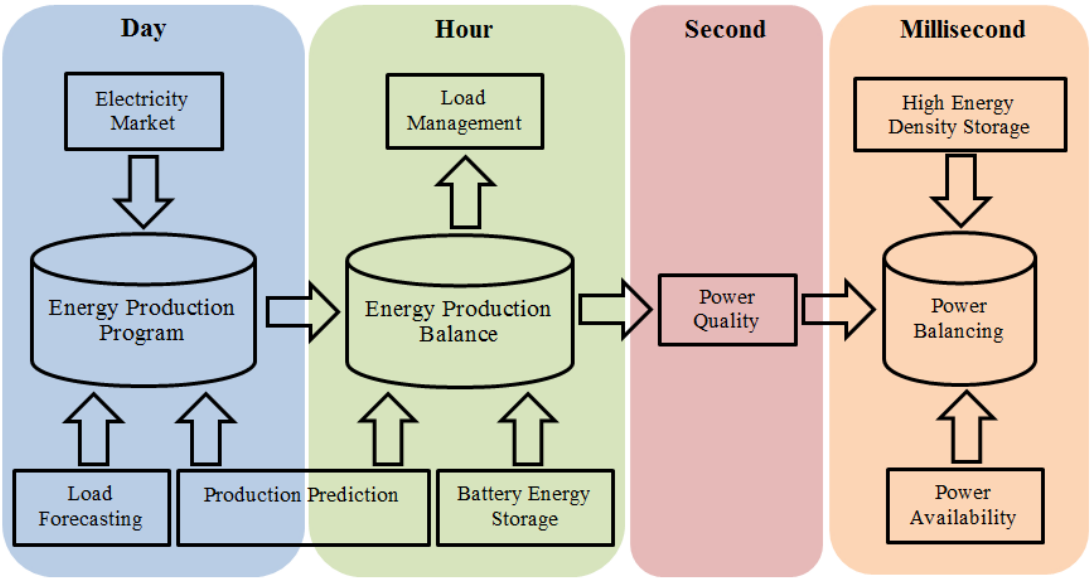

Figure 2.1 Timing classifications for EMS [20]

2.4 Battery Storage and Supercapacitor (Storage System)

Battery storage sizing is very important. There are 3 main parameters that need to be considering for every installation of battery storage system. The depth of discharge (DOD), state of charge (SOC), state of health (SOH), battery capacity, maximum battery charge and discharge power and the utility rating type [26]. Battery storage systems are being progressively used in distributed renewable energy generation nowadays. With the existence of supercapacitors, the effectiveness of the storage system will be much more reliable to be used in the near future. With the combination of battery and supercapacitors, it will increase the system efficiency as the battery will be able to store and release energy gradually, while supercapacitor effectively acts as storage device with very high power density. For a complete PV active based generator, a set of battery bank connected in a combination series-parallel in order to provide desired power to the system. The additional supercapacitor will provide a fast

response energy storage device that can reduce the effect of short term fluctuations of PV output and will enhance the whole system [21].

Basically the total produced power from the system is a total power generated from the PV, battery and supercapacitor.

$$P_T = P_{PV} + P_B + P_{sC} \tag{2.2}$$

Where;

P_T	: Total power
P_{PV}	: PV power
P_B	: Battery power
P_{sC}	: Supercapacitor power

There are a lot of research has been done for the battery storage system for PV generator. The battery dynamic equation can be represents as [27];

$$\frac{dE_B}{dt} = P_B(t) \tag{2.3}$$

Where E_B represent the amount of electricity stored at t time and P_B is the charging or discharging rate. This should be integrating with the supercapacitor to make sure that both of this storage system can be used and compatible to each other. In [25] the author focus on using the optimal use of batteries. There are several relevant resources regarding the optimization of batteries for PV. The author from [28] has proposed a battery model specifically useful for the stand-alone photovoltaic applications. Seven different levels of working zone and zone conditions has been proposed; saturation zone, overcharge zone, charge zone, changing from charge to discharge or vice versa, discharge zone, over discharge and exhaustion. As can be seen in Figure 2.4, the working condition is depends on the voltage and current that went through the battery. This is a sample of a 2V battery.

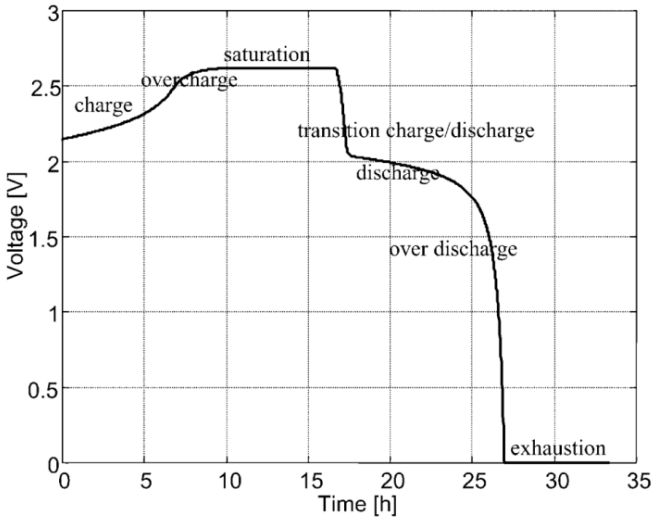

Figure 2.4 Battery working zone conditions [28]

The Fraunhofer-Institute for Solar Energy Systems (ISE) has developed a new generation of battery-management system for renewable energy system [29]. For a conventional renewable energy system, the battery often operated at the low state of charge that resulting the decreasing lifetime of the battery. By implementing a battery management system (BMS) system on the renewable energy system it improves the storage lifetime and reliability of batteries in the system and thus reduces maintenance and lifetime costs considerably. Vallve. X, Graillot and friends in [30] discussed on three basic facts on installation of storage system to a grid connected PV system. First argument is the storage system can undoubtedly improve the security of supply to the whole system; however the grid quality is the main issue. The existing grid is aging and the possibilities of interruption are high. Second; the addition of storage function might increase the performance ratio of PV generator. The third fact is large penetration of PV will definitely not be able to cover the whole load consumptions. PV source can be able to supply at least some part of overall energy consumed by specific load. These facts may lead the utility company or customer to consider on the battery and supercapacitor as a main storage structure for future housing development.

The battery storage system for PV integration is also discussed further in [31-35]. The authors in these papers discusses on the main topic related to connection of PV system to the microgrid; frequency control, voltage stability and energy storage smoothing control. These parameters are significant for a PV based active generator, since it is compulsory to get a very efficient system to make sure it can be implemented in the real system. A smoothing control method for reducing output power fluctuations and regulating battery state of charge (SOC) under typical condition is proposed. Voltage control and active

power control algorithm for centralized battery storage system is already proposed in [36].

Table 2.1 Comparison between different types of batteries [35]

Storage	Power ratings	Discharge time	Suitable Storage duration	efficiency	lifetime	
					years	cycles
PHS	100-5000	1-24hr	hrs-months	70-80	>50	>15,000
CAES	5-300	1-24hr	hrs-months	41-75	>25	>10,000
FES	0-0.25	sec-hr	sec-mins	80-90	15-20	104-107
Lead Acid	0-20	sec-hr	mins-days	75-90	3-15	250-1500
NiCd	0-40	sec-hr	mins-days	60-80	5-20	1500-3000
Li-ion	0-0.1	min-hr	mins-days	65-75	5-100	600-1200
NaS	0.05-8	sec-hr	sec-hrs	70-85	10-15	2500-4500
VRB	0.03-3	sec-10hr	hrs-months	60-75	5-20	>10,000
ZnBr	0.05-2	sec-10hr	hrs-months	65-75	5-10	1000-3650
Fuel cell	0-50	sec-24hr+	hrs-months	34-44	10-30	103-104
Supercapacitor	0-0.3	msec-1hr	sec-hrs	85-98	4-12	104-105
SMES	0.1-10	msec-8sec	mins-hrs	75-80	-	-

There are a lot of new inventions on the storage system to fit in the new grid system or microgrid. As discussed in [35] and based on evidence in [34] and [37] the utilization of VRB in microgrid has abundance of chance. Based on Table 2.1, the comparison is between five different types of energy storage; mechanical, electrochemical, chemical, electromagnet and thermal type. Pumped hydro storage (PHS), compressed air energy storage (CAES) and flywheel energy storage (FES) is considered as mechanical type of energy storage. Lead acid, Nickel-Cadmium (NiCd), Lithium-ion (Li-ion), Sodium sulfur (NaS), Vanadium Redox battery (VRB) and Zinc Bromide (ZnBr) is an electrochemical type of storage. Fuel cell is categorized as chemical type of storage, while Supercapacitor is an electromagnetic type of energy storage. Superconducting magnetic energy storage (SEMS) is a thermal type of storage, where it consists of superconductive coil, power conditioning system, refrigerator and vacuum.

This energy storage is differentiated according to their capacity of storing the energy, efficiency and lifetime. There are types of storage that has a very promising cycle of life, hence it is too expensive to be partnered with a quite

expensive PV array, this might increase the whole cost and lower the return of investment (ROI) period.

2.5 Energy Management in Microgrid Environment

For a better power delivery, the most crucial part is on the energy management side. Theoretically, it might look simple, yet it is tough. In microgrid connection, other than findings a new alternative optimization criteria and exploration of the fluctuations effect, energy management options is important to be modeled so that a reliable energy with better efficiency can be delivered without any failure to customer [38]. A deterministic energy management algorithm for a PV based active generator in Microgrid environment need to be set up for proper supervision.

Based on Figure 2.1, the PV based active generator will be coupled via a DC bus and will be connected to the microgrid through a three phase inverter. This will be connected and controlled by a microgrid controller through a droop controller for primary frequency control. A basic requirement for satisfactory operation of power system is the PV based active generator needs to maintain the nominal frequency of the grid (50Hz or 60Hz). The rules of thumb for frequency control are it depends on active power (P), while voltage is based on reactive power (Q). Thus, for better energy management for PV based active generator, a proper droop controller that will manage the voltage and frequency variation is a must. In [20, 25] and [18] has been discussing on the droop controller for PV based active generator in microgrid.

For PV based active generator, it will not engage any inertia of the mechanical system since there will be no kinetic energy involve during generating electricity from PV array. Then we can expect there will be no abrupt changes on the frequency. However, load changes might lead to significant frequency changes that might affect the whole system. It is vital to manage this kind of problems to make sure that PV based active generator in the microgrid can operate efficiently. In [20], the writer discuss on the managing the microgrid management which can be classified into two timing scale;

Table 2.2 Timing classification for energy management system in microgrid

Long Term	Short Term
✓ Electricity market ✓ Load forecasting ✓ Renewable energy production ✓ Load management ✓ Energy storage availability	✓ Voltage control ✓ Frequency control ✓ Dynamic storage availability ✓ Power capability

These are the things that need to be monitored and analyzed. For a grid connected PV based active generator, the network operators need reliable and robust PV energy output forecasting system in operational planning. PV array output depends not only on the incident solar radiation but also on the operating cell temperature as well as shading effect and its operating points. Therefore a proper forecasting methodology is required for predicting the PV array output. It is important to identify the pattern of the historical data set for predicting the output [39]. There are a lot of work has been done in this matter. Most of researchers are using artificial neural network (ANN) trained by identifying the pattern of the historical data set with genetic algorithm (GA) for predicting the PV array energy output. This can be very helpful to generate enough power for PV based active generator.

2.6 Discussion

Based on the timing classification that has been mention in Figure 2.3, power quality of the generation needs to be monitored closely and it is also important in power system analysis. The widespread uses of distributed generators are creating many power quality issues. It may lead to the multiple harmonics, voltage fluctuations, unstable operation in the power system network [40]. It will also create major issues for designing of fault protection system. The total harmonic distortion in the micro-grid environment by using PV based active generator will be studied. Also the analyses of frequency deviations will be considered for sharing the load between the distributed generators in the micro-grid environment by considering frequency – droop characteristics. It will be useful in developing some strategies in the EMS for load sharing among active generators in micro-grid.

Last but not least is the capability of the microgrid system that supplied by the PV based active generator to withstand with fault. There will be few major issues regarding the protection in the micro-grid network with higher

penetration of distributed generators. Fault currents in an islanded mode based micro-grid are not going to be similar as fault occurs in a conventional grid system. Therefore it is impossible to use the same methods for isolating the faults of the conventional grid system in the micro-grid system [10]. In micro-grid network, there are limitations on protection system due to the islanding operation mode. Also the fault clearing time is important for micro-grid stability and operation. It is needed to include control signals of the protection mechanism in the EMS [6]. Fault analysis of the PV based active generators in the micro-grid network need to be analyzed in both islanded as well as grid connected modes since there are no standards or rules on this matter up to now.

2.7 Conclusion

The utilization of PV as a source of electricity is something that needs to be emphasizing now. The dependencies on the conventional way of generating energy via 'unclean' source and method needs to be minimize. PV based active generator can be a new way of generating energy in the future. It will be clean and very promising. Since this type of generator needs a good energy storage system, battery system with Supercapacitor will be a great combination. Battery storage with the appearance of Supercapacitor will increase the system efficiency as the battery will be able to store and release energy gradually, while Supercapacitor effectively acts as storage device with very high power density.

For a better management in the micro-grid level, a new method of managing the energy needs to be implemented. The crucial part is to maintain the frequency and for this, a droop controller that will be connected with the micro-grid and the PV based active generator needs to be develop. On the energy management side, the PV forecasting, power quality concern and fault issues needs to be foresee. Forecasting the PV energy needs to be done to make sure there will be no shortage of power during operation, and if there is a power shortage, there should be a plan to overcome this problem (buying power from the conventional grid).

In order to provide reliable energy, the grid operator should monitor the grid power quality (harmonics, voltage variations). This is to avoid any deficiency to the consumer and this may lead to fault. Since in micro-grid environment there are probability on the islanding effect and this might as well affected the PV based active generator, avoiding fault is something that the operator needs to consider. Since the PV based generator has a promising future, there should be more research on the energy storage side and on the PV cells.

The impact of higher efficiency on PV cells and minimizing cost for a battery will have a significant impact to this new type of clean generator.

Chapter 3

3 Photovoltaic Based Active Generator: Aggregated Power Control System Using Stateflow Analysis[2]

This chapter focuses on architecture of energy management system for integration of PV based active generator with local load and grid. It considers two basic questions:

(i) How to manage power distribution among PV array, super-capacitor and battery?

(ii) How to reduce stress on the power distribution system during peak hours i.e. demand side management?

The control system for power management in the PV based active generator is using the Stateflow® model. Basically this method is often used to model a logic controller for dynamic outputs. Using this method, an algorithm of power management that includes PV array, battery storage system with super-capacitors and converters for their integration is presented. The Stateflow® is the event-based modeling toolbox in MATLAB and it is used to model logic for dynamically control of the energy management system. The algorithm is able

[2] *Modified from the paper published and presented in a peer reviewed conference. 11th IEEE International Conference on Power Electronics and Drive Systems (PEDS2015) Sydney, Australia. DOI: 10.1109/PEDS.2015.7203433, Pp 93-97, 2015. And in International Workshop on Integration of Solar Power into Power Systems, London, UK. ISBN 978-3-9813870-8-7. Pp 302-308, 2014.*

to control the energy usage in a PV based active generator in order to maximize the utilization of the battery storage and super-capacitors for managing the load locally and also in demand side management. But in this work Stateflow® model is used for energy management in PV based active generator.

3.1 Introduction

The basic structure for PV based active generator is given in Figure 2.1 and system components have been characterized in Stateflow® modeling. This power generation units comprises of PV arrays, batteries and super-capacitor units as storage system, DC-DC boost and buck-boost converters and an inverter. The PV array and storage system are integrated on a common DC bus through proper DC-DC converters. The energy storage system can also be used as a power fluctuate compensator for improving power quality under dynamic conditions. A coordinated use of storage units with PV array must be properly designed in order to work it as an active generator. This active generator unit is connected to the grid through a DC-AC inverter in parallel to the local load. It will also help in demand side management and energy buying / selling to the grid. In this work, these multi-source units are modelled in the MATLAB® / Simulink environment.

This simulates architecture for a grid connected PV based active generator that controls the active and reactive load demand while maintaining the frequency and the voltage stability within the system. The system architecture is designed in such a way that the load demand is achieved using the maximum available PV generated power. The grid and the energy storage including the battery and supercapacitor provide power to the loads when the maximum available PV generated power is not sufficient to meet the load demand. The total reactive power demand is achieved using the energy storage. This is has been considered in mathematical analysis and simulation. In order to analyze the system, these scopes are considered:

- Modeling the PV generation system is for maximum power operation PV generation system is required to provide the available maximum power to the loads with unity power factor. The PV integration system does not involve in controlling the active and reactive power.
- Modelling the energy storage integration for compensation of intermittent nature of PV generation.
- Integration of PV based AG into the grid. Power demand of the AC loads is partially achieved using the PV generated power and the energy

storage. The remaining power demand of the load should be taken from the grid according to a demand limit imposed by the utility.

3.2 Tier Control System

Tier control is selected for this system as it contains multi-power sources – PV, batteries, supercapacitor, and grid. In order to meet the load demand, proper power sharing among these sources is the ultimate task to be achieved. The four levels of the tier control approach are listed as:

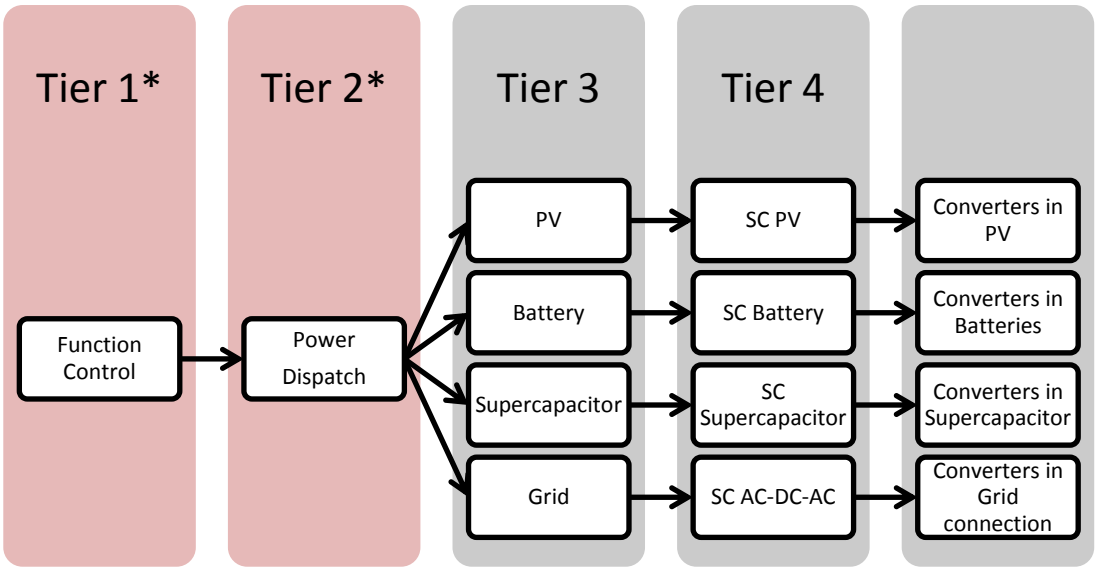

The first 2 tiers (Tier 1* and Tier 2*) identified as the main driven systems since each layer contains several mutually exclusive modes or states. The transitions among these states take place according to some logics associated with the system parameters. The other levels are selection levels based on logics that have been identified initially. Details function on each level can be defines in Table 3.1:

Table 3.1 Functions on each level in the Tier control system

Tier 1	Decides working mode for the PV based active generator by taking the limits imposed by the utility, power ratings of each storage units, current load demand and the available PV generated power into account.
Tier 2	Checks the state of each power source and enables the suitable power sources for dispatching the power according to the load demand while providing the required reference values of the active power, reactive power, frequency and the grid voltage to the next level.
Tier 3	Calculates the required direct and quadrature axis current references ($i_{d;ref}$; $i_{q;ref}$) for the next level
Tier 4	PWM signal is generated in the VSI control system to switch the converters

3.2.1 Tier 1: Function control

This stage decides the working mode for whole active generator system. The demand side management is taken into consideration to keep the power flow from the grid to the active generator in a controllable manner. This approach helps to control the peak demand which in consequence leads to maintain the stability within the grid without affecting the power fluctuations in the active generator side. In-order to accomplish an optimal load management and control with demand side management from the available power sources in the AG, limits imposed by the utility is employed in an event driven fashion to reduce the grid stresses. Figure 3.1 explains in a flow chart diagram, the function diagram flow for PV based active generator.

We do consider 3 different function controls for this tier. It is explained details in Table 3.2.

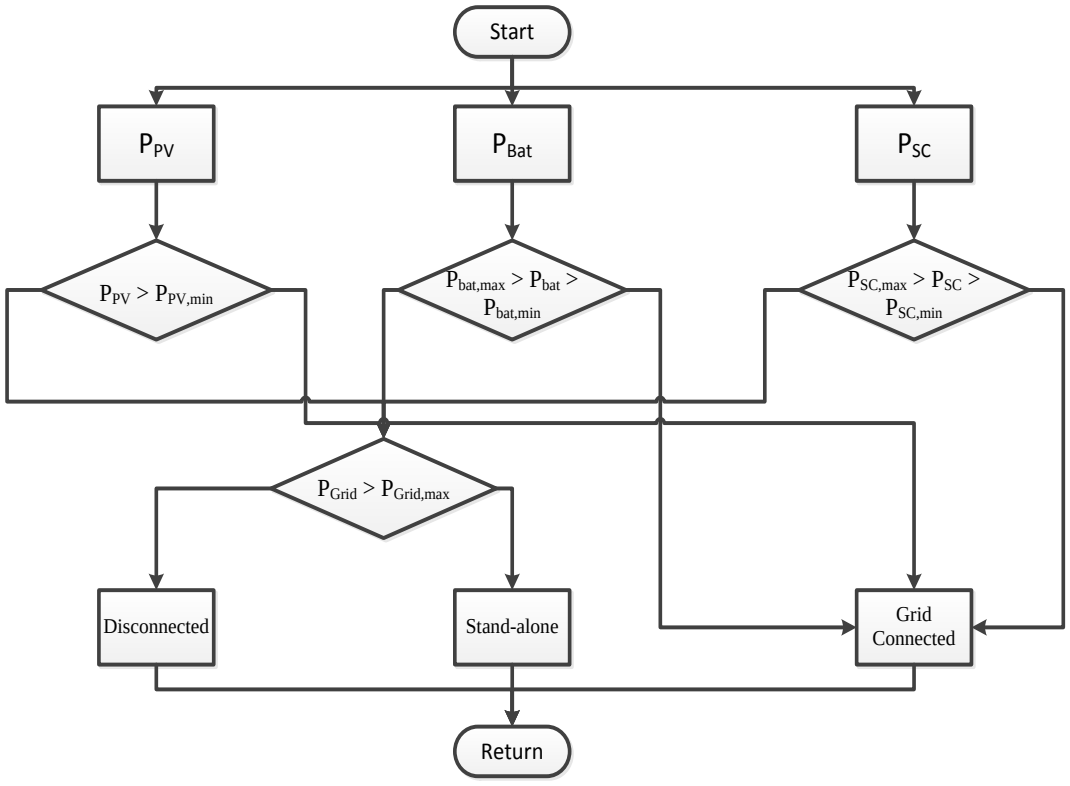

Figure 3.1 Flow chart of function control of PV based active generator

Table 3.2 Different function controls for PV based active generator

Disconnected	Stand-alone	Grid connected
•Power source cannot be accessed due to their power shares are out of the allowable working range. •To maintain the stable operation, all the sources is disconnected from the active generator system which in consequence leads to disconnect the load from the supply.	•If the power taken from the grid exceeds the prescribed limit especially at transients or high power surges, the grid should be disconnected to maintain the stable operation within the grid. •If the power shares of each storage unit and the PV array are within the corresponding minimum and maximum power limits, standalone mode is activated. •In this mode all power sources are available and accessible except the grid.	•Grid is connected to active generator as the power flow from the grid is below the grid constraints. •No peak power demand to the grid. Apart from demand limit imposed by the utility, the power ratings of each storage units are taken into •All the multi-power sources are accessible for power dispatching to meet the load demand

To execute this, transition logics is developed based on conditions that has been set initially. This logic is part of the stateflow analysis. The implementation of this tier is based on:

Table 3.3 State transition logics for tier 1: Function control

State Transition	Logics
T_1	$[(P_{grid}>P_{grid,max})\&\&(P_{bat}>P_{bat,min})\&\&(P_{bat}<P_{bat,max})\&\&(P_{sc,max}>P_{sc})\&\&(P_{sc}>P_{sc,min})\&\&(P_{pv}>P_{pv,min})]$
T_2	$[(P_{grid}<P_{grid,max})\&\&(P_{bat}>P_{bat,min})\&\&(P_{bat}<P_{bat,max})\&\&(P_{sc,max}>P_{sc})\&\&(P_{sc}>P_{sc,min})\&\&(P_{pv}>P_{pv,min})]$
T_3	$[\{(P_{bat}<P_{bat,min})\|\|(P_{bat}>P_{bat,max})\}\&\&\{(P_{sc,max}<P_{sc})\|\|(P_{sc}<P_{sc,min})\}\&\&(P_{pv}<P_{pv,min}]$
T_4	$[\{(P_{bat}<P_{bat,min})\|\|(P_{bat}>P_{bat,max})\}\&\&\{(P_{sc,max}<P_{sc})\|\|(P_{sc}<P_{sc,min})\}\&\&(P_{pv}<P_{pv,min}]$

Where:

P_{bat} : the current power delivery of the battery.
$P_{bat,\ min}$ and $P_{bat,\ max}$: minimum and the maximum power level of the battery
P_{sc} : the current power delivery of the SC
$P_{sc,\ min}$ and $P_{sc,\ max}$: minimum and the maximum power level of the SC

P_{pv} : current power generation of the PV array
$P_{pv, min}$: minimum power generation of the PV array
P_{grid} : current power delivery from the grid
$P_{grid, max}$: maximum power delivery of the grid

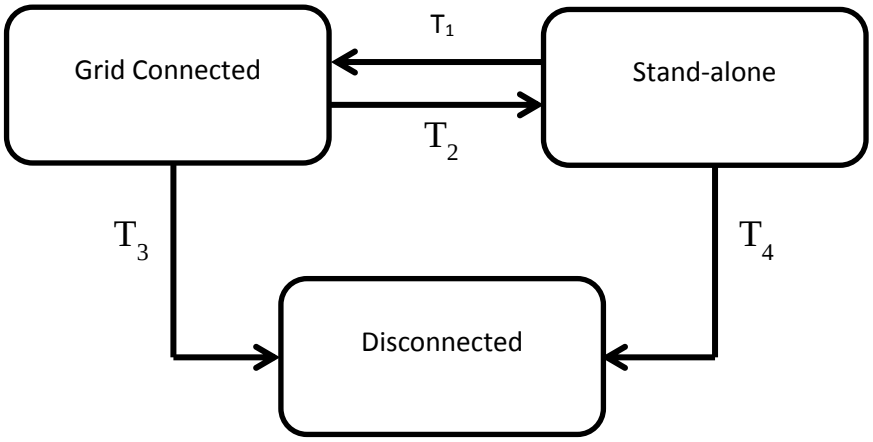

Figure 3.2 State transitional diagram

3.2.2 Tier 2: Power dispatch

This is where selected power sources will dispatch power to the system. This will base on Tier 1, hence considering state of charge (SOC) of the storage system, power generated by the PV and source from the grid. As to do this correctly, to make sure that the system is safe and the load will be supplied, power dispatching from PV array, energy storage system and power from the grid needs to be controlled. This is done by using stateflow analysis. This subsection will discuss further on controlling source from three different sources:

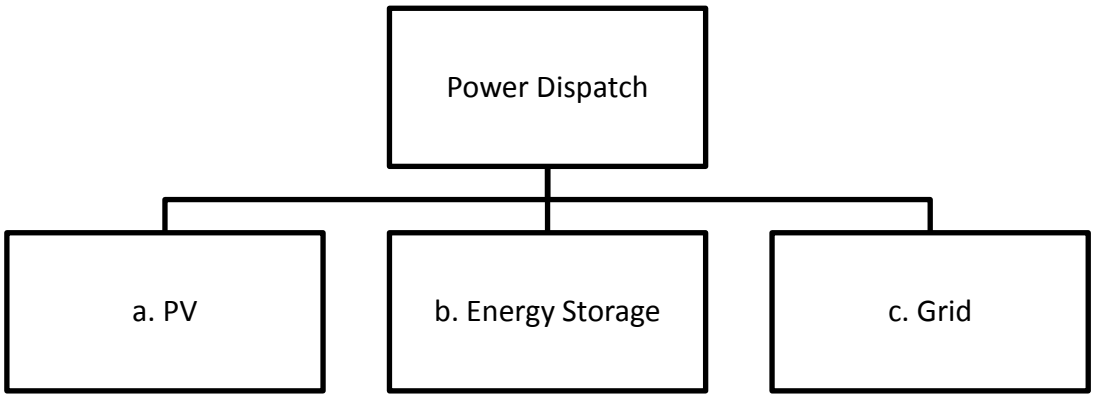

a. PV

Power flow for PV output should be in unidirectional to avoid any unnecessary effect towards the power electronic devices and this is not the purpose of PV based active generator systems. Once PV generation becoming low, it should be disconnected from the systems to avoid reverse power flow. Then, introduction of two different modes for PV array, which are:

(i) Maximum power point tracking (MPPT) state :
PV panel is available and accessible for load sharing

(ii) Disconnected state:
PV array is disconnected from the AC bus

The selection of either of these modes can be represented in the following flowchart:

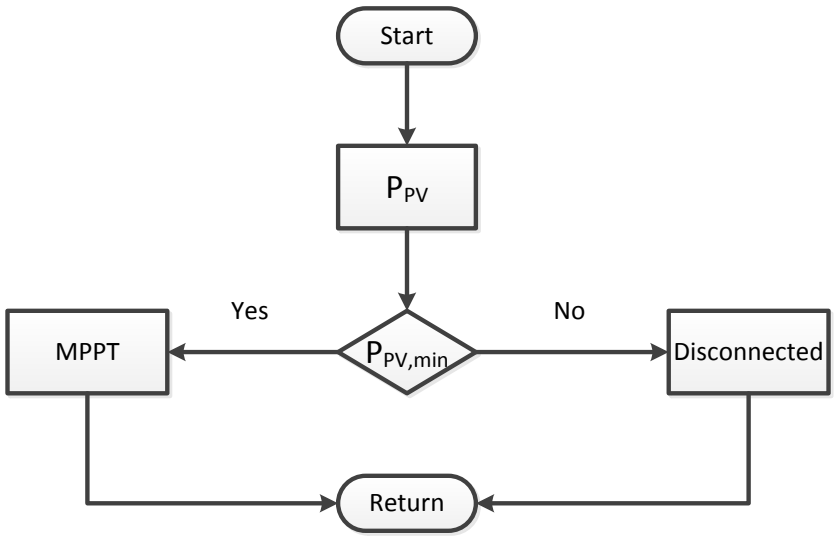

Figure 3.3 Flowchart for power dispatch in PV array

This process is then interpreted into stateflow command with the state transition logics. This logic is between transferring the command either on MPPT or disconnected state:

Table 3.4 State transition logics for PV array

State Transition	Logics
T_1	$[P_{PV} > P_{PV,min}]$
T_2	$[P_{PV} < P_{PV,min}]$

Where:

P_{PV} : current power generation of the PV array
$P_{PV, min}$: minimum power generation of the PV array

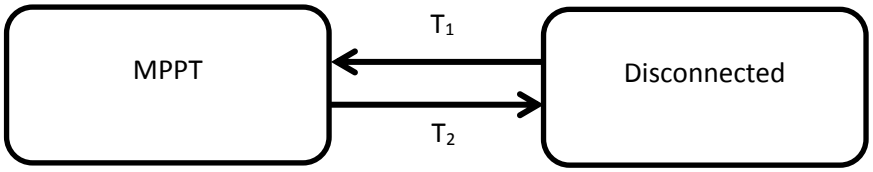

Figure 3.4 State transitional diagram for PV array

b. Energy Storage

PV based active generator's active power (P) and reactive power (Q) is controlled by the energy storage system. This comprise of battery and super capacitors. Three different states need to be considered; Dispatch state, maximum state and minimum state.

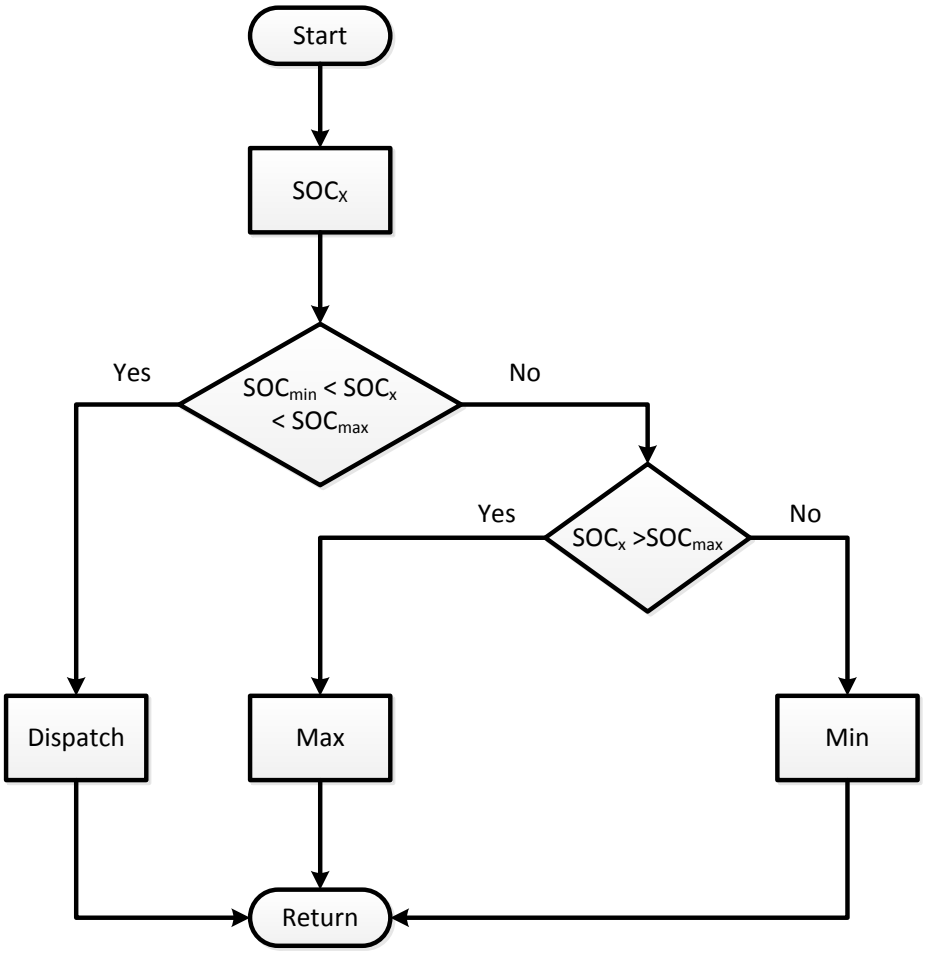

Figure 3.5 Flow chart for power dispatch control for energy storage

It begins with the state of charge for either battery or super capacitor (SOC_x) within the limit - $SOC_{min} < SOC_x < SOC_{max}$ it will directly go to the dispatch mode. The storage system will provide power to the load until the SOC is lower or equal to minimum percent ($SOC_x =< SOC_{min}$). Once the SOC is out of allowable range, it will be on the maximum or minimum state. When it is come to a specific state, it gives the required set values for active and reactive power dispatching and the reference values for the frequency and voltage control in PFC stage. At the Max state, it tends only discharging and at the Min state for charging.

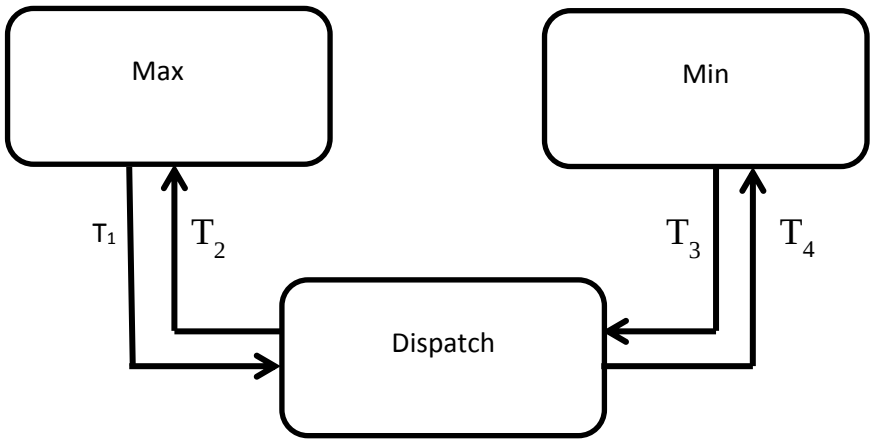

Figure 3.6 State transitional diagram for storage system

Table 3.5 State transition logics for PV array

State Transition	Logics
T_1	[SOC_x < SOCmax]
T_2	[SOC_x > SOCmax]
T_3	[SOC_x > SOCmin]
T_4	[SOC_x < SOCmin]

Where;

SOC_x : current state of charge of the source x
SOC_{max}, SOC_{min} : Maximum and minimum state of charge of the source x

c. Grid

In PV based active generator system, AC-DC-AC link is used to get the power from the grid according to the demand side. When the power deliveries from the PV array and the energy storage are not sufficient to meet the load demand, grid supplies the power to the AC load which is connected with the AC bus. It will be in a controlled way through the AC-DC-AC link. Therefore AC-DC-AC link decides the operating state of the AC-DC-AC link based on the time. In this work, two different demand limits are considered for power dispatching from the grid. The flow chart of the AC/DC/AC link is shown.

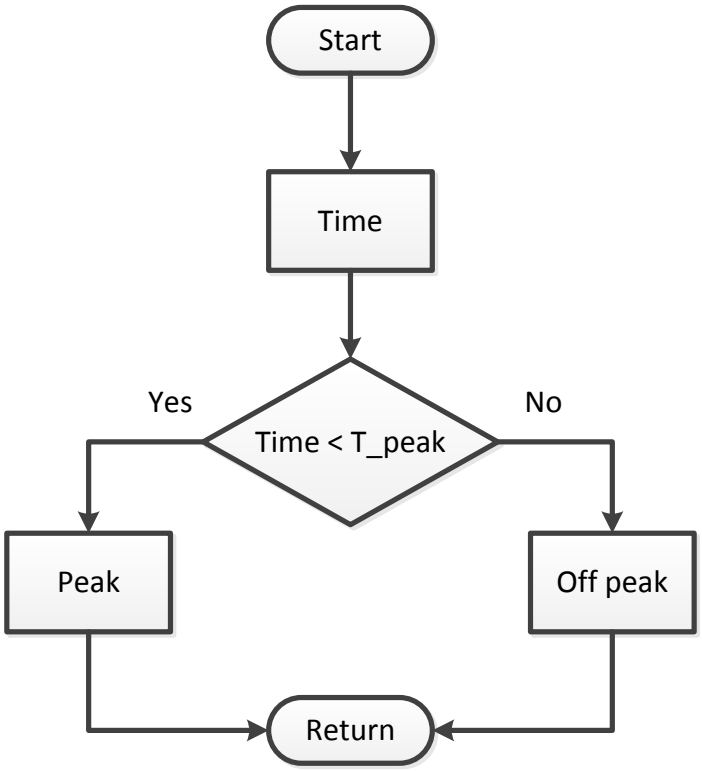

Figure 3.7 Flow chart for power dispatch control for grid connection

3.2.3 Tier 3: Power flow control

Active and reactive power in PV based active generator should be managed properly from three different sources (PV, energy storage and grid system). PV will inject active power (P) to the AC bus, while energy storage will controls P and reactive power (Q) into the AC loads. Thus controlling P and Q maintaining voltage stability and frequency control is necessary at this level.

P and Q are controlled by using voltage source inverter (VSI) controllers at both storage units (battery and supercapacitor). Then the main function of this hierarchical stage is calculating the required reference values for the pulse width

modulation (PWM) switching control of VSIs in the centralized energy storage based on the control parameters received from the tier 3 (power control) levels.

PQ theory also known as Park[3] transformation is used to extract fundamental component of the grid voltage. In this work P and Q of VSI is expressed as;

$$P = v_d i_d + v_q i_q \quad (3.1)$$
$$Q = v_d i_d - v_q i_q \quad (3.2)$$

Where;

$v_d = V_\Phi$

$v_q = 0$

V_Φ is voltage phase (magnitude) in symmetrical 3 phase circuit. Therefore it can be seen that P and Q of a VSI can be controlled independently using (i_d, i_q) components. The required reference values for the Park current components ($i_{d,ref}$, $i_{q,ref}$) are calculated using the active and reactive power controllers.

Park transformation is used to transform stationary voltage or current reference frame (V_α,V_β or I_α,I_β) to a rotating voltage or current reference frame (V_d,V_q or I_d,I_q). In a mathematical form it can be define as:

$$\begin{bmatrix} v_d \\ v_q \end{bmatrix} = \begin{bmatrix} \cos\theta & \sin\theta \\ -\sin\theta & \cos\theta \end{bmatrix} . \begin{bmatrix} v_\alpha \\ v_\beta \end{bmatrix} \quad (3.3)$$

The frequency of a system is dependent on the P. Small changes in P will affect the frequency of a simple system. While for Q, it will affect the voltage drop in a system if it is too much reactive power flowing around in the network. This might lead to excess heating and will end with a catastrophic event to a single transmission. Both of these unstable events are corrected with the implementation of VSI.

[3] Park's transformation is also known as direct-quadrature-zero transformation (dq0).

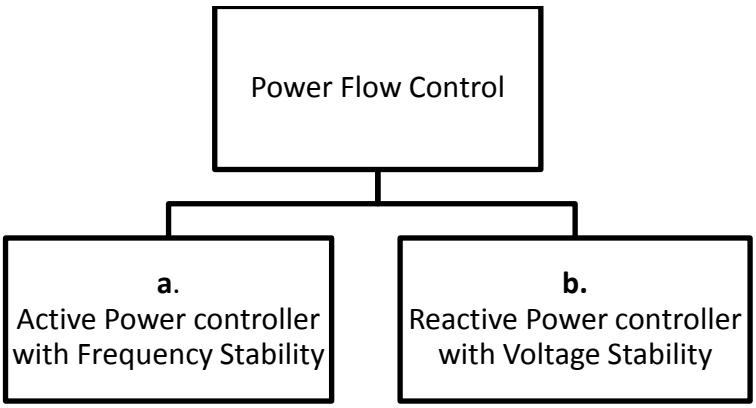

a. Active power controller with frequency stability

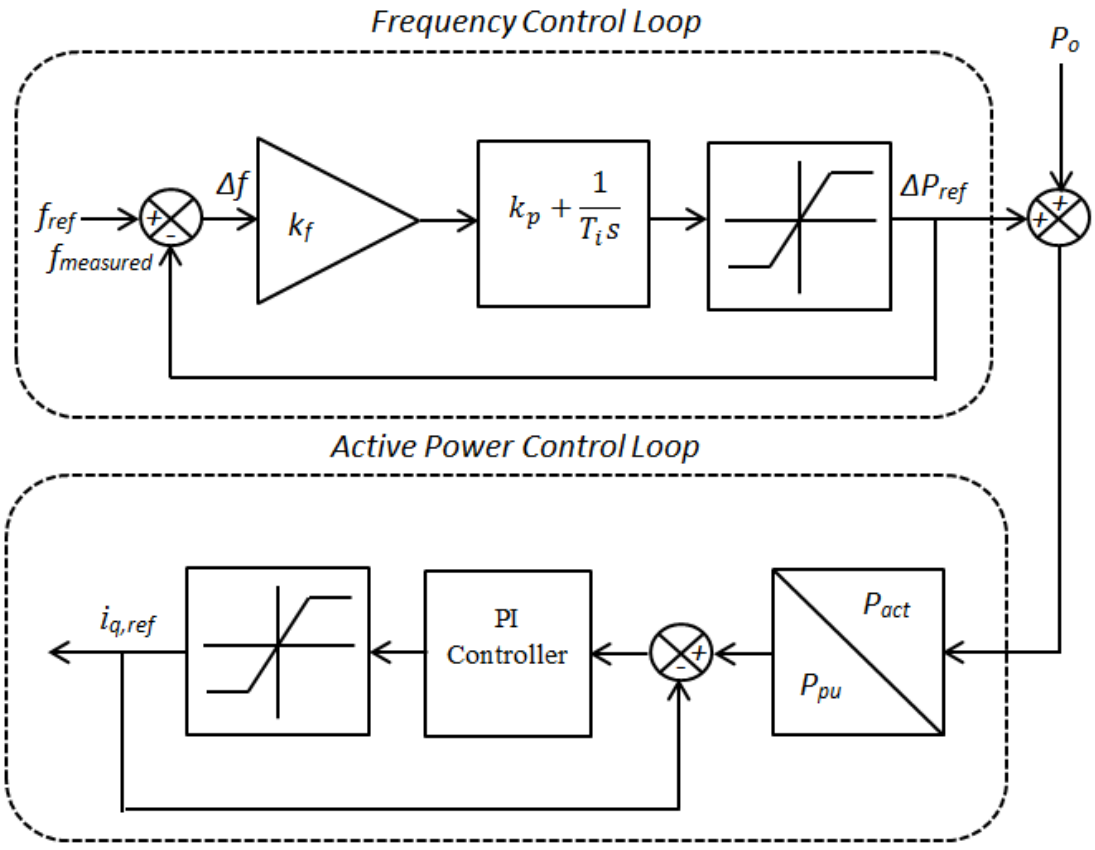

Figure 3.8 Active power controller block diagram

VSI will provide a stable active power while maintaining the frequency stability. Frequency droop characteristics need to be implemented with the active power controller. Droop controller can be defines as;

$$k_f = \frac{Changes\ in\ frequency}{Changes\ in\ active\ power} \tag{3.4}$$

$$f = f_o + k_f(P - P_o) \quad (3.5)$$

Where;

P, P_o	: Active power delivery at set point
f, f_o	: Grid frequency and nominal frequency
k_f	: frequency droop value

The required changes in active power to maintain the frequency is given as:

$$\Delta P_{ref} = P_o + k_f \Delta f \quad (3.6)$$

With the dynamic frequency changes of the system, the frequency steady state error will not be zero ($\Delta f|_{steady\ state} \neq 0$) since the frequency droop control is proportional.

From Figure 3.8, the equation can be represents as:

$$\Delta P_{ref}(S) = P_o + k_f \Delta f_{(s)} + \Delta f_{(s)}(k_p + \frac{1}{T_i s}) \quad (3.7)$$

This equation explains how equation (3.5) is altered with additional of proportional-integral (PI) controller in the droop controller.

b. Reactive power controller with voltage stability

To control the voltage stability while delivering reactive power to the system through VSI. Theoretically, in a synchronous generator when the reactive power delivered is increased, reduction of voltage terminal can be seen. However with voltage droop controller, the excitation control will adjust so that the terminal voltage magnitudes remain the same as nominal grid voltage. This relationship can be seen as an:

$$k_v = \frac{Changes\ in\ voltage}{Changes\ in\ reactive\ power} \quad (3.8)$$

$$v = v_o + k_v(Q - Q_o) \quad (3.9)$$

Where;

Q, Q_o	: Reactive power delivery at set point
v, v_o	: Grid voltage and nominal voltage
k_v	: voltage droop value

By incorporating the droop controller and reactive power controller, stable reactive power and voltage can be delivered to the system. Figure 3.9 shows the

reactive power controller with voltage stability block diagram, where voltage control and reactive power is connected together.

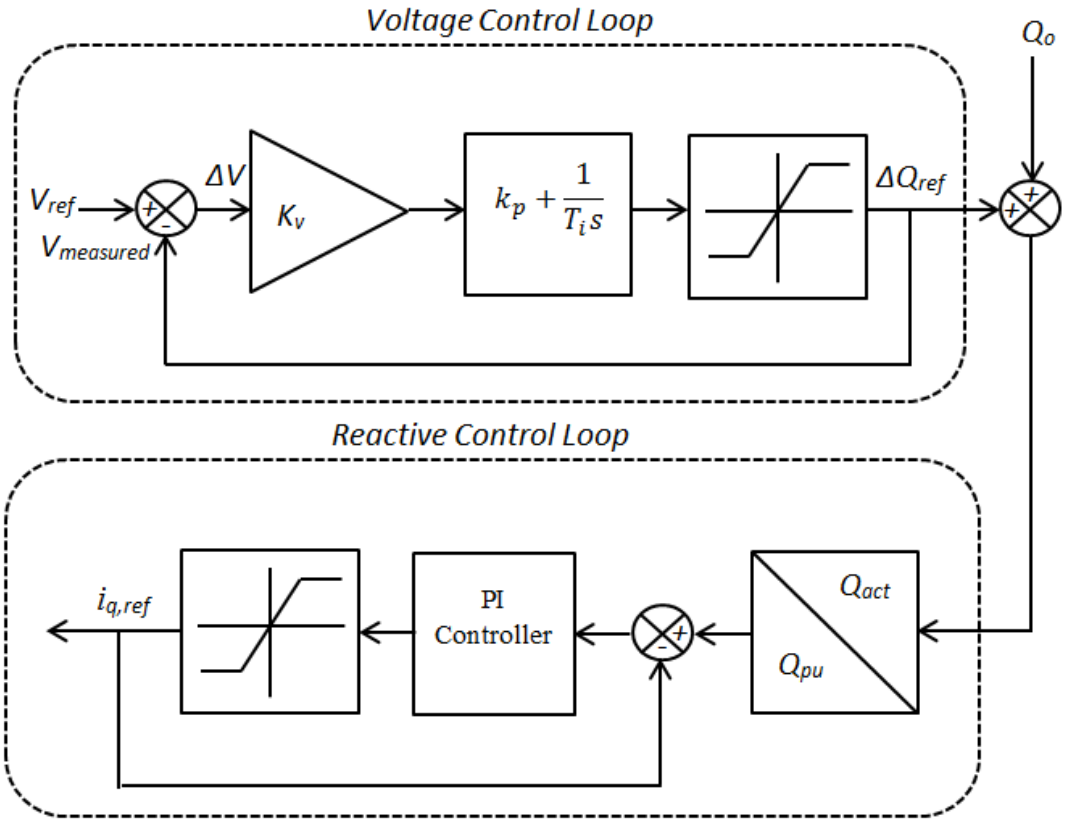

Figure 3.9 Reactive power controller block diagram

PI controller is used with voltage droop and it can be seen in Figure 3.9 and can be expressed as:

$$\Delta Q_{ref}(S) = Q_o + k_v \Delta V_{(s)} + \Delta V_{(s)}(k_p + \frac{1}{T_i s}) \qquad (3.10)$$

3.2.4 Tier 4: Switching control

Switching controls for PV, storage system and input from grid can be determine by looking into PWM switching controls of the 3ϕ VSIs from the 3 main sources. This level will generate correct PWM switching to trigger the VSIs to supply the P and Q to the system. In this sub section, PWM switching controls for a. PV, b. Energy storage and c. Grid.

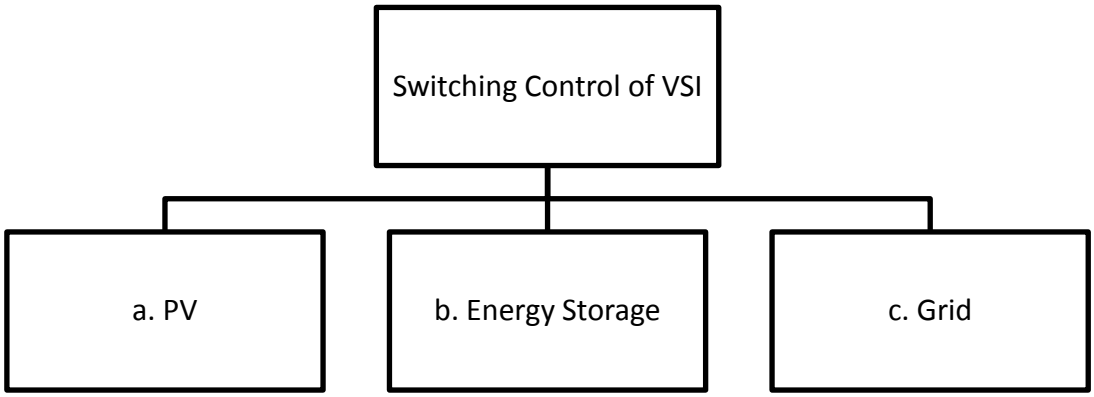

a. PV

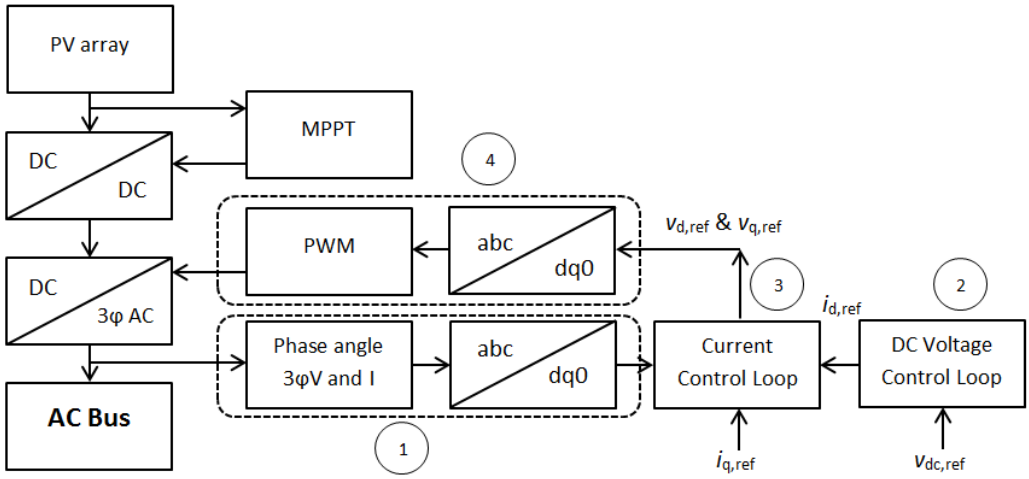

Figure 3.10 VSI control for PV system in PV based active generator

Main element has been numbered 1-4. These are the backbone of this particular system for PV array, to make sure P and Q can be delivered without compromise stability of frequency and voltage.

Table 3.6 Main parts of PV Switching control for PV based active generator

(1) Park's components and Phased locked loop (PLL)
- Measured line voltage and current waveforms at the point of common coupling (PCC) with the AC bus converted into Park components (v_d; v_q and i_d; i_q) in p.u values. - PLL is used in this subsystem for synchronization and it gives the phase angle (ωt) of the grid voltage.
(2) DC voltage control loop
- Provides reference value to Park's components - To generate required PWM signals for DC-AC 3ϕ VSI
(3) Current control loop
- To keep DC bus voltage at specific value to extract the maximum power
(4) PWM generation
- Generates required PWM signals

b. Energy storage

Three main subsystems needed in energy storage switching control. Compared to the system for PV switching control, voltage control loop is not needed, since $i_{d,ref}$ and $i_{q,ref}$ is taken from Power Control (Tier 3) output. The bidirectional power flow for the storage allows the storage to be charge using power from the grid.

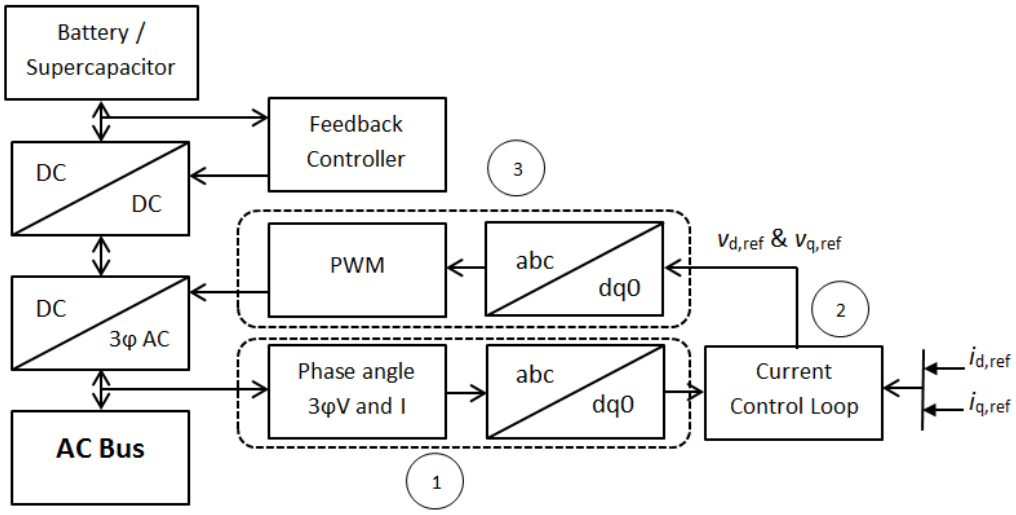

Figure 3.11 Block diagram of the switching control for the energy storage system

Based on Figure 3.11, the three main subsystems are illustrated and the same functions are expected as in PV switching control. The numbered block defined as:

(1) Park's components and Phased locked loop (PLL)
(2) Current control loop
(3) PWM generation

c. Grid

AC-DC-AC link is the connection between the electrical grid and active generator. This link will allowed the power dispatch according to the limits that been imposed by the utility provider.

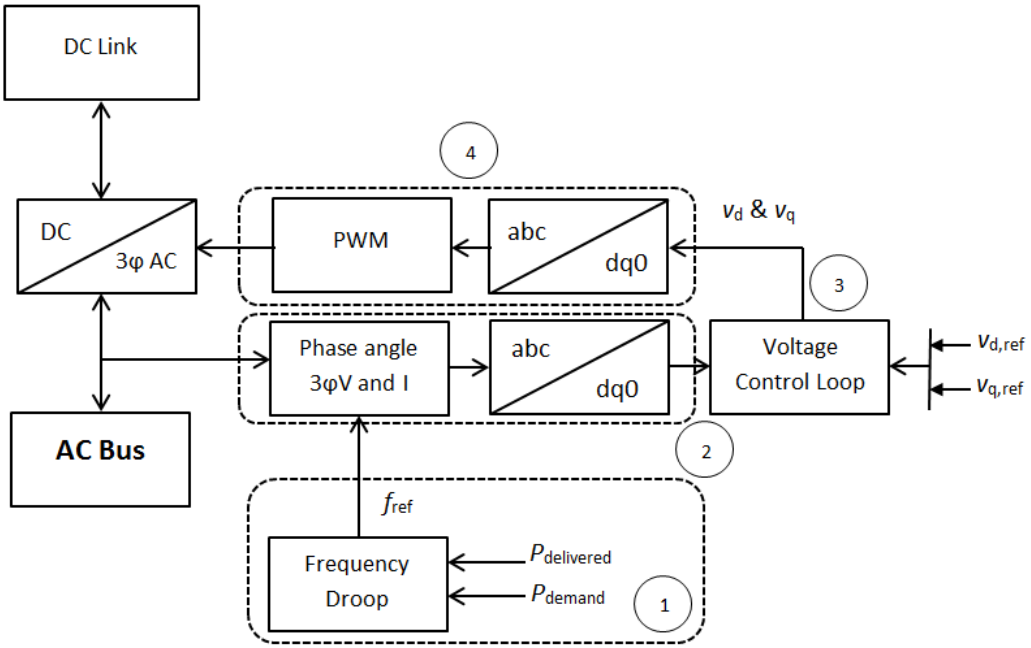

Figure 3.12 Block diagram of the switching control for the Grid (AC-DC-AC Link)

At DC link in PV generation side, PWM switching control is used to maintain the constant voltage. This can be seen at no. 4, where generated signal from parks component based on v_d and v_q will trigger PWM signal and to the DC-AC block. Based on the demand limit, DC-AC converter generates the required AC voltage signal for the AC bus of the PV based AG using frequency droop characteristics. All four blocks are defined as:

(1) Frequency control
(2) Park's components and Phased locked loop (PLL)
(3) Voltage control loop
(4) PWM generation

Except of frequency control, the rest has been explained in PV switching control. Equation 3.4 is used to decide the system frequency in frequency control block.

3.3 Test System and Base Scenario

In previous section, the architecture and the load management control of the PV based active generator has been discussed. In this section, the simulation is executed based on individual power response (P and Q) and based on the load demand and the capability of maintaining the voltage stability, frequency constancy and power quality within both the PV based active generator and conventional electrical grid is discussed. For this test system, the dynamically fluctuate real power (P), reactive power (Q) and the global tilted irradiance

(GTI) used are as below. This test is based on an aggregated load from 30 houses in the same area. Skarpnes smart house project initially proposed of 17 single-detached houses and 20 flats, and we do expect by using an estimation of 30 houses may give a good result for the system to operate.

The active power of the variable load is varied from 0 to 300kW as in Figure 3.13. The reactive power of the fixed load is set at 50 kVar, and the reactive power of the variable load is varied from 0 to 60 kVar. This can be seen in Figure 3.14. In PV based active generator, PV array is considered as the main source of power and it is operated at the maximum power point (MPP). In the simulation model, 200 kWp of PV array is considered. The PV array and the maximum power point tracker (MPPT) together are modeled as a variable current source. The PV current at the MPP is calculated using the GTI shown in Figure 3.15. These test parameters (P, Q and GTI) is based on 12 seconds of time.

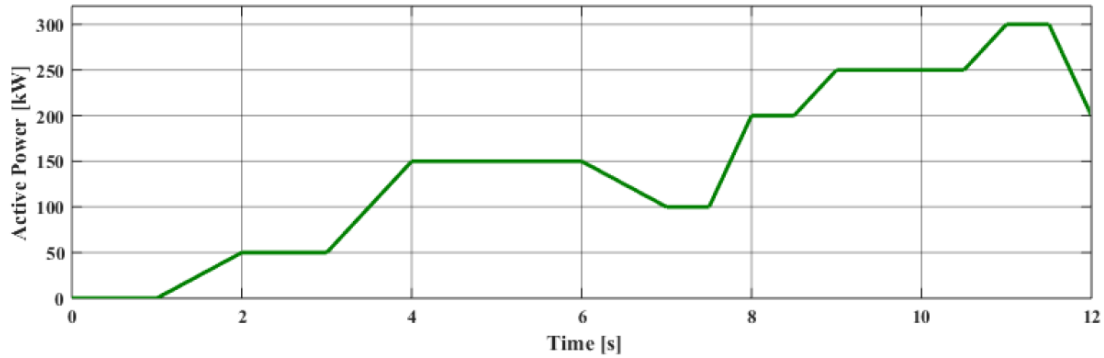

Figure 3.13 Active power (P) for variable load required for system test

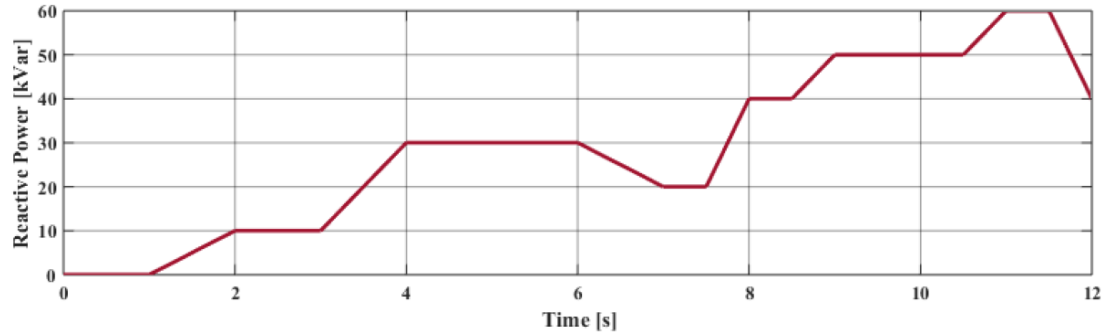

Figure 3.14 Reactive power (Q) for variable load required for system test

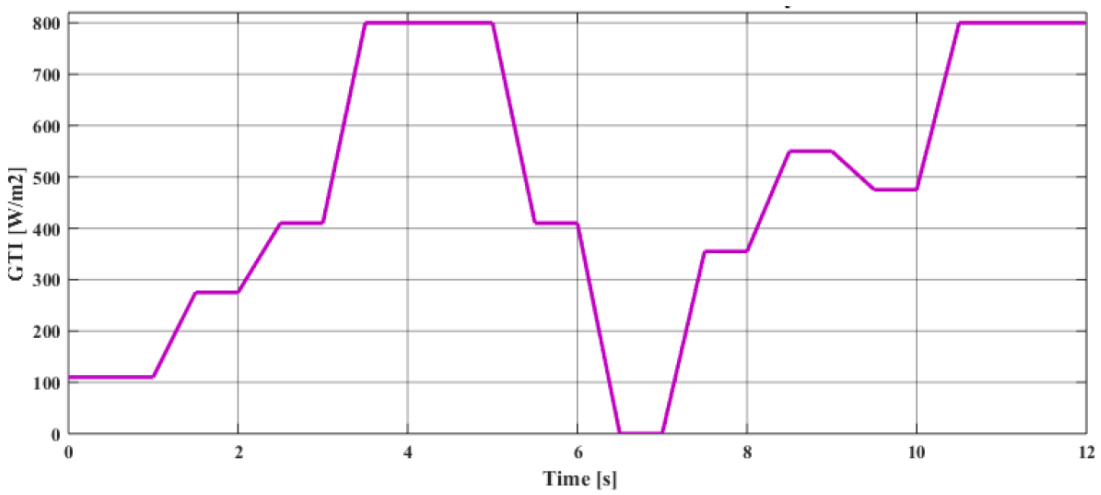

Figure 3.15 Global tilted irradiance (GTI) required for variable load for system test

3.3.1 Active and reactive power load demand

PV based active generator make sure that the P and Q is shared among the available source, with the priority is given to PV. This power transfer executed while maintaining the frequency and voltage.

3.3.1.1 Active Power Load Demand

For P it begins at the initial point (0 second) and the P demand is in blue, while the limitation that pre-set is in green. During the whole 12 second, the PV, grid, battery, supercapacitor supplying energy to the load accordingly with respect to the demand limit that has been imposed. Based on Figure 3.16, the processes are given in the following order:

(a) The system experiences a very short period of transients and becomes stable approximately after 0:35 second. During the transient period, grid power exceeds its maximum limit and the system switches to the Stand-alone mode as responses of the battery and the supercapacitor are within their allowable power range. After some time it switches back to the Grid connected mode as the centralized energy storage is continuing the power dispatching.

(b) PV array injects the maximum available power to the system. At PV generated power is around 30 kW, generated power is not sufficient to meet the load demand, however with a gradual increment of PV power and input from other sources, the load demand is supplied.

(c) In the first 5 second the system runs with an imposed limit of 200kW. Then, it is increased to 300 kW and the active power share from the grid is increased as well.

(d) During 6.50 second to the 7th second, the PV power becomes zero and it turns to the disconnected mode for preventing the reverse power entering to the PV array. In the meantime, the active power (P) share of both battery and the supercapacitor increase to meet the load demand. Supercapacitor takes the large portion of active power sharing compared to the battery due to its fast dynamic nature.

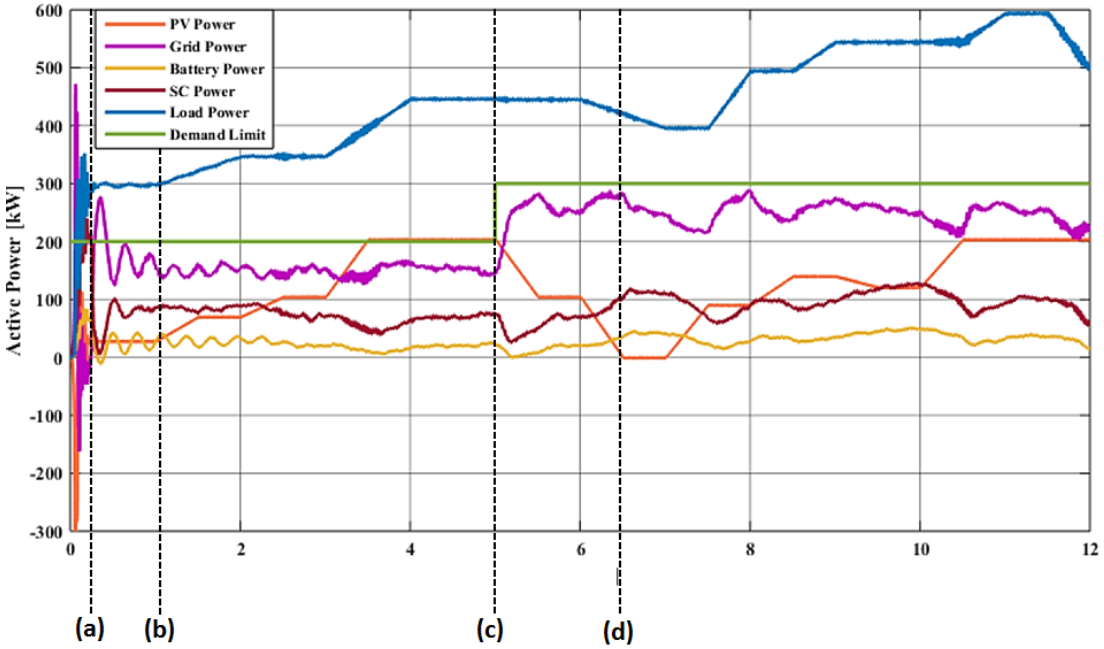

Figure 3.16 Active load demand sharing among the multi-sources in PV based active generator

3.3.1.2 Reactive Power Load Demand

PV source will only inject the P power to the system, hence the rest of the sources (battery, supercapacitor and DC link in the AC-DC-AC link) have to supply Q needed in load demand. Figure 3.17 shows the reactive load demand sharing among different sources:

(a) Between 0 second and approximately 0.35 second, the system is in a short transient before it become stable after that.

Large shares of is supplied by the DC link of the AC-DC-AC link followed by the supercapacitor and battery storage. The DC link is supplying power in an

uncontrollable manner. Oscillations seen in Figure 3.17 are a proof of this. Supercapacitor plays it role faster than the battery due to its fast dynamic response. The energy storage injects reactive power while maintaining the voltage stability within the system.

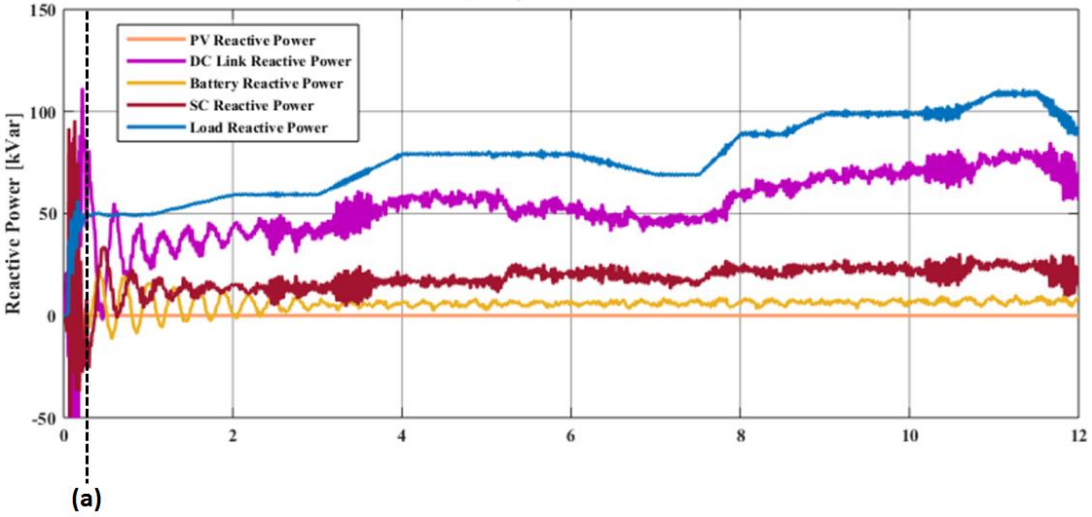

Figure 3.17 Reactive load demand sharing among the multi-sources in PV based Active Generator

3.3.2 Active and reactive power response for multi power sources

This section will discuss on the individual P and Q response, in order to study the voltage and frequency stability in the system. As for PV source, the only power response is P, while for supercapacitor, battery and grid will includes P and Q response.

3.3.2.1 Active power (P) response for PV

On the same axis, the irradiance and output power of PV is plotted. By using the Synchronous Reference Frame Converter (SRFC) in the VSI, it will only consider the injection of maximum available power to the AC bus of the active generator system [11]. It is noticed the output power do not have any significant different to the irradiance input. This can be seen in Figure 3.18

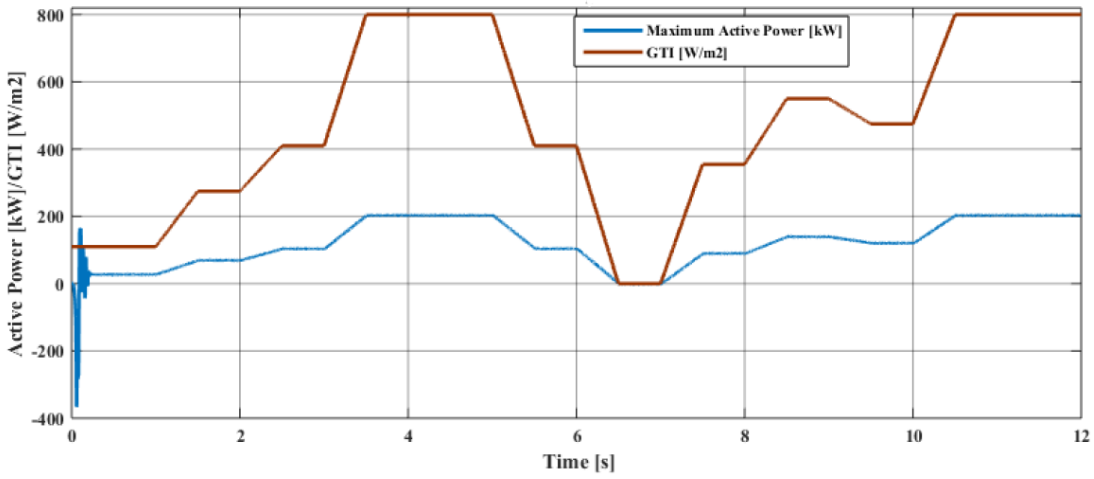

Figure 3.18 Active power response for PV in PV based active generator

3.3.2.2 Active power (P) and reactive power (Q) response for supercapacitor

Fast and dynamic fluctuations of supercapacitor in providing P and Q to the system makes it the most efficient source of providing needed power to the load. Supercapacitor plays the major role as can be seen in previous section in providing the P and Q. From Figure 3.19 and Figure 3.20, it can be seen that both P and Q injects the power accordingly to the system. It is due to controllable injection of the P and Q while maintaining voltage and frequency in the system.

From previous section, in Tier 3: Power flow control, the reference P and Q are determined here by considering the frequency and voltage stability. Then at Tier 4: Switching control, the SRFC generates required PWM signals to the VSI in the supercapacitor system through feedback and feed-forward control strategies (Figure 3.11).

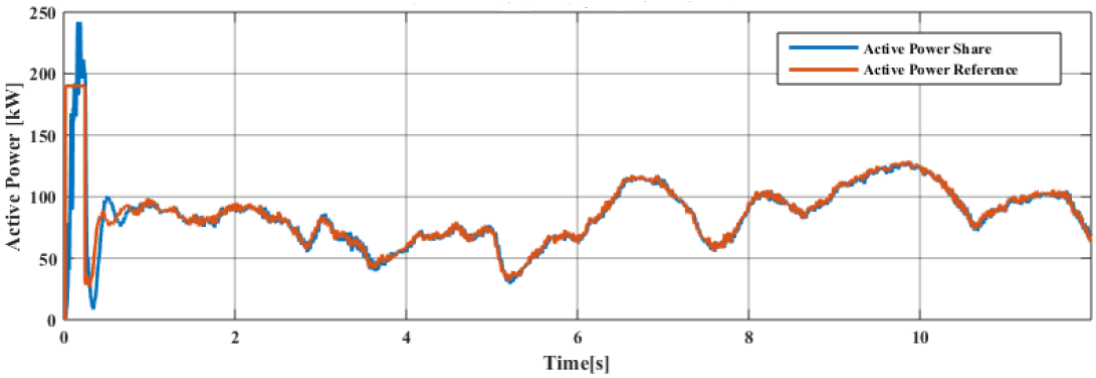

Figure 3.19 Active power (P) demand for supercapacitor in PV based active generator

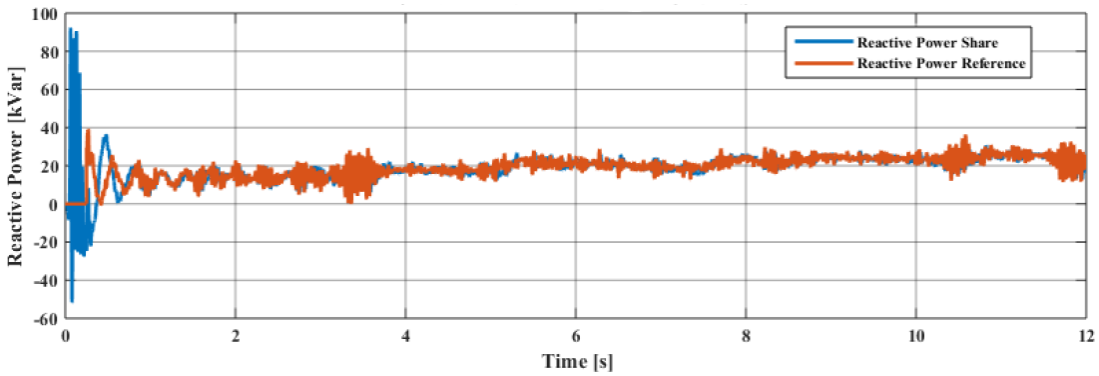

Figure 3.20 Reactive power (Q) demand for supercapacitor in PV based active generator

3.3.2.3 Active power (P) and reactive power (Q) response for battery

For long term storage, battery system is the most reliable source and it act as a power compensator in the PV based active generator system. Based on Figure 3.14, the same process as in supercapacitor will take place. Both Tier 3 and Tier 4 will be the main layers that will make sure that P and Q references are measure and calculated with reference to the voltage and frequency stability. SRFC will generates signal that requires PWM signal to VSI based on reference power.

Figure 3.21 and Figure 3.22 shows the P and Q reaction for battery system. It indicates that on earlier second there are transient happening on the system, before it is stable. The signals oscillates hence relatively are in order.

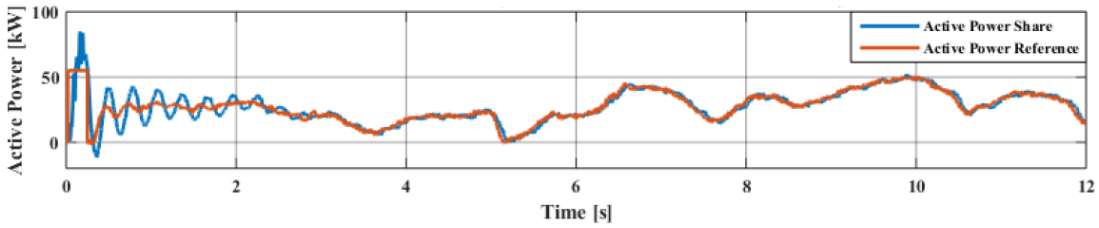

Figure 3.21 Active Power (P) response of the battery system in PV based active generator

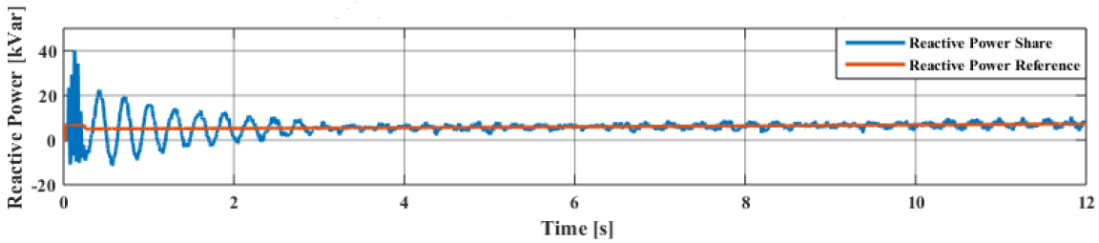

Figure 3.22 Reactive Power (Q) response of the battery system in PV based active generator

3.3.2.4 Active power (P) and reactive power (Q) response for grid

The conventional grid system and PV based active generator are isolated by the DC link and connected by AC-DC-AC link. Figure 3.23 and Figure 3.24 illustrates the active power (P) response on the grid and on the AC-DC-AC link, while Figure 3.25 and Figure 3.26 shows the reactive power (Q) response on both grid and the AC-DC-AC link. It can be seen that for both at the grid or at the link, the power is below the demand limits line (orange).

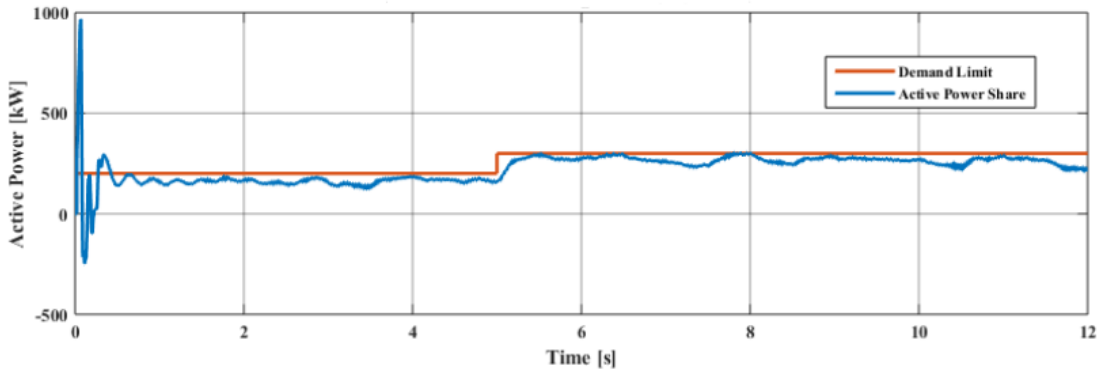

Figure 3.23 Active Power (P) response of the grid

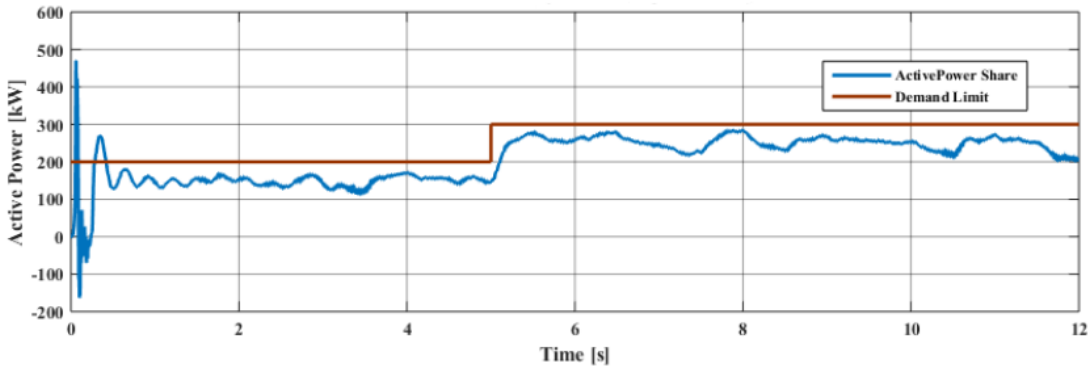

Figure 3.24 Active Power (P) response of the AC-DC-AC link

The grid system does not provide any reactive power (Q) to the PV based active generator scheme as can be seen in Figure 3.25. At the DC link supplies required reactive power (Q) as can be seen in Figure 3.26.

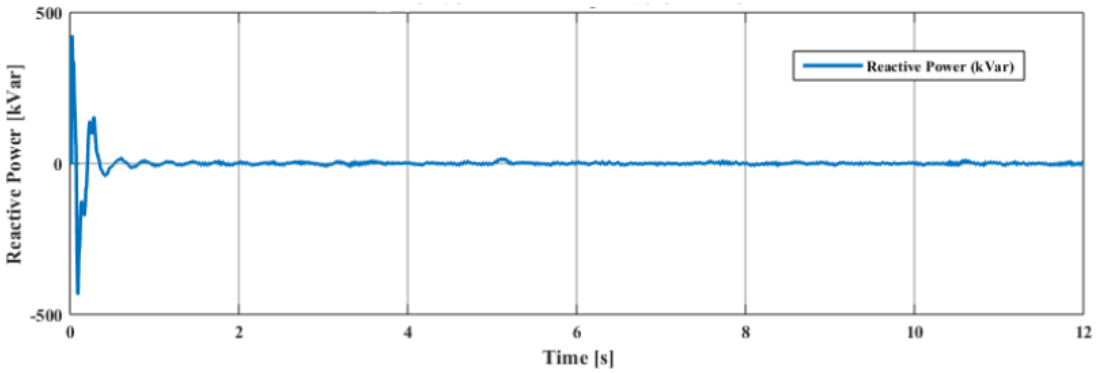

Figure 3.25 Reactive Power (Q) response of the grid

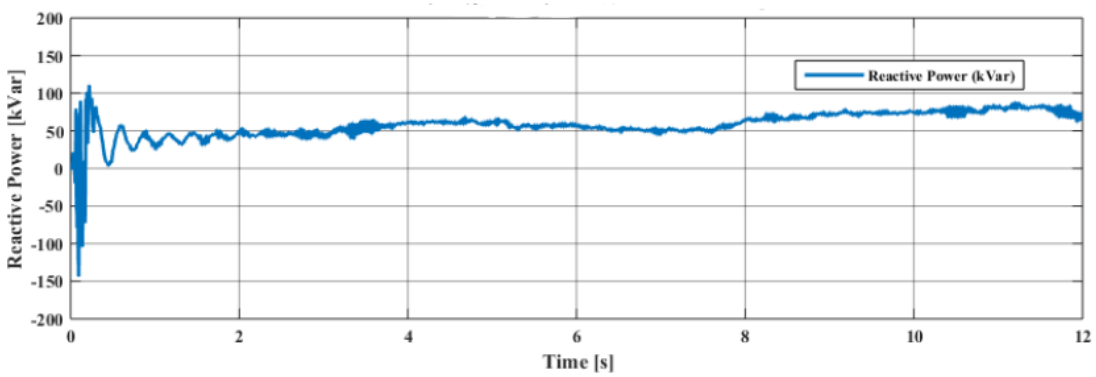

Figure 3.26 Reactive Power (Q) response of the AC-DC-AC link

3.3.3 Frequency and voltage stability

The main control strategy for PV based active generator is to ensure that the voltage stability and frequency is within the acceptable limits. This is to make sure that the system is ready to be connected to the conventional grid based on ‘plug and play’ concept.

Since the system is isolated from the grid through AC-DC-AC link, the grid parameters are not affected by the fluctuations on the active generator side. Figure 3.27 illustrates the RMS voltage at the AC bus for PV based active generator for all phases. All phases are in-phase and expected transient occurs at the beginning.

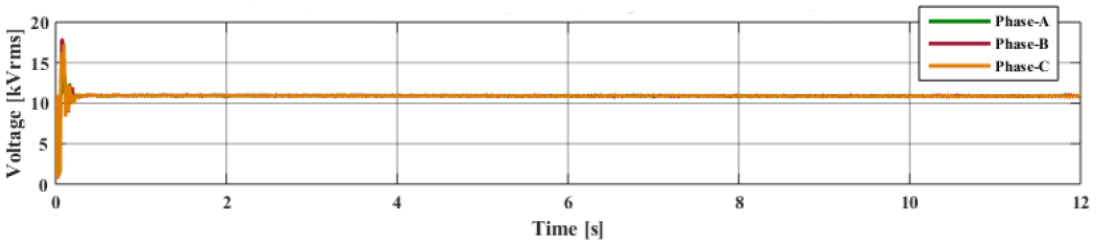

Figure 3.27 RMS voltage of the AC bus for PV based active generator

Allowable frequency fluctuation for a system is ± 5%. Based on Figure 3.28, it is within the allowable range of fluctuations.

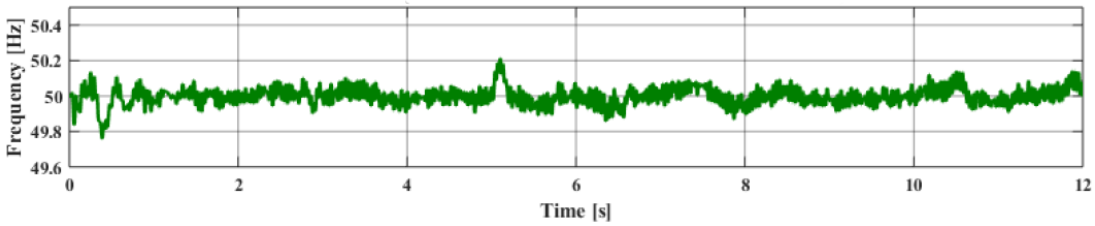

Figure 3.28 Frequency of the AC bus for PV based active generator

The grid voltage and frequency is not affected at all once it is connected to the PV based active generator. Figure 3.29 illustrates the unaffected grid RMS voltage while Figure 3.30 shows that the frequency did not change much with the connection to the PV based active generator.

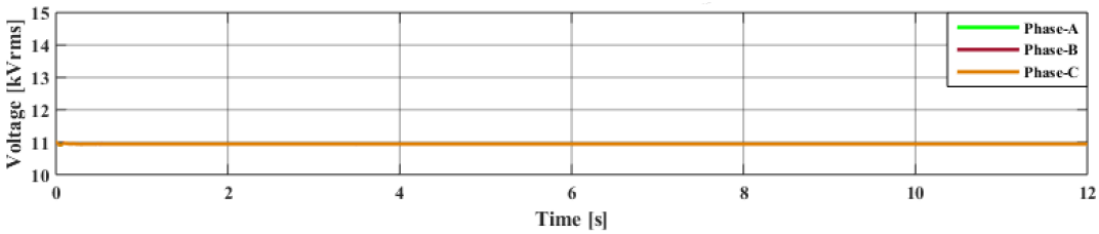

Figure 3.29 Grid RMS voltage

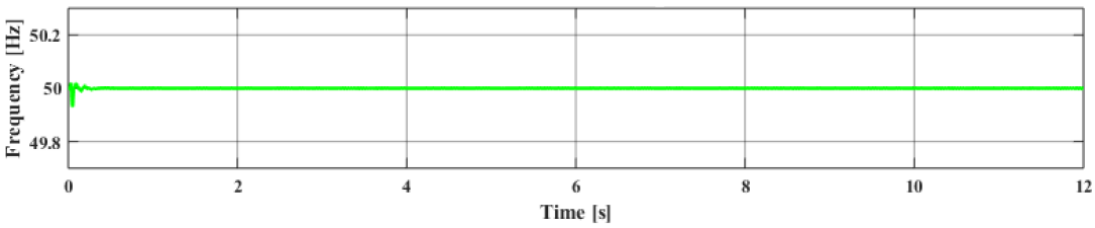

Figure 3.30 Grid frequency

Based on the test scheme that has been done using simulation, it proof penetration of PV produced power into the grid system. This can be a plug and play system that will not harm the existing grid lines. The controlling part of PV based active generator plays a major role in managing and controlling the active (P) and reactive (Q) power while maintaining the stability of voltage and frequency.

3.4 Discussion

This research is to develop PV based active generator architecture and its control strategies to meet the load demand based on the sources availability. The active power (P) and reactive power (Q) from the load demand has been managed with respect to the voltage and frequency stability. This has been done by using a hierarchical control approach using stateflow analysis with droop characteristics.

The overall control system has been developed as a hierarchical system with stateflow control and droop characteristics. The hierarchical control approach is suitable for this type of real time power management systems as it helps not only in managing and controlling the power flow but also helps in maintaining the safety and stability within the system. The top most level (Tier 1) selects the appropriate working mode based on the rated power values and the grid constraints considering the whole system as a unit. The subsequent layers concern the individual units of the active generator system. It helps to keep the SOCs of the centralized energy storage units at a relatively high values because system switches the energy storage elements between charging and discharging modes.

The implementation of droop characteristics along with the feedback control maintains the frequency and voltage stability at acceptable levels. Since the AC coupled structure is used for the PV based active generator along with a AC-DC-AC link, individual three sub systems can be identified which are having their own PWM switching control implemented using different topologies of current mode and voltage mode control of VSI. For this particular work, the PV array is considered as the main source of energy and it should inject maximum available energy to the system. The simulation results prove that the SRFC with DC voltage regulator implemented in the PWM switching control layer gives acceptable achievement of maximum power operation of the PV array. Tier 2 (Power dispatch) layer plays a major role in keeping the SOC of the energy storage units at a high value which leads to maintain the active generator system availability for the continuous operation. By using an AC-DC-AC link, the system isolation (transformer isolation and DC link isolation) is achieved in addition to demand side management control.

The centralized energy storage elements decide their power shares at Tier 3 (power flow control) based on the frequency and voltage stability to compensate the power fluctuations caused by PV generation. The method of

deciding the individual component of power sharing at lower layers helps to maintain the frequency and voltage stability within the system rather doing it at the top layers as in the conventional case.

Based on a 12 seconds testing time, the simulation based on the random data has been executed. The test is to make sure that the P and Q for the load is fully satisfied by any of the available source with a priority is given to the PV source. The test in the last section prove that the capability of the proposed architecture for managing and controlling both active and reactive power while maintaining the frequency and voltage stability within the system. The load demand to the grid can be effectively reduced by increasing the penetration of PV power as active generator systems with the help of hierarchical control strategies.

3.5 Conclusion

Four tiers hierarchical that have been introduced (Tier 1: Function control, Tier 2: Power dispatch, Tier 3: Power flow control and Tier 4: Switching control) to fully control the PV based active generator. Each of the tier will act accordingly depends on the availability of the sources. This is to make sure that the load demands is fulfill and the system does not exceeding the grid restrictions. Based on a different control methodologies on different sources, the load will be supplied effectively matching the source readiness and at the same time prohibit any unnecessary problems (voltage and frequency variations). It can be concluded that the developed architecture which provides the active power (P) and reactive power (Q) to meet the load demand helps in improving the power system dynamics and control, in addition helping on the demand side management.

Chapter 4

4 Grid Interaction Performance Evaluation of Zero Energy Building (ZEB) in the Southern Norway

The energy efficient housing development should consider that a building should produce the same amount of electrical energy as its annual requirements (i.e zero energy building (ZEB)). In future ZEBs are going to play a significant role in the upcoming smart grid development due to their contribution on on-site electrical generation, energy storage, demand side management etc. In Southern Norway, a smart village Skarpnes is developed for ZEBs. These ZEBs have Building Integrated Photovoltaic (BIPV) system. In this work the main objective is to evaluate the usefulness of ZEBs for load matching with BIPV generation profiles and grid interaction analysis. The real operational results of a year are analyzed for annual energy balance with on-site BIPV generation and local load. This work provides quantitative analysis of various grid interaction parameters suitable to describe energy performance of the BIPV. The load matching and grid interaction parameters are calculated for a house to find relationship of BIPV generation and building load. The loss of load probability is analyzed and it will be useful for finding an additional capacity for fulfilling the local load at desired reliability level. Results of this work are going to be useful for developing demand side management strategies and energy storage as well as import/export energy to the grid. This work will be beneficial for future planning of the distributed network when the BIPV penetrations are going to increase.

Nomenclature

BTS	: Building technical system
$\zeta_{sys}(t)$	: Building technical systems energy losses (excluding storage)
$\zeta_{g}(t)$	: Generation energy losses
$\zeta_{s}(t)$	: Storage energy losses
$\zeta_{l}(t)$	: Load energy losses (e.g.: distribution losses)
$g_{gross}(t)$	: Gross on-site generation
$g_{net}(t)$	: Net on-site generation
$S_{dc}(t)$	: Discharging storage energy
$S_{c}(t)$	: Charging storage energy
S_{i}	: Internal storage energy
$l_{gross}(i)$	: Gross load
$l_{net}(i)$	: Net load
$e(t)$	: Exported
$d(t)$	: Delivered
T	: Time
e	: Exported energy
d	: Delivered energy
net	: Net exported energy
PV_{net}	: On-site generation
t	: Evaluation period
t_1	: Start of the evaluation period
t_2	: End of the evaluation period
w	: Weighting factor
l	: Load
l_{net}	: Net load
e_{design}	: Designed capacity
r_{esd}	: On-site energy supply-demand index
CC_f	: Rated capacity credit factor
γ_{load}	: Load cover factor
$\gamma_{generation}$	: Generation cover factor
$LOLP$	: Loss of load probability
GM	: Generation multiple
CUF	: Capacity utilization factor
DR	: Dimensioning rate
PR_{cf}	: Power reduction capacity factor

4.1 Introduction

In future ZEBs are going to play a significant role in the upcoming smart grid due to building integrated distributed generators, energy storage, and demand side management. In southern Norway, a smart village Skarpnes is developed and at this moment five single family houses are built as per passive houses standards NS3700 [41]. In Southern Norway, a group of on-grid zero energy and zero energy building (ZEB) area with roof-mounted PV systems are developed at Skarpnes, near Arendal. Skarpnes is a small village located at 58.4° north and 8.7° east. The project is a zero energy building (ZEB) pilot project that has been executed by the local authority and is expected to be completed in four years' time. It is developed by Skanska Norge and it is a pilot project of The Research Center on Zero Emission Building and in the Norwegian '*Lavenergiprogrammet*' for evaluation of homes with low energy demand (EBLE). The actual definition of a ZEB in this project is referring to a building that produces the same amount of energy as its own demand during the operation period of a year [42]. This project location is at the southern coastline of Norway, the weather is sunny and mild with an annual mean temperature of 7.8°C, with annual solar radiation 2.43 kWh/m²/day of horizontal global solar irradiation. The solar radiation varies significantly throughout the year and in summer it can typically reach up to almost 6 kWh/m^2/day [43].

The electrical energy required in this project will be partially supplied from the PV arrays on the rooftops. For heating purposes, initial plan was the heat pumps and solar thermal collectors to be used in combination with ground heat exchangers, however this has been changed. It is expected that the annual electrical energy generated from all of the rooftop PV arrays should be sufficient to cover the total annual electrical demands of the houses. This project is providing real operational results and they are going to contribute for future building construction planning and design based on ZEBs. Results will be useful not only to the utilities for developing new business models for better energy efficiency measures but also to the urban planner and building designer [44]. Performance evaluation of ZEBs will also help in finding appropriate distributed energy storage as well as in distributed network planning and expansion. The results from this smart village may also help in analyzing the needs of traditional houses, where smart grid solutions and distributed generation units may get installed in future. Techno-economic analysis is also needed for grid expansion planning and some of the result form this specific project may be useful for doing energy business and policy analysis for future energy system [45].

4.2 Skarpnes Smart Village: Zero Energy Building Project

This Skarpnes smart village project (Figure 4.1) is based on minimizing housing energy demand through the building energy efficiency and utilizing the local PV generation. These five houses are developed as ZEBs with roof mounted building integrated PV (BIPV) system. These houses have been occupied and started collecting energy consumption and production with power quality data. This project is going to help on further investigation on load flow analysis in the distributed network on introduction of energy efficient buildings with roof mounted PV systems. Results from this project are going to be useful for doing load matching and grid interaction of such type of buildings with distributed network.

Figure 4.1 House C6 in the Skarpnes Smart house project

In this work, a house C6 is selected for doing performance analysis as well as load matching with grid interaction. This house is a single house with an area of 154 m^2. It is build facing south and Figure 4.2 shows the PV array installation on rooftop, facing to the southwest. The technical parameters of the C6 house are given in the Table 4.1. The usable roof area for C6 is 57.43 m^2, however the PV array is only covered 39.9 m^2 of this roof. Specifications of the PV modules are given in Table 4.2. Table 4.3 shows configuration of the PV array for this specific house C6.

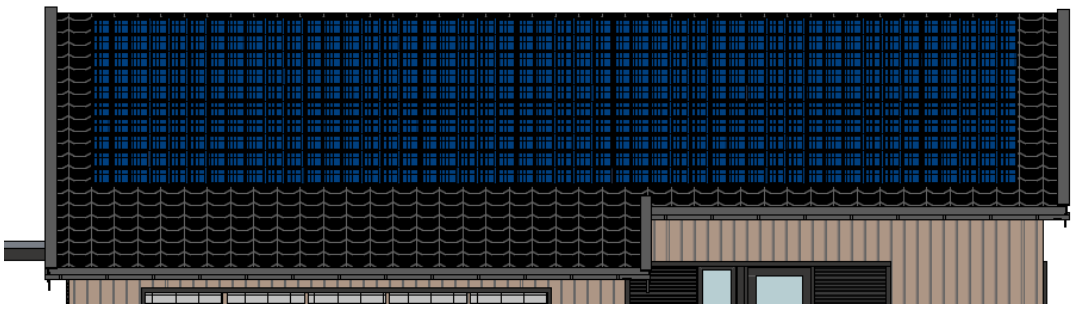

Figure 4.2 House (C6) with the PV array is facing southwest

Table 4.1 Characteristics of Skarpnes smart village house C6

Characteristic	**Value**
Increased installed PV (factor of 4.5)	7.36 kWp
Building area	154m^2
Designed capacity	16kW
Technologies	PV array

Table 4.2 Sunpower SPR 230NE-BLK-I

Peak Power (P_{max})	**230 W**
Cell Efficiency (η)	22.7 %
Panel Efficiency (η)	18.5 %
Rated Voltage (V_{mpp})	40.5 V
Rated Current (I_{mpp})	5.68 A
Open-Circuit voltage (V_{oc})	48.2 V
Short-Circuit current (I_{sc})	6.05 A
Max system voltage	600 V

Table 4.3 Overview of the installed peak capacity and PV production.

Usable Roof (south facing)			**Sunpower - SPR 230 NE-BLK-I**			
Length (m)	Width (m)	Area (m^2)	Strings	Modules	module area (m^2)	Capacity (kWp)
12.2	4.7	57.43	2	16	39.9	7.36

4.2.1 Electrical load used in designing of Skarpnes project house

Skarpnes smart village house C6 is considered in this study. C6 is representing a typical Norwegian house with common appliances those have been commonly used in other houses. Due to some engineering issues, it has been challenging to monitor power consumption of power intensive loads in C6 house and ratification process for monitoring their power consumption is continuing. In it, typical power appliances which are going to be monitored are: Heat pump, Ventilation system, Circulation pumps, Fan convector. Annual energy needs, used in planning, of a typical house of 154 m^2 area is given in

Table 4.4. It is considered in the design that the annual total energy consumption is approximately 12 MWh, where around 5.2 MWh represent electrical needs and 6.9 MWh are thermal requirements. This energy usage includes basic needs for a typical house such as lighting and heating [43].

Table 4.4 Energy fraction for planning C6 house [43]

Energy Purpose	Specific Energy (kWh/m^2 yr)	Energy Needs (kWh)
Space heating	14.9	2294.6
Hot water	29.8	4589.2
Fans	4.4	6776
Pumps	0.3	46.2
Lighting	11.4	1755.6
Technical Equipment	17.5	2695
Total net energy	**78.3**	**12058.2**

For energy saving and improved efficiency in the zero-energy houses in Skarpnes, few additional measures are considered. The installation of LED lighting to replace the conventional lighting system will obviously reduce the energy consumption. Initially the heating was planned to be provided by a solar thermal collector system and ground heat from 160 meters of underground pipes, but this proposal has been withdrawn by the developers.

ZEBs will be part of upcoming smart grid with its role as integrating with the grid as distributed generator as well as load balancing. As the existing power system network has hierarchical arrangement with unidirectional power flow, consequently grid interaction analysis of such type of ZEBs is important for further planning and enhancement of the grid. Analysis of grid integration and load matching of ZEBs with seasonal variation will be useful in the framework of the smart cities planning [46].

4.2.2 BIPV Energy output for C6 House

The installed PV array on C6 can produce nearly 7 MWh energy annually. This is close enough for estimated/approximately annual electricity consumption of a typical house. Therefore, this house can be considered as ZEB. The PV array output is continuously monitored and the hourly PV electrical energy production (of C6 house) for a year (September 2015 – August 2016) is given in Figure 4.3. It is observed that there are big variations with intermittency of PV production ranging from 0 kWh to 6.5 kWh hourly. The lowest PV

production is in the month of December and house may have more electricity demand in this month.

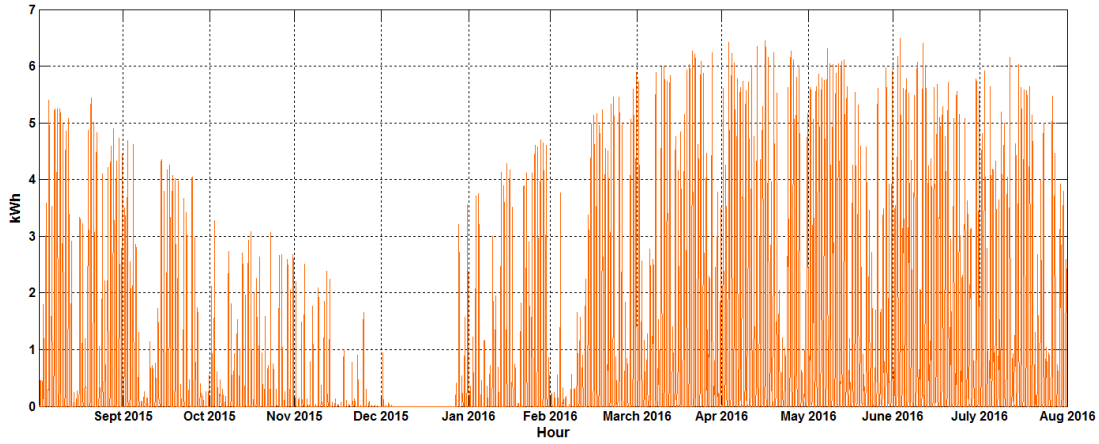

Figure 4.3 Hourly PV electrical energy in 12 months

The monthly PV generation is calculated and given in Figure 4.4. It is observed that the PV production is relatively low during winter months in November, December and January. This is due to the short day length and the snow fall. Cumulative energy for these three months is 295.75 kWh, which is not even half of the monthly output of May. In May, almost 1110 kWh is generated from the PV array. The daily PV production for December is given in Figure 4.5. In May as can be seen in Figure 4.6, the energy generated from the array is the highest among other months. The highest is at 6.41 kWh on May 16th at 1400 hours.

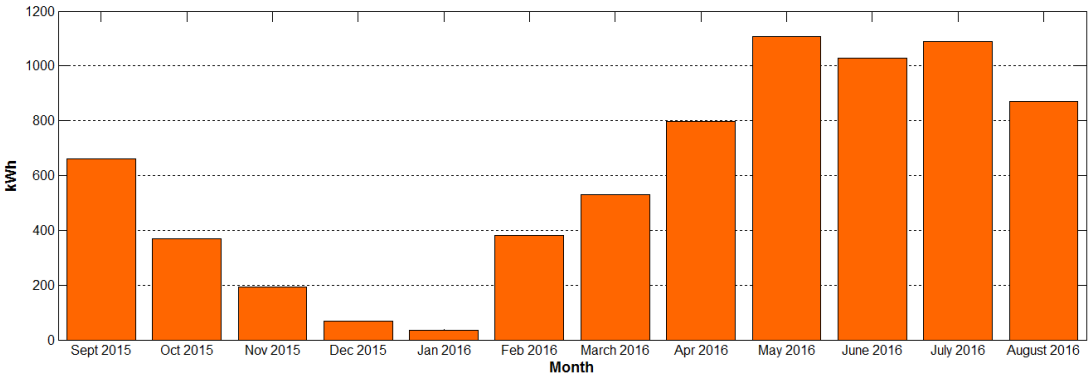

Figure 4.4 Total PV generation monthly.

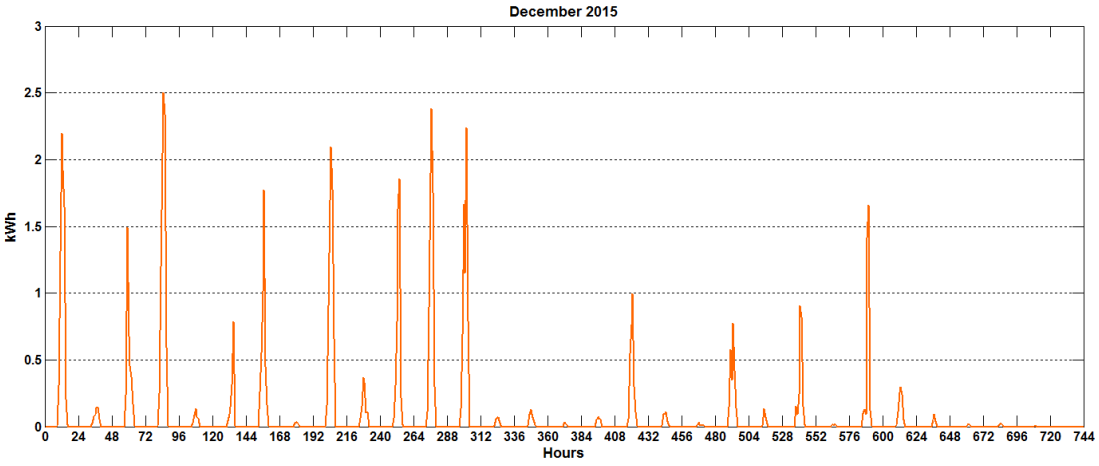

Figure 4.5 PV generation profile, December 2015.

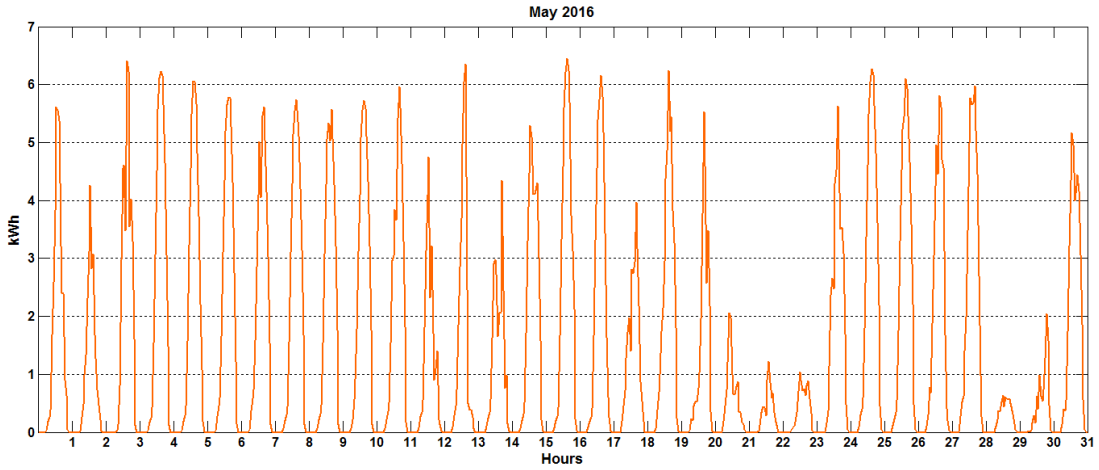

Figure 4.6 PV generation profile, May 2016.

4.2.3 Real time annual load curve for C6 house

The instrumentations have been organized to measure the real time power of various power intensive loads of the house. But due to some engineering problems, installations of these meters have to be rectified. The overall real time net power consumption of the house is monitored through the ELSPEC power quality instrument and it can provide the measurements at minimum of 20 μ sec [47]. In this work, total hourly net power consumption of the house is collected through ELSPEC and it is given in Figure 4.7 for 12 months (September 2015 - August 2016). It is observed that the highest net demand is coming in the mid of February with net hourly energy demand of 7 MWh and in the month of December**,** the minimum net power consumption is 1000 kWh for whole month due to continuous heating demand of the house.

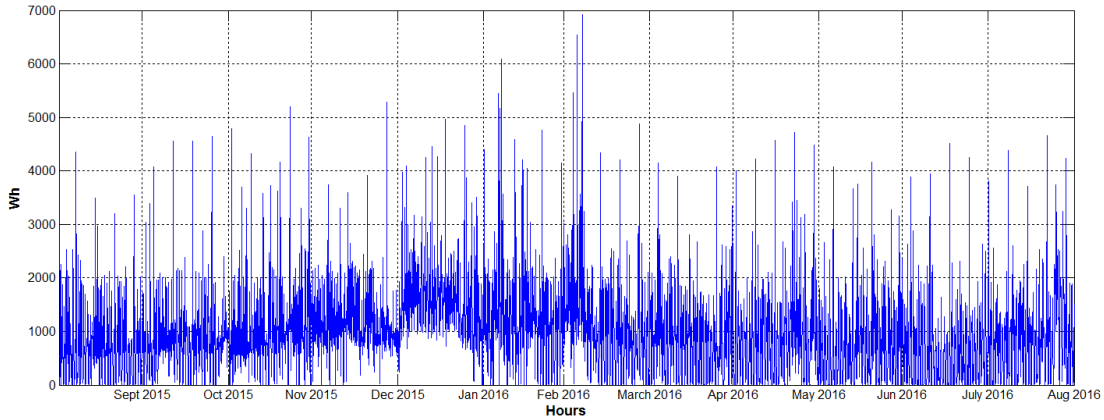

Figure 4.7 Electric load curve for the C6

A typical winter time weekend net real time load curve and a typical weekday net load curve are given in Figure 4.8 and Figure 4.9 respectively. It is observed there is substantial difference on net load patterns for both weekday and weekend. Net peak occurrence timings as well as minimum net load occurrence timing are quite different. Therefore, the grid interaction on weekdays and weekend are going to be different and they also depend on the user behavior as well as weather conditions, physical characteristics of dwellings, types of appliances and user occupancy [48] [49].

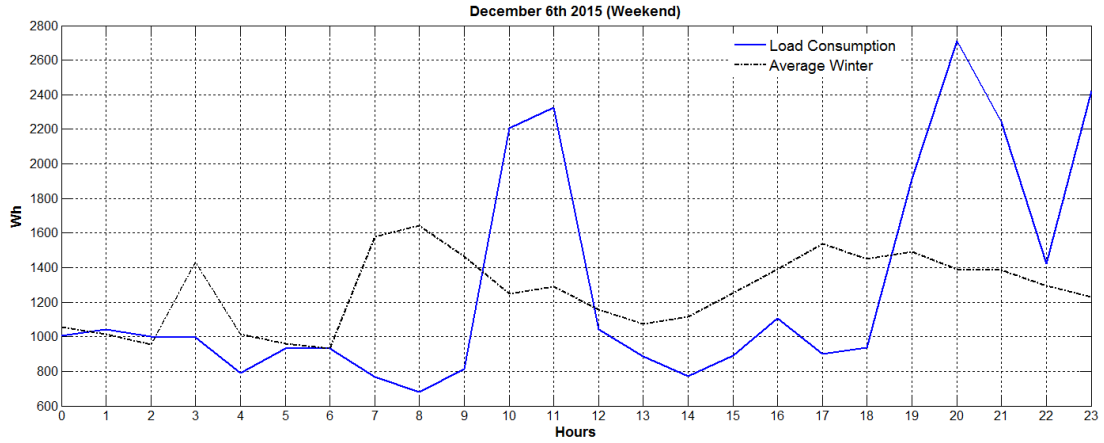

Figure 4.8 Daily net load curve on typical weekend during winter season

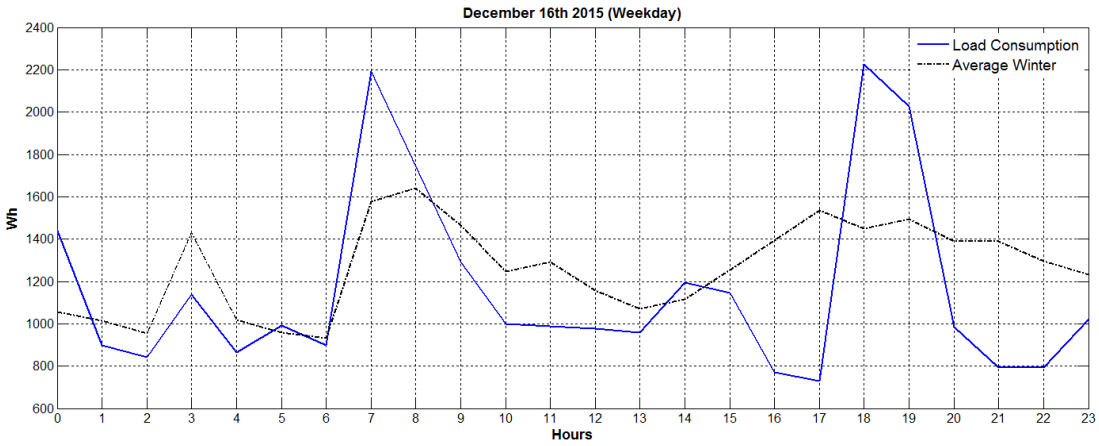

Figure 4.9 Daily net load curve on typical weekdays during winter season

In southern Norway the month of July is considered as summer vacation period. Therefore, real time net load profile of July for typical weekday and typical weekend are considered. It is observed that for C6 house, throughout summer month (June to August), the hourly average minimum load is 970 W and maximum 1587 W. The hourly average load profile for weekday and weekend, during summer month, are also given in Figure 4.10 and Figure 4.11 respectively.

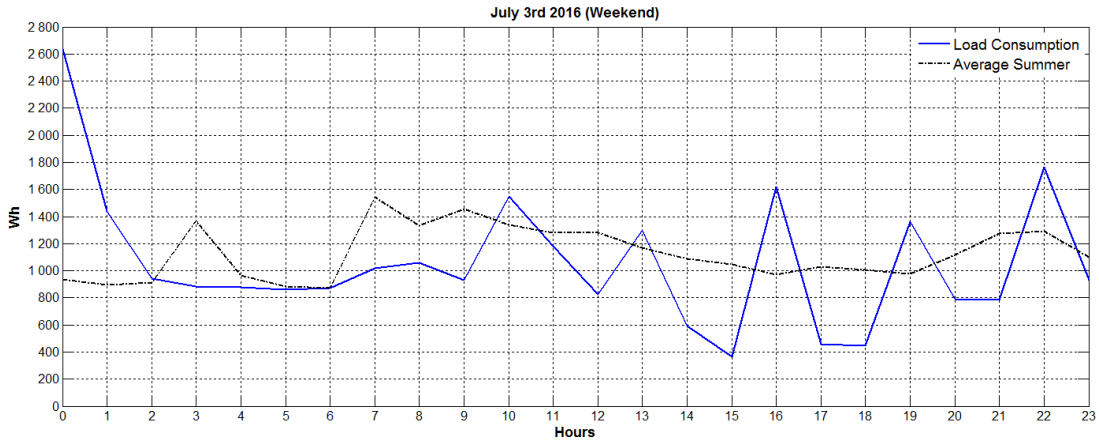

Figure 4.10 Daily net load curve on typical weekend during summer season

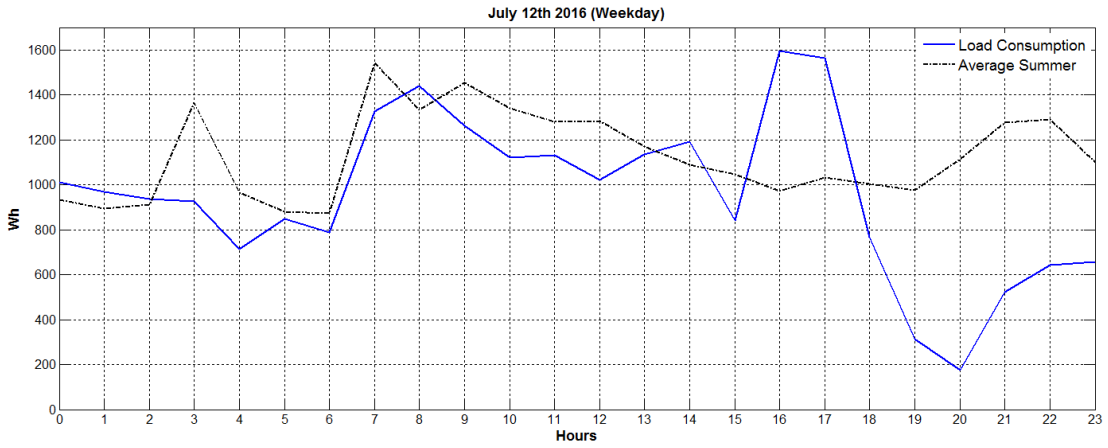

Figure 4.11 Daily net load curve on typical weekday during summer season

4.3 Mismatching of real time load with the on-site PV generation

The real time hourly PV production (Figure 4.3) and the hourly load consumption (Figure 4.7) are analyzed for finding the net export/import of hourly real time energy from the grid and it is reported in Figure 4.12. The maximum export of the energy happens on June 21st at 1700 hours and the maximum import occurs on February 29th at 0600hours.

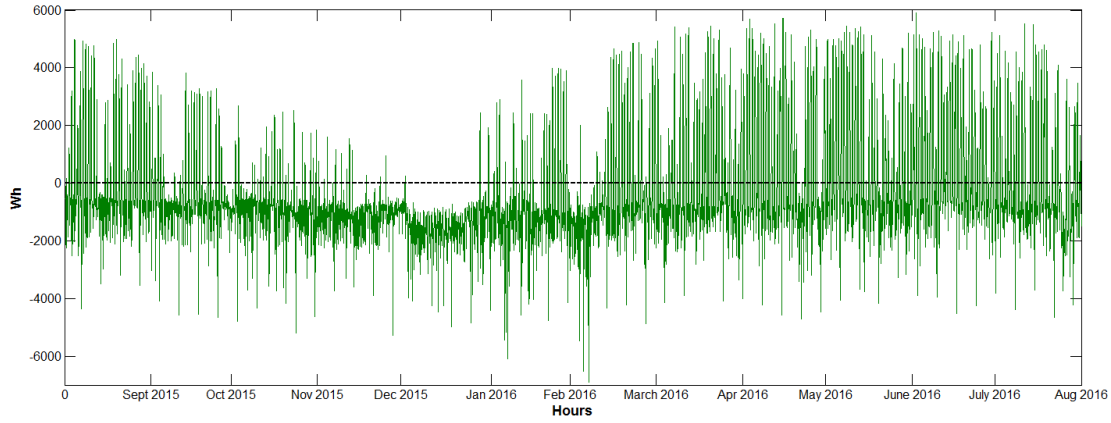

Figure 4.12 Net export/import of hourly real time energy

The hourly net energy from the grid is analyzed on monthly basis to measure monthly energy taken from the grid and supplied to the grid (Table 4.5). Also the on-site monthly PV measured production as well as the C6 monthly measured energy consumption are given in the Table 4.5. It is observed during May 2016 the monthly PV productions are high, therefore the energy has been exported to the grid. In the month of January the PV production is the lowest compared to other months, hence the demand is the highest. The monthly PV

energy production is varied from < 3% (in January) to 125% (in May) with reference to the monthly total electrical energy consumption. The mismatching of the monthly energy export and import of C6 is analyzed and it is noticed that maximum export is 29% with reference to PV production in the month of July. However, in the month of January the PV production is the lowest, therefore the import of 3232% of energy with reference to PV production can be seen. With the reference to the monthly energy consumption of C6, the variation of C6 energy supply and requirement to/from the grid are analyzed; and it is found that the monthly energy supplied by the house to the grid is from 41.2% and monthly energy required by the house from the grid is 97%.

Table 4.5 Summary of monthly net energy and PV generation

Month	Energy IN (kWh)	Energy OUT (kWh)	Mismatch (kWh)	PV Production (kWh)	Consumption (kWh)
September	448.65	507.62	-58.97	660.249	601.27
October	603.05	228.39	374.66	369.83	744.49
November	688.09	95.02	593.07	193.54	786.61
December	823.10	22.53	800.57	67.949	868.52
January	1119.88	12.23	1107.65	34.264	1141.92
February	815.31	203.10	612.22	380.361	992.58
March	778.87	348.65	430.22	529.974	960.20
April	568.44	507.43	61.01	798.582	859.59
May	640.03	863.61	-223.58	1108.23	884.65
June	448.08	680.98	-232.90	1027.64	794.74
July	416.52	734.57	-318.05	1090.63	772.58
August	594.29	535.44	58.85	870.97	929.82
Annual Total	**7943.07**	**4739.56**		**7132.22**	**10335.73**
Average	**662.026**	**394.964**		**594.352**	**861.414**

It was expected that typical house in Skarpnes smart village should produce on-site PV generation approximately equal to the electrical energy consumption of the house annually. For this typical year, the on-site annual PV production of C6 house is lower than the annual electrical consumption (Figure 4.13). Deviation of annual (September 2015 – August 2016) exported and imported energy of C6 with reference to net zero line, is given in Figure 4.14 and due to changing weather patterns it may vary. Load consumption as well as the PV production will vary and may depend on the climatic conditions as well as change in user behavior, load pattern, home energy management system[50]**.** The energy efficient loads and home energy management system may help in reducing annual energy consumption and matching with PV production.

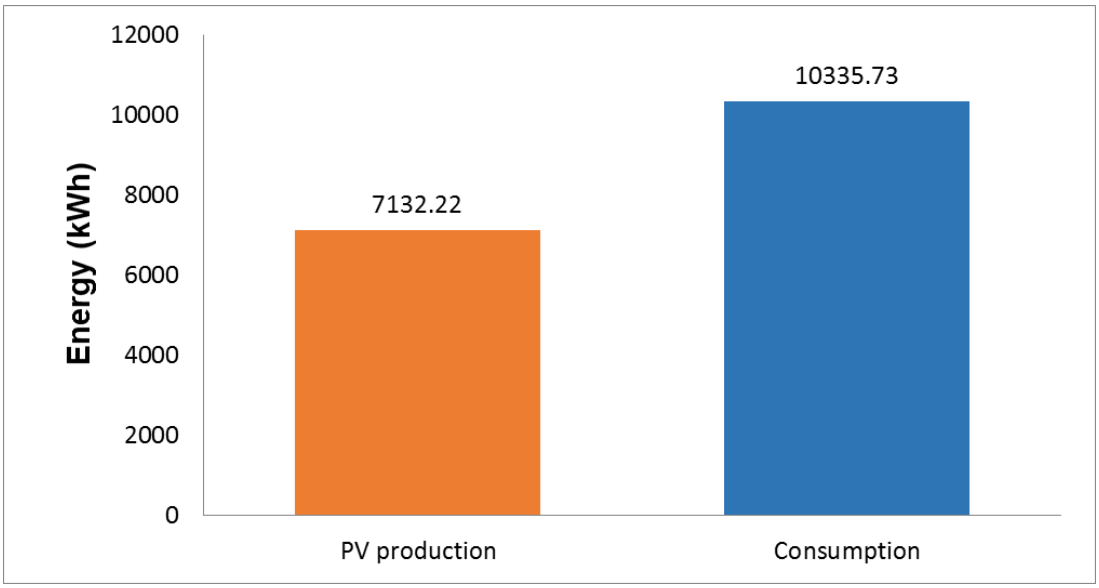

Figure 4.13 Aggregated energy balance and electric loads and the PV generation

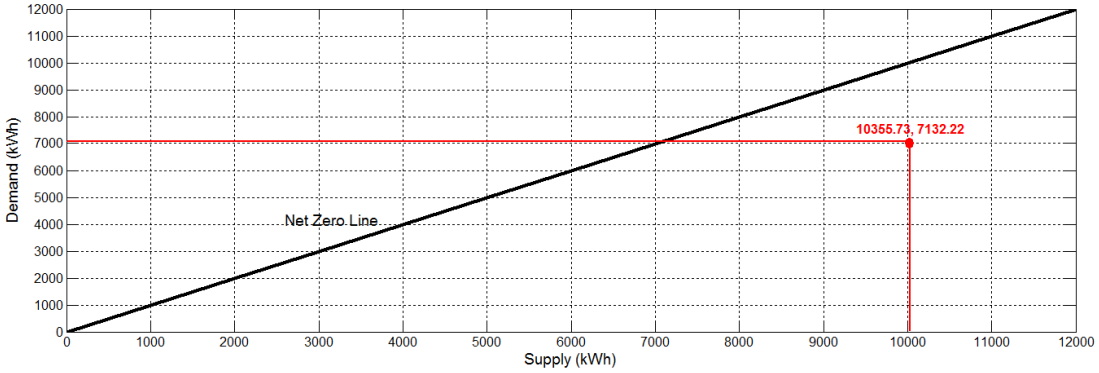

Figure 4.14 C6 final energy balance

4.4 Grid Interaction Indicators of BIPV

Quantitative analysis of near net ZEB is important for investigating on-site energy generation with reference to local load [51]. Quantitative grid interaction refers the energy import/export between ZEB and distribution network. This investigation is going to help for understanding load matching with on-site PV generation and profile of supplying power to the grid [52]. In this section, grid interaction indicators are explained and they are used in subsequent sections.

In this work load matching with PV generation and grid integration for a year are analyzed for this C6 ZEB. IEA Task 40 [53] has emphasized the importance of grid interaction of the ZEB and presented a sketch for energy

flows in ZEB. If the building is equipped with PV, solar thermal and smart energy meter then its typical energy flows will be as given in Figure 4.15.

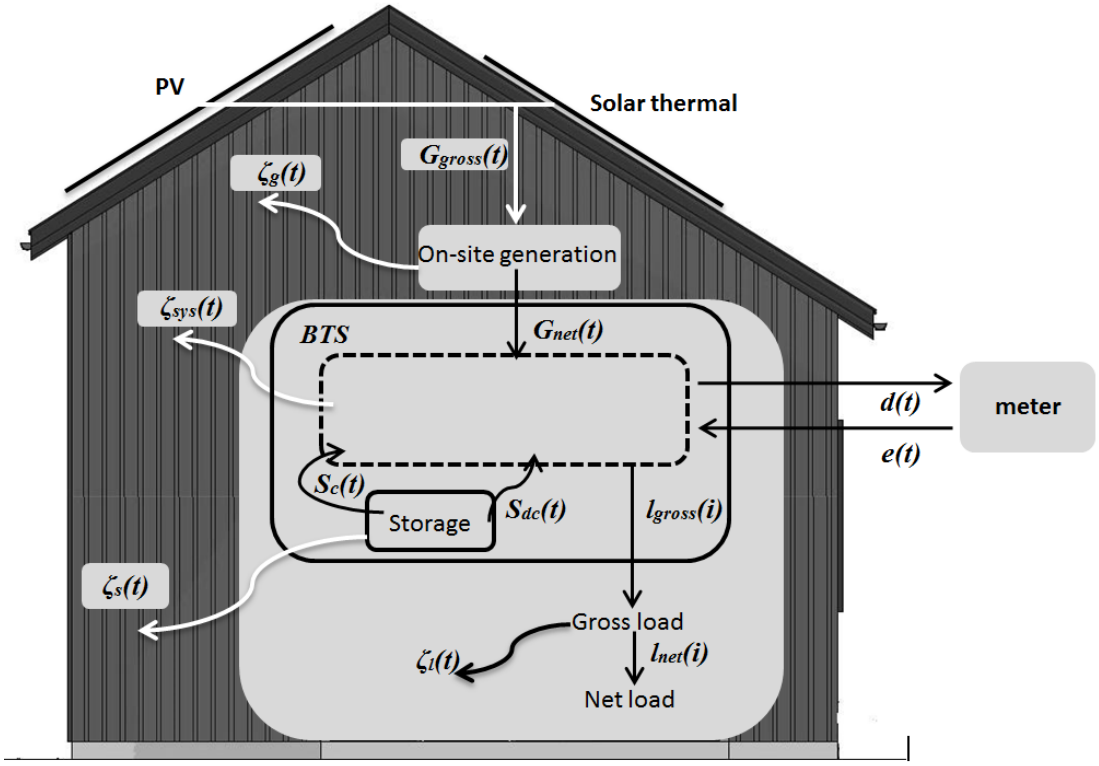

Figure 4.15 Energy flows for a typical ZEB

The energy delivery for ZEB can be represents in an equation form. The end expression is the net exported energy (net). A general energy flows for a typical ZEB, considered all on-site generations, losses, storage and grid interactions, is:

$$G_{net}(t) + d(t) = l_{net}(t) + [\Sigma\ losses] + e(t) + \frac{dS_i}{dt}, \qquad (4.1)$$

where the cumulative losses ($\Sigma\ losses$) that have been taken as:

$\zeta_{sys}(t)$	: Building technical systems energy losses (excluding storage)
$\zeta_s(t)$	: Storage energy losses
$\zeta_l(t)$	: Load energy losses (e.g.: distribution losses)

While for storage system (S) and the gross load (l_{gross}), the equation considered are:

$$S(t) = S_c(t) - S_{dc}(t) = \zeta_s(t) + \frac{dS_i}{dt} \qquad (4.2)$$

$$l_{gross}(t) = l_{net}(t) + \zeta_l(t) \tag{4.3}$$

So, by integrate equation (4.1) with respect to equation (4.2) and equation (4.3), between times ranges from t_1 to t_2, (4.1) may be represents as:

$$\int_{t_2}^{t_1} G_{net}(t) + \int_{t_2}^{t_1} d(t) = \int_{t_2}^{t_1} l_{gross}(t) + \int_{t_2}^{t_1} \zeta_{sys}(t) + \int_{t_2}^{t_1} e(t) + \int_{t_2}^{t_1} \zeta_s(t) + \Delta S_i \tag{4.4}$$

For $\Delta S_i \approx 0$,

$$\int_{t_2}^{t_1} G(t) + \int_{t_2}^{t_1} d(t) = \int_{t_2}^{t_1} l_{net}(t) + \int_{t_2}^{t_1} \zeta(t) + \int_{t_2}^{t_1} e(t) \tag{4.5}$$

By simplifying equation (4.5), the net exported energy is:

$$net\ (t) = e(t) - d(t) \tag{4.6}$$

4.4.1 On-site energy supply-demand index (r_{esd})

This index (r_{esd}) is defined as the ratio of cumulative energy supplied by on-site generation to the load during a specific time period. If this index is higher, the coincident among the on-site generation and load is superior. This index is express as:

$$r_{esd} = \frac{\int_{t_2}^{t_1} PV(t)dt}{\int_{t_2}^{t_1} l(t)dt} \tag{4.7}$$

If at the site local energy storage have been used, then this relation needs to be modified considering the on-site generation, energy storage power flow including losses and load variation during the specified time period.it can be define as:

$$r_{esd,storage} = \frac{\int_{t_2}^{t_1} [PV(t) \pm Storage\ (t) - losses(t)]dt}{\int_{t_2}^{t_1} l(t)dt} \tag{4.8}$$

4.4.2 Rated capacity credit factor (CC_f)

On-site BIPV generation varies from time to time with weather conditions. As the penetration of on-site BIPV increases intermittent output is going to become important feature of distributed network. It will impact capacity amount which is required for meeting the peak demand and also on the operation of the generators. The net export load profile can be used for analyzing the impact of BIPV on network capacity. The difference between the peaks of the load duration curve with net load export curve represents the BIPV contribution. This BIPV contribution to the local load can be express as percentage of the rated installed BIPV capacity.

4.4.3 Load and generation cover factor (γ_{load} and $\gamma_{generation}$)

The building integrated PV system is contributing to fulfil the local load and reducing the demand on the grid. It can be quantified as cover factor(s) and can be referenced with the on-site load and generation. Load cover factor is expressed as the ratio of local demand supplied by on-site PV generation to the local load during the specific time period. Similarly generation cover factor is expressed as the ratio of local demand supplied by on-site PV generation to the on-site PV generation during the specific time period.

$$\gamma_{load} = \frac{\int_{t_2}^{t_1} min[PV(t), l(t)]dt}{\int_{t_2}^{t_1} l(t)dt} \tag{4.9}$$

$$\gamma_{generation} = \frac{\int_{t_2}^{t_1} min[PV(t), l(t)]dt}{\int_{\tau_2}^{\tau_1} PV(t)dt} \tag{4.10}$$

The factor $min[PV(t), l(t)]$ is representing the load supplied by the on-site PV generation at particular time, taking into account minimum value of PV generation or load.

Load cover factor: quantifies the local demand supplied by PV and during daytime with more PV output, this factor is going to increase and can reach up to a maximum value. While installing the PV system, with local load consideration, the load cover factor should be considered to have as maximum as possible. The maximum load cover factor will depend on the day length and PV production time period. The maximum load cover factor is more useful for

doing analysis over daily, monthly or yearly time period and it can be expressed as:

$$\gamma_{load,max}^{(t_1,t_2)} = \frac{\int_{sunset}^{sunrise}[\, l(t)]dt}{\int_{t_2}^{t_1} l(t)dt} \tag{4.11}$$

The analysis of load cover factor and generation cover factor are going to help in understanding the role of home energy management system (HEMS) for time shift able power intensive domestic loads [50]. These cover factors are useful in managing operation of power intensive non-critical loads with reference to the on-site PV generation.

4.4.4 Loss of load probability (LOLP)

In the electrical energy system, loss of load probability (LOLP) is useful for finding the system of availability. The BIPV system, the LOLP can be express as the time which on-site PV generation is not able to fulfil the local demand, and therefore how often the required energy should be provided by the grid. It can be expressed as:

$$LOLP = \frac{\int_{t_1}^{t_2} dt|_{l(t)>PV(t)}}{t_2 - t_1} \tag{4.12}$$

LOLP analysis is useful for determining the amount of capacity which will be needed for fulfilling the desired reliability level of domestic load.

4.4.5 Generation multiple (GM)

The generation multiple [54], has been used for relating the capacity of on-site PV generation with the total load of the house which has been used in the design study. It is defined as ratio of generation capacity to designed load of the house.

$$GM_{PV/l} = \frac{rated\ PV\ capacity}{rated\ or\ designed\ peak\ load} \tag{4.13}$$

Generation multiple information is useful for power system network planning on estimating the on-site peak PV generation compared to peak load. This factor may help in designing operational strategies for HEMS. The GM can be configured by considering delivering energy profiles to the grid and acquiring energy from the grid. The GM can be expressed using the delivering (*e(t)*) and

acquiring energy (*d(t)*) profiles using maximum power values from these profiles.

$$GM_{e/d} = \frac{peak\ [e(t)]}{peak\ [d(t)]} \tag{4.14}$$

4.4.6 Net energy export and range

While designing the BIPV with considered designed load profile, the net export energy (e_{design}) is analyzed and it can be used for normalizing the on-site net energy export to the grid with designed value. It can be expressed as:

$$net(t)_{norm} = \frac{net(t)}{e_{design}} \tag{4.15}$$

Net energy export profile can be considered for doing further analysis of GM. With reference to the energy export profile, the GM analysis can be done through the maximum (peak) of export profile and the minimum of it. It can be calculated as:

$$GM_{net(100/0)} = \frac{max|net(t)|}{min|net\ (t)|} \tag{4.16}$$

The net energy export profile can be studied using percentile of maximum and minimum power values. The net energy export profile curve can be configured as load duration curve for doing further sensitivity analysis. In this analysis, the changes of the peak values (power) of the export energy as well as of reducing/changing input values (power) from the grid can be investigated. Reduction to the grid export and load peak reduction can be reviewed using the net exported of the load duration curve. This investigation can help in finding the scope of HEMS for peak shaving in the load side. Variation in the peak export power to the grid and also in the peak demand from the grid can be used for understanding the range which may be useful for power system network planning. The GM with variation of export peak (P_{up}) and reduction in peak demand (P_{down}) can be analyzed using:

$$GM_{net(P_{up}/P_{down})} = \frac{\left|net_{P_{up}}\right|}{\left|net_{P_{down}}\right|} \tag{4.17}$$

4.4.7 Capacity utilization factor (CUF)

The capacity utilization factor is considered as the ratio of actual net energy of the house to the maximum possible energy based on designed capacity. Net energy exchange with grid can be analyzed with the design value of peak capacity of the grid connection (e_{design}).

$$CUF = \frac{\int_{t_1}^{t_2} |net(t)| dt}{e_{design}.(t_2 - t_1)} \quad (4.18)$$

4.4.8 Dimensioning rate (DR)

The maximum absolute net power profile value at a particular time with reference to the designed capacity of the house can be expressed as dimensioning rate (DR).

$$DR = \frac{max[|net(t)|]}{e_{design}} \quad (4.19)$$

DR can be used for analyzing the capacity of power reduction from the grid. This analysis may be useful for considering different control strategies for domestic power reductions scenarios on the grid. It can be quantified as power reduction capacity factor and expressed as:

$$PR_{cf} = 1 - DR \quad (4.20)$$

If the house is not having on-site generation then accordingly the power reduction capacity factor can be modified.

4.5 Performance Evaluation and Grid Interaction of C6 house

Previously, in most of the studies the load matching analysis and grid interaction of on-site generation of ZEBs have been out of scope. Annual energy load profile of the house is going to describe the energy performance with peak demands. The importance of load matching analysis and grid interaction is increasing due to development in more complex dynamic energy systems with increasing penetration of renewable energy sources, energy storage, demand side management, and smart metering.

In power system analysis of BIPV system, the maximum power delivered/received to/from the grid information is very important from

distributed network planning/expansion. From the grid point of view, net ZEB analysis is necessary to analyze the peak demand from the grid especially in the winter month which will be similar to the other houses. This information is useful for finding the requirements of additional network capacity as well as generation capacity. Therefore, the ZEB quantitative analyses of load matching and grid interactions are important [55].

In this work, Skarpnes smart village houses are monitored for PV generation profiles with load consumption and also the load matching analysis and grid interaction of on-site generation. Main interest of balancing power with local on-site generation with the electricity grid is to increase the grid efficiency. The main focus is to not only analyzing PV on-site production but also the impact of such type of buildings on grid power quality. However, with large penetration of such type of buildings to the grid may contribute to the power quality as well as power management problems. It is important to analyze the real operational performance of BIPV through grid interaction indicators, which will help in making future planning of the distributed network when the BIPV penetrations are going to increase.

The C6 single family house has been monitored for the power quality using ELSPEC investigator, and PV production SMA power conditioning device. Details of the C6 house are given in the Table 1. Throughout this section, quantitative indicators analysis of grid interaction and load matching are presented. These indicators are vital to be analyzed for a ZEB to see the performance of energy exchange between the BIPV and grid. Various grid interactions and load matching parameters are explained in previous section. These parameters are analyzed considering the real time operational data of C6 house. These analyses are going to be useful for distributed network planning and expansion.

4.5.1 Analysis of Load duration curve and cover factors

It is essential to analyze the load distribution which will help in dimensioning cables and transformers for avoiding overloading as well as keeping the voltage regulation within the prescribe limit. For increasing penetration of BIPVs, injected power to the grid may create considerable concerns on power flows direction, voltage fluctuations, local losses, power system dynamics stability and control.

The analysis of ZEBs is going to help the distributed network planner to consider housing loads and on-site PV generation for handling the highest load demand and the highest injected power to the grid. It is also going to help the network planner on getting correlation between on-site PV generation with load and weather conditions. In future there may be requirements from the network operators to BIPV to operate as an active generator for frequency control as well as use the time of used (TOU) electrical pricing for reducing the peak demand (DSM).

The hourly load power consumption of the C6 house is given in the Figure 8 for a year (September 2015 till August 2016). It is noticed that the highest load demand is occurring in the mid of February with hourly energy demand of 7MWh. It is seen that the continuous interplay among on-site PV generation and the local load is resulting with import/export of energy with grid. This hourly load profile (Figure 4.7) is used for plotting the load duration curve (Figure 4.16). Similarly the hourly profile of the on-site PV generation for a year is given in the Figure 4.4.

This hourly PV generation is used for plotting generation duration curve. In the duration curves, the maximum hourly demand value load/generation considered (load has taken as negative and generation is taken as positive, but plotting considered individual peak values at starting of the curve). The contribution of net hourly power profile for a year from the grid with reference to the on-site PV generation and load is measured through ELSPEC investigator (Figure 4.7). This net grid contribution is plotted as duration curve (Figure 4.16). Graphical representations of load, PV generation, net contribution from the grid in the duration curve is useful in understanding supplied and exported highest values from the grid. The duration when the house is supplying or taking energy to and from the grid can be measured from the duration curve. From September 2015 to August 2016, it is observed from Figure 4.17 that the net export of the energy is around 2008 hours (4739.56 kWh) and for the remaining period of the year the energy is being imported from the grid (7493.07 kWh). This net energy contribution from grid can help in doing further analysis for finding the appropriate energy storage capacity for seasonal variations.

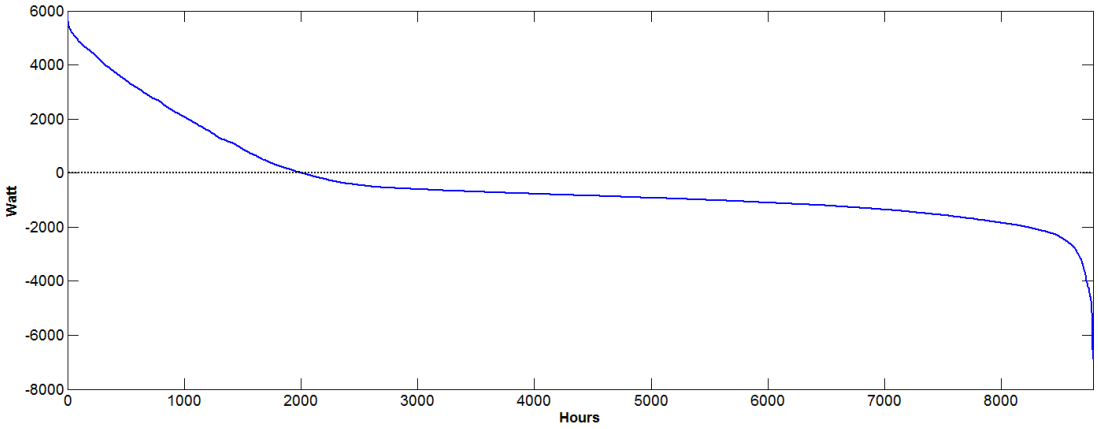

Figure 4.16 Net exported energy for house C6

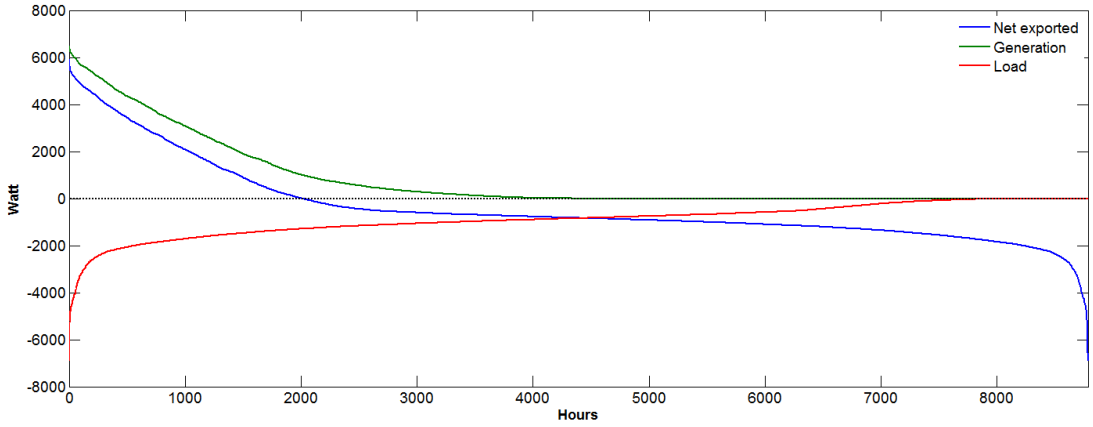

Figure 4.17 Load duration curve for generation, load and net exported energy for C6

Based on year load consumption and PV profiles, the CC_f for C6 house is at 80% and it may vary due to considerable variation of the weather. This CC_f analysis with probability distribution can help on finding capacity credit calculation to estimate additional capacity required for maintaining system competency in the presence of BIPV.

The annual cumulative energy produced by the on-site PV system is quantified with referenced to the annual cumulative load for the same time period. Quantification factor is defined as on-site energy supply-demand index (r_{esd}) equation (4.7), and for C6 house from September 2015 to August 2016, it is 0.8932. This index should have higher values to ensure better coincident with on-site PV generation and the load. It is necessary to evaluate the effectiveness of BIPV with reference to the load for reducing the grid dependency. This evaluation can be quantified using load cover factor and generation cover factor, which are explained in previous section in equation (4.9) and equation (4.10). In evaluating the load cover factor, during the specific time period the minimum value of on-site PV generation or the load is taken into account with reference to the load consumption during the specific time. Similarly the generation cover

factor is evaluated with reference to the power generation during the specific time.

In this study of this C6 house, the load cover factor is analyzed on an hourly basis and illustrated in Figure 4.18 and Figure 4.19, and generation cover factor is in Figure 4.20 and Figure 4.21. There is significant seasonal variation in both γ load and γ generation and these factors may help for demand side management. This is going to benefit the utility provider and consumer to plan and understanding in managing the power supply. The daily average of load cover factor and generation cover factor is analyzed and given in Table 4.6 and Table 4.7. Through these tables the seasonal variation of the load and the generation can be used for creating local demand side management profiles.

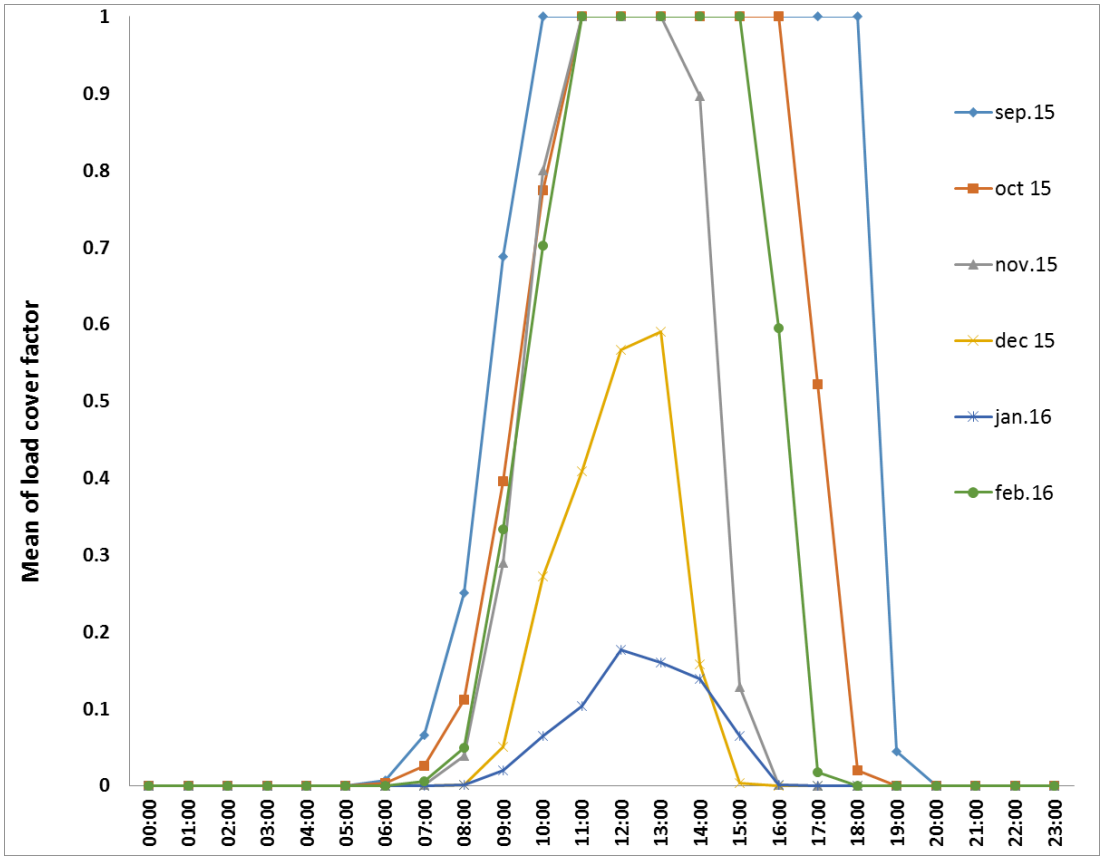

Figure 4.18 Mean hourly load cover factor (September 2015 – February 2016)

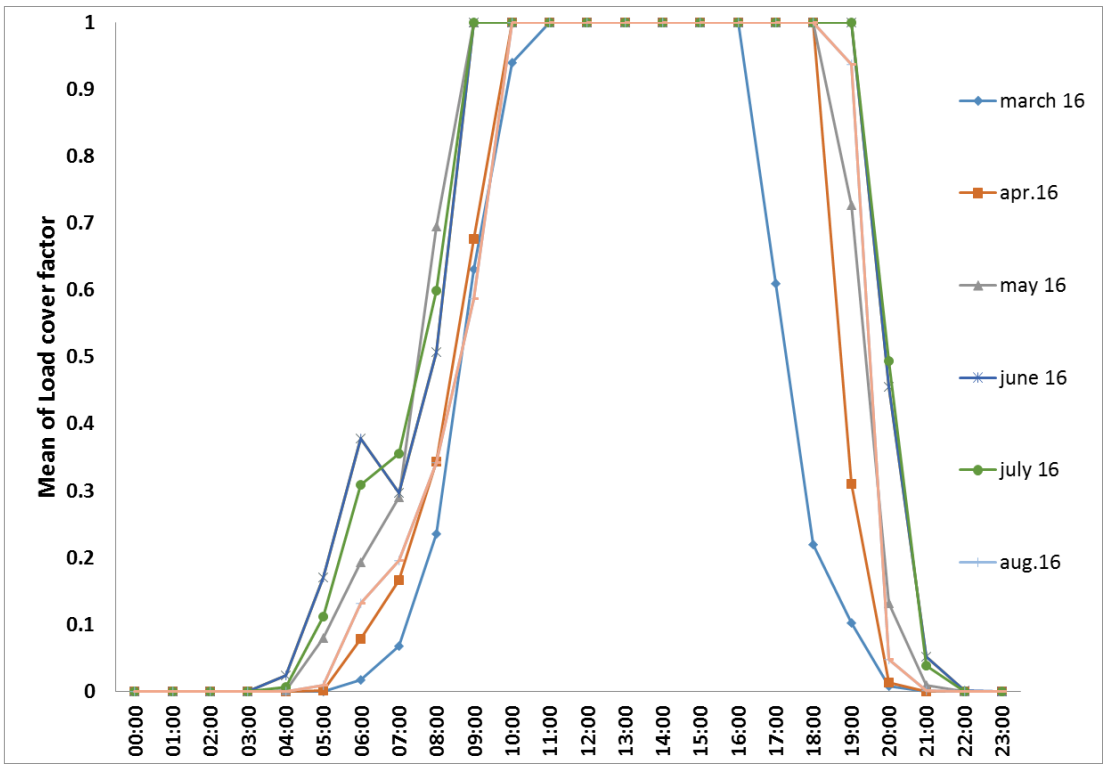

Figure 4.19 Mean hourly load cover factor (March 2016 – August 2016)

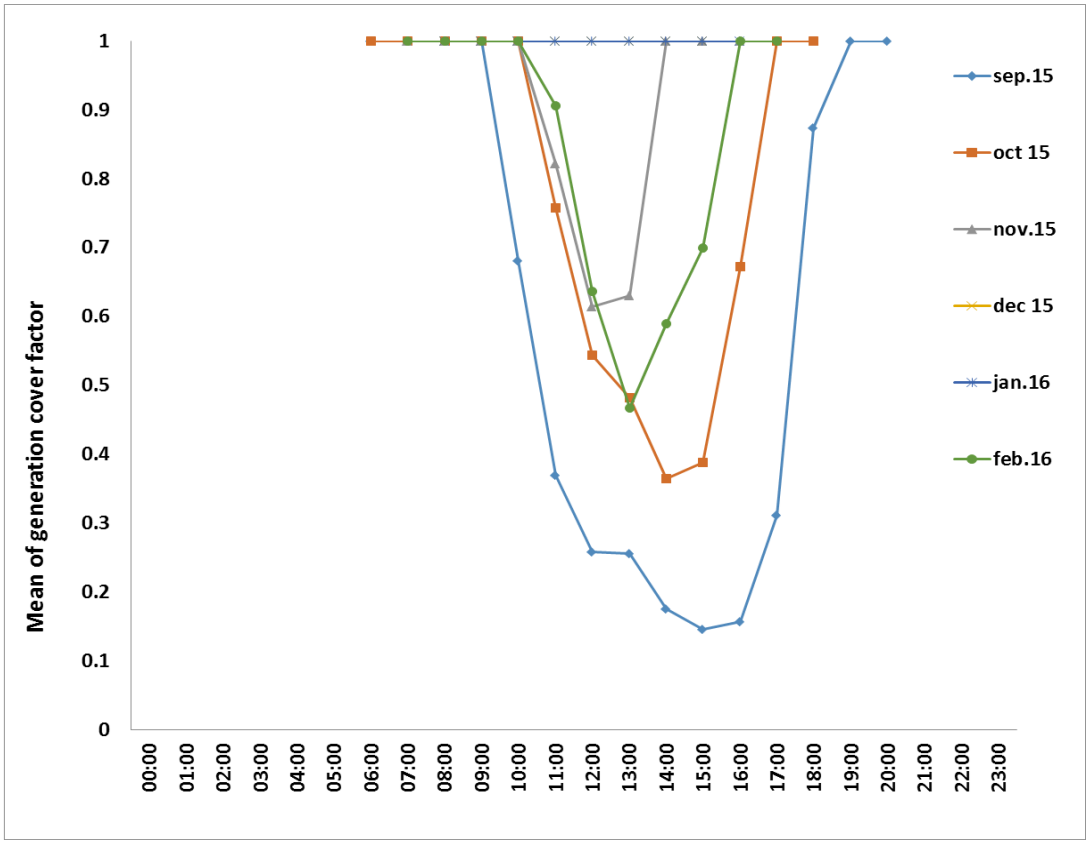

Figure 4.20 Mean hourly generation cover factor (September 2015 – February 2016)

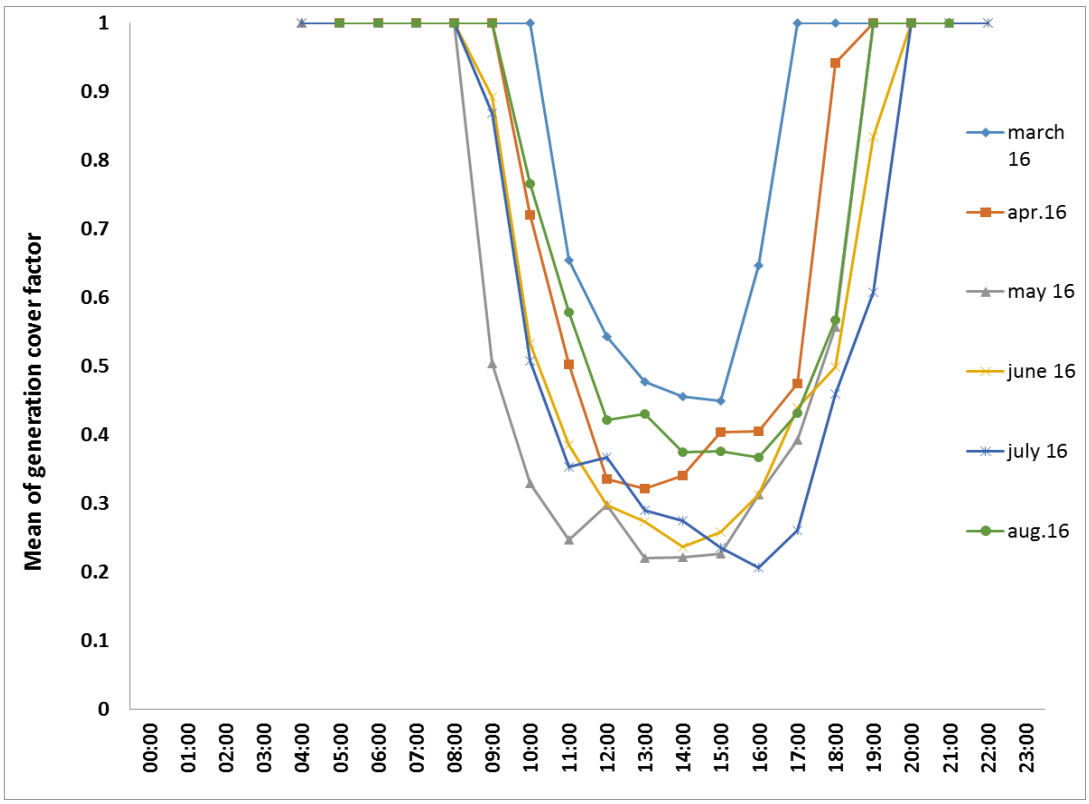

Figure 4.21 Mean hourly generation cover factor (March 2016 – August 2016)

For the first six months, it covers winter season (November - January). γ load diagram shows that in December 2015 and January 2016 there are no significant peaks compared to other months in the same Figure (Figure 4.18). The lowest peak recorded in January at 0.1770. This result tells us that the dependency to the grid is so high on January and on daily average is 3.05% (0.305) of load demand is covered by PV production. This can be seen from Table 6. For a clear comparison, for γ load = 1, the building energy is self-sufficient.

The rest of the months September, October, November and February the percentage of both factors (γ load and γ generation), change quite significantly. This can be seen through mean daily cover factor as in Table 4.6 (shaded columns is winter season). It has been mention earlier that, by adding storage system, the ratio of both factors will be better. Other option is adding geothermal storage system that can be utilized as a heating source.

Table 4.6 Mean daily cover factors for C6 (September 2015 – February 2016)

	Sept 2015	Oct 2015	Nov 2015	Dec 2015	Jan 2016	Feb 2016
γ load	0.4190	0.3237	0.2148	0.0854	0.0305	0.279
γ generation	0.6150	0.7850	0.9066	1.000	1.000	0.8453

Table 4.7 Mean daily cover factors for C6 (March 2016 – August 2016)

	March 2016	April 2016	May 2016	June 2016	July 2016	Aug 2016
γ load	0.3679	0.4412	0.5053	0.5368	0.5380	0.4688
γ generation	0.8150	0.7151	0.6820	0.6821	0.6540	0.7243

For the other six months (March 2016 – August 2016), this includes summer season. Based on Table 4.7, the changes for γ load is not that much compared to the value in Table 4.6. During summer months (orange shaded columns), with the longer day and good solar radiation, the load consumption will be supplied by the on-site generation and it can export the energy surplus to the grid, especially at noon. This pattern can be seen in Figure 4.20 and Figure 4.21. Based on Skarpnes energy output in 2016 May and July recorded the highest value. Figure 4.21 explains this phenomenon. The mean generation cover factor for both of these months recorded at the plotted curvature. Significant variations for both factors along the year can be seen. For example γ load is varies from 3.05% to 53.8%, while for γ generation it is from 61.5% to 100%. Based on the energy summary given in Table 4.8, and compared with Figure 4.20 and Figure 4.21 (Mean hourly generation cover factor), we can see the substantial effect on the curvature of γ generation on the months where the energy mismatch occurred.

Table 4.8 Energy mismatch summary for selected month where there are power delivered to the grid from on-site generation

Month	Energy IN (kWh)	Energy OUT (kWh)	Mismatch (kWh)	PV Production (kWh)	Consumption (kWh)
September 2015	448.65	507.62	-58.97	660.249	601.27
May 2016	640.03	863.61	-223.58	1108.23	884.65
June 2016	448.08	680.98	-232.90	1027.64	794.74
July 2016	416.52	734.57	-318.05	1090.63	772.58

4.5.2 Analysis on Loss of Load probability

In order to find the quantitative value on the performance of generated energy on-site compared to the load consumption, the loss of load probability factor (LOLP) can be used. LOLP is explained in previous section and expressed through equation (4.12). LOLP suggests how of the on-site BIPV supply does not meet the local demand. Annual LOLP for C6 house is calculated and given in Table 4.9. Also, the annual values of load cover factor and supply cover factor are presented together with the LOLP. For this house 35% time of the year, the load is not covered by BIPV generation. Since this is just a numerical ratio and it is not providing further information on exact amount of electricity supply. However, based on the cumulative real-time data from ELSPEC, the result signifies the LOLP ratio. PV production for the whole 12 months is 7.132 MWh, while the load consumption is 10.33 MWh. The energy deficit calculated is 37%: means that this is the amount the load is not covered by the on-site generation.

Table 4.9 Annual grid interactions parameters for C6 house

Parameter	C6
r_{esd}	0.893
LOLP	0.354
Annual γ load	0.3512
Annual γ generation	0.7809
$GM_{PV/l}$	0.9390
$GM_{e/d}$	0.854

4.5.3 Analysis on Generation Multiple

Once the building is connected to the conventional electrical grid, utility provider, and ancillary services needs to make sure the connection is 'healthy'. The needs of knowing generation multiple (GM) is crucial. Generation multiple (GM) is explained in previous section and expressed as in equation (4.13). In order to verify the effectiveness of generation strategies with respect to the grid operation, the GM can be very valuable information. For C6, the calculated GM is (0.939). The $GM_{PV/l}$ is around unity, which means that the peak PV production is approximately equal to the designed peak load. The same pattern of values can be seen for $GM_{e/d}$. For C6 the ratio is 0.854 as can be seen in Table 4.9.

The different GM ratios are analyzed with considerable design ranges using percentile values of supplied time of net exported energy. This has been explained in previous section and expressed in equation (4.16). To describe the nature of the data from all calculations and comparison that has been done,

statistical analysis on GM can be executed. This is a good method to explore the relation of the data. This is a ratio of higher percentile to the lower percentile and expressed as in equation (4.17). This ratio is to see the performance of each ratio in statistical approach. Higher percentile used are 99, 95, 90 and 75, while lower percentile considered are: 1, 5, 10, and 25. Graphically, this means:

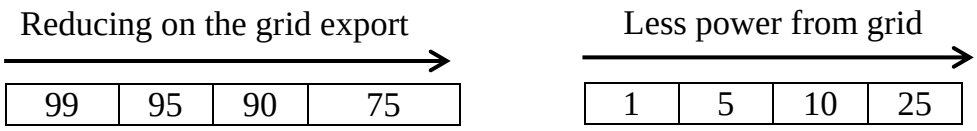

The result for this statistical analysis is presented in Table 4.10. This parameter is to find the changes of the peak power values of the export energy as well as of reducing or changing input power values from the grid. For power system network planning, variation in the peak export power to the grid and also in the peak demand from the grid can be used.

4.5.4 Analysis on Capacity Utilization Factor and Dimensioning Rate

Capacity utilization factor (CUF) for C6 house has been calculated based on the ratio of actual net energy of the house to the possible energy on the designed capacity. This parameter is as important as the Dimensioning rate (DR) factor. This factor is considered as maximum total net power profile value at a certain defined timeframe with reference to the designed capacity. This parameter may be useful for considering different control strategies for domestic power reductions scenarios on the grid. The CUF and DR for C6 house is calculated by using (4.18) and equation (4.19) and the results are as seen in Table 4.10.

Table 4.10 GM parameters for 3 different buildings

Values and ranges	C6
e_{design} (kW)	16
$load_{norm}$	0.432
PV_{norm}	0.406
$net_{norm,min}$	-3.879
$net_{norm,max}$	3.713
$GM_{net,\ 100/0}$	0.957
$GM_{net,\ 99/1}$	1.774
$GM_{net,\ 95/5}$	2.259
$GM_{net,\ 90/10}$	1.923
$GM_{net,\ 75/25}$	0.173
$GM_{net,\ 99/0}$	0.808
$GM_{net,\ 95/0}$	0.609
$GM_{net,\ 90/0}$	0.418
CUF	0.023
DR	0.015

4.6 Performance Comparison of C6 House (Norway) with Flamingo House (FH) and Energy Flex House (EFH) of Denmark

The grid interactions and load matching comparison with other such type of buildings are important. In ref [54], analysis of these parameters for some of the European buildings are reported. Among them the two buildings (i.e. Flamingo house (Taulov) –FH, Energy Flex house (Taastrup) – EFH) are used for making comparison with the Skarpnes ZEB. In this section, all of the grid indicators and load factors that have been evaluated and discussed in the previous subchapter are compared with these two buildings located in the Denmark at Taulov and Taastrup.

4.6.1 Flamingo house (Taulov) –FH

This single family house was built in 2008 and the hourly result collected and compared is based on 1 hour resolution 2012 data. It is not a ZEB house; hence it was built with a PV array, geothermal and solar thermal. The in and out energy is being monitored since February 2009. This is a private owned house. The details are as in Table 4.11.

Table 4.11 Flamingo house basic characteristics

Characteristic	Value
Initial installed PV	2.0 kWp
Increased installed PV (factor of 4.5)	10.0 kWp
Building area	166m^2
Designed capacity	10kW
Technologies	PV/ Heat pump and Solar thermal

4.6.2 Energy Flex house (Taastrup) – EFH

This building begins its operation by autumn 2009. With a 12 minutes resolution of data, this building is considered a typical design of Danish single family house. It was built with PV array on top of the roof and heat pumps and solar thermal as a source of heat. The data recorded for this building is excluded the electric vehicle usage and basic parameter of this building is as in Table 4.12. This is a test facility for the 'Green lab for energy Efficient Buildings' (GLEEB). It is owned by the Danish Technological Institutes.

Table 4.12 EF house basic characteristics

Characteristic	Value
Initial installed PV	10.6 kWp
Building area (double storied)	216 m^2
Designed capacity	25.2kW
Technologies	PV/ Heat pump and Solar thermal

Based on the normalized load for all buildings, EFH has the lowest with only 0.249, while for C6 it is 0.432 and FH is 0.526. For EFH with the lower load requirement and larger building size (216m^2) and greater installed PV area (60m^2), the result looks convincing compared to the other two dwellings. For PV output, based on the normalized values, FH location looks promising with 1.040 contrasted with normalized values for C6 (0.406) and EFH (0.361). Based on this, both buildings in Denmark is way ahead of C6. Even with a lower normalized PV values, EFH installed PV area is higher than in C6. These differences give a significant impact on other calculations based on the data for all buildings. Based on this, we can measure the maximum and minimum values for the buildings. Net exported basically is energy in subtracted with energy out. This value is important to see the energy flows and energy balance. It seems like in C6, energy flows in and out is extremely high. The result is as seen as in Table 4.13.

Comparing $GM_{net,100/0}$ C6, FH and EFH, the value for the houses in Denmark scores a ratio of >1.0. For a real ZEB, the GM should have the ratio

of energy in and out at least 1.0. FH is a non-ZEB house; initial ratio for FH initially was 0.268. The data for this house has been generated artificially and the PV capacity has been increase by the factor of 4.5. Thus, the new output shows the GM for this house is reaching ZEB status. By doing rough calculation, C6 may increase the generation multiple ratio by increasing the PV installed capacity to 10kWp to at least achieve 1.0 GM ratio. By varies the higher and lower percentile for each of the building output, we may know the performance of the net exported energy. From Table 4.13, for FH and EFH we can see the decreasing trend, as we reduce the export power to the grid. However, for C6 the there is no specific trends. By delivering power to the grid at 95% and 5% of power from the grid, the ratio reaches up to 2.259. It indicates that at that ratio, the probability of power exchange from the grid to the house and vice versa is the highest. Hypothetically, when the lower percentile is zero, there is no peak shaving happening. For $GM_{net,99/0}$, $GM_{net,99/0}$ and $GM_{net,90/0}$ it is a calculation based on C6 data on what are the ratio if the buildings is only using on-site energy with different value of higher percentile (99, 95 and 90). The lower the grid export values, the lower the ratio goes. Similar trends occur on FH and EFH. Since both are ZEB, the ratio is rather lower than the non-ZEB results (C6).

Table 4.13 Comparison of parameters between 3 different cases

Parameter	C6	FH	EFH
LOLP	0.354	0.701	0717
CF	0.023	0.151	0.069
DR	0.015	0.725	0.345
$GM_{PV/l}$	0.939	1.967	1.449
$GM_{e/d}$	0.854	1.377	1.398
e_{design} (kW)	16	10	25.2
$load_{norm}$	0.432	0.526	0.249
PV_{norm}	0.406	1.040	0.361
$net_{norm,min}$	-3.879	-0.526	-0.247
$net_{norm,max}$	3.713	0.7245	0.345
$GM_{net,\ 100/0}$	0.957	1.377	1.398
$GM_{net,\ 99/1}$	1.774	2.174	1.845
$GM_{net,\ 95/5}$	2.259	1.990	1.779
$GM_{net,\ 90/10}$	1.923	1.539	1.500
$GM_{net,\ 75/25}$	0.173	0.451	0.213
$GM_{net,\ 99/0}$	0.808	1.223	1.228
$GM_{net,\ 95/0}$	0.609	0.950	0.897
$GM_{net,\ 90/0}$	0.418	0.670	0.605

4.7 Techno-economic analysis of ZEB house

Other important variable that needs to be understood is techno- economic assessment. It is required prior to executing any project. For the house in Skarpnes, main supply of electrical energy is the grid and the PV array installed on the roof. For a residential BIPV system, 45% of the capital cost of PV systems is coming from the hardware (modules, inverter, racking), while 44% is based on soft cost (engineering, procurement and construction) and 11% is for installation and labor cost [56]. As per 2015 the variable and its prices can be concluded as below (Table 14). This is based on National Renewable Energy laboratory (NREL) reports, November 2015 [20]. The price varies according to the region and countries; however this can be used as a base price.

With the high initial cost of developing BIPV, it is expected that the return of investment (ROI) will be longer. The payback period of this project based on results [3] is 21 years, assuming that the energy price is static and that the price of PV panel and installation will be decreasing by 2.1 % every year. This period will vary depending on the fluctuations of energy price from the grid and the price of PV systems, which is expected to continue to decrease in the near future.

Analysis has been done with a few estimation and assumptions in order to evaluate the economic feasibility of the project. It is important to know the net present cost (C_{NPC}) of the project [43]. C_{NPC} values will define the project acceptability in terms of investment, and consider the variance in current value of the future investment. Positive C_{NPC} values are an indicator of a potentially feasible project.

The following equation has been used to calculate:

$$C_{NPC} = \frac{C_{TAC}}{CRF_{(i,N)}} \tag{4.21}$$

Where C_{NPC} is the total net present cost, C_{TAC} is the total annualized cost, and $CRF_{(i,N)}$ is the capital recovery factor. To get the it, the following equation [43] applies;

$$CRF_{i,N} = \frac{I(1+i)^N}{(1+i)^{N-1}} \tag{4.22}$$

where *i* is the annual interest rate or the discount rate and *N* is the number of years. From HOMER simulation the NPC value in this case study is NOK 173,579 (≅USD 20,624)[4] and the levelized cost of energy (LCOE) is NOK 1.59 (≅ USD 0.189) per kWh. Operating cost ($C_{operating}$) is defined as the annualized all costs ($C_{ann,total}$) minus the initial capital cost ($C_{ann,cap}$). It can be represented by the equation:

$$C_{operating} = C_{ann,total} - C_{ann,cap} \tag{4.23}$$

Analysis is done based on 25 years of system lifetime. In the analysis, it is assumed that all prices are escalating at the same rate, and where 'annual real interest rate' is used rather than the 'nominal interest rate' [57].

The energy price will significantly change the whole economic assessment. This depends on type of fuels, transmission and distribution system and regulations from different regulators. In Norway it is controlled and basically it is unchanged due to increase in the tax on the consumption of electricity. The energy price is based on Norwegian energy price available in Statistics Norway. The energy price is relatively flat throughout the day. There is no time of use (TOU) price allocated for Norwegian energy pricing, hence there is no concern for the customer to particularly running appliances according to peak and off-peak price.

4.8 Discussion and Conclusion

The Skarpnes residential development is initially expected to demonstrate zero energy and zero emission building. This is done by trying to implement the conventional technologies, hence in an innovative manner so that the building will be an optimal solution for a so-called zero energy building. This is with regard to energy production, tenant comfort and energy utilization.

The smart house is located at the southern part of Norway, where it has most sunshine days in Norway. Initial plan is to monitor the production and consumption of a group of houses at the similar area, hence this is far from occurring. However based on few houses that has been build and connected to the sensors and advanced smart meters, daily, weekly and annual load profile can be captured, thus the plan on developing a new business model that can benefits the energy provider and consumer [58].

[4] USD 1.00 = NOK 8.42

Real time PV output monitoring is the crucial parameters in this work. Based on the data collected from house C6 rooftop PV array, the energy output can be determined. Mismatch data for one year (September 2015 – August 2016) has been captured and calculated to see the C6 hose performance. Imported energy to and from the grid as well as the load profile for C6 is concluded. Based on all of this data, the house condition, the performance of the house can be seen through energy mismatch plot (Figure 4.13) and this is based on the measured data from Figure 4.13. Based on this Figure, it seems like C6 is in an 'unhealthy' for ZEB conditions.

The load matching index, load duration curve and grid interaction index have been analyzed for grid integration of the ZEB. The result for C6 house shows that the building has its capability of imported energy to the grid during summer. This is based on load cover factor and generation cover factor results. These have been presented thoroughly in graphical method (Figure 4.17, Figure 4.18, Figure 4.19 and Figure 4.20) and in a table form (Table 4.6 and Table 4.7). The load and generation cover factor is a quantified value with reference to the on-site generation and the load.

The loss of load probability factor has been evaluated to see the performance of on-site energy generation. C6 house has a fairly good ratio, where the score is 35%. Then, calculation on generation multiple (GM) for the building is executed to relate the on-site generation result with reference to the local demand. For C6 house, the $GM_{PV/l}$ is around unity, which tells us that the peak demand is almost equal to the designed peak load. While for $GM_{e/d}$ the result is at 0.854, which is relatively good. Based on statistical method of calculation, different GM ratio can be calculated. By varying the input and output energy, the house and grid interaction can be verified (Table 4.10). Capacity utilization factor and dimensioning rate for the house has been analyzed. Both of this parameter is crucial for consideration of different control strategies for the ZEB and to implement the HEMS.

To see the Skarpnes smart house performance in the real world, comparison with another two different buildings (i.e. Flamingo house (FH) and Energy flex house (EFH)) in Denmark has been considered. C6 house, Flamingo house (FH) and Energy flex house (EFH) is being compared based on the similar parameters. Based on the output as exhibited in Table 4.13, C6 is in a good position in achieving ZEB status if only there are several modifications are made. Location wise, installation of solar thermal collectors will definitely help

in achieving zero. Battery storage is another innovative invention that might lead C6 towards achieving ZEB status.

Achieving ZEB goal, which is an environment of energy balance is rather ambitious. Assuming all electric appliances is in a good state and very energy efficient is one challenge that the project owner needs to confront. Other than that, primary concern is the house owner lifestyle, as this might give a huge impact on the output. Initial plan to use geothermal energy as a solution of thermal heating might be a good solution for the house to achieve ZEB status. Electrical energy consumption during winter will be ridiculously high, by using natural thermal energy might save a lot. The existence of electric vehicles might lead into negative energy balance to the house and the energy mismatch might change a lot. For a pilot project, this is a good start as researchers may use this Skarpnes Smart Village project as benchmarks to achieve ZEB status and better energy mismatch.

Chapter 5

5 Impact of Increasing Penetration of Photovoltaic (PV) Systems on Distribution Feeders[5]

This chapter investigates impact of increasing photovoltaic (PV) penetration on distribution feeders. The main focus of this work is on 'how different amount of PV systems can influence the protective devices in the distribution feeder'. Roles of PV systems in a feeder have been analyzed considering 3ϕ fault, fault location and protective devices (PDs) settings (e.g. time of PDs operation before a fault gets cleared by it). It is also emphasizing on 'how the penetration of PV can affect voltage quality / unbalance in the distribution feeder'. The considered distribution feeders are supplying domestic area and therefore loading on different phases are unbalanced. The voltage quality at different nodes is analyzed not only due to domestic load distribution but also due to integrated PV systems output variations. The results show that increasing PV penetration can escalate PDs' operating time during 3ϕ faults. This work has been carried out using DigSilent PowerFactory®. The system is representation of a huge system of PV based active generator without storage system.

[5] *Modified from the paper published and presented in a peer review conference. IEEE International Conference on Smart Grid and Clean Energy Technologies (2015 ICSGCE), Offenburg, Germany. DOI: 10.1109/ICSGCE.2015.7454271, Pp: 70-74, 2015.*

5.1 Introduction

Large scale penetration of intermittent renewable energy sources (e.g. PV systems) and other distributed generators in the smart grid environment require the development of a load dispatching methodology by considering not only the active inertia of the power system but also using frequency-droop characteristics like conventional generators approach. The integration of intermittent renewable energy and other efficient distributed energy resources into existing and future electricity networks represents significant technical and economic challenges. The widespread development of such systems requires a thorough analysis of all technical and commercial aspects of renewable energy sources and other decentralized generation units in the distribution network. In power system network, the power quality is very important. Due to PV power output fluctuations; there are some chances for power quality disturbances e.g. voltage transients due to intermittency, harmonics, active and reactive power management, power delivery angles and a lot more reasons. In the conventional grid connected PV generators, hybrid filters are used to improve the power quality [59]. However, for multiple PV based active generators (e.g. group of buildings with BIPV), the power quality issues require more detailed analysis. Also it is important to analyze the fault protection system [60].

The higher penetrations of distributed generators are going to create different possibilities of the faults not only in the micro-grid network, but also at the higher voltage power system network. Fault detection and isolation mechanism is very important for power system operation. It is needed to analyze the fault protection system under increasing penetration of PV systems (e.g. fault current levels, relay settings, fault clearing time in the micro-grid environment). During fault or any unwanted events and abnormal conditions at the micro-grid network, the grid may be disconnected, and islanding effect may occur in micro-grid [43]. Fault currents in an islanded mode based micro-grid are not going to be similar as fault occurs in a conventional grid system. Therefore methods for isolating the faults of the conventional grid system are needed modification in the micro-grid system [1]. In a micro-grid network, there are limitations on protection system due to the islanding operation mode. Also the fault clearing time is important for micro-grid stability, operation and safety. It is needed to include/coordinate control signals of the protection mechanism in the EMS of micro grid. In this work, the fault analysis of the PV systems in the micro-grid network are analyzed in both islanded as well as grid connected modes.

Examination on the effects of high diffusion PVs on a distribution feeder's protection and operation is reported in [4]. Increasing penetration of PV systems on a feeder will affect the voltage variation due to change in solar radiations. In this work, the considered distribution network topology is based on [61]. This work is using DigSilent PowerFactory® simulation software. It has the ability for doing load flow calculations with integration of PV systems, electromagnetic transients and as well as transient events during abnormal operation of the distributed network.

5.2 Distribution feeder modelling

The grid system modelled in PowerFactory® is represented as a single line diagram, which is given in Figure A26 (Appendix A) and it is based on [61]. The load symbol in the figure is representing a group of houses. Each PV system in its lumps a number of separate PV modules connected in parallel as an aggregated PV system. The rating of each PV module is equal to the peak of the load and it is represented as:

$$P_{PV,peak} = P_{load,peak} \quad (5.1)$$

The considered network has three voltage levels: (i) external grid at 69 $kV_{line-line}$, (ii) distribution feeders 12 $kV_{line-line}$, and (iii) domestic buildings 0.24 $kV_{line-ground}$. In this distribution network, considered loads are domestic and PV systems are connected in a single phase and thus, the system is going to be unbalanced. In the PowerFactory® software the following load parameters for a private home are used: peak load of 1.14 kW with power factor 0.95 lagging. Based on equation (1), each house's PV system rating has taken as 1.14 kW.

5.3 Power flow analysis

The power flow calculations are studied for considered distribution network topology (Figure A26) for following some scenarios (Table 5.1). The variation of loads between 50% and 100% are considered, and PV system outputs variations are considered from 0% to 100% based on PV availability. These scenarios may change in real conditions, but considered scenarios are going to provide some information on voltage quality of the network. Legends of these scenarios are given in Table 5.1 and they are referred in Figure 5.1, Figure 5.2 and Figure 5.3 for each phase voltages.

Table 5.1 Some Scenarios for Variation of Load and PV

Scenario	Load (%)	PV (%)	Legend
1	100	0	
2	100	50	
3	50	50	
4	50	100	
5	50	0	

5.3.1 Distribution feeder voltage level and balance

In this section the investigation on how the voltage levels are affected by PV is simulated. The distribution feeders are unbalanced and the voltage levels must be within the limits that has been decided by TSO (transmission system operator) and based on the PDs capabilities. Based on Table 5.1, voltage levels are plotted for node 1 to node 16 (refer: Figure 5.1 for node identification), to see how the voltage level varies in each phase for different scenarios.

The voltage variation that occurs as seen in Fig. 2, Fig. 3 and Fig.4 is an expected problem due to PV penetration into distribution feeders. For future simulation work, reactive compensation device (e.g STATCOM) will be included to overcome huge voltage variation and reverse power flow problem [62].

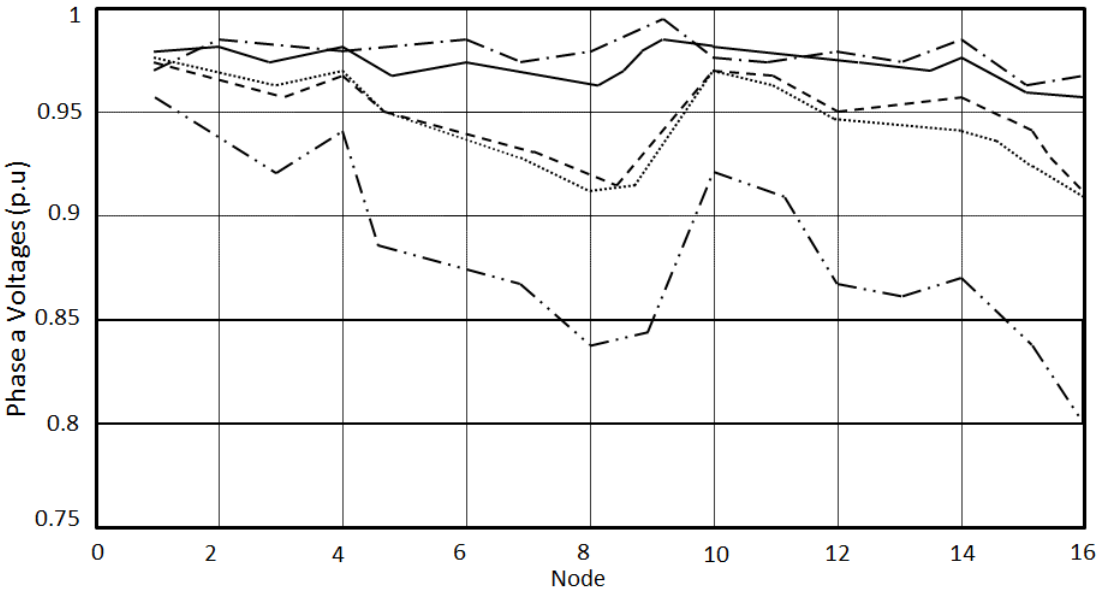

Figure 5.1 Phase a voltage magnitude for the system nodes

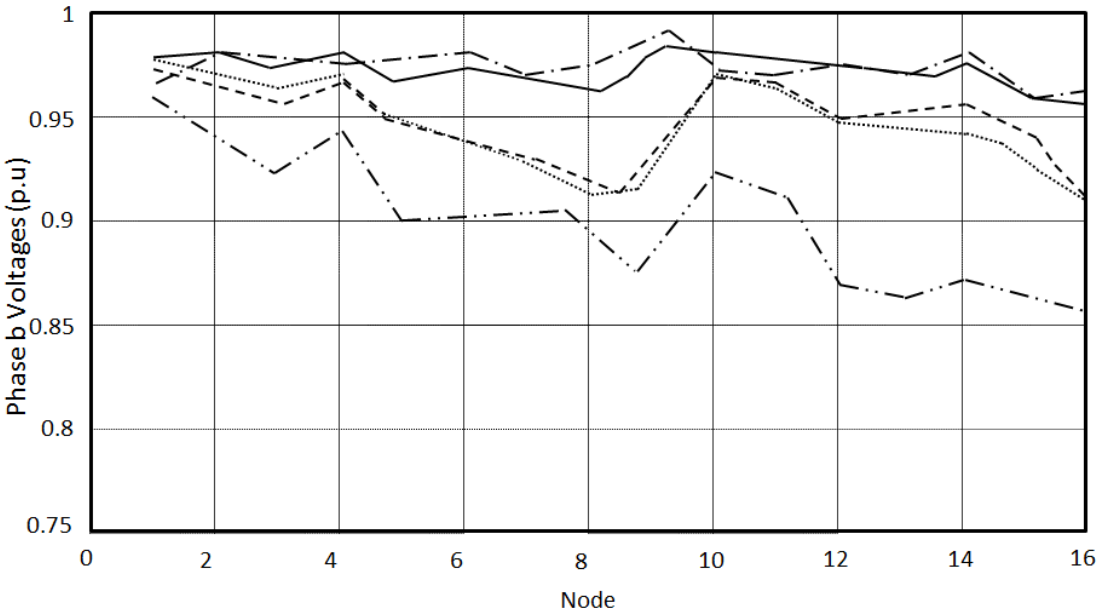

Figure 5.2 Phase b voltage magnitude for the system nodes

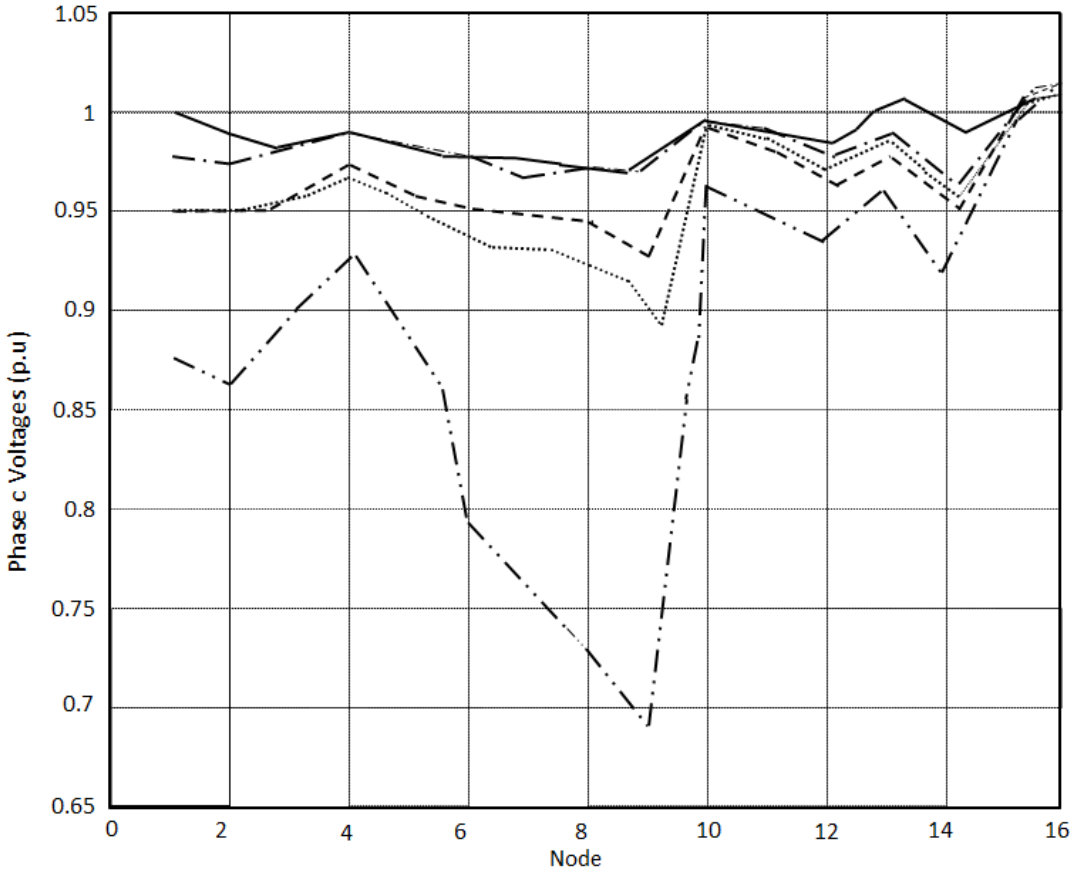

Figure 5.3 Phase a voltage magnitude for the system nodes

It can be seen that when $P_{PV} \approx P_{load}$ voltage curves are almost flat and the losses is quite small. However, with no PV (PV = 0%) the voltage is dropping along the line. Hence, with no PV (PV = 0%), the losses are quite high. In phase c, the

voltage drop significantly at node no: 7, with the voltage p.u is less than 0.7.

5.4 Photovoltaic Operation and Protection Devices- Relay

In this section the influence of PVs on fault current simulation and protection devices (PDs) are investigated. At first the documentation of the modelled PDs are presented, then some simulations are performed to see how the PDs perform considering various levels of PV generation with the fault current analysis. Three different positions of protection devices are evaluated. There are standards used for fault calculations by International Electrotechnical Commission (IEC), Verband der Elektrotechnik (VDE), Institute of Electrical and Electronics Engineers (IEEE), British standards (BS) and American National Standards Institute (ANSI). Here are the lists of standards [63] that are available to calculate short circuit currents;

1) IEC 60909-2001
2) VDE 0102:2002-07
3) IEEE 141-1993
4) ANSI C37.010.1999
5) ANSI C37.5
6) BS 7639:1993
7) BS EN 60909-0:2016 which replaces (1)

For this particular chapter, IEC 60909-2001 is used. This is referred to the selection in the DigSilent PowerFactory® [63].

5.4.1 Protection Device

There are four main protection devices in the system. These devices are breakers or switches that are supervised by over current relays. Fig. 1 shows the position of each of the PD. Based on this figure, there are two PDs for each feeder. At this point the PVs are set to 0% generation and the loads are at 100 %. This simulation is to see the amount of rated currents that will flow through the PDs. Thus, all PVs are set to be ‘off’ and an unbalanced power flow algorithm is simulated. The results can be seen in Table II.

Table 5.2 Maximum currents flowing through PDs under normal conditions

Protection Device	Current (A)
PD 1-1	605
PD 1-2	196
PD 2-1	571
PD 2-2	184

The scheme for the Over Current Relays (OCR) in PowerFactory® is developed from 5 working blocks (refer: Figure 5.4). The current are measured by a current transformer (CT). The CT will be given a rated value, corresponding to the currents in the recent power flow (refer: Table 5.2). In the blocks labelled 'I >' and 'I >>', the maximum allowed current magnitude for the PDs are set. Time limit for the current are also set, for the duration that the system can endure the currents before the breaker gets activated. If current with magnitude of larger than 'I >>' are flowing to the PD, the switch will disconnect and isolate the respective line. 'I >' will only respond to fault that are smaller amount but continuous over some time.

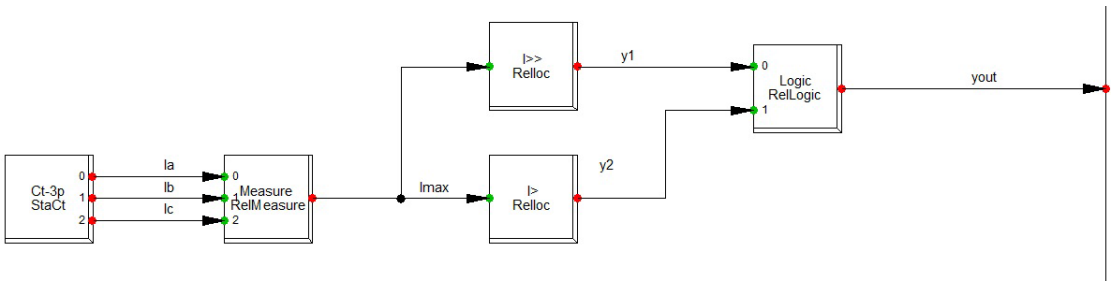

Figure 5.4 PowerFactory ® Over current relay scheme

The parameters given in the over current relay can be seen in Table 5.3:

Table 5.3 Over current relay parameters for Circuit breakers

Response	Magnitude (pu)	Time (s)
Slow response (I >)	1.2	1
Fast response (I>>)	2	0.02

These parameters are used for relays. It can be seen from Table III if the current magnitude are 20 % above rated, for a time larger than 1 second, the PD will disconnect the respective branch from the grid. Under abnormal conditions where the current is larger than 2.0 p.u, fast response will be executed.

5.4.2 PV Protection

For a PV system that connected in parallel with the electric utility, there are special recommendations made by the IEEE standards committee. This is to ensure the safety of workforces, utility system operations and equipment protection [64]. Based on the IEEE Std 929-2000 (IEEE Recommended Practice for Utility Interface of Photovoltaic (PV) Systems), the response time to abnormal changes for any voltage disturbance can be define as:

Table 5.3 Protection scheme for a domestic PV array

Voltage*	Max trip time
V<60	6 cycles
60≤V<106	120 cycles
106≤V≤132	Normal Operation
132<V<165	120 cycles
165≤V	2 cycles

*Based on a system voltage assume at nominal 120V

The protection scheme for PV array in PowerFactory ® is given with 3 parameters that can be change. Switch-off threshold, switch-on threshold and switch –on delay. The switch 'off' value is set as 0.5 p.u and the switch 'on' value as 0.9 p.u. Hence, the PV gets disconnected if the PV terminal voltage is below 0.5 p.u in 0.010s. The protection scheme will reconnect the PV automatically according to the Switch-on Delay time.

5.5 Analysis on fault

For this paper, the fault analysis has been done only at node 4 (refer Fig. 1). In Table V the fault scenario parameters are given. The fault resistance in transmission lines can be calculated by using different model of arc resistance [65]. The common equation that has been used as based equation is the Warrington equation:

$$R_i = \frac{(28707.35\ x\ L)}{I} \tag{5.2}$$

Where:

R_i = Arc resistance (Ω)

L = Arc length (m)

I = RMS value of fault current

This equation is derived from the Warrington's test with an assumption of bad measurement was omitted. The weakness of this model is that the range of arc current is below 1kA which is low and new formula introduced by V.Terzija and Koglin [66, 67]. Since then, a few others expression has been introduced to find the real magnitude of arc current. The parameter that has been used in this simulation is based on Table 5.4, this is based on data from [61].

Table 5.4 Fault resistance parameter (at node 4)

Phase	Fault resistance (Rf)
3	0
3	0.11
1	0
1	0.17

A short circuit event is created for each scenario. Then the RMS analyses are simulated. The idea is to see if the level of solar radiation will have an impact on the PD response time. Based on Fig. 6, it shows that solar radiation has an impact on how fast the PD disconnects during fault. Hence, the time variation is quite small.

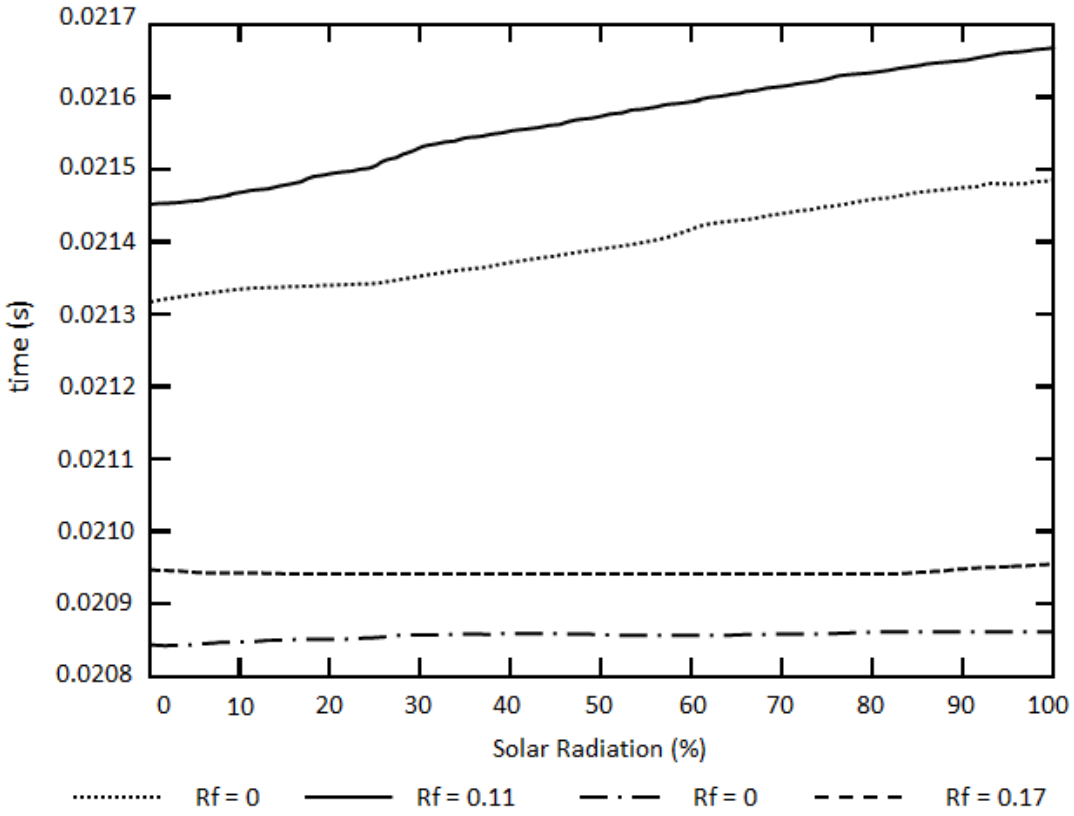

Figure 5.5 Effects of PVs on the operating time of PD at node 4

For a 3ϕ fault with Rf of 0 Ω, the operating time is increasing from 21.36 millisecond (msec) to approximately 21.4 msec. The most significant rise can be seen for 3ϕ fault with Rf of 0.11 Ω. It grows from 21.47 msec to nearly 21.70 msec. This variation is rather small, however in protection system, every micro-second is vital [68]. There are obvious impacts on PV based on fault current magnitude. This can be simulated by applying a fault at one of the branch (refer Fig. 1).

During fault, the PD will react automatically. Figure 5.6 shows the p.u voltage drops down significantly after the PD is activated. During the fault occur, PV 1(refer Figure A26) will shut down. Figure 5.7 shows that fault current is almost 5 kA before it is drop to 0A once the PD system is activated. The same pattern of voltage and current parameter is anticipated on the other PV system in the same distribution system. Nevertheless, with a large number of PV connection throughout the distribution feeders, the vast effect should be expected and the most common thing is fault current transients in distributed generation will have initial high "subtransient component" [69]. Further work will consider more nodes in the distribution feeders and comparisons between faults in a conventional feeders and distributed generation with a great number of PV systems will be executed.

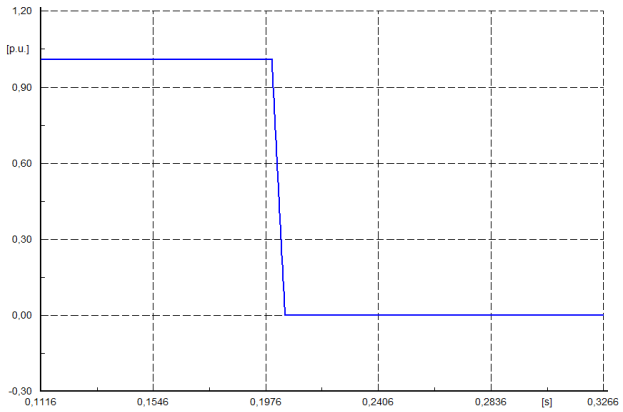

Figure 5.6 Voltage at Node 1 during fault (voltage in pu versus time in sec)

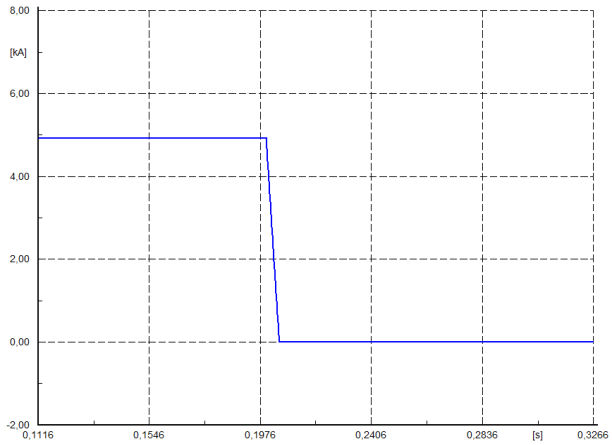

Figure 5.7 Current from PV at Node 1 during fault (current in kA versus time in sec)

5.6 Conclusions

Power quality is important in power system analysis. The widespread uses of distributed generators (DGs) are creating many power quality issues. It may lead to the multiple harmonics, voltage fluctuations, and unstable operation in the power system network. This work has considered into the most important thing in DGs, the fault analysis. High PV penetration into the distribution system will give a huge impact to the protection system. The existence of PV array in a huge quantity in a system may prejudice the grid safety in terms of protection scheme and safety. Based on the simulation, the results show that high penetration PVs will give a significant impact on voltage profile. It will also affect the overall system protections. Fig. 2, Fig. 3 and Fig. 4 is the comparison of the per-unit voltage under different system of operating at a different node. The highest p.u voltage is happening in scenario 4, where the PV generation exceeds the load. This result may vary if the PV array output is taken into account, meaning that for a different geographical location, it might affect the PV array output.

Based on IEEE Standards 929-2000, PV systems protection scheme needs to be monitored so that the response time will meet the regulation within the range. The PDs and all protection devices need to act as the standards. In PowerFactory® settings, the result in Figure 5.6 and Figure 5.7 can be seen with a total shut down after fault. As for future work, the impact of the high penetration of DGs especially PV in a transmission lines can be simulate in a different load profile with a different season (winter or summer). Purpose of this work is to get understanding of increasing PV systems and to replace the network topology using local Norwegian distribution network parameters, which will be reported in further work.

Chapter 6

6 Conclusion

PV based active generator is an active solution for the increasing penetration of PV into the conventional grid system. Thus, this dissertation has presented an ideas on PV based active generator, its application on Skarpnes smart house project, power management for short term and power balancing in a circuit and protective scheme on the system. This is somehow covers many of the pertinent issues on the PV based active generator to be implemented in the real world.

Chapter 2 has presented analysis of PV based active generator in microgrid. Its utilization is discussed for operational planning of the power system and also for instantaneous power flow management in the smart grid environment. The application of this system is part of a solution on handling a large scale deployment of grid connected distributed generators, especially PV system. By implementing the PV based active generator, it will be very flexible able to manage the power delivery from the active generator sources (e.g. PV system, energy storage technologies, active power conditioning devices).

PV based active generator architecture and its control strategies have been discussed in Chapter 3. They can be implemented into managing the power while maintaining the reliable supply to the load. The active and reactive component has been managed and controlled by using a hierarchical control approach. Based on the simulation, PV based active generator is able to manage power locally by taking grid constraints into consideration. The developed architecture can provide the active and reactive power to meet the load demand reliably and at the same time improving the power system operation as well as helping demand side management. The analysis shows that synchronous

reference frame converter with DC voltage regulator can be implemented in the PWM switching control layer for giving acceptable achievement.

The usefulness of ZEBs for load matching with BIPV generation profiles and grid interaction analysis are presented in Chapter 4. In this chapter the real operational results of a year from a ZEB house of Skarpnes smart house project are analyzed for annual energy balance with on-site PV generation and local load. The load matching index, load duration curve and grid interaction index have been evaluated for the grid integration of the ZEB. The loss of load probability factor has been assessed to see the performance and it will be useful for finding an additional capacity of PV as well as energy storage for fulfilling the local load at desired reliability level. The generation multiple with different percentile of net energy are investigated, which will be useful for DSM as well as energy storage capacity. Performance evaluation of a ZEB from Southern Norway is compared with two different buildings from Denmark.

Impact of increasing PV penetration in distributed network on power flow as well as fault analysis is discussed in Chapter 5. Fault execution in certain areas is investigated for protection devices settings, where a large number of PV source are connected in distributed network. Also, voltage quality at different nodes is analyzed not only due to domestic load distribution but also due to BIPV systems output variations. The results are analyzed by considering for 3ϕ fault, fault location and protective devices (PDs) settings.

The most significant contribution of this dissertation is on the PV based active generator as a tertiary source to be connected to a conventional electrical grid system. Given the available technology nowadays, there is no doubt that this system may turn into a huge thing one day with a proper design, higher equipment efficiency, and better planning. The on-going problems are the expenses of implementing PV array with battery and supercapacitor. The price is still outstandingly high and the return of investment and payback period is stretched long. Hence, with a proper planning and as the technology is expanding, it is possible to make the system worth to implement and providing efficient energy.

6.1 Scope for Further Work

This research will be more interesting to be extended further. Recommendations for future research are divided into several parts. There are:

- It would be interesting to integrate the Skarpnes smart house project with the active demand side management. By combining the DSM and storage system in the ZEB might give a better output on grid interactions parameter and the ZEB performance will be increased. Based on the data that exist from the Skarpnes project can be used to get the proper dimension for storage system. By doing this, the consumer and utility can expect the maximization of self-consumption energy and reducing the dependency on the grid.

- Based on the higher level logical control used in stateflow analysis of PV based active generator, by implementing this system to the house with some additional controller on the demand side, an efficient clean energy can be utilized. New analysis based on this can be done which might benefits the consumer and utility.

- To improve the power quality and reduce the system harmonics in the power controlling system, proper tuning or designing LC filters for minimizing the impact of harmonics/unbalance current in the neutral is required. And also more robust control techniques can be used for power flow control with system stability analysis. This will contribute for a better controlling method.

References

[1] M. Kolhe, "Smart grid: charting a new energy future: research, development and demonstration," *The Electricity Journal,* vol. 25, pp. 88-93, 2012.

[2] Y. J. Reddy, Y. P. Kumar, K. P. Raju, and A. Ramsesh, "Retrofitted Hybrid Power System Design With Renewable Energy Sources for Buildings."

[3] H. Kanchev, V. Lazarov, and B. Francois, "Environmental and economical optimization of microgrid long term operational planning including PV-based active generators," in *Power Electronics and Motion Control Conference (EPE/PEMC), 2012 15th International*, 2012, pp. LS4b-2.1-1-LS4b-2.1-8.

[4] F. Corno and F. Razzak, "Intelligent Energy Optimization for User Intelligible Goals in Smart Home Environments," 2012.

[5] M. Kolhe, "Techno-economic optimum sizing of a stand-alone solar photovoltaic system," *Energy Conversion, IEEE Transactions on,* vol. 24, pp. 511-519, 2009.

[6] M. Pipattanasomporn, H. Feroze, and S. Rahman, "Securing critical loads in a PV-based microgrid with a multi-agent system," *Renewable Energy,* vol. 39, pp. 166-174, 2012.

[7] F. Grimaccia, M. Mussetta, and R. E. Zich, "Advanced predictive models towards PV energy integration in smart grid," in *Fuzzy Systems (FUZZ-IEEE), 2012 IEEE International Conference on*, 2012, pp. 1-6.

[8] P. Basak, S. Chowdhury, S. Halder nee Dey, and S. Chowdhury, "A literature review on integration of distributed energy resources in the perspective of control, protection and stability of microgrid," *Renewable and Sustainable Energy Reviews,* vol. 16, pp. 5545-5556, 2012.

[9] W. Najy, H. Zeineldin, and W. Woon, "Optimal Protection Coordination for Microgrids with Grid-Connected and Islanded Capability," 2013.

[10] A. Kasem Alaboudy, H. Zeineldin, and J. L. Kirtley, "Microgrid stability characterization subsequent to fault-triggered islanding incidents," *Power Delivery, IEEE Transactions on,* vol. 27, pp. 658-669, 2012.

[11] R. Teodorescu and M. Liserre, *Grid converters for photovoltaic and wind power systems* vol. 29: John Wiley & Sons, 2011.

[12] V. Chairperson and S. A. Kunsman, "PROTECTIVE RELAYING AND POWER QUALITY."

[13] M. L. Kolhe, K. I. U. Ranaweera, and A. S. Gunawardana, "Techno-economic sizing of off-grid hybrid renewable energy system for rural electrification in Sri Lanka," *Sustainable Energy Technologies and Assessments,* vol. 11, pp. 53-64, 2015.

[14] G. Zubi, R. Dufo-López, G. Pasaoglu, and N. Pardo, "Techno-economic assessment of an off-grid PV system for developing regions to provide electricity for basic domestic needs: A 2020–2040 scenario," *Applied Energy,* vol. 176, pp. 309-319, 2016.

[15] A. Ghafoor and A. Munir, "Design and economics analysis of an off-grid PV system for household electrification," *Renewable and Sustainable Energy Reviews,* vol. 42, pp. 496-502, 2015.

[16] A. S. Al Busaidi, H. A. Kazem, A. H. Al-Badi, and M. F. Khan, "A review of optimum sizing of hybrid PV–Wind renewable energy systems in oman," *Renewable and Sustainable Energy Reviews,* vol. 53, pp. 185-193, 2016.

[17] S. A. Kunsman, "PROTECTIVE RELAYING AND POWER QUALITY."

[18] H. Kanchev, D. Lu, B. Francois, and V. Lazarov, "Smart monitoring of a microgrid including gas turbines and a dispatched PV-based active generator for energy management and emissions reduction," in *Innovative Smart Grid Technologies Conference Europe (ISGT Europe), 2010 IEEE PES*, 2010, pp. 1-8.

[19] D. Lu, T. Zhou, H. Fakham, and B. Francois, "Design of a power management system for an active PV station including various storage technologies," in *Power Electronics and Motion Control Conference, 2008. EPE-PEMC 2008. 13th*, 2008, pp. 2142-2149.

[20] H. Kanchev, D. Lu, F. Colas, V. Lazarov, and B. Francois, "Energy management and operational planning of a microgrid with a PV-based active generator for smart grid applications," *Industrial Electronics, IEEE Transactions on,* vol. 58, pp. 4583-4592, 2011.

[21] R. Shah and N. Mithulananthan, "A comparison of ultracapacitor, BESS and shunt capacitor on oscillation damping of power system with large-scale PV plants," in *Universities Power Engineering Conference (AUPEC), 2011 21st Australasian*, 2011, pp. 1-6.

[22] C. A. Hill, M. C. Such, D. Chen, J. Gonzalez, and W. M. Grady, "Battery energy storage for enabling integration of distributed solar power generation," *Smart Grid, IEEE Transactions on,* vol. 3, pp. 850-857, 2012.

[23] J. M. Guerrero, J. C. Vasquez, J. Matas, L. G. de Vicuña, and M. Castilla, "Hierarchical control of droop-controlled AC and DC microgrids—a general approach toward standardization," *Industrial Electronics, IEEE Transactions on,* vol. 58, pp. 158-172, 2011.

[24] J. Zhang, J. Wang, and X. Wu, "Research on Supercapacitor Charging Efficiency of Photovoltaic System," in *Power and Energy Engineering Conference (APPEEC), 2012 Asia-Pacific*, 2012, pp. 1-5.

[25] D. Lu and B. Francois, "Strategic framework of an energy management of a microgrid with a photovoltaic-based active generator," in *Advanced Electromechanical Motion Systems & Electric Drives Joint Symposium, 2009. ELECTROMOTION 2009. 8th International Symposium on*, 2009, pp. 1-6.

[26] A. Aichhorn, M. Greenleaf, H. Li, and J. Zheng, "A cost effective battery sizing strategy based on a detailed battery lifetime model and an economic energy management strategy," in *Power and Energy Society General Meeting, 2012 IEEE*, 2012, pp. 1-8.

[27] Y. Ru, J. Kleissl, and S. Martinez, "Storage size determination for grid-connected photovoltaic systems," 2011.

[28] D. Guasch and S. Silvestre, "Dynamic battery model for photovoltaic applications," *Progress in Photovoltaics: Research and applications*, vol. 11, pp. 193-206, 2003.

[29] R. Kaiser, "Optimized battery-management system to improve storage lifetime in renewable energy systems," *Journal of Power Sources*, vol. 168, pp. 58-65, 2007.

[30] X. Vallvé, A. Graillot, S. Gual, and H. Colin, "Micro storage and demand side management in distributed PV grid-connected installations," in *Electrical Power Quality and Utilisation, 2007. EPQU 2007. 9th International Conference on*, 2007, pp. 1-6.

[31] H.-J. Yoo, H.-M. Kim, and C. H. Song, "A coordinated frequency control of Lead-acid BESS and Li-ion BESS during islanded microgrid operation," in *Vehicle Power and Propulsion Conference (VPPC), 2012 IEEE*, 2012, pp. 1453-1456.

[32] H. Chen, T. N. Cong, W. Yang, C. Tan, Y. Li, and Y. Ding, "Progress in electrical energy storage system: A critical review," *Progress in Natural Science*, vol. 19, pp. 291-312, 2009.

[33] H. Zhao, Q. Wu, S. Hu, H. Xu, and C. N. Rasmussen, "Review of energy storage system for wind power integration support," *Applied Energy*, vol. 137, pp. 545-553, 2015.

[34] T. A. Nguyen, X. Qiu, T. T. Gamage, M. L. Crow, B. M. McMillin, and A. Elmore, "Microgrid application with computer models and power management integrated using PSCAD/EMTDC," in *North American Power Symposium (NAPS), 2011*, 2011, pp. 1-7.

[35] G. Wang, M. Ciobotaru, and V. G. Agelidis, "PV power plant using hybrid energy storage system with improved efficiency," in *Power Electronics for Distributed Generation Systems (PEDG), 2012 3rd IEEE International Symposium on*, 2012, pp. 808-813.

[36] K. Le Dinh and Y. Hayashi, "Coordinated BESS control for improving voltage stability of a PV-supplied microgrid," in *Power Engineering Conference (UPEC), 2013 48th International Universities'*, 2013, pp. 1-6.

[37] G. Wang, M. Ciobotaru, and V. G. Agelidis, "Minimising output power fluctuation of large photovoltaic plant using vanadium redox battery storage," in *Power Electronics, Machines and Drives (PEMD 2012), 6th IET International Conference on*, 2012, pp. 1-6.

[38] D. Quiggin, S. Cornell, M. Tierney, and R. Buswell, "A simulation and optimisation study: Towards a decentralised microgrid, using real world fluctuation data," *Energy*, vol. 41, pp. 549-559, 2012.

[39] E. Matallanas, M. Castillo-Cagigal, A. Gutiérrez, F. Monasterio-Huelin, E. Caamaño-Martín, D. Masa, *et al.*, "Neural network controller for Active Demand-Side Management with PV energy in the residential sector," *Applied Energy*, vol. 91, pp. 90-97, 2012.

[40] R. Kumar, A. Mohanty, S. Mohanty, and N. Kishor, "Power quality improvement in 3-Φ grid connected photovoltaic system with battery storage,"

in *Power Electronics, Drives and Energy Systems (PEDES), 2012 IEEE International Conference on*, 2012, pp. 1-6.

[41] S. Norge, "NS 3700: Criteria for passive houses and low energy houses (residential buildings)," 2010.

[42] M. Thyholt, T. H. Dokka, and R. Rasmussen, "The Skarpnes Residential Development: A Zero Energy Pilot Project," in *The 2012 Nordic Passive House Conference. Trondheim*, 2012.

[43] A.-N. Azmi, M. L. Kohle, and A. G. Imenes, "On-grid residential development with photovoltaic systems in Southern Norway," in *Clean Energy and Technology (CEAT), 2013 IEEE Conference on*, 2013, pp. 93-97.

[44] A. Kylili and P. A. Fokaides, "European smart cities: The role of zero energy buildings," *Sustainable Cities and Society*, vol. 15, pp. 86-95, 2015.

[45] A. N. Azmi and M. L. Kolhe, "Photovoltaic based active generator: Energy control system using stateflow analysis," in *2015 IEEE 11th International Conference on Power Electronics and Drive Systems*, 2015, pp. 18-22.

[46] M. Cellura, F. Guarino, S. Longo, and M. Mistretta, "Different energy balances for the redesign of nearly net zero energy buildings: An Italian case study," *Renewable and Sustainable Energy Reviews*, vol. 45, pp. 100-112, 2015.

[47] P. Solutions. (24 June). *Data Acquisition and Process*. Available: http://elspec-ltd.com/power-quality-software-pqscada-software/

[48] A. Songpu, M. L. Kolhe, L. Jiao, N. Ulltveit-Moe, and Q. Zhang, "Domestic demand predictions considering influence of external environmental parameters," in *2015 IEEE 13th International Conference on Industrial Informatics (INDIN)*, 2015, pp. 640-644.

[49] M. Alirezaei, M. Noori, and O. Tatari, "Getting to net zero energy building: Investigating the role of vehicle to home technology," *Energy and Buildings*, vol. 130, pp. 465-476, 2016.

[50] M. Kolhe, "Algorithms for Demand Response and Load Control," SEMIAH-WP5-D5.1, European Comission FP7 Program (FP7-ICT-2013-11-619560), 2015.

[51] A. J. Marszal, P. Heiselberg, J. S. Bourrelle, E. Musall, K. Voss, I. Sartori, *et al.*, "Zero Energy Building–A review of definitions and calculation methodologies," *Energy and buildings*, vol. 43, pp. 971-979, 2011.

[52] A. J. Marszal and P. Heiselberg, "Life cycle cost analysis of a multi-storey residential net zero energy building in Denmark," *Energy*, vol. 36, pp. 5600-5609, 2011.

[53] T. IEA, "40/Annex 52, 2008. Towards Net Zero Energy Solar Buildings, IEA SHC Task 40 and ECBCS Annex 52," ed, 2010.

[54] A. J. M. Jaume Salom, José Candanedo, Joakim Widén, Karen Byskov Lindberg, Igor Sartori, "Analysis of load match and grid interaction indicators in net zero energy buildings with high resolution data," Catalonia Institute for Energy Research, IREC, Barcelona, SpainOctober, 2013 2013.

[55] A. Allouhi, R. Saadani, T. Kousksou, R. Saidur, A. Jamil, and M. Rahmoune, "Grid-connected PV systems installed on institutional buildings: Technology

comparison, energy analysis and economic performance," *Energy and Buildings,* vol. 130, pp. 188-201, 2016.

[56] D. Chung, C. Davidson, R. Fu, K. Ardani, and R. Margolis, "US Photovoltaic Prices and Cost Breakdowns: Q1 2015 Benchmarks for Residential, Commercial, and Utility-Scale Systems," NREL Technical Report, In Preparation 2015.

[57] O. Hafez and K. Bhattacharya, "Optimal planning and design of a renewable energy based supply system for microgrids," *Renewable Energy,* vol. 45, pp. 7-15, 2012.

[58] A. N. Azmi, M. L. Kolhe, and A. G. Imenes, "Review on photovoltaic based active generator," in *2015 9th International Symposium on Advanced Topics in Electrical Engineering (ATEE)*, 2015, pp. 812-815.

[59] P. Basak, S. Chowdhury, S. H. nee Dey, and S. Chowdhury, "A literature review on integration of distributed energy resources in the perspective of control, protection and stability of microgrid," *Renewable and Sustainable Energy Reviews,* vol. 16, pp. 5545-5556, 2012.

[60] A. N. Azmi, M. L. Kolhe, and A. G. Imenes, "Review on photovoltaic based active generator," in *Advanced Topics in Electrical Engineering (ATEE), 2015 9th International Symposium on*, 2015, pp. 812-815.

[61] M. E. Baran, H. Hooshyar, Z. Shen, and A. Huang, "Accommodating high PV penetration on distribution feeders," *Smart Grid, IEEE Transactions on,* vol. 3, pp. 1039-1046, 2012.

[62] C.-H. Lin, W.-L. Hsieh, C.-S. Chen, C.-T. Hsu, and T.-T. Ku, "Optimization of photovoltaic penetration in distribution systems considering annual duration curve of solar irradiation," *Power Systems, IEEE Transactions on,* vol. 27, pp. 1090-1097, 2012.

[63] D. PowerFactory, "DIgSILENT PowerFactory 15 User Manual," ed: August, 2015.

[64] IEEE, *IEEE Recommended Practice for Utility Interface of Photovoltaic (PV) Systems*: IEEE, 2000.

[65] V. D. Andrade and E. Sorrentino, "Typical expected values of the fault resistance in power systems," in *Transmission and Distribution Conference and Exposition: Latin America (T&D-LA), 2010 IEEE/PES*, 2010, pp. 602-609.

[66] N. Zamanan, J. Sykulski, and A. Al-Othman, "Arcing high impedance fault detection using real coded genetic algorithm," 2007.

[67] V. V. Terzija and H.-J. Koglin, "On the modeling of long arc in still air and arc resistance calculation," *Power Delivery, IEEE Transactions on,* vol. 19, pp. 1012-1017, 2004.

[68] D. Salomonsson, L. Söder, and A. Sannino, "Protection of low-voltage DC microgrids," *Power Delivery, IEEE Transactions on,* vol. 24, pp. 1045-1053, 2009.

[69] M. E. Baran and I. El-Markaby, "Fault analysis on distribution feeders with distributed generators," *Power Systems, IEEE Transactions on,* vol. 20, pp. 1757-1764, 2005.

Appendix A : Data Tables and Graphs

Table A1 Summary of solar radiation data (global horizontal) per month from different sources.

	PVGIS (Wh/m2/day)	Helio-Clim3 (Wh/m2/day)	Meteornorm (Wh/m2/day)
January	326	582	333
February	865	1096	767
March	1830	2516	2300
April	3300	4668	3900
May	4610	5214	5533
June	5200	6086	6033
July	4850	5541	5767
August	3650	4503	4267
September	2330	2841	2633
October	1110	1361	1267
November	436	491	433
December	219	329	233
Total	28726	35228	33466

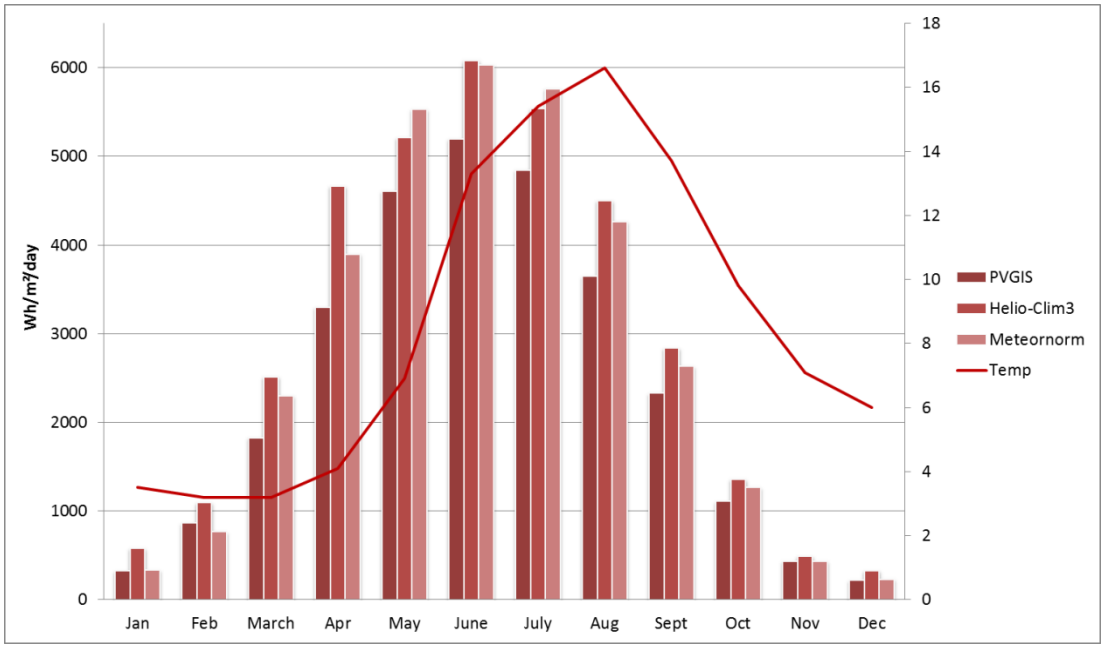

Figure A1 Summary solar radiation data per month from different sources.

Table A2 Cover factors for Sept 2015 to Feb 2016

	September 2015		October 2015		November 2015		December 2015		January 2016		February 2016	
	γ load	γ supply	γ load	γ supply	γ load	γ supply	γ load	γ supply	γ load	γ supply	γ load	γ supply
00:00	0.0000		0.0000		0.0000		0.0000		0.0000		0.0000	
01:00	0.0000		0.0000		0.0000		0.0000		0.0000		0.0000	
02:00	0.0000		0.0000		0.0000		0.0000		0.0000		0.0000	
03:00	0.0000		0.0000		0.0000		0.0000		0.0000		0.0000	
04:00	0.0000		0.0000		0.0000		0.0000		0.0000		0.0000	
05:00	0.0000		0.0000		0.0000		0.0000		0.0000		0.0000	
06:00	0.0066	1.0000	0.0032	1.0000	0.0000		0.0000		0.0000		0.0000	
07:00	0.0655	1.0000	0.0261	1.0000	0.0008	1.0000	0.0000		0.0000		0.0052	1.0000
08:00	0.2503	1.0000	0.1119	1.0000	0.0386	1.0000	0.0004	1.0000	0.0010	1.0000	0.0496	1.0000
09:00	0.6887	1.0000	0.3963	1.0000	0.2895	1.0000	0.0501	1.0000	0.0196	1.0000	0.3330	1.0000
10:00	1.0000	0.6810	0.7748	1.0000	0.8003	1.0000	0.2722	1.0000	0.0645	1.0000	0.7025	1.0000
11:00	1.0000	0.3694	1.0000	0.7568	1.0000	0.8214	0.4089	1.0000	0.1039	1.0000	1.0000	0.9063
12:00	1.0000	0.2576	1.0000	0.5434	1.0000	0.6143	0.5668	1.0000	0.1770	1.0000	1.0000	0.6361
13:00	1.0000	0.2554	1.0000	0.4812	1.0000	0.6307	0.5900	1.0000	0.1606	1.0000	1.0000	0.4674
14:00	1.0000	0.1748	1.0000	0.3639	0.8963	1.0000	0.1580	1.0000	0.1390	1.0000	1.0000	0.5895
15:00	1.0000	0.1457	1.0000	0.3874	0.1280	1.0000	0.0031	1.0000	0.0642	1.0000	1.0000	0.6992
16:00	1.0000	0.1563	1.0000	0.6727	0.0007	1.0000	0.0000		0.0014	1.0000	0.5946	1.0000
17:00	1.0000	0.3107	0.5224	1.0000	0.0000		0.0000		0.0000		0.0170	1.0000
18:00	1.0000	0.8737	0.0200	1.0000	0.0000		0.0000		0.0000		0.0000	
19:00	0.0439	1.0000	0.0000		0.0000		0.0000		0.0000		0.0000	
20:00	0.0001	1.0000	0.0000		0.0000		0.0000		0.0000		0.0000	
21:00	0.0000		0.0000		0.0000		0.0000		0.0000		0.0000	
22:00	0.0000		0.0000		0.0000		0.0000		0.0000		0.0000	
23:00	0.0000		0.0000		0.0000		0.0000		0.0000		0.0000	

Table A3 Cover factors for March 2015 to August 2016

	March 2016		April 2016		May 2016		June 2016		July 2016		August 2016	
	γ load	γ supply	γ load	γ supply	γ load	γ supply	γ load	γ supply	γ load	γ supply	γ load	γ supply
00:00	0.0000		0.0000		0.0000		0.0000		0.0000		0.0000	
01:00	0.0000		0.0000		0.0000		0.0000		0.0000		0.0000	
02:00	0.0000		0.0000		0.0000		0.0000		0.0000		0.0000	
03:00	0.0000		0.0000		0.0000		0.0000		0.0000		0.0000	
04:00	0.0000		0.0000		0.0009	1.0000	0.0240	1.0000	0.0064	1.0000	0.0000	
05:00	0.0000		0.0017	1.0000	0.0804	1.0000	0.1698	1.0000	0.1115	1.0000	0.0096	1.0000
06:00	0.0174	1.0000	0.0778	1.0000	0.1932	1.0000	0.3776	1.0000	0.3084	1.0000	0.1316	1.0000
07:00	0.0683	1.0000	0.1658	1.0000	0.2901	1.0000	0.2969	1.0000	0.3558	1.0000	0.1952	1.0000
08:00	0.2355	1.0000	0.3435	1.0000	0.6949	1.0000	0.5066	1.0000	0.5987	1.0000	0.3415	1.0000
09:00	0.6306	1.0000	0.6754	1.0000	1.0000	0.5033	1.0000	0.8923	1.0000	0.8679	0.5871	1.0000
10:00	0.9396	1.0000	1.0000	0.7194	1.0000	0.3286	1.0000	0.5331	1.0000	0.5071	1.0000	0.7663
11:00	1.0000	0.6541	1.0000	0.5019	1.0000	0.2459	1.0000	0.3849	1.0000	0.3525	1.0000	0.5785
12:00	1.0000	0.5425	1.0000	0.3354	1.0000	0.2967	1.0000	0.2965	1.0000	0.3667	1.0000	0.4218
13:00	1.0000	0.4767	1.0000	0.3207	1.0000	0.2193	1.0000	0.2736	1.0000	0.2900	1.0000	0.4306
14:00	1.0000	0.4557	1.0000	0.3396	1.0000	0.2215	1.0000	0.2365	1.0000	0.2744	1.0000	0.3745
15:00	1.0000	0.4491	1.0000	0.4033	1.0000	0.2265	1.0000	0.2584	1.0000	0.2347	1.0000	0.3760
16:00	1.0000	0.6469	1.0000	0.4044	1.0000	0.3129	1.0000	0.3123	1.0000	0.2063	1.0000	0.3673
17:00	0.6091	1.0000	1.0000	0.4749	1.0000	0.3927	1.0000	0.4393	1.0000	0.2601	1.0000	0.4316
18:00	0.2192	1.0000	1.0000	0.9422	1.0000	0.5561	1.0000	0.4990	1.0000	0.4591	1.0000	0.5670
19:00	0.1021	1.0000	0.3105	1.0000	0.7260	1.0000	1.0000	0.8337	1.0000	0.6070	0.9368	1.0000
20:00	0.0084	1.0000	0.0136	1.0000	0.1319	1.0000	0.4554	1.0000	0.4934	1.0000	0.0484	1.0000
21:00	0.0000		0.0000		0.0094	1.0000	0.0514	1.0000	0.0386	1.0000	0.0009	1.0000
22:00	0.0000		0.0000		0.0000		0.0009	1.0000	0.0001	1.0000	0.0000	
23:00	0.0000		0.0000		0.0000		0.0000		0.0000		0.0000	

PV profiles hourly

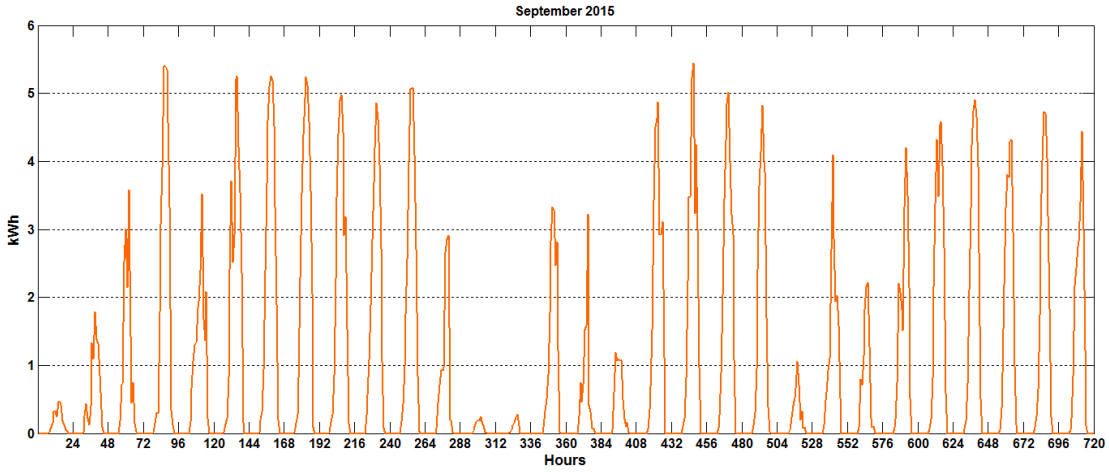

Figure A2 September 2015 hourly PV profile

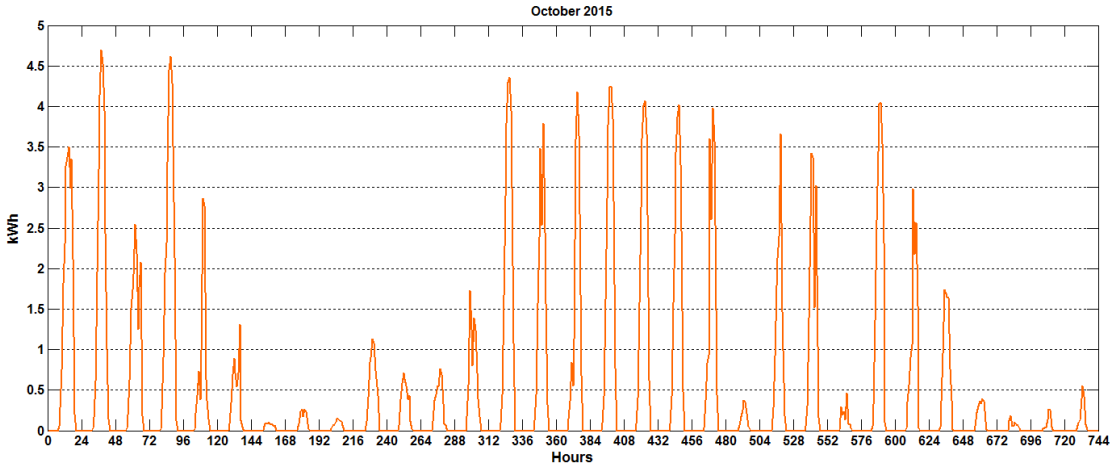

Figure A3 October 2015 hourly PV profile

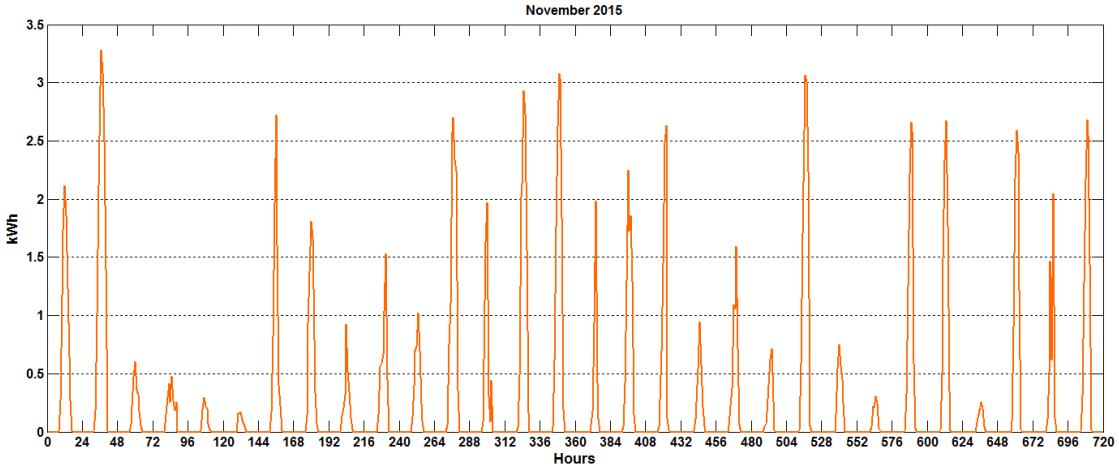

Figure A4 November 2015 hourly PV profile

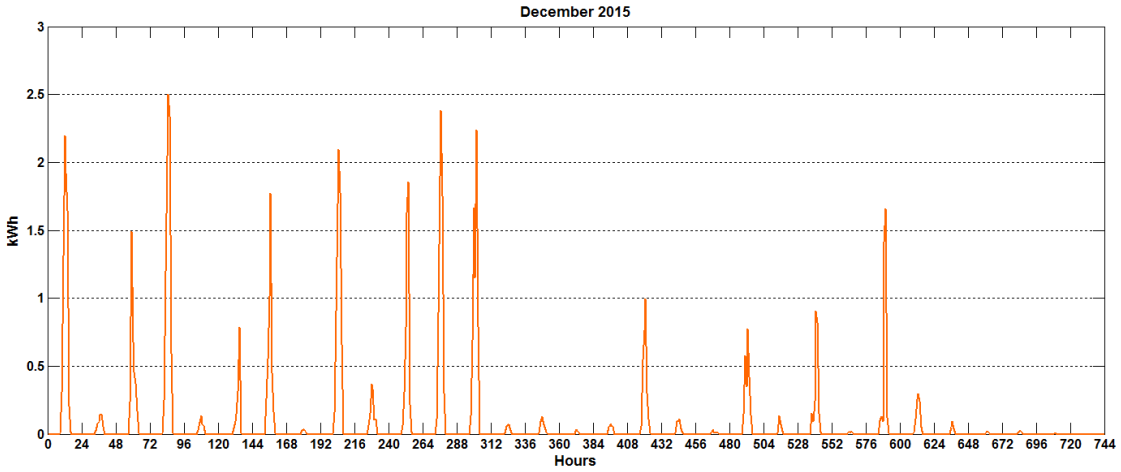

Figure A5 December 2015 hourly PV profile

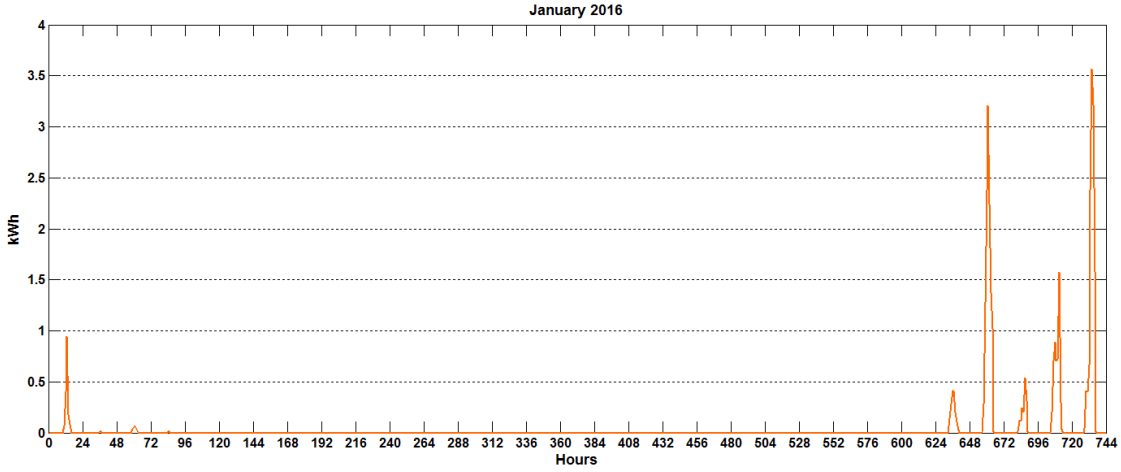

Figure A6 January 2016 hourly PV profile

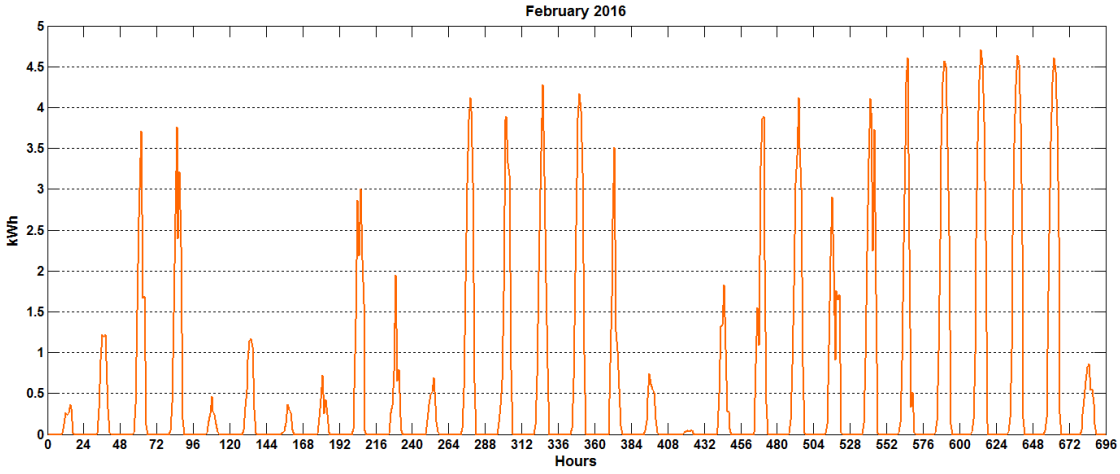

Figure A7 February 2016 hourly PV profile

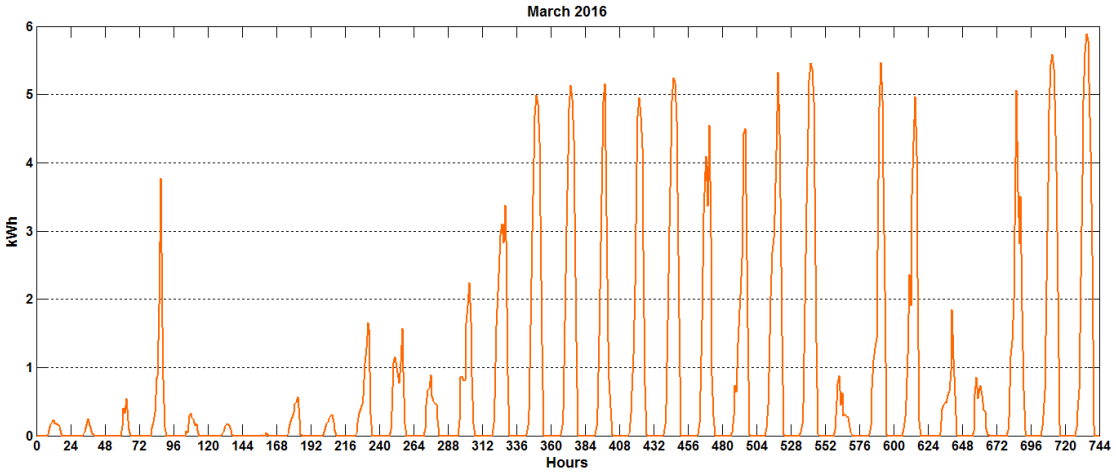

Figure A8 March 2016 hourly PV profile

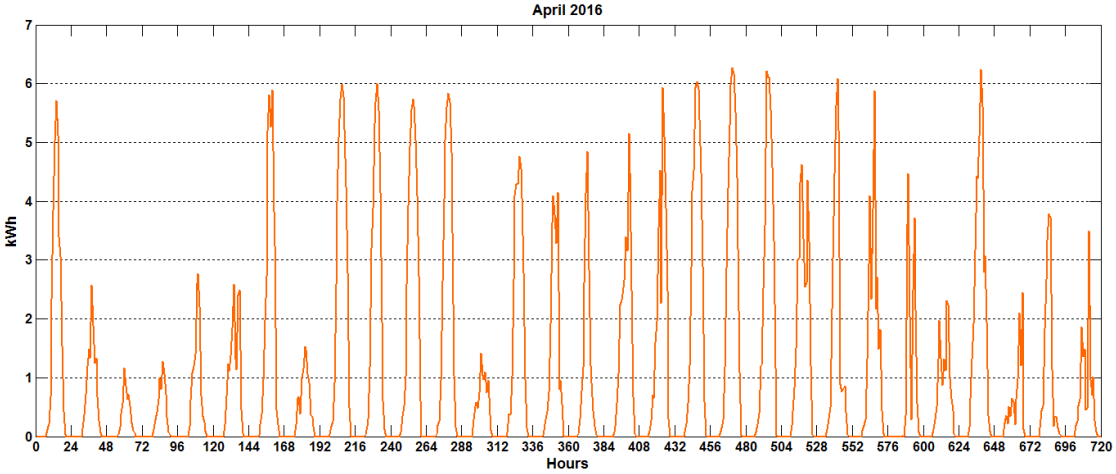

Figure A9 April 2016 hourly PV profile

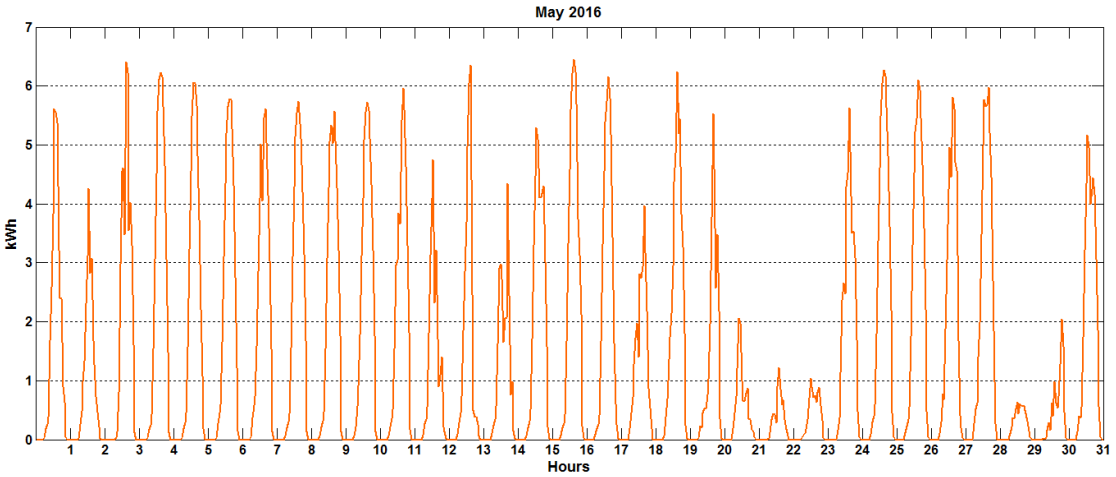

Figure A10 May 2016 hourly PV profile

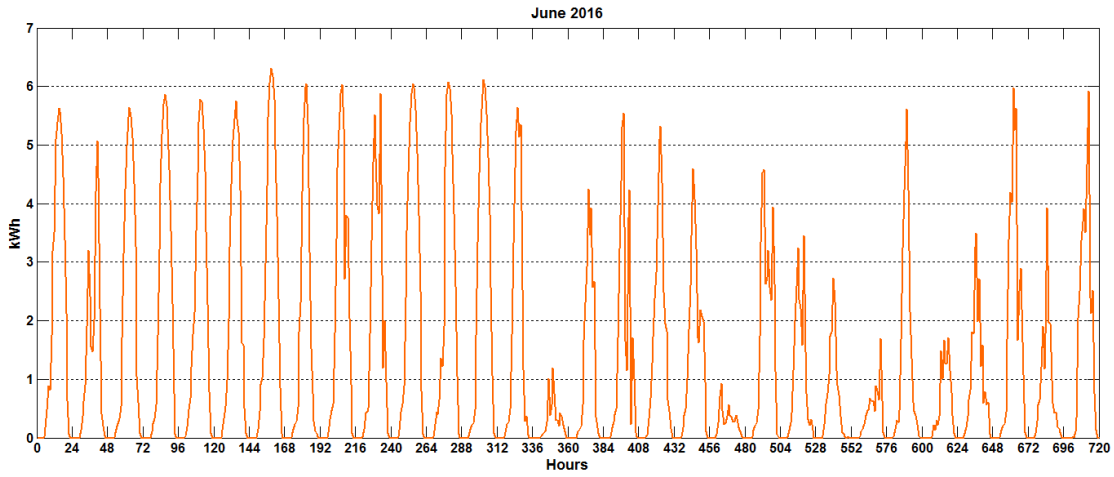

Figure A11 June 2016 hourly PV profile

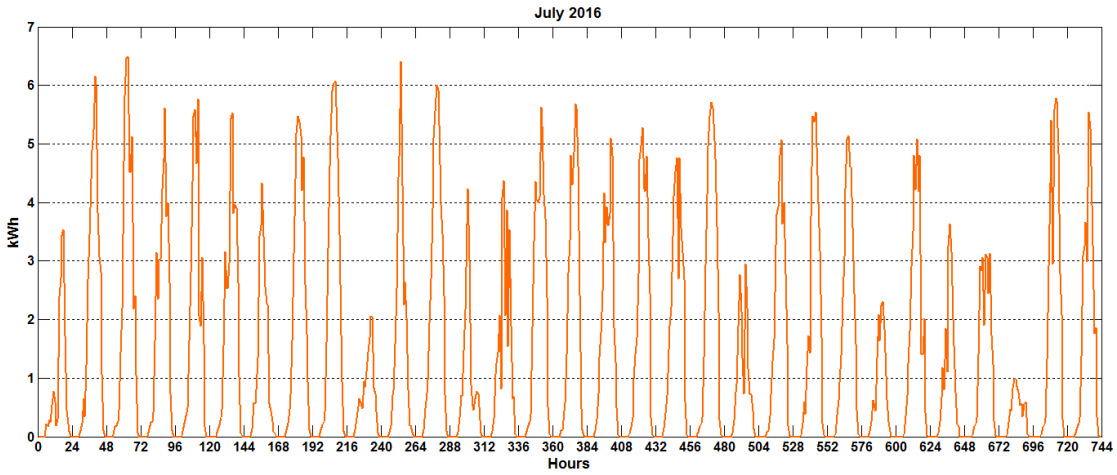

Figure A12 July 2016 hourly PV profile

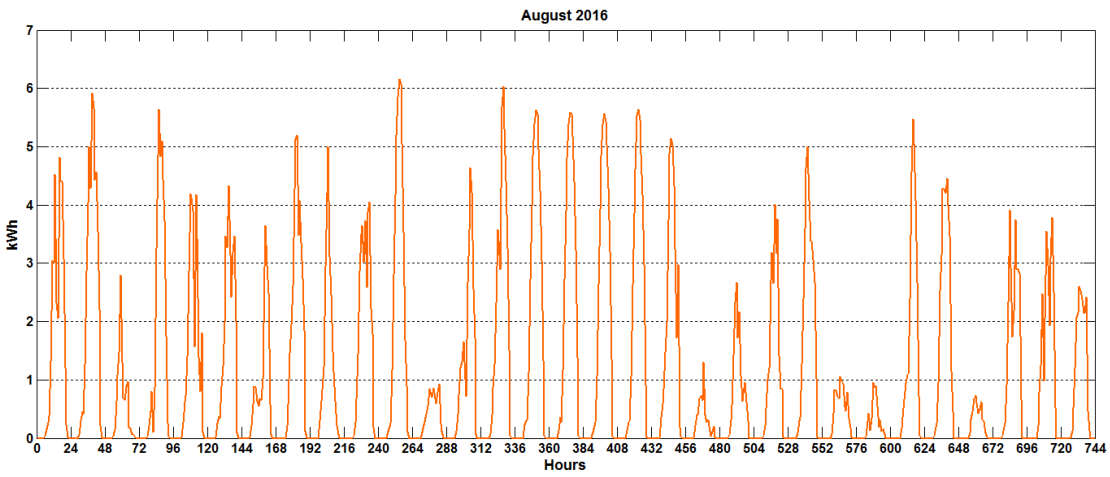

Figure A13 August 2016 hourly PV profile

Load profiles hourly

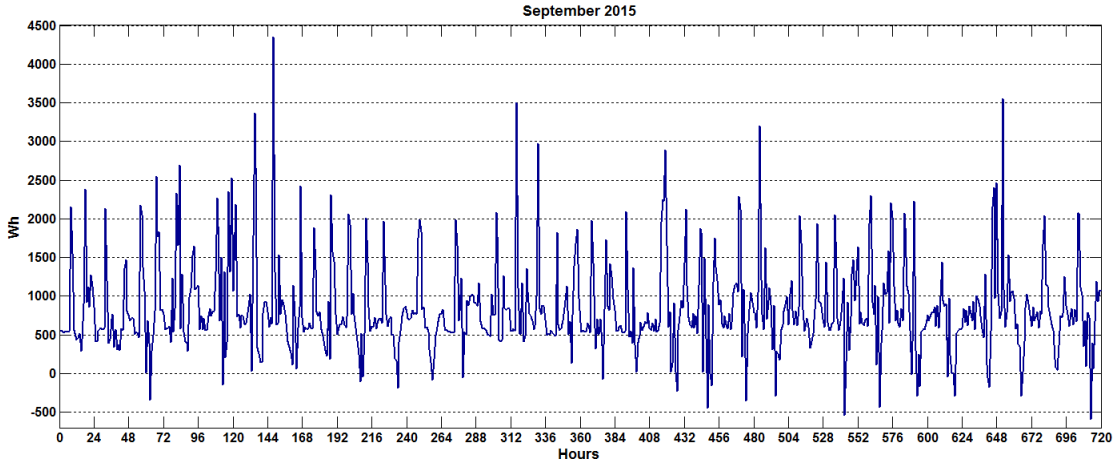

Figure A14 September 2015 hourly load profile

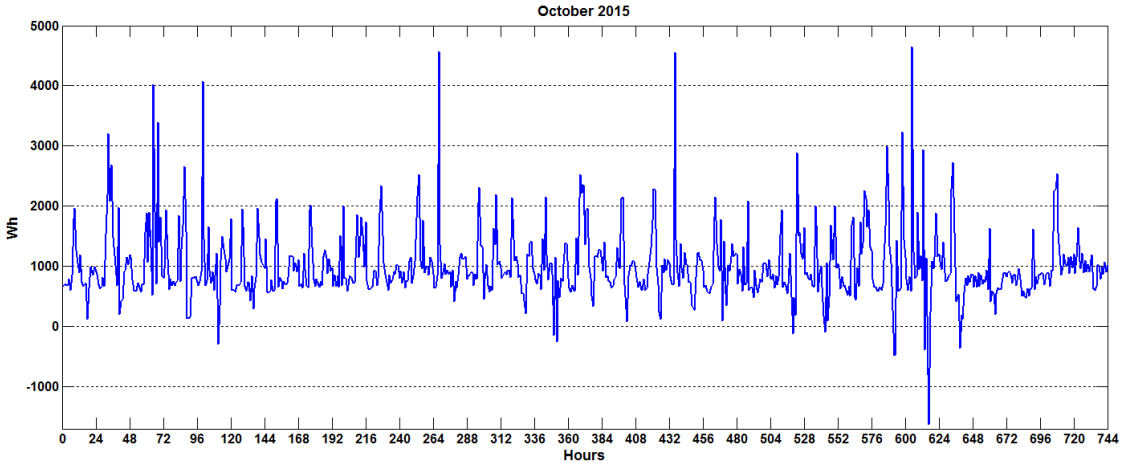

Figure A15 October 2015 hourly load profile

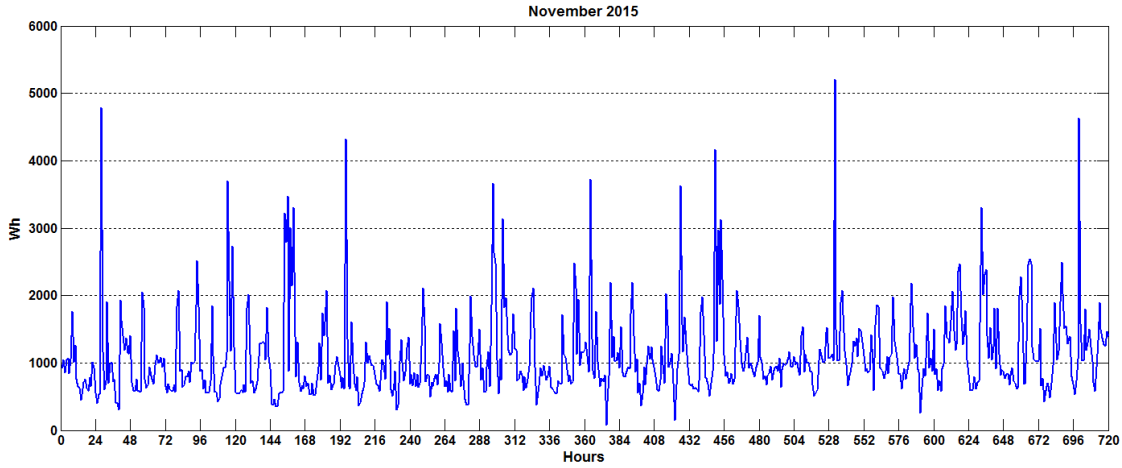

Figure A16 November 2015 hourly load profile

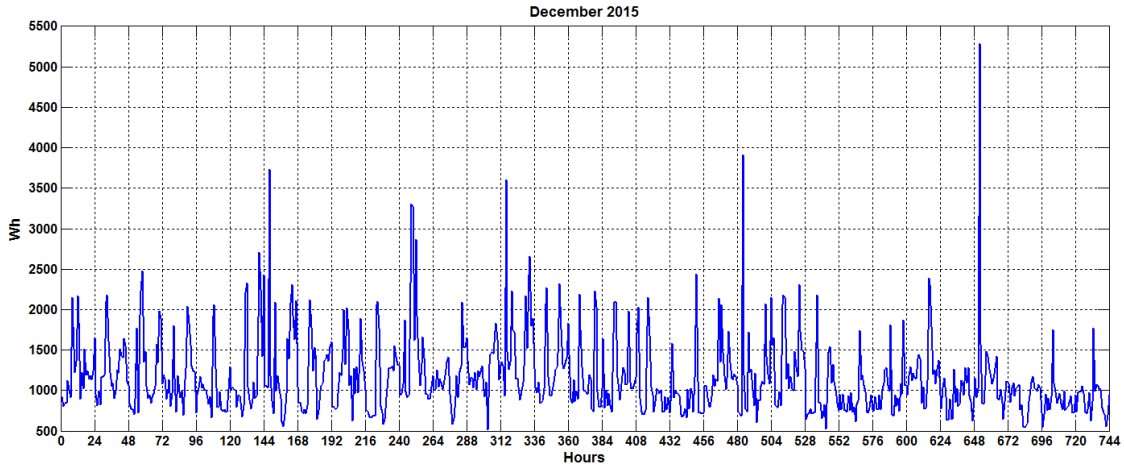

Figure A17 December 2015 hourly load profile

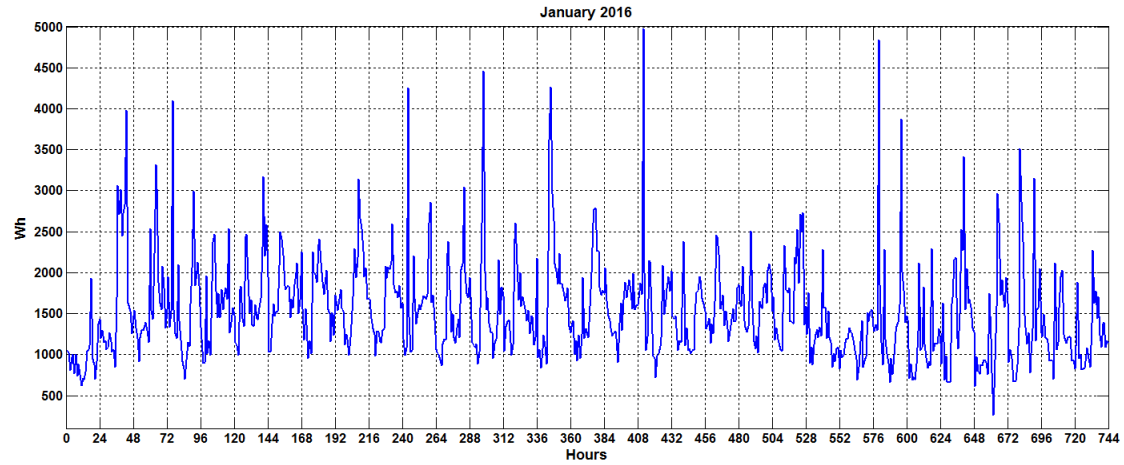

Figure A18 January 2016 hourly load profile

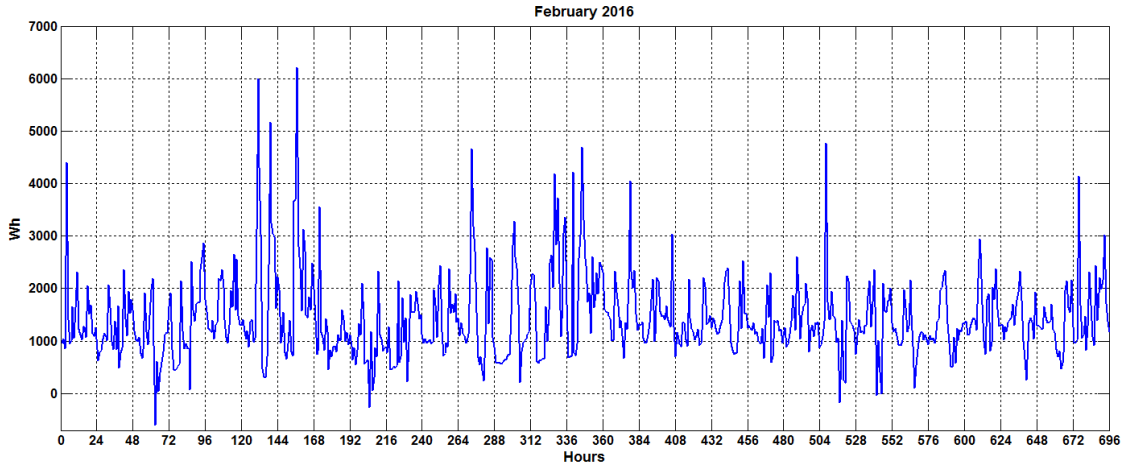

Figure A19 February 2016 hourly load profile

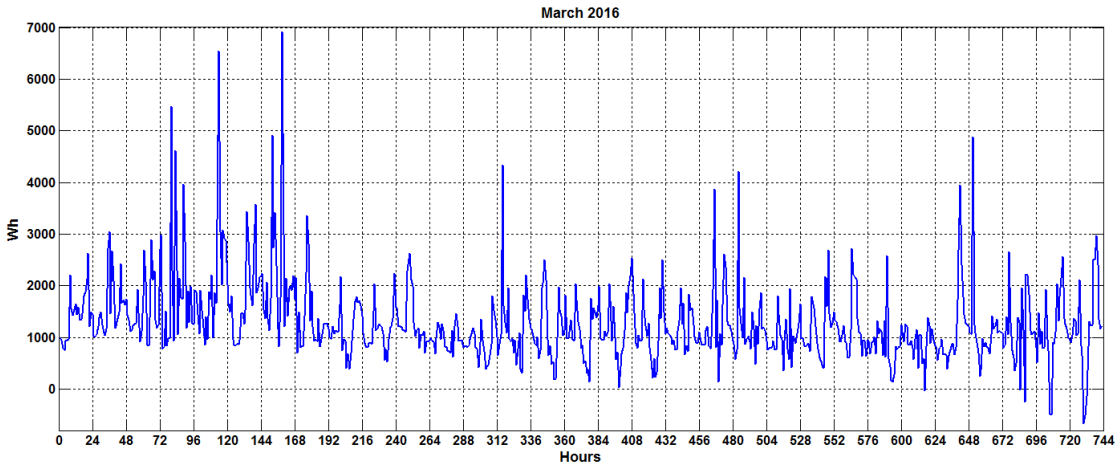

Figure A20 March 2016 hourly load profile

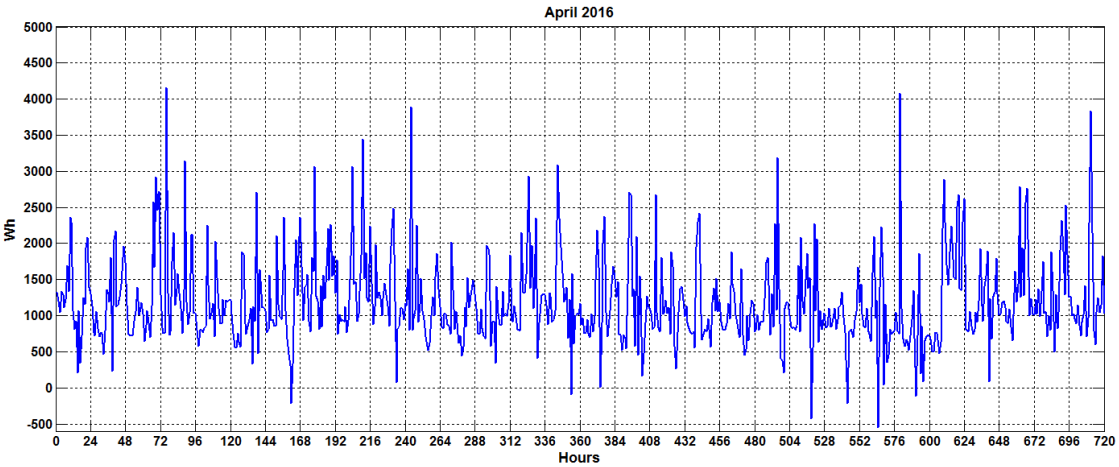

Figure A21 April 2016 hourly load profile

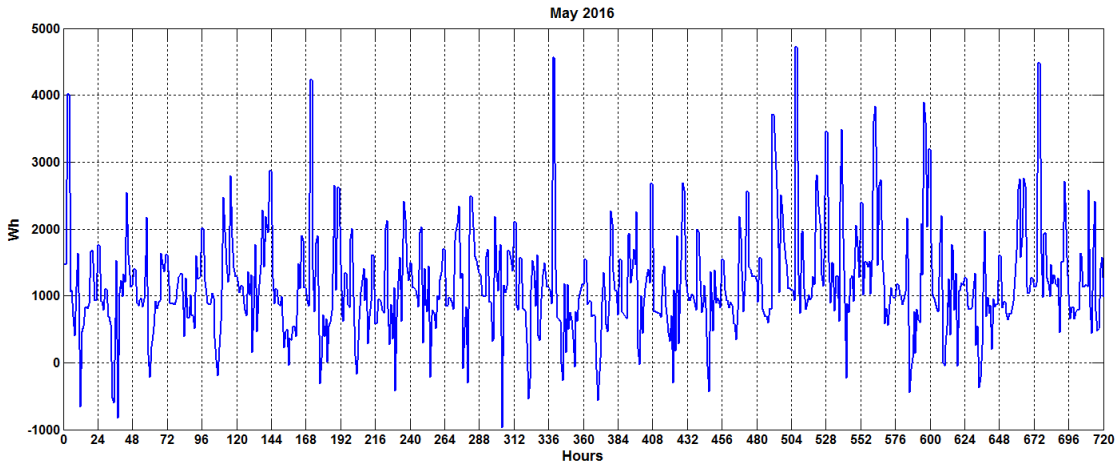

Figure A22 May 2016 hourly load profile

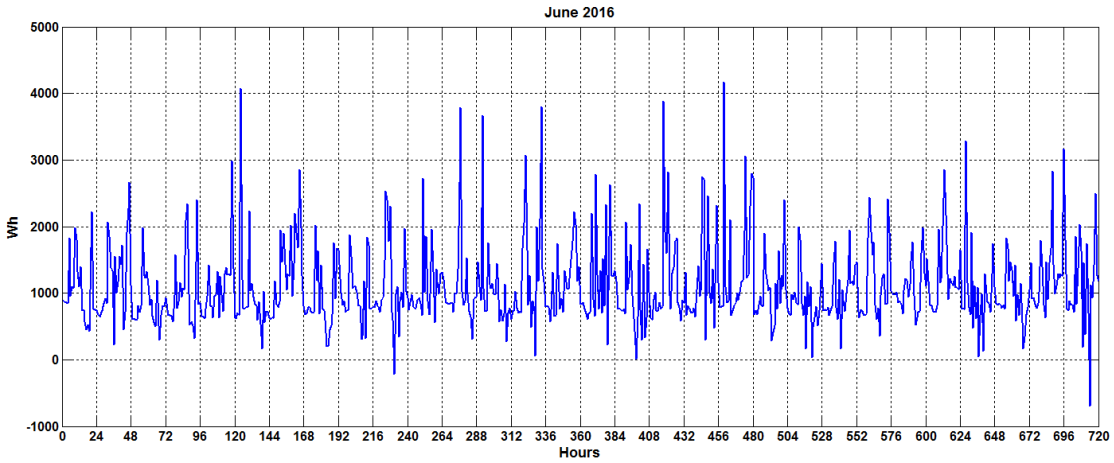

Figure A23 June 2016 hourly load profile

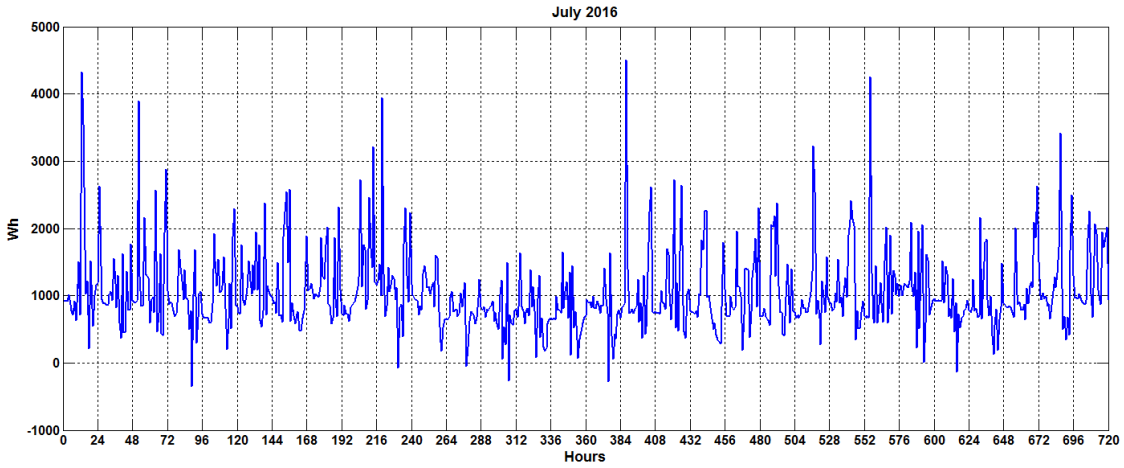

Figure A24 July 2016 hourly load profile

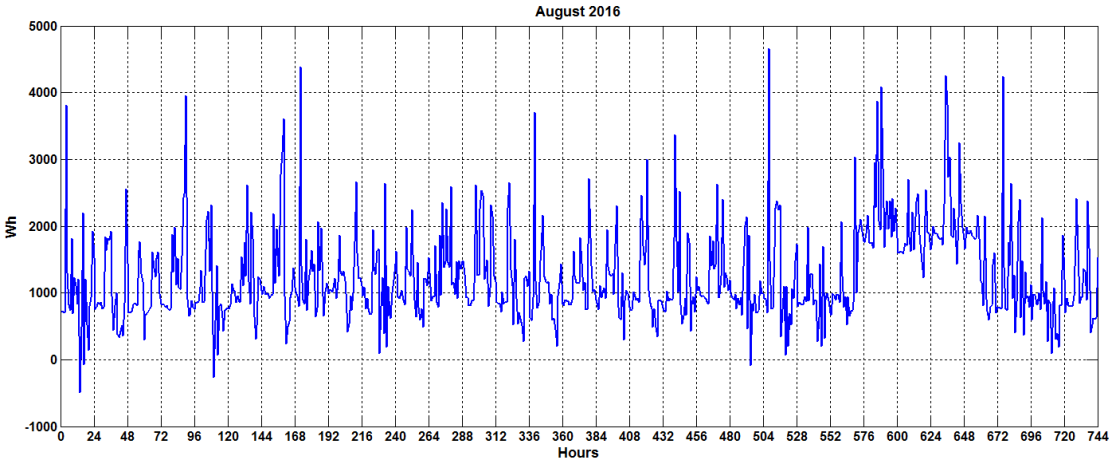

Figure A25 August 2016 hourly load profile

Table A4 Building properties according to NS 3700 vs Skarpnes building properties [42]

Properties	NS3700	Skarpnes
Total glass – window and door area (BRA)	< 20 % of heated area	n/a
U-value walls [W/m^2 K][1]	< 0.15	0.12
U-value roof [W/m^2 K] [1]	< 0.13	0.08
U-value floor to ground and to open space [W/m^2 K] [1]	< 0.15	0.09
U-value glass/windows/doors [W/m^2 K] [1]	< 0.80	< 0.80
Specific cold bridge value [W/m^2 K] [1]	< 0.03	n/a
Air tightness [1/h] [1]	< 0.6	0.6 (@50 Pa)
Heat recovery system [%][1]	> 80	85
Specific fan power in ventilation system, SFP-factor [kW/(m^3 s)] [1]	< 1.5	1.5
Ventilation air flow rate [m^3 /hm^2] [2]	> 1.2	n/a
Maximum heat loss number [W/(m$_2$ K)] [3]	0.6	n/a
Based on (NS3700): **[1] Table 5** **[2] Table A.1** **[3] Table 2**		

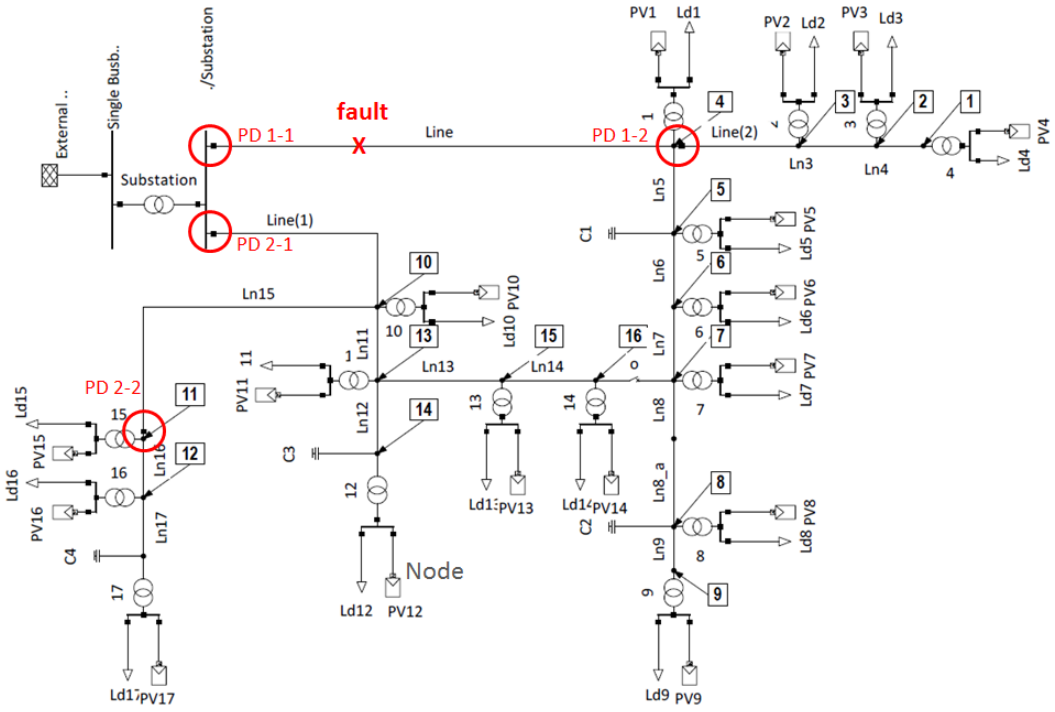

Figure A26 Single line diagram with node reference of distribution feeders in PowerFactory® environment

Appendix B : Research Papers

Paper 1: A.N Azmi, M.L Kolhe, *Primary Frequency Control through Grid Connected Photovoltaic Active Generator*, 3rd International Workshop on Integration of Solar Power into Power Systems London, United Kingdom. Pp: 32-38, 2013. **ISBN: 978-3-9813870-8-7**

Paper 2: A.N Azmi, M.L Kolhe, A.G Imenes, *Techno-Economic Analysis of On-Grid Smart House in Southern Norway*, 2013 IEEE Conference on Clean Energy and Technology (CEAT 2013), Langkawi, Malaysia. pp: 93 - 97, 2013. **DOI: 10.1109/CEAT.2013.6775606**

Paper 3: A.N Azmi, M.L Kolhe, A.G Imenes, *Technical and Economic Analysis for a Residential Grid Connected PV System with Possibilities of Different Battery Energy Storage Capacities(Case Study: Southern Norway),* 4th International Workshop on Integration of Solar Power into Power Systems, Berlin. pp: 486 – 49, 2014. **ISBN: 978-3-9816549-0-5**

Paper 4: A.N Azmi, M.L Kolhe, *Photovoltaic Based Active Generator Energy Controlling System by Using Stateflow Analysis*, 11th IEEE International Conference on Power Electronics and Drive Systems (PEDS2015) Sydney, Australia. pp: 18 – 22, 2015. **DOI: 10.1109/PEDS.2015.7203433**

Paper 5: A.N Azmi, M.L Kolhe, A.G Imenes, *Review on Photovoltaic Based Active Generator*, IEEE International Symposium on Advanced Topics in Electrical Engineering (ATEE 2015), Bucharest, Romania. pp: 812 – 815, 2015. **DOI: 10.1109/ATEE.2015.7133914**

Paper 6: A.N Azmi, I.N Dahlberg M.L Kolhe, A.G Imenes, *Impact of Increasing Penetration of Photovoltaic (PV) Systems on Distribution Feeders.* IEEE International Conference on Smart Grid and Clean Energy Technologies (2015 ICSGCE), Offenburg, Germany. pp: 70 – 74, 2015. **DOI: 10.1109/ICSGCE.2015.7454271**

Journal Article under review: A.N Azmi, M.L Kolhe, Grid Interaction Performance Evaluation of Zero Energy Building (ZEB) in the Southern Norway, '*Energy and Buildings' (Elsevier)*, **ISSN: 0378-7788.**

Book Chapter: "PV System Design for Off-Grid Applications," in Solar Photovoltaic System Applications, A guidebook for off-grid electrification, Springer International Publishing, 2015, pp: 49-84. DOI: 10.1007/978-3-319-14663-8_3
Online ISBN: 978-3-319-14663-8.

3rd International Workshop on Integration of Solar Power into Power Systems London, United Kingdom. ISBN: 978-3-9813870-8-7

Primary Frequency Control through Grid Connected Photovoltaic Active Generator

Aimie Nazmin Azmi
Faculty of Engineering & Science and FKE
University of Agder and UTeM
Norway and Malaysia

Mohan Kolhe
Faculty of Engineering & Science
University of Agder
Grimstad, Norway

Abstract*—the penetrations of grid connected photovoltaic (PV) systems are increasing exponentially due to government policies / climate legislations etc and they involve large fluctuations of the frequency, power and voltage in the grid. At present, grid connected PV systems are operating at maximum power points. Active generator has the capacity to support frequency control, instantaneous power balance. The grid operator adjusts the power dispatch of generators according to power demand fluctuations. PV based active generator (with embedded energy storage units) can be used as load following generator as other power dispatch generators. This new type of distribution system, based on active generators, needs new innovative management and operation strategies for increasing the penetration of intermittent renewable energy systems. In this paper, a PV based active generator with integrated storage units is proposed to provide frequency regulation and power balance for power system stability. A coordinated use of PV source with storage units is needed to make it as a PV active generator. A proper coordination between storage units and PV source must be designed within the energy availability at sources. The system value can be increased significantly for the grid operation, because this active generator can be able to provide active / reactive power balance with frequency control / regulation. In this work, a strategy for short term power balancing and frequency control based on PV source and energy storage units' coordination are discussed. This strategy is based on conventional grid operation of synchronous generator and it is using the frequency droop characteristics and the virtual moment of inertia of the PV based active generator. In this strategy energy storage units charging / discharging cycles is considered to increase the life time of the storage units and the role of hybrid active generator for power system stability at micro grid level.

I. INTRODUCTION

PV system is increasing rapidly worldwide and has the potential to become a major source of renewable energy in the urban environment. Compared to other sources, PV systems offer reduced economic costs and improved environmental performance due to its zero emissions and almost maintenance free nature. However, since PV energy is dependent on the weather condition, the power controlling part will be slightly complex. Traditional PV system will involve the delivery of power direct to the load or grid. The latest innovation on PV system is through active generator. This system will include the battery storage system or ultracapacitor or both and will be connected direct to inverter via DC-DC converter. Figure 1 show the PV based active generator block diagram.

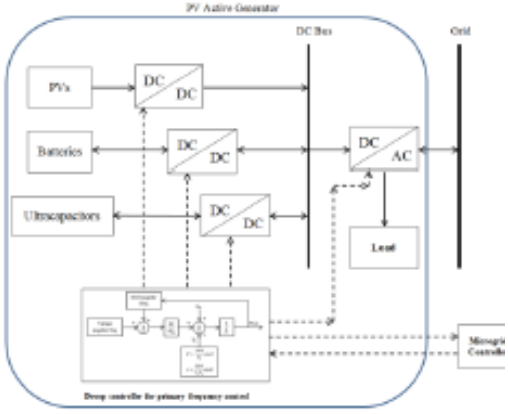

Figure 1. PV based active generator block diagram

This PV based active generator must continually manage the fluctuations of the load and output power of the PV field to maintain the nominal frequency of the grid (50 Hz or 60 Hz). This is a basic requirement for the satisfactory operation of power system. The rules of thumb for frequency control are it depends on active power (P), while voltage is based on reactive power (Q). For a great operation of grid system, it is crucial to keep the frequency and voltage close to their nominal values.

The goal of frequency control is to maintain the synchronous operation of the synchronous generator in the system and to maintain the power balance. By using droop controller this can be solve Basic frequency control will be based on energy and inertia. Frequency deviation is dependent on the inertia of the system and it is expected when the frequency deviation exceeds the pre-defined limit, it will be adjust by the droop controller. Common droop controller equations are:

The first author Aimie Nazmin Azmi would like to acknowledge the funding support received from Universiti Teknikal Malaysia Melaka (UTeM) to carry out his PhD programs at University of Agder, Norway

$$f = f_o - k_p(P - P_o) \quad (2)$$

$$V_1 = V_o - v(Q - Q_o) \quad (3)$$

f_0 and V_0 are the base frequency and voltage while P_0 and Q_0 are the temporary set points for the real and reactive power of the system. In the droop control mechanism, it has the inherent trade-off between active power sharing and frequency accuracy. This will deviate the frequency value from its nominal value. Thus, it is desirable to restore a controller that would restore the frequency to its nominal value [1].

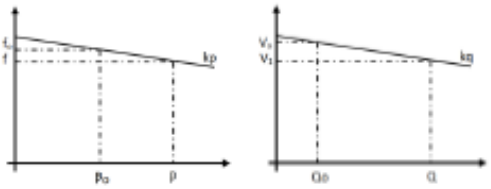

Figure 2. Droop controller characteristic plot

From the droop equation (1) and equation (2), the droop controller characteristic can be plot as seen in Figure 2. The real power on the load increase, the droop controller will allow the system to regulate to its initial frequency value.

It is obvious that for a PV active generator, it will not involve the inertia of the mechanical system which will abruptly change the frequency. However, load changes might lead to some significant frequency changes in the whole system. Furthermore, unlike the synchronous generator, lack of control over primary power source imposes a rigid limit to the active power that been injected to the grid [2].

In this paper, battery storage system and ultracapacitor is proposed to be used as primary frequency control. Then, droop controller will be introducing as a medium to regulate frequency for PV based active generator. A 'mirror' characteristic of synchronous generator will be used to mimic the exact operation and plays a similar role as the kinetic energy in the PV based active generator system that might solve the unstable frequency problems in proposed grid connected PV based active generator.

II. BATTERY STORAGE AND ULTRACAPACITOR

Battery energy storage systems are increasingly being used in the integration of PV system and grid. Battery storage with the appearance of ultracapacitor will increase the system efficiency as the battery will be able to store and release energy gradually, while ultracapacitor effectively act as storage device with very high power density. For a complete PV active based generator, a set of battery bank connected in a combination series-parallel in order to provide desired power to the system. The additional ultracapcitor will provide a fast response energy storage device that can reduced the effect of short term fluctuations of PV output and will enhance the whole system [3]. The dynamic of ultracapacitor can be seen from an equation:

$$\frac{C_e}{\omega}\frac{\partial V_e}{\partial t} = \frac{1}{R_e}\left[\left(\frac{1-d}{d}\right)V_{dc} - V_e\right] \quad (4)$$

Where:
C_e = capacitance value
R_e = series resistance of ultracapacitor
V_e = ultracapacitor voltage
d = duty cycle.

The duty cycle is implemented the proportional and integration controller (PI).

For a better output for the PV based active generator, battery storage system sizing is crucial. There are a few parameters that need to be considering determining the battery sizing for the system. Those parameters are; the depth of discharge (DOD), state of charge (SOC), state of health (SOH), battery capacity, maximum battery charge and discharge power and the utility rating type [4]. DOD defines as the lower and upper limits of the battery SOC while SOH is the merit condition of a certain battery compares to its initial conditions. The battery that is suitable is the lithium-ion for its good lifetime performance and high energy density.

Battery and ultracapacitor will enables smoothing fluctuations for solar array generation units. Battery as a storage system are capable to absorb and delivering both real (P) and reactive power (Q) with sub second response. For a renewable energy application, the battery storage system will be operated under the partial state of charge duty (PSOC) [5]. In this condition, the battery or ultracapacitors will be partially discharge at all time, in order to make sure the system will be able to absorb or discharging power to the grid as it is needed [6].

These storage elements are really important since for a primary voltage and frequency control, this can be used to balance the energy between the distributed generation units and the storage elements. For systems that complete with a storage system, the frequency droop equation can be representing as:

$$\omega = \omega_o - \frac{\alpha}{\beta}.(P - P_o) \quad (5)$$

Where:
α = frequency droop coefficient
β = level of charge (p.u)

Clearly, the storage system for PV based active generator will provide a fast response and proper power and frequency balancing for the system.

III. FREQUENCY RESPONSE ANALYSIS

For small and low-voltage systems, the frequency deviation will not be harmful for the whole system. However, based on the BS EN 50160:2000 (Table I) the frequency deviation of public electricity supplied by public distribution systems must be within the range of 49.5 Hz to 50.5 Hz for a high voltage system with huge amount of loads. Since frequency variation might give an adverse effect onto the whole system, it is important to control it. For a primary frequency control through grid connected photovoltaic active generator, this system will try to embed the battery storage system with ultracapacitor to control the frequency when it crosses certain threshold as stated in BS EN 50160:2000.

For a primary frequency control for the grid connected photovoltaic active generator, the strategy begins with consideration of basic inertia equation that might lead to the implementation of the whole controller into the system. Fundamental of basic inertia equation is:

$$I = b\, m\, r^2 \tag{6}$$

Where b is inertial constant, m is the mass and r is the distance between axis and rotation angle. Vital parameter for grid connected photovoltaic active generator system is the regulated inertial constant where it can be defined as:

$$k = \frac{stored\ kinetic\ energy}{VA\ rating} \tag{7}$$

For a complex system with one or more connected generator that has been tripped, the kinetic equation can be outlined as (assuming that this will lead to the frequency variation):

$$k = \frac{1}{2}\left(\frac{-(generator\ rating)}{\frac{\partial \omega_\alpha}{\partial t}}\right)\frac{\omega_\alpha}{P_\alpha} \tag{8}$$

And it can be simplified as:

$$k = \frac{-(generator\ rating)f}{2P_\alpha\left(\frac{\partial f}{\partial t}\right)} \tag{9}$$

Where:
ω_α = system angular speed
P_α = power balance after trip
f = system frequency

It can be determine that for a small power system scheme, the smaller the k value will be [5].

The battery and ultracapcitor storage system will started to act once the frequency is over or under the rated value. Droop response from battery storage system will use the proportional control to drive the whole system and lead the system to its equilibrium condition. The relationship between frequency and power as in Figure 3 can be seen that for every frequency drop the real power needs to be supplied by the battery storage system and ultracapacitor. It wills goes vice versa for an over rated frequency.

In order for the battery storage system and ultracapacitor to control the process, battery SOC, DOD and power density parameter is critical.

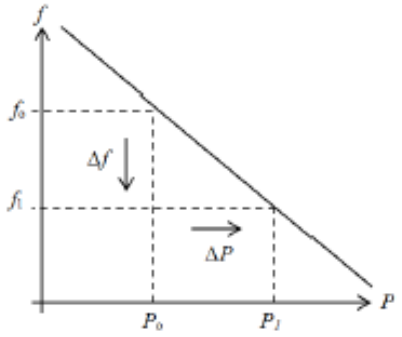

Figure 3. Real power and frequency relationship [7]

IV. FREQUENCY DROOP CONTROLLER AND REAL POWER REGULATION

Droop controller in PV based active generator will be able to act as a primary controller for any disruption that might affect the frequency nominal value. Currently, there is no regulations or requirement to provide frequency regulation services to the power system [8]. However, with the increasing penetration of renewable generation especially PV array, the impact on frequency regulation will be significant. Principally, the typical values of the frequency droop is 100% of increasing power for any reducing of frequency between 3% to 5% of the actual values [9].

Basically for a conventional frequency droop control for PV array with storage system, the irradiance and temperature or the PV cells will affected the operating conditions of the droop controller. The controller will act when the frequency falls from f_0 to f. This indicates that there are changes happening in load and more active power is needed (Figure 3). This is where the appearance of synchronous generator parameters is needed and to do such thing, the system needs to imitate the synchronous generator.

In order for the system to mimics the actual operations of synchronous generator, a fake synchronous generator will be embedded as a controller in the system. This is done by emulate the swing equation of synchronous generator with the new equation, based on the droop controller

characteristics [10]. The frequency droop mechanism can be executed based on Figure 4.

Virtual angular speed and the nominal frequency value from grid are compared before multiplied with gain. This equation involving the total torque ($\Delta\tau$) and angular frequency (Δf_a) changes, where it can be define as the droop coefficient for the whole system that might affect the output frequency. There are three basic synchronous generators parameters that are vital in the system, real power (P), reactive power (Q) and the electromagnetic torque which is labeled as (τ). These parameters are calculated based on simplified lagging power factor phasor diagram for synchronous generator (Figure 5).

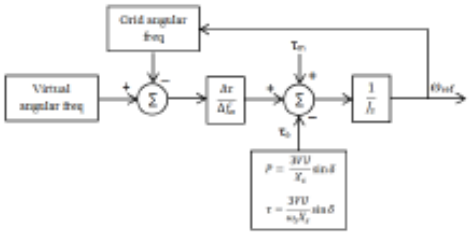

Figure 4. Frequency droop controller block diagram.

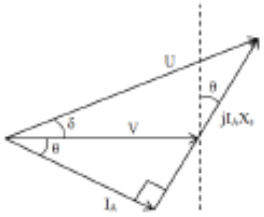

Figure 5. Simplified lagging power factor phasor diagram for synchronous generator.

V. System Under Study

Figure 3 show the proposed system for Primary frequency control through grid connected photovoltaic active generator. The controllers' equation can be expressed as:

$$\omega_{ref} = \frac{1}{J_s}(P_e - P_m) + \frac{\Delta\tau}{\Delta f_a} - \omega_g + \omega_f \qquad (10)$$

This equation is analyzed on its performance based on the dynamics and steady-state. Both of these performances are crucial to make sure that the system can be implemented in further works.

Equation (5) can be rewrite as a power system measurement for a low pass-filter analysis:

$$\omega^* = -\frac{\alpha}{\beta(\tau_s+1)}P^* \qquad (11)$$

Where P* and ω* denotes as a perturbed value of real power and frequency. For a steady-state performance, the controller frequency is equal to the grid frequency; hence by comparing equation (6) and (7) there are similarities. However, it may be a slight different due to variations in the controller parameters if it is connected to the real system. For a real system, damping control is required to run the controller smoothly.

VI. Conclusion

Control and operation energy storage in relation to the power system is a vital issue nowadays as the penetration of photovoltaic system and others renewable energy sources into the market. Based on this paper a PV based active generator with integrated storage units is proposed to provide frequency regulation and power balance for power system stability. A proper ground work for coordination between storage units PV source and generator has been discussed. The frequency droop characteristics and the virtual moment of inertia of the PV based active generator is presented supported by equations that will be used for future design of primary frequency control for grid connected photovoltaic active generator.

References

[1] R. Bhatt and B. Chowdhury, "Grid frequency and voltage support using PV systems with energy storage," in *North American Power Symposium (NAPS), 2011*, 2011, pp. 1-6.

[2] Y. L. Huanhai Xin, Zhen Wang, Deqiang Gan, Taicheng Yang, "A New Frequency Regulation Strategy for Photovoltaic Systems Without Energy Storage," *IEEE Transactions on Sustainable Energy*, vol. 1, pp. 1-9, 23 April 2013 2013.

[3] R. Shah and N. Mithulananthan, "A comparison of ultracapacitor, BESS and shunt capacitor on oscillation damping of power system with large-scale PV plants," in *Universities Power Engineering Conference (AUPEC), 2011 21st Australasian*, 2011, pp. 1-6.

[4] A. Aichhorn, M. Greenleaf, H. Li, and J. Zheng, "A cost effective battery sizing strategy based on a detailed battery lifetime model and an economic energy management strategy," in *Power and Energy Society General Meeting, 2012 IEEE*, 2012, pp. 1-8.

[5] C. A. Hill, M. C. Such, D. Chen, J. Gonzalez, and W. M. Grady, "Battery energy storage for enabling integration of distributed solar power generation," *Smart Grid, IEEE Transactions on*, vol. 3, pp. 850-857, 2012.

[6] J. M. Guerrero, J. C. Vasquez, J. Matas, L. G. de Vicuña, and M. Castilla, "Hierarchical control of droop-controlled AC and DC microgrids—a general approach toward standardization," *Industrial Electronics, IEEE Transactions on*, vol. 58, pp. 158-172, 2011.

[7] H.-J. Yoo, H.-M. Kim, and C. H. Song, "A coordinated frequency control of Lead-acid BESS and Li-ion BESS during islanded microgrid operation," in *Vehicle Power and Propulsion Conference (VPPC), 2012 IEEE*, 2012, pp. 1453-1456.

[8] M. Datta, T. Senjyu, A. Yona, T. Funabashi, and C.-H. Kim, "A voltage and frequency control approach by grid-connected MW class PV systems," in *Electrical Machines and Systems (ICEMS), 2010 International Conference on*, 2010, pp. 475-480.

[9] Q.-C. Zhong and G. Weiss, "Synchronverters: Inverters that mimic synchronous generators," *Industrial Electronics, IEEE Transactions on*, vol. 58, pp. 1259-1267, 2011.

[10] Y. D. J. Guerrero, L. Chang, J. Su, and M. Mao, "Modeling, Analysis, and Design of a Frequency-Droop-

Based Virtual Synchronous Generator for Microgrid Applications."

APPENDIX

TABLE I BS EN 50160:2000 VOLTAGE CHARACTERISTICS OF ELECTRICITY SUPPLIED BY PUBLIC DISTRIBUTION SYSTEMS STANDARDS

Supply Voltage Phenomenon	Acceptable Limits	Measurement Interval	Monitoring Period	Acceptance Percentage
Grid frequency	49.5 Hz to 50.5 Hz	10s	1 week	95%
Slow voltage changes	230V ± 10%	10mins	1 week	95%
Voltage sags or dips (≤ 1 min)	10 to 1000 times/ year	10ms	1 year	100%
Short interruptions (≤ 3mins)	10 to 1000 times/ year	10ms	1 year	100%
Accidental, long interruptions (> 3mins)	10 to 500 times/ year	10ms	1 year	100%
Temporary over-voltages (line to ground)	< 1.5kV	10ms	N/A	100%
Transient over-voltages (line to ground)	< 6kV	N/A	N/A	100%
Voltage unbalanced	2%, 3%	10 min	1 week	95%
Harmonics voltages	8% THD	10 min	1 week	95%

2013 IEEE Conference on Clean Energy and Technology (CEAT 2013).
DOI: 10.1109/CEAT.2013.6775606

On-Grid Residential Development with Photovoltaic Systems in Southern Norway

Aimie-Nazmin Azmi
Faculty of Engineering & Science
University of Agder
Grimstad, Norway
aimie.n.azmi@uia.no

Mohan Lal Kohle
Faculty of Engineering& Science
University of Agder
Grimstad, Norway
mohan.l.kohle@uia.no

Anne Gerd Imenes
Teknova AS
Kristiansand, Norway
agi@teknova.no

Abstract – **The application of residential photovoltaic (PV) systems is increasing rapidly worldwide. In Southern Norway, a group of on-grid smart houses with embedded PV systems, solar thermal collectors, and geothermal heat pumps are under development at Skarpnes. In this paper, performance analysis based on simulations of an on-grid residential house with PV system located at Skarpnes is presented. This project is expected to demonstrate zero energy and zero emission housing in Norway. This paper discusses a theoretical study of home energy consumption with electricity production for a single house from a PV system, including simulations of irradiation conditions and tilt angles, and of the PV system's levelized energy cost compared with average grid energy price. The results show that an annual zero-energy budget for electrical needs could be achieved, and that under certain assumptions the system may be economically feasible.**

Keywords - Smart house, Photovoltaic system (PV), Building energy, Solar energy

I INTRODUCTION

Building integrated (BIPV) and roof-mounted photovoltaic systems are increasing rapidly worldwide and have the potential to become a major contributor of renewable energy in the urban environment. Compared to centralized PV plants, BIPV systems may offer reduced economic costs and improved environmental performance [1, 2]. The use of residential PV systems can be economically viable also in the Nordic countries, and especially in sunny areas such as Southern Norway [3, 4]. In Southern Norway, a group of on-grid zero energy and zero-emission housing area with roof-mounted PV systems, solar thermal collectors, and geothermal heat pumps (borehole heat exchangers) are under development at Skarpnes. The proposed project is a zero energy pilot project that has been approved by the local authority and is expected to be completed in four years' time, with residents moving in to the first houses in 2014. It will be developed by Skanska Norge and is a pilot project in The Research Center on Zero Emission Building (ZEB) and in the Norwegian '*Lavenergiprogrammet*' for evaluation of homes with low energy demand (EBLE) [5]. The definition of a zero energy building in this project is referring to a building that produces the same amount of energy as its own demand during the operation period of a year. The electricity use for appliances is not included in the net energy balance account.

The energy required in this project will be partially supplied from the PV arrays on the rooftops. For heating purposes, heat pumps and solar thermal collectors will be used in combination with borehole heat exchangers. Based on preliminary system specifications, the developer is planning to install a PV area of around 45 m^2 on the roof of each single house unit. The PV array installation is going to affect the cost of development of smart houses. It is expected that the energy generated from all of the rooftop PV arrays should be sufficient to cover the total annual electrical needs for the housing development. This project will give results for the specific situation in the local region and collect extensive data from field measurements. Results from the project will be helpful in finding the future optimal mix of storage, local energy generation and grid power in zero energy houses.

The results may also help in analyzing the needs of traditional houses where smart grid solutions and distributed generation units may get installed in future. Skarpnes is a small village located at 58.4° north and 8.7° east. Based on results from PVsyst simulation it will receive an annual average 2.43 kWh/m^2/day of horizontal global solar irradiation. The solar radiation varies significantly throughout the year and in summer it can typically reach up to almost 6 kWh/m^2/day [3, 4].

The techno-economic analysis and evaluation of a PV system is the main requirement for its proliferation in any application [6]. In this paper, a techno-economic performance analysis of a smart house with PV system located at Skarpnes is presented. The PV system performance is influenced by incident solar radiation, tilt angle of the modules, and also by any partial shading that can be caused by surrounding objects. It is however assumed here that the housing development will not be significantly affected by shading. This paper discusses a study of home energy consumption and local PV electricity production with levelized energy cost and grid energy price comparison. These analyses have been done by using the HOMER [7] and PVsyst [8] software packages. These results will be compared with the real operational data once the smart houses are in operation. HOMER and PVsyst are sizing tools software, which help the user to execute a simulation to explore techno-economic performance analysis.

This paper is organized as follows: Section II provides a discussion on the electrical load consumption (profile) of a typical house in Norway. Other vital parameters included are the PV panel parameters and the solar radiation profile. Section III presents the techno-economic analysis, focusing on the energy generation per month and the cost involved. Section IV provides conclusions drawn from the obtained simulation results.

II Data Collection

A. *Typical load profile:*

The smart houses, which are under development at Skarpnes (Norway), are going to be built based on the zero energy and zero emission concepts. The development is complying NS 3700 standard. In this paper, the estimated load is based on a basic home energy requirement with a size of 154 m^2. Typical daily load profile for a standard house including basic electrical needs and heating is presented in Figure 1. This is the average data based on [16] and [17]. As this house will be heated by a heat pump and solar thermal collector system, the electricity consumption required for house heating will be less than for a traditional Norwegian home. The electricity usage patterns vary with time of day, seasons and weather conditions. Realistic seasonal / daily load profiles will be considered in further studies for doing more accurate performance analysis of the system. Real operational results will be collected over a few years and compared with the simulated results.

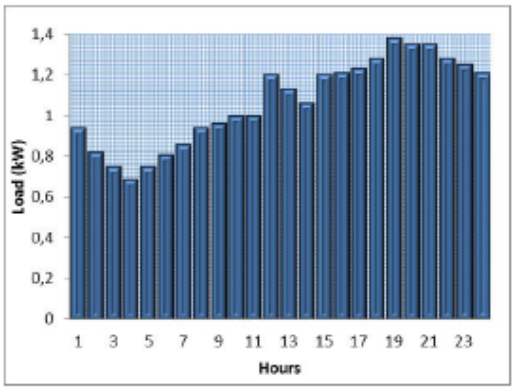

Figure 1: Daily load profile for a typical house, based on [16,17].

B. *Solar Resources at Skarpnes*

In the case studied here, the solar panels will be mounted at a fixed tilt angle of 30° and facing due south. The actual houses will have different orientations, facing either to the south-west or south-east. Based on the predicted solar irradiance at Skarpnes, the potential of using solar as a source of electricity and heat is promising. Figure 2 shows the simulation results from 3 different sources - meteronorm, PVGIS website and PVsyst simulation. Based on the average value of these three databases, Skarpnes has an average annual insolation of 2.84 kWh/m^2/day on a 30° tilted roo facing due south. As expected, during mid-winter (Dec) th solar radiation is as low as 0.31 kWh/m^2/day (meteronorm and it is expected that the house will use the electricity fro the grid during winter, and will be able to sell the electricit generated from the PV system to the grid in summer.

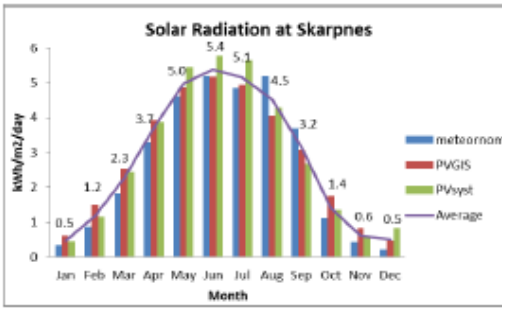

Figure 2: Average solar radiation at Skarpnes, based on meteonorm, PVGI and PVsyst simulations for 30° tilted to the south.

Figure 3 shows the annual solar path at Skarpnes, base on PVsyst simulation. The longest day in summer will hav around 17.8 hours of sunshine, and 22nd December marks th shortest period of sunshine in Skarpnes.

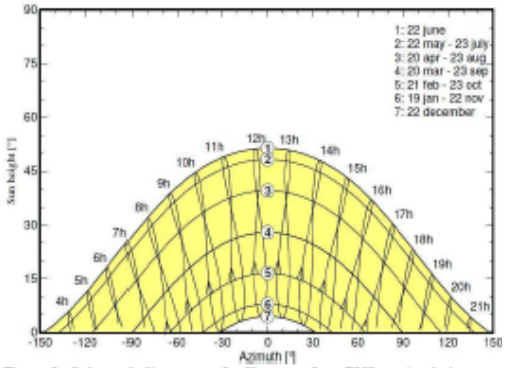

Figure 3: Solar path diagramme for Skarpnes from PVSyst simulation.

For the house studied here, the PV tilt angle is fixed a 30° due to the angle of the tilted roof. In this article, we als consider the possibilities of other tilt angles for maximizin incident solar radiation. Figure 4 shows the average annua solar insolation for different tilt angles, based on results fro PVsyst. OPT is the tilt angle for annual maximum output This tilt angle is 39° and during January-March an September-December, it results in slightly higher inciden solar radiation. However, the difference is relatively sma and the chosen rooftop angle is close to the optimum angle i terms of the energy output from the PV array.

III RESULTS AND DISCUSSION

A. *Electric Energy Profile of the System*

PV array selection is crucial for the developer in order to get high efficiency of output power when the available area is limited. For simulation purposes, a total of 28 polycrystalline silicon modules, each 230 W, are assumed to cover an area of 45 m^2 for each house. The expected total generation of electricity from this PV array is 6353 kWh/year.

TABLE I. ENERGY NEEDS FOR SMALL HOUSE IN SKARPNES [18]

Energy Purpose	Specific Energy (kWh/m^2)	Energy Needs (kWh)
Space heating	13.3	2058
Hot water	29.8	4609
Fans	4.4	678
Pumps	1.3	197
Lighting	9.3	1446
Technical Equipment	17.5	2712
Ventilation Cooling (cooling coils)	0.6	94
Total net energy	**76.2**	**11794**

Table 1 shows the energy needs for a small house with a 154 m^2 area. It is expected that the annual total energy consumed is approximately 11.8 MWh, where around 6.1 MWh represent electrical needs and 5.7 MWh are thermal requirements. This energy usage includes basic needs for a typical house such as lighting and heating. For energy saving and improved efficiency in the zero-energy houses in Skarpnes, there are a few additional measures that will be considered. The installation of LED lighting to replace the conventional lighting system will reduce the energy consumption. Heating will be provided by a solar collector system and ground heat from 160 meters of underground pipes. Thicker insulation and 3-layered glass windows will reduce heat losses.

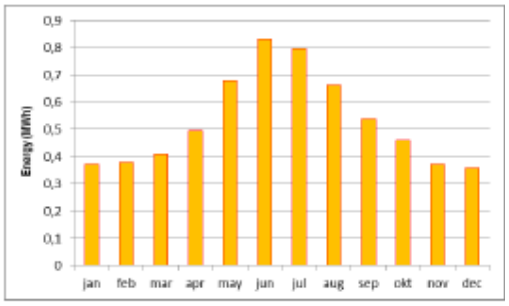

Figure 5: Monthly energy generated from the PV rooftop system (based on HOMER simulation).

From HOMER simulation, the bar chart in Figure 5 shows that it is expected that the 45 m^2 PV rooftop system will be able to supply a maximum of 0.83 MWh in June and 0.80 MWh July, and a minimum of around 0.38 MWh during December and January. There is some deviation between the monthly irradiation distribution results from PVsyst simulations and the monthly energy production from HOMER, especially mid-winter. It is possible that this could be due to different meteorological reference data used by the two software programs, and this will be further investigated.

The total energy generated based on the HOMER simulation is 6.4 MWh/yr. Compared with the electrical needs displayed in Table I of approximately 6.1 MWh/yr, it shows that the Skarpnes house should be able to fulfill the requirement for a zero-energy building since all electrical needs may be covered by the PV system. The most important thing in this work is to see the ability of the house to generate electricity for domestic usage and its capacity to sell the electricity back to the operator in the energy consumer-energy supplier concept (prosumers).

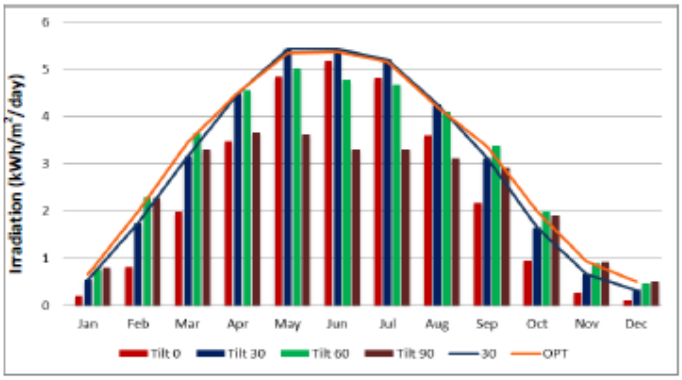

Figure 4: Average solar insolation for different tilt angles of the solar roof, where 39° is the optimum angle.

B. Economic Assessment

For this section, the values and figures that have been used do not reflect the exact Skarpnes housing project but are estimations done by the writer with a few assumptions in order to evaluate the economic feasibility of the project. In this section the most important parameter is the net present cost (NPC). NPC values will define the project acceptability in terms of investment, and consider the variance in current value of the future investment. Positive NPC values are an indicator of a potentially feasible project [13]. The following equation has been used to calculate NPC [14]:

$$C_{NPC} = \frac{C_{TAC}}{CRF_{(i,N)}} \quad , \qquad (1)$$

where C_{NPC} is the total net present cost, C_{TAC} is the total annualized cost, and CRF $(_{i,N})$ is the capital recovery factor. To get the capital recovery factor, the following equation applies;

$$CRF_{i,N} = \frac{i(1+i)^N}{(1+i)^{N-1}} \quad , \qquad (2)$$

where i is the annual interest rate or the discount rate and N is the number of years. From HOMER simulation the NPC value in this case study is NOK 21,2 (USD 3,6) and the levelized cost of energy (LCOE) is NOK 0.29 (USD 0.05) per kWh. Operating cost is defined as the annualized all costs ($C_{ann,total}$) minus the initial capital cost ($C_{ann,cap}$). It can be represented by the equation

$$C_{operating} = C_{ann,total} - C_{ann,cap} \quad , \qquad (3)$$

All simulations are made based on 25 years of lifetime. For HOMER, there are assumptions that already pre-set in the software, where it is assumed that all prices escalate at the same rate, and where 'annual real interest rate' is used rather than the 'nominal interest rate' [14].

Figure 6: Comparison of cost of energy from PV+Grid (prosumer mechanism) and total purchase from the grid (HOMER).

Figure 6 shows comparison of LCOE of PV generated electrical energy and monthly average market grid price. The grid price depends on the dynamics of the energy market. In this figure the price for PV+Grid is a levelized price by using the average price of the energy, while the grid energy price is a monthly average price collected from Nord Pool[1] website. Both prices are excluding tax and VAT. Average tax and VAT price based on 2012 statistics on average is 17 % of the total energy price that the consumer needs to pay per month [16]. For this simulation purpose, the energy price for PV+Grid is considered as a flat rate, whereas the actual energy rate will fluctuate around this average value with maximum values during winter and minimum values during summer.

The Payback period of this project based on the simulation is 21 years, assuming that the energy price is static and that the price of PV panel and installation will be decreasing by 2.1 % every year. This period will vary depending on the fluctuations of energy price from the grid and the price of PV systems, which is expected to continue to decrease in the near future.

C. Discussion

From simulations and calculations, it is obvious that the implementation of PV system is costly and it has many years of return of investment. Nevertheless, the result shows that the payback period is shorter than the expected lifetime of the system, and on-grid PV systems may have a good future in Norway since the cost of PV systems is expected to continue to decrease. For future analysis, the load profiles will be updated with real data from measurements at Skarpnes and will provide valuable insights into the behavior and performance of zero-energy houses of the future. This will give important feedback to the whole simulation, energy price and payback period analysis for the system.

Towards the year 2020, the anticipated 'nearly zero-energy' standards will start to take place. This project will contribute knowledge for future building construction based on environmental friendly and sustainable energy. After the construction of this project is completed, the exact result based on data from actual inhabited houses can be generated. This will guide the energy provider to develop new business models for better energy efficiency measures and improved design processes.

V CONCLUSION

In this paper, a roof-mounted residential PV system based on site data from Skarpnes in Southern Norway has been studied. From simulations and the predicted annual average solar irradiance at Skarpnes, the result of local energy generation has been presented. A techno-economic analysis has been performed by using the HOMER and PVsyst

[1] Nord Pool is a leading power market in Europe and the biggest in the world. It operates in Norway, Denmark, Sweden, Finland, Estonia and Lithuania.

simulation tools. Typical load profiles for a household's energy consumption and the average electricity price have been used to evaluate the planned smart houses at Skarpnes with a size of 154 m^2. This study found that the total electricity that can be generated from a 45 m^2 PV system with an average efficiency of 15 % is around 6 MWh/year. Since the houses in Skarpnes will be connected to the grid, each of the houses will sell the energy generated to the grid, with net export during summer months and net import during winter months. The comparison of the PV system's levelized energy cost with grid energy price is estimated to have a payback period of 21 years based on assumptions that the energy price is static and that the price of PV panel and installation will be decreasing by 2.1 % every year. This shows that the project may become economically feasible, since the payback period is less than the assumed system lifetime of 25 years.

IV Acknowledgement

The authors gratefully acknowledge the support of the Research Council of Norway and project partners in the project 'Electricity Usage in Smart Village Skarpnes'. Aimie Nazmin Azmi would also like to acknowledge the funding support received from Universiti Teknikal Malaysia Melaka (UTeM) for his PhD study at University of Agder (Norway).

References

[1] M. Oliver, T. Jackson, "Energy and economic evaluation of building-integrated photovoltaics", Energy, vol.26, issue 4, pp. 431-439, 2001.

[2] B. Agrawal, G.N. Tiwari, "Optimizing the energy and exergy of building integrated photovoltaic thermal (BIPVT) systems under cold climatic conditions", Applied Energy, vol.87, issue 2, pp. 417-426, 2010.

[3] O-M. Midtgard, T.O. Sætre, G. Yordanov, A.G. Imenes, C.L. Nge, "A qualitative examination of performance and energy yield of photovoltaic modules in southern Norway", Renewable Energy, vol.35, issue 6, pp. 1266-1274, 2010.

[4] H.G. Beyer, G.H. Yordanov, O.M. Midtgard, T.O. Sætre, A.G. Imenes, "Contributions to the knowledge base on PV performance: Evaluation of the operation of PV systems using different technologies installed in southern Norway", 37th IEEE Photovoltaic Specialists Conference (PVSC), pp. 3103-3108, 2011.

[5] Marit Thyholt, Tor Helge Dokka, Roald Rasmussen. "The Skarpnes Residential Development: A Zero Energy Pilot Project". The 2012 Nordic Passive House Conference. Trondheim. October, 2012.

[6] M. Kolhe, "Techno-economic optimum sizing of a stand-alone solar photovoltaic system". IEEE Transaction on Energy Conversion Transaction, vol. 24, issue 2, pp. 511-519, June 2009.

[7] HOMER Energy, 2334 Broadway, Suite B, Boulder, CO 80304, USA.

[8] PVSyst, Photovoltaic System Software, Route du Bois-de-Bay 107, 1242 Satigny, Switzerland.

[9] Greg Rosenquist, Michael McNeil et al. "Energy Efficiency Standards for Residential and Commercial Equipment: Additional Opportunities". University of California, Berkeley LBNL-56207. 2004.

[10] Dave Turcotte, Michael Ross, Farah Sheriff. "Photovoltaic Hybrid System Sizing and Simulation Tools: Status and Needs. Cost of solar energy generated using PV panels". PV Horizon: Workshop on PV Hybrid Systems. Montreal, Sept 10, 2001.

[11] SolarBuzz. Retail Price Summary 2012. March 2012. www.solarbuzz.com

[12] M.N El-Kordy et al. "Economical Evaluation of Electricity Generation Considering Externalities". Renewable Energy Journal. February. 2002.

[13] G.J. Dalton, D.A. Lockington, T.E. Baldock. "Feasibility Analysis of Stand-alone Renewable Energy Supply Options for a Large Hotel". Renewable Energy Journal. July 2008.

[14] Omar Hafez, Kankar Bhattacharya. "Optimal Planning and Design of a Renewable Energy based Supply System for Microgrids". Renewable Energy Journal. February 2012.

[15] Renewable Energy Technologies: Cost Analysis Series. International Renewable Energy Agency (IRENA). Abu Dhabi, UAE. June 2012.

[16] Statistics Norway. Statistisk Sentralbyrå (www.ssb.no). http://ssb.no/en/energi-og-industri/statistikker/husenergi

[17] D. H. Joe Wiehagen, "Review of Residential Electrical Energy Use Data," 2001, http://www.toolbase.org/PDF/CaseStudies/ResElectricalEnergyUseData.pdf

[18] Rasmussen R., Skarpnes Boligfelt: Søknad om støtte til ny teknologi for fremtidens bygg. Application to Enova, archive doc. 13/683-5, 27 August 2013. Unpublished document, Skanska Norge AS.

4th International Workshop on Integration of Solar Power into Power Systems Berlin, Germany. ISBN: 978-3-9816549-0-5

Technical and Economic Analysis for a Residential Grid Connected PV System with Possibilities of Different Battery Energy Storage Capacities.

(Case Study: Southern Norway)

Aimie-Nazmin Azmi[1, 2], Mohan Lal Kolhe[1], Anne Gerd Imenes[1,3]
[1]Faculty of Engineering & Science, University of Agder, Norway
[2]Fakulti Kejuruteraan Elektrik, Universiti Teknikal Malaysia Melaka, Malaysia
[3]Teknova AS, Kristiansand, Norway
aimie.n.azmi@uia.no, mohan.l.kolhe@uia.no, agi@teknova.no

***Abstract*— -Battery energy storage systems are likely to have substantial influence in small scale grid connected building integrated photovoltaic (PV) system. Grid connected PV system with proper storage technologies and power conditioning devices can also work as an active generator for controllable dispatch of active and reactive power. The importance of power conditioning devices and energy storage technologies has been increasing due to implementation of future intelligent / smart grid technologies for power dispatch, demand side management, and peak load reduction. This work presents a typical annual techno-economic analysis of a grid connected PV system with different possibilities of battery energy storage capacities. It will also demonstrate the impact of PV penetration and battery storage on energy production. The assessment criteria involve net present value, levelized energy cost production from PV system, renewable fraction as well as contribution from/to grid for fulfilling the residential electrical energy requirements. A typical energy storage capacity is going to be determined by taking into account daily PV production with reference to the daily load profile. It is going to consider different battery energy storage capacities, with reference to a typical value, for doing techno-economic analysis. In this study, a typical annual load profile of Southern Norway region is considered for a distinctive planned building integrated PV system. A basic Norwegian house with the size of 154 m² and 45 m² of PV area is used. The results of this work will be very useful for planning of inclusion of battery energy storage systems for grid connected building integrated PV system in smart grid environment especially in Norway.**

Keywords-Battery storage, photovoltaic, battery capacity, cost

I. INTRODUCTION

TABLE I. EXAMPLES OF RECEIVED SOLAR RADIATION AND ENERGY CONSUMPTION

Annual received solar radiation by the earth	7.81×10^{17} kWh
Annual global energy use	1.40×10^{14} kWh
Annual received solar radiation in Norway	2.91×10^{12} kWh
Annual energy use in Norway	3.12×10^{11} kWh
Annual insolation in Kristiansand	ca 1.0 kWh/m²
Annual energy use, passivehouse	ca 0.1 kWh/m²

Believing in the future of solar power is the motivation of the analysis which has been done in this paper. The increased energy consumption globally and of the problem with conventional fossile energy sources that lead to environmental issues, has brought attention to the utilization of renewable energy and especially solar power. Table I shows numerical examples on the enormous solar radiation resource available and the potential for its utilization. Based on local Norwegian data for total energy usage [1], it is obviously that annual received solar radiation is more than enough to supply energy throughout the country. Based on this fact, research on fully utilizing the solar resource is needed.

This paper will discuss an analysis of a photovoltaic system in typical Norwegian house in Southern part of Norway. The coordinates of the town Kristiansand have been used in collecting the irradiation data, and the Skarpnes[1] zero energy village project description is the background study for this analysis. The recommended PV tilt angle for the region is about 35°-40°, and the chosen tilt angle in this project simulation is 38°. By doing a repetition simulation in HOMER[2] and using solar irradiation result from PVGIS[3], the output of the whole project has been evaluated. By taking into account the economical prospect of the project, 5 kW PV capacity is chosen in this case study.

Since the system is designed for domestic residence, the roof area required for PV should not be larger than 50 m², unless the owner of the property is willing to build a standalone PV system in the home compound. However, for any installation of PV system, the user needs to consider the storage system. Apart from considering grid storage, this can be battery storage or a series of batteries with ultracapacitors.

With the existence of the storage system, undoubtedly it will improve the security of supply for the whole system. However, the biggest challenge is it still high cost with a short lifetime. Based on the daily load profile of a typical Norwegian residential home and the available solar radiation,

[1] http://www.skarpnes-nullhus.no/
[2] http://www.homerenergy.com/
[3] http://photovoltaic-software.com/pvgis.php

different capacity of battery storage system ranging from 20% up to 160% has been simulated. This simulation is based on two extreme days, the 28th of January and the 21th of July, representative of mid-winter and mid-summer respectively. For this particular work, the lead acid battery is chosen. With different selections of the battery capacity it is clear that the result will be affected.

When evaluating the overall system economicsconsidering the maximum PV battery lifetime of around 7-15 years [1] with respect to charging and discharging, it will end up with a significant cost. Therefore, proper sizing of the battery for a grid connected PV system is essential to a have a minimum operating cost with a higher utilization efficiency. This is the challenge for a researcher. It is needed to discover an optimal value for the battery energy storage size such that the total operation cost remains at a minimum. If the battery size is larger or smaller than the optimal battery size, the total operation cost is increased.

II. LOAD PROFILE

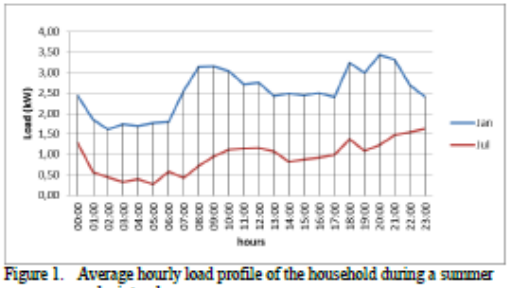

Figure 1. Average hourly load profile of the household during a summer and winter day.

Figure 1 show the average load profile of the residence of a typical Norwegian home with a size of 154 m^2. The load profile for mid-winter (January) and mid-summer (July) is plotted. Average daily consumption for the summer day is 0.89 kW while for the winter day it is 2.58 kW. Obviously, the electricity usage patterns vary with time of day, seasons and weather conditions. The average daily energy consumption throughout the year is 2.07 kW. On average, the difference between these two seasons is almost 52 %. It is a significant amount with a large impact on the system design. Therefore, proper system sizing is necessary in order to supply energy efficiently and at minimum cost.

III ENERGY STORAGE

Energy storages can be classified in four main categories: Electrical, Chemical, Electromechanical and Mechanical. Each of these types have the same purpose with different method of operation. Energy storage offers a broad range of approaches on controlling the power system units and it is able to create flexibilities in an electrical network. For renewable energy systems, generally three major types of lead acid battery are being used. Those are: AGM batteries, flooded type and gelled electrolyte sealed [2]. Each of these batteries has its own benefit that might be used for a different type of installation. For a proper development of a renewable energy system, battery sizing is crucial by considering battery parameters.

There are four main parameters that need to be considered for every installation of battery storage system. These are battery capacity, state of charge (SOC), charging and discharging rates, and battery efficiency [3]. By considering all of these crucial parameters, battery sizing and method to optimize the battery size can be achieved.

TABLE II. INPUT PARAMETERS FOR BATTERY

Variable	Notation	Value
Ageing coefficient	Z	5×10^{-4}
Minimum state of charge	SOC_{min}	30 %
Maximum state of charge	SOC_{max}	90 %
Self-discharging factor	a	2.5% per month
Minimum charging/ discharging time	t_{min}	10 hours
PV inverter efficiency	η_{pv}	97 %
Battery inverter efficiency	η_{bat}	94 %
Battery charging efficiency	η_{charge}	90 %
Battery discharging efficiency	$\eta_{discharge}$	90 %
Nominal battery voltage	V	12 V
Sampling time interval	$r\Delta t$	1 hour
Capital recovery factor	CRF	0.1233
Real interest rate	i	4 % per annum
Inverter Lifetime	N	10 years
Battery inverter cost		\$606 /kW
Battery investment cost rate		\$200 / kWh

Table II shows battery parameters that are used in this study. The above mentioned parameters are kept constant while simulation is done for different nominal battery capacities. For battery sizing purposes, load calculations need to be taken into consideration. Then, the days of autonomy for the battery to be operated needs to be determined. Based on the following battery equations, and by referring to Table II, the cumulative battery capacity loss can be calculated. Then this will lead to battery lifetime calculations and the cost and nominal battery capacities.

Charging,

$$SOC(d,t) = SOC(d,t-\Delta t)\times(1-a)+\eta_{charge}\frac{P_{DC,bat}(d,t)}{C_{bat}(d,t)V}\Delta t \quad (1)$$

Discharging,

$$SOC(d,t) = SOC(d,t-\Delta t)\times(1-a)+\frac{P_{DC,bat}(d,t)}{\eta_{discharge}\,C_{bat}(d,t)V}\Delta t \quad (2)$$

where,

C_{bat} : Usable battery capacity (Ah)

P_{DC_bat} : Charge/Discharge rate of the battery (kW)

Then, the cumulative battery capacity loss at the charging and discharging process of the battery can be determined.

$$C_{loss,cumi}(d,t) = \begin{cases} C_{loss,cumi}(d,t-\Delta t) - Z\,P_{DC,bat}\,\Delta t, & P_{DC,bat}(d,t) < 0 \\ C_{loss,cumi}(d,t-\Delta t), & P_{DC,bat}(d,t) > 0 \end{cases} \quad (3)$$

where,

$C_{loss,cumi}$:Cumulative battery capacity loss (kWh)

The battery capacity loss at any given time can be determined by;

$$C_{loss}(d,t) = C_{loss,cumi}(d,t) - C_{loss,cumi}(d,t-1) \quad (4)$$

where,

C_{loss} : Battery capacity loss (kWh)

The maximum battery charge rate at DC side is given by;

$$P_{DC\_bat,ch,max}(d,t) = P_{DC\_bat,disch,max}(d,t) = \frac{C_{bat}(d,t) \times V}{t_{min}} \quad (5)$$

IV PHOTOVOLTAIC DATA

The typical PV production data is based on Global Tilted Irradiance (GTI) measurement in Kristiansand area (58.15°, 8.00°) with a 38° tilting angle. This is measured through the year for 365 days. Several factors such as cloud cover, pollution and ground reflectionsmay influence the irradiation levels.

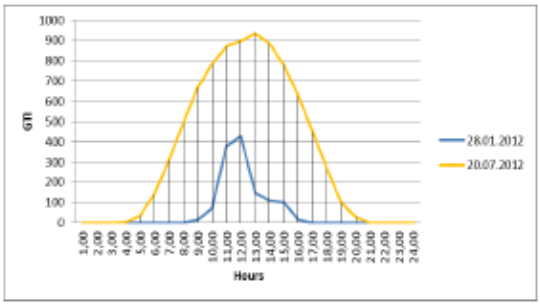

Figure 2. Average hourly irradiation profile in summer (July) and winter (January)

From Figure 2, it can be seen that the irradiance on a specific date in July (21st July) gives significantly high irradiance values due to summer season. On 28th of January, when it is winter and the ambient temperature is between -4 to 2°C, the maximum irradiance is seen at 12:00.

The equation for output energy from the PV panels is:

$$E = A \times Y \times H \times PR \quad (6)$$

Where:
E : energy (kWh)
A : PV panels active area (m^2)

H : annual average solar radiation on panels (shading is not included)
Y : yield%
PR : performance ratio.

For this specific simulation the parameters for the PV system has been identified as:

TABLE III. INPUT PARAMETERS FOR PV SYSTEMS

PV system size (kW)	5
Array type	Fixed-roof mount
DC-to-AC derate factor	0.78
Tilt angle(deg)	37.8
Derating factor	80%
Lifetime (years)	20
PV area (m^2)	54.5

V ANALYSIS

In this section, two types of analysis has been executed One analysis on (A) winter conditions and (B) summe conditions, and one analysis on (C) operational cost an benefits. The two representative days for the winter an summer seasons show significant variation, asseen from th daily PV insolation and the way the energy is being use (load profile). The energy price will also show variation. Fo this simulation, the author intentionally selected a flat rate o USD 0.05/ kWh for usage of energy. If there is a Feed-i Tariff (FiT) scheme, the consumer will gain benefits fro this scheme, preferrably executed with the implementatio of import and export energy prices. Up to this date, there i no such scheme implemented in Norway.

A. Analysis for Winter (January 28th)

During winter, the solar insolation is low as shown i Figure 2. For this particular paper, the author has chose January 28th as a reference for a winter day. Based on Figur 1, the highest load consumption will be during 20:00 t 21:00, while the lowest is between 02:00 and 03:00 where ranges between 1.98kW to 3.46kW. When the PV production profile is plotted together with battery storag charge/discharge rates based on the load profile for Januar 28th, the output can be seen in Figure 3. This simulation i based on a battery capacity of 1200 Ah with the lifetime o 13 years. On this particular date, the highest PV insolation i at 12:00 with the GTI almost 450 Wh/m^2.

Figure 3 shows the sequence of power transfer on typica winter day. It can be seen that the house is dependent on th power gain from the grid, with a very minimum input fro PV power and battery storage. Approximately from 12:00 t 15:00, where the solar radiation is sufficiently high, it i possible to charge the battery storage system, while the loa is still supplied by power from the grid. During this perio of time, the power from PV is just enough to recharge th

storage system. The battery then will be used the next morning. In this particular system, it is possible to charge the storage system by using power from the grid.

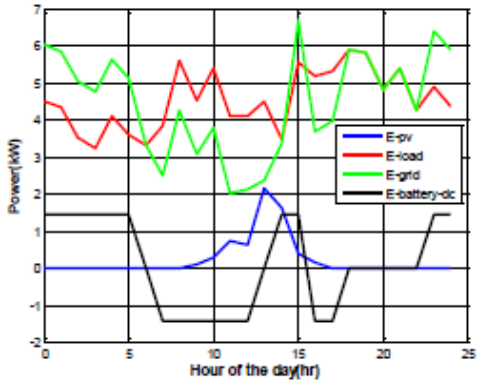

Figure 3. Power transfer sequence of the PV-storage system on 28th January (winter)

For four different values of battery capacity (Ah), the output of the power sequence is displayed in Figure 5. This figure shows battery capacity of 500 Ah, 700 Ah, 900 Ah and 1200 Ah that has been simulated. Based on these different values, it can be seen that a battery capacity at 1200 Ah will provide more power with higher cost compared to other capacities (refer Table II for battery parameters). Equations in Section III are used to find the optimum battery capacity to use in the system, taken into consideration the battery SOC and battery capacity loss.

B. *Analysis for Summer (July 21st)*

In mid-July, the solar insolation rose up to 950 Wh/m^2, as can be seen from Figure 2. During this season, the load profile is reduced nearly 34 %. The reduction of energy usage during this period is linked to the warmer temperatures and reduced heating demand. According to weather observations[4] during this period, the temperature varies from around 19°C to 28°C with an average wind speed of 3 m/s.

Figure 4 shows the power transfer sequence for the given summer day in July. The dependency on the power from grid is much less compared to Figure 3 during winter. However there is some interval of time when the load will be 100 % dependent on the grid, i.e. during night and in the early morning.

[4] www.yr.no

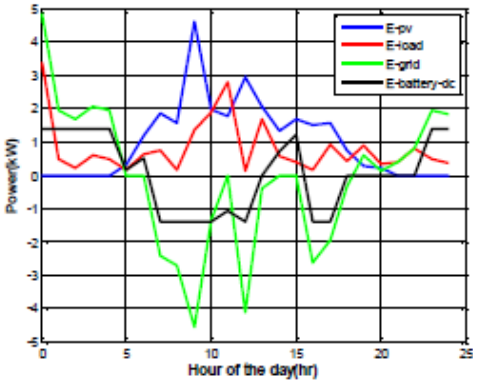

Figure 4. Power transfer sequence of the PV-storage system on 21st July (summer)

By simulating four different battery capacities, Figure 6 shows the power output from PV vs power from battery. It is compared to the power needed to supply the load. It is noticeable that with the high PV power output, the battery is less needed. However, it is crucial to make sure that the battery storage is charging and discharging within the limit at all time. With the battery capacity of 1200 Ah, the flow of the power remains smooth with fluctuations of charging and discharging process throughout the day. By using 500 Ah 700 Ah and 900 Ah, a different curve of power output will result. The lower the capacity, the lower the costs will be but by using equation (1), (2), (4) and (5), it is more cost efficient to use 1200 Ah compared to other capacities.

C. *Operational Cost and Benefits*

Grid connected PV system with storage system can give good benefits in terms of operational cost. The major cost that is related to this system is the cost of purchasing electricity and the cost of battery capacity loss, which is related to the discharging process. To determine the battery capacity loss during any particular hour that the system operates, that the following equation is used [4];

$$BCL_{cost}(d,t) = \frac{C_{loss}(d,t) \times B_{invest\_cost}}{1 - SOH_{min}} \quad (7)$$

Where,

BCL_{cost} : Cost of battery capacity loss ($)

B_{invest_cost} : Investment cost rate of the battery ($/kWh)

In this section the most important parameter is the net present cost (NPC). NPC values will define the project acceptability in terms of investment, and consider the variance in current value of the future investment. Positive NPC values are an indicator of a potentially feasible project. The following equation has been used to calculate NPC [5]:

$$C_{NPC} = \frac{C_{TAC}}{CRF_{(i,N)}} \quad (8)$$

By doing simulation in HOMER, the NPC that this system has is $62,320, which is relatively high. The cost of energy for every kWh ($/kWh) is $0.291. All simulations are made based on 25 years of lifetime. For HOMER, there are assumptions that already pre-set in the software, where it is assumed that all prices escalate at the same rate, and where 'annual real interest rate' is used rather than the 'nominal interest rate'.

TABLE IV. ELECTRICAL SUMMARY FOR THE SYSTEM

Production	kWh/yr	%
PV array	4,435	24
Grid purchases	14,358	76
Total	18,793	100

Based on Table IV, the electrical fraction of the whole system can be determined. 24 % of total energy used in the house is from renewable energy while the rest is from the grid. This means that most of the time, the house will use the energy purchased from the grid. This is illustrated in Figure 7, which shows the monthly average electric PV production and grid supplied power during the whole year. With the renewable fraction estimated at 0.24, this system is feasible to be used.

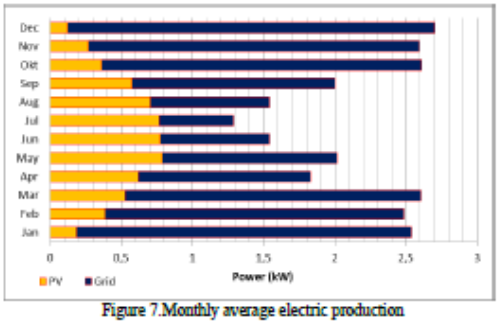

Figure 7.Monthly average electric production

For this simulation, a flat rate price of power purchased from the grid has been used. The energy market in Norway is dependent on the dynamic energy market prices from Nord Pool[5]. Thus, the price that should be considered will include tax and VAT price. Average tax and VAT price based on 2012 statistics on average is 17 % of the total energy price that the consumer needs to pay per month [6].

VI CONCLUSION

In this paper a typical annual techno-economic analysis of a grid connected PV system with different possibilities of battery energy storage capacities has been presented. The simulation for different battery capacities for 2 seasons winter and summer, has been presented in section V. For a house of 154 m^2, the suitable battery storage that will suit well is approximately at 1200 Ah. This storage system will efficiently work during summer and winter, with large variation in insolation. With an annual production from the PV system at 4,435 kWh and grid purchase at 14,358 kWh this system met the entire electrical load (refer Figure 3 and Figure 4) needed. By using HOMER, the NPC and COE has been calculated. It is expected that the NPC can be reduced if the exact energy price per kWh is used instead of the assumed flat rate. In the near future, the storage price is expected to decrease. This can reduce the capital cost for the whole system. For future work, exact price of energy in Norway will be taken account and the system will simulated for a larger range of load profiles and with different types of households.

ACKNOWLEDGMENT

The authors gratefully acknowledge the support of the Research Council of Norway and project partners in the project 'Electricity Usage in Smart Village Skarpnes'. Aimie Nazmin Azmi would also like to acknowledge the funding support received from Universiti Teknikal Malaysia Melaka (UTeM) for his PhD study at University of Agder (Norway).

REFERENCES

[1] S. Manya, M. Tokunaga, N. Oda, T. Hatanaka, and M. Tsubota, "Development of long-life small-capacity VRLA battery without dry-out failure in telecommunication application under high temperature environment," in *Telecommunications Energy Conference, 2000. INTELEC. Twenty-second International*, 2000, pp. 42-45.

[2] N. K. Medora and A. Kusko, "An enhanced dynamic battery model of lead-acid batteries using manufacturers' data," in *Telecommunications Energy Conference, 2006. INTELEC'06. 28th Annual International*, 2006, pp. 1-8.

[3] A. Aichhorn, M. Greenleaf, H. Li, and J. Zheng, "A cost effective battery sizing strategy based on a detailed battery lifetime model and an economic energy management strategy," in *Power and Energy Society General Meeting, 2012 IEEE* 2012, pp. 1-8.

[4] M. Gitizadeh and H. Fakharzadegan, "Battery capacity determination with respect to optimized energy dispatch schedule in grid-connected photovoltaic (PV) systems," *Energy*, vol. 65, pp 665-674, 2014.

[5] A.-N. Azmi, M. L. Kohle, and A. G. Imenes, "On-grid residential development with photovoltaic systems in Southern Norway," in *Clean Energy and*

[5] Nord Pool is a leading power market in Europe and the biggest in the world. It operates in Norway, Denmark, Sweden, Finland, Estonia and Lithuania.

Technology (CEAT), 2013 IEEE Conference on, 2013, pp. 93-97.

[6] S. N. S. Sentralbyrå. (2014). Available: http://ssb.no/en/energi-og-industri/statistikker/husenergi

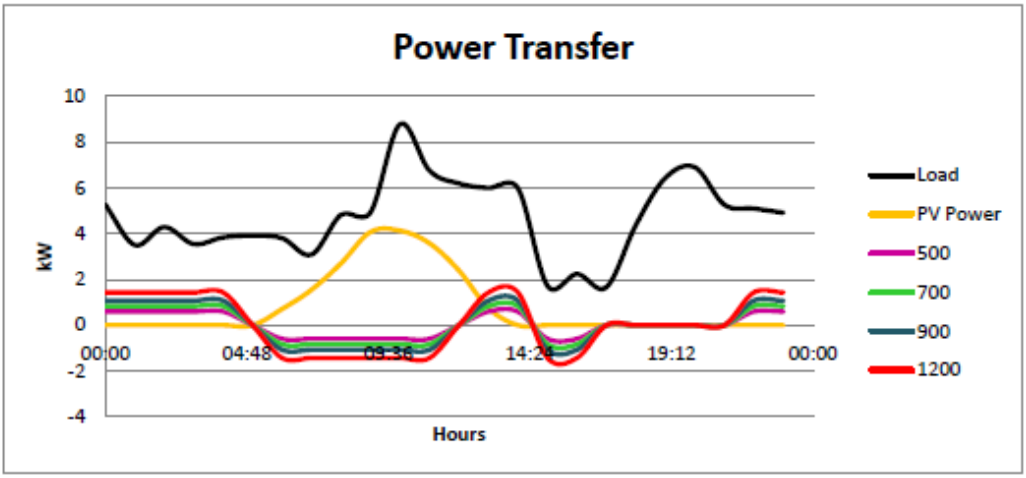

Figure 5. Different battery capacity vs PV power and typical daily load in winter

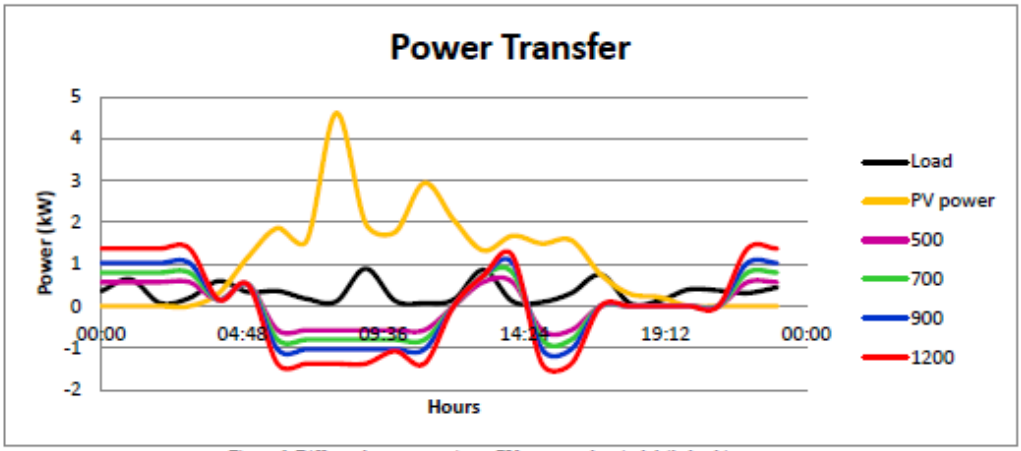

Figure 6. Different battery capacity vs PV power and typical daily load in summer

11th IEEE International Conference on Power Electronics and Drive Systems (PEDS2015). DOI: 10.1109/PEDS.2015.7203433

IEEE PEDS 2015, Sydney, Australia
9 – 12 June 2015

Photovoltaic Based Active Generator: Energy Control System Using Stateflow Analysis

Aimie Nazmin Azmi[1, 2], Mohan Lal Kolhe[1],
[1]Faculty of Engineering & Science, University of Agder, Norway
[2]Fakulti Kejuruteraan Elektrik, Universiti Teknikal Malaysia Melaka, Malaysia
E-mail(s): aimie.n.azmi@uia.no, mohan.l.kolhe@uia.no,

***Abstract* — At present, most of the grid connected photovoltaic (PV) systems are operating at maximum power points and injecting power in uncontrolled way. Thus, active generator will be a good solution to support instantaneous power balance, frequency control and maintaining the power quality with controllable power injection. This new mode of active generator needs innovative power management. The new proposed energy control system for active generator might help to manage the energy within the micro-grid environment. In this work, the focus is to manage the energy among the PV based active generator, load and interconnected grid and energy controller architecture for that purpose is presented. It considers availability of the solar resources, storage system and load requirements. If there is lack of energy from the active generator, then the grid supplies remaining energy. For architecture of energy controller, Stateflow ® model is used. It uses available energy information from PV array, battery storage with super-capacitors and load requirements for managing the energy flow and it provides control signals to the power conditioning devices, which are used for integrating the sources. The presented energy management algorithm will be useful for the future smart grid system and also for building integrated PV based active generator system and demand side management.**

Keywords—PV active generator, stateflow; energy controller

I. INTRODUCTION

Distributed generators (DGs) in electrical network might be very helpful for reducing the demand on the conventional power generators. One of the prominent sources for renewable energy sources is the PV system. However, there are problems related to the deployment of PV system due to their stochastic nature. Standalone PV system with battery storage system is well studied for their optimum sizing configurations based on load requirements [1]. To overcome this, PV based active generator concept can be implemented. PV based active generator (with embedded energy storage units) can be used as load following generator as other controllable power dispatch generators [2, 3]. This new type of distribution system, based on active generators, needs new innovative management and operation strategies for increasing the penetration of intermittent renewable energy systems e.g. PV system. The energy sources and loads are heterogeneous and it is needed to have real time management through active generator in coordination with grid at load end and it will also improve the energy efficiency. Energy management system in PV based active generator is a co-ordination of produced PV energy with the energy storage systems (together wit battery and super-capacitors) and load requirements. A battery controller for distributed energy system is presente in [4], but it has not considered PV and super-capacitor. A proper controller / algorithm are needed for controlling th energy flow among PV array, battery, and super-capacito with load requirements.

This paper focuses on architecture of energ management system for integration of PV based activ generator with local load and grid. It considers two basi questions: (i) How to manage energy distribution among P array, super-capacitor and battery? (ii) How to reduce stres on the power distribution system during peak hours i.e demand side management? These points are considered i this paper. The control system for energy management i the PV based active generator is using the Stateflow® model. Basically this method is often used to model a logi controller for dynamic outputs. Using this method, a algorithm of energy management that includes PV array battery storage system with super-capacitors and converter for their integration is presented. The Stateflow® is th event-based modeling toolbox in MATLAB and it is used t model logic for dynamically control of the energ management system. The algorithm is able to control th energy usage in a PV based active generator in order t maximize the utilization of the battery storage and super capacitors for managing the load locally and also in deman side management. This work is based on ref [5] and it ha used Petri-nets analysis. But in this work Stateflow® mode is used for energy management in PV based activ generator.

II. PV BASED ACTIVE GENERATOR

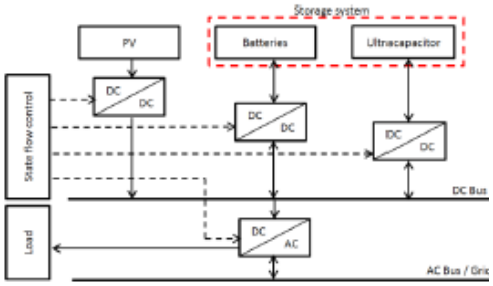

Figure 1. Basic structure of the PV based active generator

978-1-4799-4402-6/15/$31.00 ©2015 IEEE

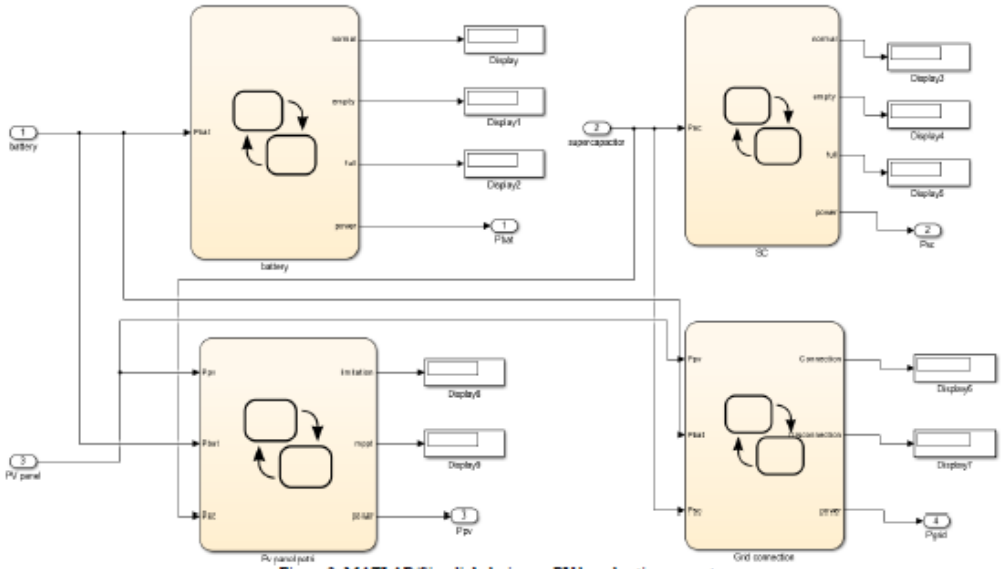

Figure 2. MATLAB/Simulink design on PV based active generator

The basic structure for PV based active generator is given in Fig. 1 and system components have been characterized in Stateflow® modeling. This power generation units comprises of PV arrays, batteries and super-capacitor units as storage system, DC-DC boost converters and an inverter. The PV array and storage system are integrated on a common DC bus through proper DC-DC converters. The energy storage system can also be used as a power fluctuate compensator for improving power quality under dynamic conditions. A coordinated use of storage units with PV array must be properly designed in order to work it as an active generator. This active generator unit is connected to the grid through a DC-AC inverter in parallel to the local load. It will also help in demand side management and energy buying / selling to the grid.

In this work, these multi-source units are modelled in the MATLAB® / Simulink environment. These models are integrated and their parameters are given in Section III. In Fig 2, battery storage system is labelled as No 1, super-capacitor is labelled as No 2 and the PV array is labelled as No 3, while No 4 is the grid reference.

III. COMPONENT MODELLING

The power generation units in this system comprises of four core modules: Energy storage, PV array, DC-DC converters, and DC-AC inverter. Each of these components needs functions and parameters. The component parameters are taken from [5].

A. Storage System

For long-term energy storage, the batteries are considered. A special operation management for battery charging and discharging strategies and knowledge of battery state of charge (SOC) is necessary. The ageing mechanism of the battery may result from many factors and it may affect the operational performance of the batteries [6]. In this work, the battery operations based on performance factors are not considered and they will be considered in further work. For this work, a simple battery model is used from MATLAB/Simulink. The battery parameters are given in Table I:

TABLE I. PARAMETERS FOR BATTERY

Parameters	Data
Nominal Voltage	144V
Rated Capacity	69.4Ah
Initial State Of Charge	100%
Fully Charged Voltage	156.8V
Nominal Discharge Current	13.9V
Internal Resistance	0.02 Ω
Capacity(Ah)@Nominal Voltage	21.53Ah
Exponential zone[Voltage, Capacity]	[146.6V 0.2Ah]

The storage system includes super-capacitor. In this work, the aging factors of super-capacitor have not been considered. The super-capacitor parameters are given in Table II:

TABLE II. PARAMETERS FOR SUPERCAPACITOR

Parameters	Data
Rated capacitance	198F
Equivalent DC series resistance	2.1×10^{-3} Ω
Rated voltage	150V
Surge voltage	155V
Number of series capacitors	2
Number of parallel capacitors	4
Initial voltage	16V
Leakage current	5×10^{-3}A
Operating temperature(Celsius)	15

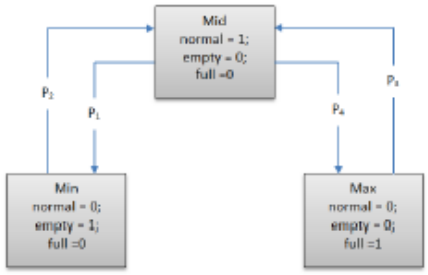

Figure 3. Stateflow diagram of the battery management system

For load management purposes, three conditions have been adapted in the simulation: maximum, mid and minimum conditions (Fig. 3). The energy storage system is represented for battery as P_{bat} and for super-capacitor as P_{sc}. The battery is at normal mode if ($P_{bat,min} < P_{bat} < P_{bat,max}$) while for 'full' condition it is at ($P_{bat} = P_{bat,max}$). It is defined as 'empty' if ($P_{bat} = P_{bat,min}$) . Basically, the flow of process is representing the digital signal as either 1 for available or 0 for not available. As shown in Figure 3, for a four transitions which are; P_1: $P_{bat} = P_{bat,min}$, P_2: $P_{bat} > P_{bat,min}$, P_3: $P_{bat} < P_{bat,max}$, and P_4: $P_{bat} = P_{bat,max}$. The same model is applied to super-capacitor.

B. PV Array and Input

PV module that is used in this paper is BP 3160N. 18 PV modules are used to supply energy to the system. The technical data is given in Table III:

TABLE III. PARAMETER FOR PV MODULE

Electrical data	Parameters
Nominal output P_{mpp}	160 W
Max. Voltage system	1000 V
Nominal Voltage V_{mpp}	35.1 V
Nominal current I_{mpp}	4.55 A
Open circuit voltage V_{oc}	44.2 V
Short circuit current I_{sc}	4.8 A
Module conversion efficiency	12.7 %

To analyse the output of the developed system, it is necessary to know the PV array output. The PV array output depends on the incident solar radiation, temperature and PV array parameters. In this work, the solar radiation data of Kristiansand (Latitude: 58° 15' 3521" N, Longitude: 8° 00' 2497" E) is used. A sample time period of few hours from the last day of May is selected as input for the PV array. The sample time period from 11:00 to 15:00 is taken and the global tilted irradiance (*GTI*) data for this period is as below:

TABLE IV. GTI DATA ON 31ST MAY 2012

Time	GTI (W/m²)	Time	GTI (W/m²)
10:56:00	970	13:11:00	801
11:11:00	977	13:26:00	821
11:26:00	974	13:41:00	794
11:41:00	903	13:56:00	805
11:56:00	869	14:11:00	786
12:11:00	863	14:26:00	761
12:26:00	827	14:41:00	722
12:41:00	794	14:56:00	680
12:56:00	739	15:11:00	638

From this table, the approximate output power can b determine by:

$$P_{PV} = GTI \times \eta \times A \quad (1$$

Where;

GTI : Global Titled Irradiation
η : Efficiency of the solar panel
A : Panel area

And the approximate output is on 31st May 2012 from 10:5 to 15:11 in 15 minutes interval has been given in Figure 4.

PV panel will be represented as P_{PV} and in this work; th simulation has been done into 2 different situations:

1) ($P_{pv} >= P_{\_req}$) and ($P_{bat} = P_{bat,max}$) and ($P_{sc} = P_{sc,max}$)
2) ($P_{pv} < P_{\_req}$) or ($P_{bat} = P_{bat,min}$) or ($P_{sc} = P_{sc,min}$)

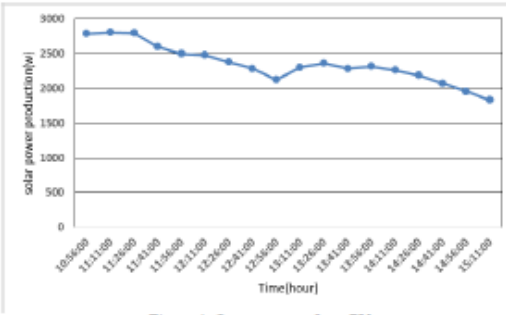

Figure 4. Output power from PV

$P_{\_req}$ is a power required by the load. In the first situatio the PV power is more than the required power, and th storage system is in a good capacity. The second condition give an impression of the conditions where the powe available from PV is lower than the required power.

IV. MODELLING ALGORITHM

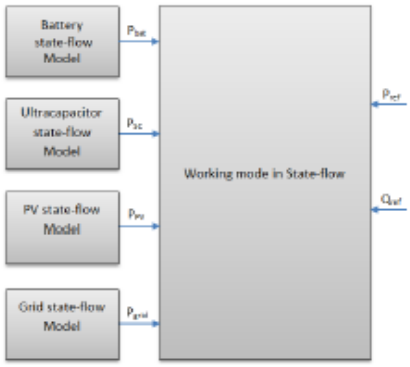

Figure 5. Stateflow algorithm flow diagram

Three different conditions have been tested. Mode 1 refers to the condition where the battery and super-capacitor are ready to use ($P_{bat,min} < P_{bat} < P_{bat,max}$ and $P_{SC,min} < P_{SC} < P_{SC,max}$. In this mode, PV array can supply power to load as well as to energy storage system.

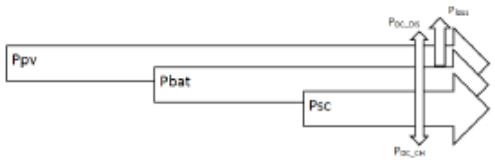

Figure 6. Power flow in Mode 1

The exchanged power of capacitor which belongs to input voltage of DC/DC inverter is P_{DC}. This power is disintegrated in 2 terms: P_{DC_CHA} indicates the capacitor is loaded and P_{DC_DIS} represents the capacitor is unloaded. The power flow is shown in Fig.6.

In Mode 2, the conditions are: super-capacitor and battery are fully charged ($P_{bat} = P_{bat,max}$ and $P_{SC} = P_{SC,max}$) and the produced PV power is higher than the reference power ($P_{PV} > P_{ref}$). At this mode the power production from PV needs to be controlled. This need to be done to make sure that the storage system is not overcharged as it may shorten the lifetime.

In this mode there is excess power from PV array that needs to be limited. Since the super-capacitor and battery are fully charged, excess power will be not accepted. So in this working mode the storage units are setup in stand by condition, and can be represented in:

$$P_{\_(Sto\_ref)} = P_{\_(bat\_ref)} = P_{\_(sc\_ref)} = 0 \quad (2)$$

In addition, PV array has gained more power than the required power $P_{\_req}$. All these reasons make it crucial to limit solar power production in this particular mode. Thus, the required power must be equal as solar power in reference. It is possible to supply the excess power to the grid.

Mode 3 refers to conditions where the batteries and super-capacitor are charging since both power sources are too low to deliver power. No power is supplied to the grid. Batteries and super-capacitor are charged. These working modes are embedded in the system as given in Figure 5.

In this working mode, the solar power production is insufficient. At the same time, supercapacitor and batteries are empty. This is the reason of the priority of power delivery from PV panels is given to supercapacitor and batteries for charging. As a result of this, the grid is supplying the load and charging battery and super-capacitor

V. Results and Discussion

Overall Stateflow® design of this whole system is given in Figure 2. This includes all modes that have been discussed in the previous sections. For this work the simulation result are only based on Mode 1. Figure 7 shows typical load requirement for 4 hours on 31st May 2012. Maximum load requirement is 6000 Watt while the lowest us 2000 Watt. The simulation results for battery, super-capacitor and PV power contributions for the mentioned load are given in Figure 8. In all these diagrams, 0 point from time offset signifies the measurement of testing time starts from 11:00, and it will last 4 hours till 15:00. In the beginning of the first hour shows that the total power production from battery and PV array is not enough to meet the requirement from the load. With the compensation from supercapacitor, the problem has been solved. This result proves that the generated power reaches the required power needed.

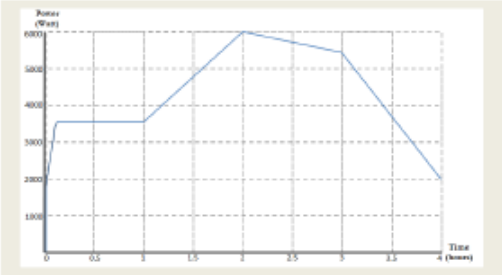

Figure 7. Load power requirement from 10:56 until 15:11

VI. Summary and Further Work

In this work, an overall power management system for a simple distributed generator, which includes storages (battery and super-capacitor) and PV array has been presented. Control strategy has been developed in Stateflow® in MATLAB. Hierarchical control algorithm is utilized to organize and identify the level of control system. Different modes of working methods are presented. The states of every power source are modelled in Stateflow® and simulated. Later, the power management system selects the relevant working mode and computes the power reference for each source. The active electric power has been considered. Other discussed operating modes with grid interaction will be considered as further work taking a day load profile.

Acknowledgment

A.N. Azmi would like to acknowledge the funding support received from the Universiti Teknikal Malaysia Melaka (UTeM) for his PhD study at the University of Agder (UiA), (Norway). The authors are very grateful to Mr. Su Haocheng, who has partially contributed in this work as part of his master thesis at UiA.

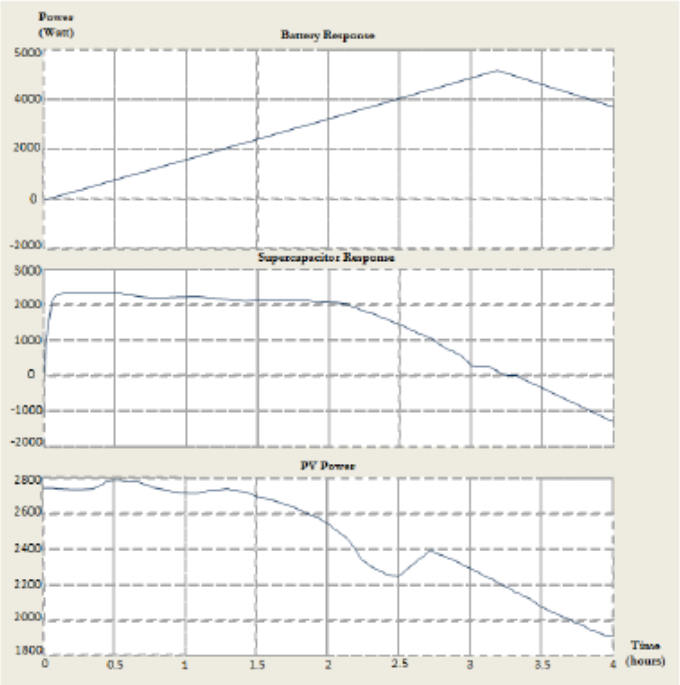

Figure 8. Power response from super-capacitor, battery and PV array

REFERENCES

[1] M. Kolhe, "Techno-economic optimum sizing of a stand-alone solar photovoltaic system," *Energy Conversion, IEEE Transactions on,* vol. 24, pp. 511-519, 2009.

[2] H. Kanchev, D. Lu, F. Colas, V. Lazarov, and B. Francois, "Energy management and operational planning of a microgrid with a PV-based active generator for smart grid applications," *Industrial Electronics, IEEE Transactions on,* vol. 58, pp. 4583-4592, 2011.

[3] A.N. Azmi, M. L. Kolhe, "Primary Frequency Control through Grid Connected Photovoltaic Active Generator," *3rd International Workshop on Integration of Solar Power into Power Systems* pp. 116-122, 2013.

[4] V. Virulkar, M. Aware, and M. Kolhe, "Integrated battery controller for distributed energy system," *Energy,* vol. 36, pp. 2392-2398, 2011.

[5] D. Lu, H. Fakham, T. Zhou, and B. François, "Application of Petri nets for the energy management of a photovoltaic based power station including storage units," *Renewable energy,* vol. 35, pp. 1117-1124, 2010.

[6] R. Kaiser, "Optimized battery-management system to improve storage lifetime in renewable energy systems," *Journal of Power Sources,* vol. 168, pp. 58-65, 2007.

IEEE International Symposium on Advanced Topics in Electrical Engineering (ATEE 2015). DOI: 10.1109/ATEE.2015.7133914

THE 9th INTERNATIONAL SYMPOSIUM ON ADVANCED TOPICS IN ELECTRICAL ENGINEERING
May 7-9, 2015
Bucharest, Romania

Review on Photovoltaic Based Active Generator

Aimie Nazmin Azmi[1,2], Mohan Lal Kolhe[1] , Anne Gerd Imenes[1,3]
[1]Faculty of Engineering & Science, University of Agder, PO Box 422, NO 4604 Kristiansand, Norway
[2]Fakulti Kejuruteraan Elektrik, Universiti Teknikal Malaysia Melaka, Durian Tunggal, 76100, Malaysia
[3]Teknova AS, Gimlemoen 19, NO 4630 Kristiansand, Norway
aimie.n.azmi@uia.no, mohan.l.kolhe@uia.no, AnneGerd.Imenes@teknova.no

***Abstract*— An active generator has the capacity to support frequency control and instantaneous power balance. The grid operator adjusts the power dispatch of generators according to power demand fluctuations. Photovoltaic (PV) based active generators can be used as load following generators in the same manner as other power dispatch generators. This new type of distribution system, based on active generator(s), needs new innovative management and operation strategies for increasing the penetration of intermittent renewable energy systems. The considered PV based active generator has three units, i.e., PV array, battery storage and super capacitor. In this review paper, the management and operation approaches of PV based active generators are discussed.**

Keywords: Photovoltaic (PV); Active generator; Microgrid; Smart Grid

I. INTRODUCTION

At present, most of the world-wide grid connected photovoltaic (PV) systems are operating at maximum power points and not contributing effectively towards the energy management in the power system network. Unless properly managed and controlled, large scale deployment of grid connected PV generators may create problems such as voltage fluctuations, frequency deviations, power quality problems in the power system network, changes in fault currents and protections settings, and congestion in the distributed network. A solution to these problems is the concept of active generators. The active generators will be very flexible and able to manage the power delivery as in a conventional generator system. This active generator includes the PV array with combination of energy storage technologies and proper power conditioning devices. The PV array output is weather dependent and therefore the PV power output predictability is important for operational planning of the micro-grid as well as centralized generators. In conventional grid connected PV generators, hybrid filters are used to improve the power quality [1]. But for multiple PV based active generators (e.g., a group of buildings with BIPV), the power quality issues require more analysis. Evaluation of fault protection systems will be needed to account for unknown situations that might interrupt the energy flow on the grid and reduce the efficiency of the grid performance.

II. OVERVIEW OF PV BASED ACTIVE GENERATOR

A PV based active generator is a system comprising of a PV array and a battery storage system with a capacity of storing energy both for long and short term local usage (long term: storage period in weeks or month. Short term: hour and days) [2]. The system should be able to generate, stor and release energy as long as the electricity is neede depending on the system sizing and house daily load. Thi can be done with a proper hierarchical monitoring and energ management system. Figure 1 shows such a system. Powe management is crucial to control the whole energy flow in th PV based active generator. As discussed in [3], the author put an emphasis on the power management algorithm o active PV station with a battery storage. Four hierarchica positions have been introduced and each level has its ow task, as shown in Figure 2. This PV based active generator i expected to offer new flexibilities to the consumer an operator. The system will be operated in a micro-gri environment and will have parameters that need to b considered such as frequency, voltage, storage capacities an PV forecasting.

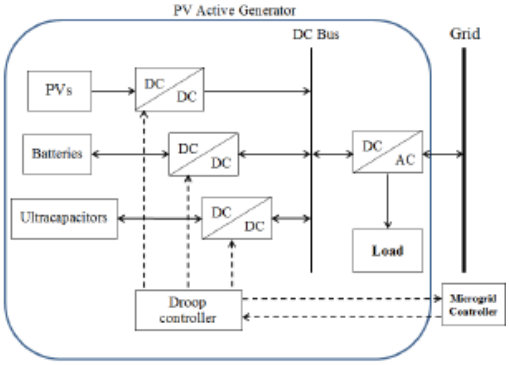

Fig. 1. Scheme of a PV based active generator

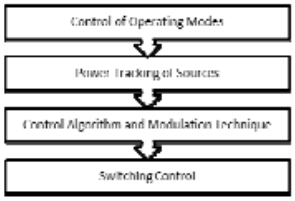

Fig. 2. Control levels of a PV based active generator

It has been observed that main disadvantage for thi system is the stochastic nature of solar radiation and PV arra

978-1-4799-7514-3/15/$31.00 ©2015 IEEE

output. In order to solve this problem, the PV based active generator has been introduced. Further discussion on applications, environmental and economic aspects may be found in [2, 4]. For a complete PV active based generator, a set of battery banks are connected in a series-parallel combination in order to provide desired power to the system. The additional ultra-capacitor will provide a fast response energy storage device that can reduce the effect of short term fluctuations of PV output and quick power delivery and it will enhance power quality of the whole system [5]. For such type of PV system, the battery storage system will be operated under the partial state of charge duty (PSOC) [6]. In this condition, the battery will be partially discharged at all times, in order to make sure the system will be able to absorb or discharge power to the grid as it is needed [7]. To charge-discharge the ultra-capacitor, a few methods as discussed in [8] can be used. Based on simulation results, the latter reference [8] found that constant power charging mode is preferred for charging ultra-capacitors in a PV system. However, it is not yet proven that this strategy will be suitable for a micro-grid system. It needs more investigation and in our further work it will be reported.

III. PV Based Active Generator in a Micro-grid Environment

A micro-grid is a system that operates at low voltage and has one or more distributed energy resources for electricity production (e.g. PV, wind turbines, micro-turbines, etc.) With proper energy management and systematic supervision, a micro-grid can be an effective new way of generating and transmitting energy near to the load. Examples of PV based active generators integrated into the micro-grid can be found in Kytnos Island and Mannheim-Wallstadt [2]. Energy supervision and management for the whole system is compulsory, and the authors in [9] have divided the system into two different parts: (i) central energy management of the micro-grid, and (ii) supervision and management of the active generator. On the micro-grid side, the operator needs to manage energy between the sources and load. This includes the active and reactive powers, frequency regulation, and voltage fluctuations. It has been noticed in [4] and [9] that a strategic framework of executing PV based active generators in a smart grid environment with more rules considering the long term energy management and the short term power balancing. In [4] the optimization of environmental and economic criteria have been developed on 24 hours of PV prediction. Reference [2] has provided long term operational planning for energy management of a micro-grid. It has presented a micro-grid system with energy sources from three gas turbines and a PV based active generator and a micro-grid central energy management system (MCEMS) has been given with parameters that include environmental effects, long term energy and short term power prediction, and energy market. Based on all of these crucial parameters, the micro-grid system need to be organized properly and the output of the system can be optimised for more efficient and environmentally friendly operation.

IV. Battery Storage and Ultra-Capacitor (Energy Storage System)

Battery storage systems are being progressively used in distributed renewable energy generation. With the additional introduction of ultra-capacitors in the near future, the effectiveness and reliability of the energy storage systems will be improved. The combinations of battery and ultra-capacitors will increase the system efficiency as the battery will be able to store and release energy gradually. In [9], the authors evaluate the optimal use of batteries for PV, and in [10] a battery model is proposed that is specifically useful for stand-alone PV applications. In it seven different levels of working zone and zone conditions are proposed: saturation zone, overcharge zone, charge zone, changing from charge to discharge or vice versa, discharge zone, over discharge, and exhaustion.

Vallvè et al. [11] has discussed three basic aspects of the installation of storage for grid connected PV systems. The first argument concerns the fact that the storage system can undoubtedly improve the security of supply for the whole system, however, the power quality is the main issue. Second the addition of storage units may increase the performance of the PV generator for controlling the power flow. The third aspect concerns the fact that even with large penetration of PV, it will not be possible to cover the whole load consumption, but the PV source can supply at least some part of the overall energy consumption by some loads. These facts may lead the utility company or customer(s) to consider the battery and ultra-capacitor system as a main storage structure for future housing development in order to integrate PV system as well as play role in demand side management. The battery storage system for PV integration is also discussed in[12], [13] and [14]. The authors in these papers have discussed the power quality issues related to the integration of PV systems in the micro-grid, i.e., frequency control, voltage stability, and energy storage smoothing control. These parameters are very important for implementing controlled power flows from a PV based active generator.

Several new technologies have been proposed for energy storage system to fit into the grid or micro-grid. The utilization of Vanadium Redox Battery (VRB) is a good solution. As discussed in [15] and based on evidences reported in [16] and [17], the utilization of VRB in micro-grids is considered to have high potential for successful integration. The comparisons between different types of batteries are given in Table 1.

V. Energy Management in Micro-Grid Environment

In a micro-grid connection, other than finding new alternative optimization criteria and exploration of the power fluctuation effects, it is important to model energy management options so that a reliable energy supply with improved efficiency can be delivered without any failure to customer [18]. A deterministic energy management algorithm for a PV based active generator in a micro-grid environment needs to be set up for proper supervision. Based on Figure 1, the PV based active generator will be coupled

TABLE I. COMPARISON BETWEEN DIFFERENT TYPES OF BATTERIES FOR IMPLEMENTATION WITH PV BASED ACTIVE GENERATOR IN MICRO-GRIDS.

Parameter/Technology	Li-ion	Na S	Lead-Acid	VRB	Flow Battery
Energy density [17]	Average	High	Low	Low	Varies (lower than Li-ion)
Efficiency	High (near 100%)	High (~ 92%)	85%	~ 85%	60% ~ 85%
Lifecycle	500-1000[1]		200-300[1]	High	
Toxicity	Non-toxic (electrolyte may be harmful)	Highly Corrosive	Sulphuric acids in the lead is highly corrosive	No fire hazard No highly reactive or toxic substances	Low toxicity
Cost	High (above ~ $600)	High (up scaling)	Low	High	Low on average (depends on type of chemical)
Other		High operation temperature (heating process needed)	Requires regular maintenance	Independent energy and power rating More complicated technology	High power and capacity for load levelling in grid system

via a DC bus and it will be connected to the micro-grid through a three phase inverter. This will be connected and controlled by a micro-grid controller through a droop controller for primary frequency control.

A basic requirement for satisfactory operation of power system is that the PV based active generator needs to maintain the nominal frequency of the grid (50 Hz or 60 Hz) within the standard threshold limit of ±0.02 Hz [19]. The rule of thumb for frequency control is that it depends on the active power (P), whereas voltage control is based on reactive power (Q). In [2], [4, 9], the droop controller for a PV based active generator in a micro-grid has been discussed, and it does not engage any inertia of mechanical systems since there is no kinetic energy involved during electricity generation from the PV array [20]. As load changes might lead to significant frequency changes that can affect the whole system, it is vital to manage the frequency control aspect to ensure efficient operation of the micro-grid. In [4], the authors have discussed micro-grid management in terms of two timing scales; long term and short term. Long term in this micro-grid management is defined as days and hour while for short term, it is outlined in a seconds and milliseconds. The parameter of this timing classification can be seen in Table II.

TABLE II. TIMING CLASSIFICATION FOR ENERGY MANAGEMENT SYSTEM IN MICRO-GRID

Long Term	Short Term
- Electricity market - Load forecasting - Renewable energy production - Load management - Energy storage availability	- Voltage control - Frequency control - Dynamic storage availability - Power capability

For a grid connected PV based active generator, the network operators need a reliable and robust PV energy output forecasting system for operational planning purposes. Therefore, a proper forecasting methodology is required for predicting the PV array output. One approach can be based on identification of patterns in historical data sets for predicting the future output, see for instance [21]. A lot of work has been done in this area, where researchers are using different methods to predict the PV array energy output. The continuous development in this area will be very helpful to achieve increased implementation and energy generation share of PV based active generators in the main grid as well as in local micro-grids.

VI. CONCLUSION

This paper has reviewed the PV based active generator in combination with battery storage and ultra-capacitors. Active generator may increase the overall system efficiency as the battery will be able to store and release energy gradually, while the ultra-capacitor can act as a storage device of high power density with fast response times for effective power management and delivery. Different types of battery technologies have been compared, and it is observed that Vanadium Redox Battery looks promising for the near future application in PV based active generators. On the energy management side, the PV forecasting methods, controlled power (active & reactive) delivery, power quality management and potential fault issues needs to be taken into account. Since the PV based generator has a promising future for increasing its penetration and it will be having greater impact on the green energy market. The continuous research on both the energy storage side and PV system will be important to ensure high power quality, reliability, and cost for this new type of clean energy generator.

ACKNOWLEDGMENT

The authors gratefully acknowledge the partial support of the Research Council of Norway and partners in the project 'Electricity Usage in Smart Village Skarpnes'. Aimie Nazmin Azmi would also like to acknowledge the funding support received from the Universiti Teknikal Malaysia Melaka for his PhD study at the University of Agder (Norway).

REFERENCES

[1] P. Basak, S. Chowdhury, S. Halder nee Dey, and S. Chowdhury, "A literature review on integration of distributed energy resources in the perspective of control, protection and stability of microgrid," Renewable and Sustainable Energy Reviews, vol. 16, pp. 5545-5556, 2012.

[2] H. Kanchev, D. Lu, B. Francois, and V. Lazarov, "Smart monitoring of a microgrid including gas turbines and a dispatched PV-based active generator for energy management and emissions reduction," in Innovative Smart Grid Technologies Conference Europe (ISGT Europe), 2010 IEEE PES, 2010, pp. 1-8.

[3] D. Lu, T. Zhou, H. Fakham, and B. Francois, "Design of a power management system for an active PV station including various storage technologies," in Power Electronics and Motion Control Conference, 2008. EPE-PEMC 2008. 13th, 2008, pp. 2142-2149.

[4] H. Kanchev, D. Lu, F. Colas, V. Lazarov, and B. Francois, "Energy management and operational planning of a microgrid with a PV-based active generator for smart grid applications," Industrial Electronics, IEEE Transactions on, vol. 58, pp. 4583-4592, 2011.

[5] R. Shah and N. Mithulananthan, "A comparison of ultracapacitor, BESS and shunt capacitor on oscillation damping of power system with large-scale PV plants," in Universities Power Engineering Conference (AUPEC), 2011 21st Australasian, 2011, pp. 1-6.

[6] C. A. Hill, M. C. Such, D. Chen, J. Gonzalez, and W. M. Grady, "Battery energy storage for enabling integration of distributed solar power generation," Smart Grid, IEEE Transactions on, vol. 3, pp. 850-857, 2012.

[7] J. M. Guerrero, J. C. Vasquez, J. Matas, L. G. de Vicuña, and M. Castilla, "Hierarchical control of droop-controlled AC and DC microgrids—a general approach toward standardization," Industrial Electronics, IEEE Transactions on, vol. 58, pp. 158-172, 2011.

[8] J. Zhang, J. Wang, and X. Wu, "Research on Supercapacitor Charging Efficiency of Photovoltaic System," in Power and Energy Engineering Conference (APPEEC), 2012 Asia-Pacific, 2012, pp. 1-5.

[9] D. Lu and B. Francois, "Strategic framework of an energy management of a microgrid with a photovoltaic-based active generator," in Advanced Electromechanical Motion Systems & Electric Drives Joint Symposium, 2009. ELECTROMOTION 2009. 8th International Symposium on, 2009, pp. 1-6.

[10] D. Guasch and S. Silvestre, "Dynamic battery model for photovoltaic applications," Progress in Photovoltaics: Research and applications, vol. 11, pp. 193-206, 2003.

[11] X. Vallvé, A. Graillot, S. Gual, and H. Colin, "Micro storage and demand side management in distributed PV grid-connected installations," in Electrical Power Quality and Utilisation, 2007. EPQU 2007. 9th International Conference on, 2007, pp. 1-6.

[12] V. Virulkar, M. Aware, and M. Kolhe, "Integrated battery controller for distributed energy system," Energy, vol. 36, pp. 2392-2398, 2011.

[13] X. Li, D. Hui, and X. Lai, "Battery energy storage station (BESS)-based smoothing control of photovoltaic (PV) and wind power generation fluctuations," 2013.

[14] H.-J. Yoo, H.-M. Kim, and C. H. Song, "A coordinated frequency control of Lead-acid BESS and Li-ion BESS during islanded microgrid operation," in Vehicle Power and Propulsion Conference (VPPC), 2012 IEEE, 2012, pp. 1453-1456.

[15] G. Wang, M. Ciobotaru, and V. G. Agelidis, "PV power plant using hybrid energy storage system with improved efficiency," in Power Electronics for Distributed Generation Systems (PEDG), 2012 3rd IEEE International Symposium on, 2012, pp. 808-813.

[16] T. A. Nguyen, X. Qiu, T. T. Gamage, M. L. Crow, B. M. McMillin, and A. Elmore, "Microgrid application with computer models and power management integrated using PSCAD/EMTDC," in North American Power Symposium (NAPS), 2011, 2011, pp. 1-7.

[17] G. Wang, M. Ciobotaru, and V. G. Agelidis, "Minimising output power fluctuation of large photovoltaic plant using vanadium redox battery storage," in Power Electronics, Machines and Drives (PEMD 2012), 6th IET International Conference on, 2012, pp. 1-6.

[18] D. Quiggin, S. Cornell, M. Tierney, and R. Buswell, "A simulation and optimisation study: Towards a decentralised microgrid, using real world fluctuation data," Energy, vol. 41, pp. 549-559, 2012.

[19] P. Mercier, R. Cherkaoui, and A. Oudalov, "Optimizing a battery energy storage system for frequency control application in an isolated power system," Power Systems, IEEE Transactions on, vol. 24, pp. 1469-1477, 2009.

[20] Aimie Nazmin Azmi, M. L. Kolhe, "Primary Frequency Control through Grid Connected Photovoltaic Active Generator," in 3rd International Workshop on Integration of Solar Power into Power Systems, London, UK, 2013.

[21] E. Matallanas, M. Castillo-Cagigal, A. Gutiérrez, F. Monasterio-Huelin, E. Caamaño-Martín, D. Masa, and J. Jiménez-Leube, "Neural network controller for Active Demand-Side Management with PV energy in the residential sector," Applied Energy, vol. 91, pp. 90-97, 2012.

IEEE International Conference on Smart Grid and Clean Energy Technologies (2015 ICSGCE), DOI: 10.1109/ICSGCE.2015.7454271

2015 International Conference on Smart Grid and Clean Energy Technologies

Impact of Increasing Penetration of Photovoltaic (PV) Systems on Distribution Feeders

Aimie Nazmin Azmi, Ivan Nordnes Dahlberg, Mohan Lal Kolhe, and Anne Gerd Imenes

Faculty of Engineering & Science, University of Agder, PO Box 422, NO 4604 Kristiansand, Norway

e-mail: aimie.n.azmi@uia.no, ivandahlberg@hotmail.com, mohan.l.kolhe@uia.no, AnneGerd.Imenes@teknova.no

***Abstract*—This paper investigates impact of increasing photovoltaic (PV) penetration on distribution feeders. The main focus of this work is on 'how PV systems penetration can influence operation of the protective devices in the distribution feeder?'. PV systems' impact, in a distribution feeder, for 3ϕ fault has been analyzed. It considers fault location and protective devices (PDs) settings (e.g. time of PDs operation before a fault gets cleared by it). This paper is also emphasizing on 'how the penetration of PV can affect voltage quality / unbalance in the distribution feeder'. The considered distribution feeders are supplying residential network and therefore loading on different phases are going to be unbalanced. The voltage quality at different nodes is analyzed, not only due to domestic load distribution, but also due to output variations from integrated PV systems. The obtained results show that increasing PV penetration can escalate PDs' operational time during 3ϕ faults. This work has been carried out using DigSilent PowerFactory®.**

Keywords-photovoltaic; fault; protection devices; PowerFactory®

I. INTRODUCTION

Large scale penetration of intermittent renewable energy sources (e.g. PV systems) and other distributed generators in the smart grid environment require the development of a load dispatching methodology by considering not only the active inertia of the power system but also using frequency-droop characteristics like conventional generators approach. The integration of intermittent renewable energy and other efficient distributed energy resources into existing and future electricity networks represents significant technical and economic challenges. The widespread development of such systems requires a thorough analysis of all technical and commercial aspects of renewable energy sources and other decentralized generation units in the distribution network. In power system network, the power quality is very important. Due to PV power output fluctuations; there are some chances for power quality disturbances e.g. voltage transients due to intermittency, harmonics, active and reactive power management, power delivery angles and a lot more reasons. In the conventional grid connected PV generators, hybrid filters are used to improve the power quality [1]. However, for multiple PV based active generators (e.g. group of buildings with BIPV), the power quality issues require more detailed analysis. Also it is important to analyze the fault protection system [2].

The higher penetrations of distributed generators are going to create different possibilities of the faults not only in the micro-grid network, but also at the higher voltage power system network. Fault detection and isolation mechanism is very important for power system operation. It is needed to analyze the fault protection system under increasing penetration of PV systems (e.g. fault current levels, relay settings, fault clearing time in the micro-grid environment). During fault or any unwanted events and abnormal conditions at the micro-grid network, the grid may be disconnected, and islanding effect may occur in micro-grid [3]. Fault currents in an islanded mode based micro-grid are not going to be similar as fault occurs in a conventional grid system. Therefore methods for isolating the faults of the conventional grid system are needed modification in the micro-grid system [4]. In a micro-grid network, there are limitations on protection system due to the islanding operation mode. Also the fault clearing time is important for micro-grid stability, operation and safety. It is needed to include/coordinate control signals of the protection mechanism in the EMS of micro grid. In this work, the fault analysis of the PV systems in the micro-grid network are analyzed in both islanded as well as grid connected modes.

Examination on the effects of high diffusion PVs on a distribution feeder's protection and operation is reported in [4]. Increasing penetration of PV systems on a feeder will affect the voltage variation due to change in solar radiations. In this work the considered distribution network topology is based on [5]. This work is using DigSilent PowerFactory® simulation software. It has the ability for doing load flow calculations with integration of PV systems, electromagnetic transients and as well as transient events during abnormal operation of the distributed network.

II. DISTRIBUTION FEEDER MODELLING

The grid system modelled in PowerFactory® is represented as a single line diagram, which is given in Fig. 1 and it is based on [5]. The load symbol in the figure is representing a group of houses. Each PV system in its lumps a number of separate PV modules connected in parallel as an aggregated PV system. The rating of each PV module is equal to the peak of the load and it is represented as:

$$P_{PV;peak} = P_{load;peak} \quad (1$$

The considered network has three voltage levels: (i) external grid at 69 $kV_{line\text{-}line}$, (ii) distribution feeders 12 $kV_{line\text{-}line}$, and (iii) domestic buildings 0.24 $kV_{line\text{-}ground}$. In this distribution network considered loads are domestic and PV systems are connected in a single phase and thus, the system is going to be unbalanced. In the PowerFactory® software the following load parameters fo

978-1-4673-8734-7/15/$31.00 ©2015 IEEE

a private home are used: peak load of 1.14 kW with power factor 0.95 lagging. Based on equation (1), each house's PV system rating has taken as 1.14 kW.

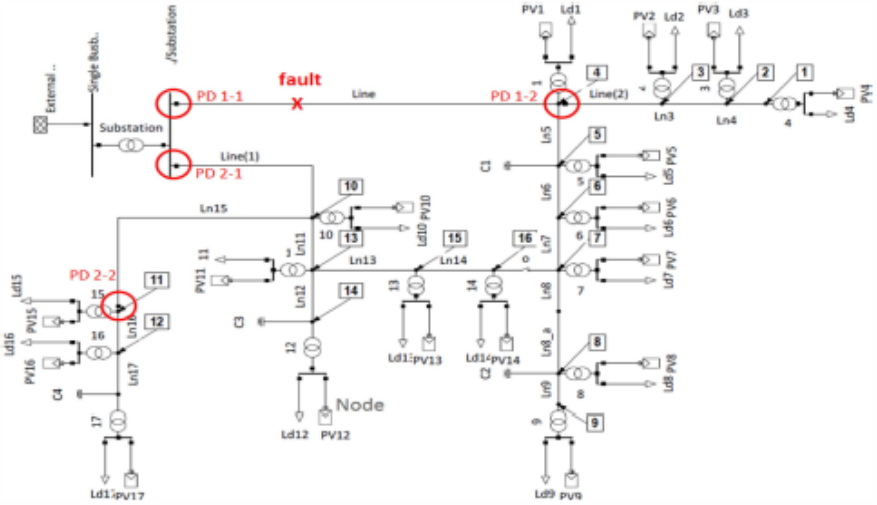

Figure 1.Single line diagram with node reference of distribution feeders in PowerFactory® environment

III. Power Flow Analysis

The power flow calculations are studied for considered distribution network topology (Fig. 1) for following some scenarios (Table I). The variation of loads between 50% and 100% are considered, and PV system outputs variations are considered from 0% to 100% based on PV availability. These scenarios may change in real conditions, but considered scenarios are going to provide some information on voltage quality of the network. Legends of these scenarios are given in Table I and they are referred in Fig. 2, Fig. 3 and Fig. 4 for each phase voltages.

TABLE I. Some Scenarios for Variation of Load and PV

Scenario	Load (%)	PV (%)	Legend
1	100	0	
2	100	50	
3	50	50	
4	50	100	
5	50	0	

A. Distribution Feeder Voltage Level and Balance

In this section the investigation on how the voltage levels are affected by PV is simulated. The distribution feeders are unbalanced and the voltage levels must be within the limits that has been decided by TSO (transmission system operator) and based on the PDs capabilities. Based on Table I, voltage levels are plotted for node 1 to node 16 (refer. Fig. 1 for node identification), to see how the voltage level varies in each phase for different scenarios.

The voltage variation that occurs as seen in Fig. 2, Fig. 3 and Fig. 4 is an expected problem due to PV penetration into distribution feeders. For future simulation work, reactive compensation device (e.g STATCOM) will be included to overcome huge voltage variation and reverse power flow problem [6].

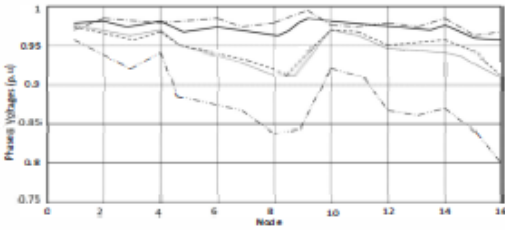

Figure 2. Node voltages for phase (a).

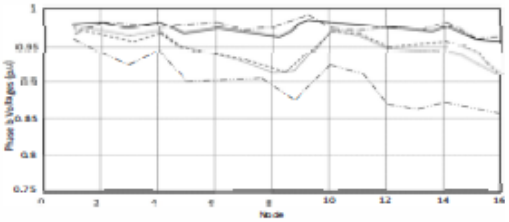

Figure 3. Node voltages for phase (b).

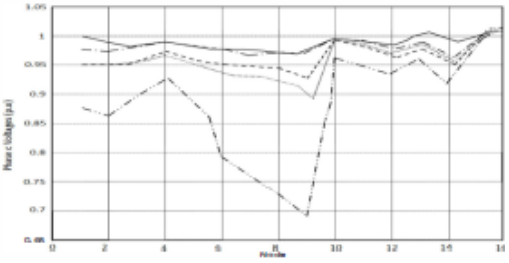

Figure 4. Node voltages for phase (c).

It can be seen that when $P_{PV} \approx P_{load}$ voltage curves are almost flat and the losses is quite small. However, with no PV (PV = 0%) the voltage is dropping along the line. Hence, with no PV (PV = 0%), the losses are quite high. In phase c, the voltage drop significantly at node no. 7, with the voltage p.u. is less than 0.7.

IV. PDs and PVs Operation

In this section the influence of PVs on PDs are investigated. At first the documentation of the modelled PDs are presented, then simulations are performed to see how the PDs perform, based on a single node in the distribution feeders. Four different positions of PDs are evaluated. These devices are breakers or switches that are supervised by over current relays.

A. Protection Device

There are four main protection devices in the system. These devices are breakers or switches that are supervised by over current relays. Fig. 1 shows the position of each of the PD.

Based on this figure, there are two PDs for each feeder. At this point the PVs are set to 0% generation and the loads are at 100 %. This simulation is to see the amount of rated currents that will flow through the PDs. Thus, all PVs are set to be 'off' and an unbalanced power flow algorithm is simulated. The results can be seen in Table II.

TABLE II. Maximum Currents Flowing Through PDs under Normal Conditions

Protection device	Current (A)
PD 1-1	605
PD 1-2	196
PD 2-1	571
PD 2-2	184

The scheme for the Over Current Relays (OCR) in PowerFactory® is developed from 5 working blocks (refer: Fig 5). The current are measured by a current transformer (CT). The CT will be given a rated value, corresponding to the currents in the recent power flow (refer: table II). In the blocks labelled 'I >' and 'I >>', the maximum allowed current magnitude for the PDs are set. Time limit for the current are also set, for the duration that the system can endure the currents before the breaker gets activated. If current with magnitude of larger than 'I >>' are flowing to the PD, the switch will disconnect and isolate the respective line. 'I >' will only respond to fault that are smaller amount but continuous over some time.

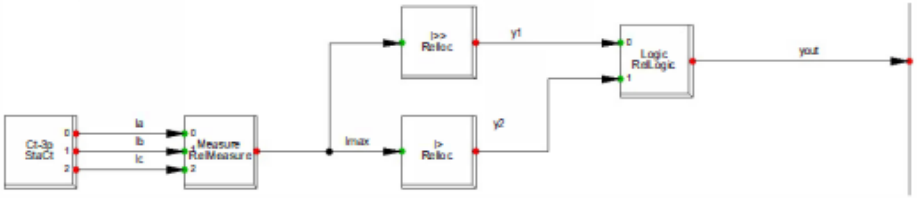

Figure 5. PowerFactory ® Over current relay scheme.

The parameters given in the over current relay can be seen in Table III:

TABLE III. Over Current Relay Parameters for Circuit Breakers

Response	Magnitude (pu)	Time (s)
Slow response (I >)	1.2	1
Fast response (I>>)	2	0.02

These parameters are used for relays. It can be seen from Table III if the current magnitude are 20 % above rated, for a time larger than 1 second, the PD will disconnect the respective branch from the grid. Under abnormal conditions where the current is larger than 2.0 p.u., fast response will be executed.

B. PV System

For a PV system that connected in parallel with the electric utility, there are special recommendations made by the IEEE standards committee. This is to ensure the safety of workforces, utility system operations and equipment protection [7]. Based on the IEEE Std 929-2000 (IEEE Recommended Practice for Utility Interface of Photovoltaic (PV) Systems), the response time to abnormal changes for any voltage disturbance can be define as:

TABLE IV. Protection Scheme for a Domestic PV Array

Voltage*	Max trip time
V<60	6 cycles
60≤V<106	120 cycles
106≤V≤132	Normal Operation
132<V<165	120 cycles
165≤V	2 cycles

*Based on a system voltage assume at nominal 120 V

The protection scheme for PV array in PowerFactory ® is given with 3 parameters that can be change. Switch-off threshold, switch-on threshold and switch –on delay. The switch 'off' value is set as 0.5 p.u. and the switch 'on' value as 0.9 p.u. Hence, the PV gets disconnected if the PV terminal voltage is below 0.5 p.u. in 0.010s. The protection scheme will reconnect the PV automatically according to the Switch-on Delay time.

V. Analysis on Fault

For this paper, the fault analysis has been done only at node 4 (refer Fig. 1). In Table V the fault scenario parameters are given. The fault resistance in transmission lines can be calculated by using different model of arc resistance [8]. The common equation that has been used as based equation is the Warrington equation:

$$R_f = (28707.35 \times L) / I \qquad (2)$$

where:

R_f = Arc resistance (Ω)
L = Arc length (m)
I = RMS value of fault current

This equation is derived from the Warrington's test with an assumption of bad measurement was omitted. The weakness of

this model is that the range of arc current is below 1kA which is low and new formula introduced by Terzija and Koglin [9], [10]. Since then, a few others expression has been introduced to find the real magnitude of arc current. The parameter that has been used in this simulation is based on Table V, this is based on data from [5].

TABLE V. FAULT RESISTANCE PARAMETER (AT NODE 4)

Phase	Fault resistance (Rf)
3	0
3	0.11
1	0
1	0.17

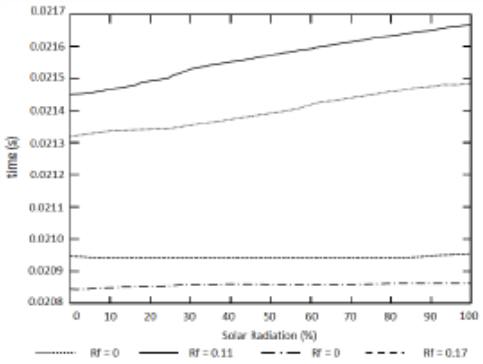

Figure 6. Effects of PVs on the operating time of PD at node 4.

A short circuit event is created for each scenario. Then the RMS analyses are simulated. The idea is to see if the level of solar radiation will have an impact on the PD response time. Based on Fig. 6, it shows that solar radiation has an impact on how fast the PD disconnects during fault. Hence, the time variation is quite small.

For a 3ϕ fault with Rf of 0 Ω, the operating time is increasing from 21.36 millisecond (msec) to approximately 21.4 msec. The most significant rise can be seen for 3ϕ fault with Rf of 0.11 Ω. It grows from 21.47 msec to nearly 21.70 msec. This variation is rather small, however in protection system, every micro-second is vital [11]. There are obvious impacts on PV based on fault current magnitude. This can be simulated by applying a fault at one of the branch (refer Fig. 1).

During fault, the PD will react automatically. Fig. 7 shows the p.u voltage drops down significantly after the PD is activated. During the fault occur, PV 1(refer Fig. 1) will shut down. Fig. 8 shows that fault current is almost 5 kA before it is drop to 0A once the PD system is activated. The same pattern of voltage and current parameter is anticipated on the other PV system in the same distribution system. Nevertheless, with a large number of PV connection throughout the distribution feeders, the vast effect should be expected and the most common thing is fault current transients in distributed generation will have initial high "subtransient component" [12]. Further work will consider more nodes in the distribution feeders and comparisons between faults in a conventional feeders and distributed generation with a great number of PV systems will be executed.

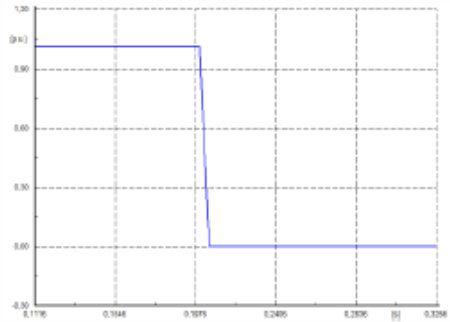

Figure 7. Voltage at Node 1 during fault (voltage in pu versus time in sec).

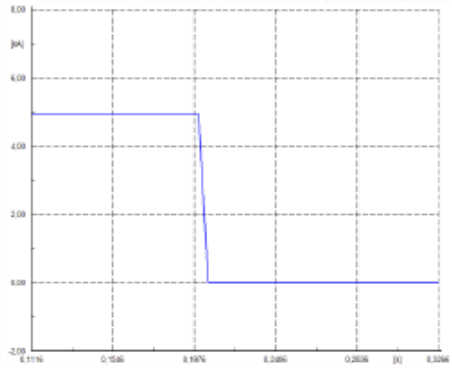

Figure 8.Current from PV at Node 1 during fault (current in kA versus time in sec).

VI. CONCLUSION

Power quality is important in power system analysis. The widespread uses of distributed generators (DGs) are creating many power quality issues. It may lead to the multiple harmonics, voltage fluctuations, and unstable operation in the power system network. This work has considered into the most important thing in DGs, the fault analysis. High PV penetration into the distribution system will give a huge impact to the protection system. The existence of PV array in a huge quantity in a system may prejudice the grid safety in terms of protection scheme and safety. Based on the simulation, the results show that high penetration PVs will give a significant impact on voltage profile. It will also affect the overall system protections. Fig. 2, Fig. 3 and Fig. 4 is the comparison of the per-unit voltage under different system of operating at a different node. The highest p.u voltage is happening in scenario 4, where the PV generation exceeds the load. This result may vary if the PV array output is taken into account, meaning that for a different geographical location, it might affect the PV array output.

Based on IEEE Standards 929-2000, PV systems protection scheme needs to be monitored so that the response time will meet the regulation within the range. The PDs and all protection devices need to act as the standards. In PowerFactory® settings, the result in Fig. 7 and Fig. 8 can be seen with a total shut down after fault. As for future work, the impact of the high penetration of DGs especially PV in a transmission lines can be simulate in a different load profile with a different season

(winter or summer). Purpose of this work is to get understanding of increasing PV systems and to replace the network topology using local Norwegian distribution network parameters, which will be reported in further work.

ACKNOWLEDGMENT

The authors gratefully acknowledge the support of the Research Council of Norway and project partners in the project 'Electricity Usage in Smart Village Skarpnes'. Aimie Nazmin Azmi would also like to acknowledge the funding support received from Universiti Teknikal Malaysia Melaka (UTeM) for his PhD study at University of Agder (Norway).

REFERENCES

[1] P. Basak, S. Chowdhury, S. H. nee Dey, and S. Chowdhury, "A literature review on integration of distributed energy resources in the perspective of control, protection and stability of microgrid," *Renewable and Sustainable Energy Reviews*, vol. 16, pp. 5545-5556, 2012.

[2] A. N. Azmi, M. L. Kolhe, and A. G. Imenes, "Review on photovoltaic based active generator," in *Proc. 2015 9th International Symposium on Advanced Topics in Electrical Engineering (ATEE)*, 2015, pp. 812-815.

[3] A.-N. Azmi, M. L. Kohle, and A. G. Imenes, "On-grid residential development with photovoltaic systems in Southern Norway," in *Proc. 2013 IEEE Conference on Clean Energy and Technology (CEAT)*, 2013, pp. 93-97.

[4] M. Kolhe, "Smart grid: charting a new energy future: research, development and demonstration," *The Electricity Journal*, vol. 25, no. 2, pp. 88-93, 2012.

[5] M. E. Baran, H. Hooshyar, Z. Shen, and A. Huang, "Accommodating high PV penetration on distribution feeders," *IEEE Transactions on Smart Grid*, vol. 3, no. 2, pp. 1039-1046, 2012.

[6] C.-H. Lin, W.-L. Hsieh, C.-S. Chen, C.-T. Hsu, and T.-T. Ku, "Optimization of photovoltaic penetration in distribution systems considering annual duration curve of solar irradiation," *IEEE Transactions on Power Systems*, vol. 27, no. 2, pp. 1090-1097, 2012.

[7] IEEE, *IEEE Recommended Practice for Utility Interface of Photovoltaic (PV) Systems*: IEEE, 2000.

[8] V. D. Andrade and E. Sorrentino, "Typical expected values of the fault resistance in power systems," in *Proc. 2010 IEEE/PES Transmission and Distribution Conference and Exposition: Latin America (T&D-LA)*, 2010, pp. 602-609.

[9] N. Zamanan, J. Sykulski, and A. Al-Othman, "Arcing high impedance fault detection using real coded genetic algorithm," in *Proc. the 3rd IASTED Asian Conference on Power and Energy Systems*, 2007, pp. 35-39.

[10] V. V. Terzija and H.-J. Koglin, "On the modeling of long arc in still air and arc resistance calculation," *IEEE Transactions on Power Delivery*, vol. 19, no. 3, pp. 1012-1017, 2004.

[11] D. Salomonsson, L. Söder, and A. Sannino, "Protection of low-voltage DC microgrids," *IEEE Transactions on Power Delivery*, vol. 24, no. 3, pp. 1045-1053, 2009.

[12] M. E. Baran and I. El-Markaby, "Fault analysis on distribution feeders with distributed generators," *IEEE Transactions on Power Systems*, vol. 20, no. 4, pp. 1757-1764, 2005.